

**HIGHLY STABLE POLYMERIC MATERIALS  
FOR ELECTRO-OPTICAL MODULATORS**

This research has been supported by the Dutch Technology Foundation STW, applied science division of NWO, grant number TOE 6067.

© Faccini Mirko, Enschede, 2008

No part of this work may be reproduced by print, photocopy or any other means without the permission in writing of the author.

ISBN 978-90-365-2675-3

# HIGHLY STABLE POLYMERIC MATERIALS FOR ELECTRO-OPTICAL MODULATORS

PROEFSCHRIFT

ter verkrijging van  
de graad van doctor aan de Universiteit Twente,  
op gezag van de rector magnificus,  
prof. dr. W.H.M. Zijm,  
volgens besluit van het College voor Promoties  
in het openbaar te verdedigen  
op donderdag 26 Juni 2008 om 13.15 uur

door

**Mirko Faccini**

geboren op 6 Juni 1978  
te Orzinuovi, Italië

Dit proefschrift is goedgekeurd door:

Promotor: Prof. Dr. Ir. D. N. Reinhoudt

Assistent-promotor: Dr. W. Verboom

# Contents

## CHAPTER 1

<b>General Introduction</b>	1
1.1 References	4

## CHAPTER 2

### **Nonlinear Optical Polymeric Materials**

2.1 Introduction	6
2.2 General Background	6
2.3 Applications of Electro-optical Materials	9
2.4 Material Requirements	11
2.5 Chromophore Design	12
2.6 Guest-Host Systems	16
2.7 Side-Chain Systems	18
2.7.1 Polyimides	18
2.8 Main-Chain Systems	22
2.9 Cross-linked Systems	23
2.10 Dendritic Systems	27
2.10.1 3D-shaped Dendritic NLO Chromophores	28
2.10.2 Crosslinkable NLO Dendrimers	31
2.10.3 Side-chain Dendronized NLO Polymers	34
2.11 Self-assembled Systems	36
2.11.1 Langmuir-Blodgett (LB) Films	37

2.11.2	Covalent Layer-by-Layer Assemblies	38
2.11.3	Hydrogen Bonded and Supramolecular Assemblies	41
2.12	Conclusions and Outlook	44
2.13	References	46

## **CHAPTER 3**

### **Enhanced Poling Efficiency in Highly Thermal and Photostable Nonlinear Optical Chromophores**

3.1	Introduction	56
3.2	Results and Discussion	59
3.2.1	Synthesis	59
3.2.2	Linear Optical Properties	61
3.2.3	Optical Loss Measurements	62
3.2.4	Thermal Analysis	64
3.2.5	Photobleaching Test	64
3.2.6	Hyper-Rayleigh Scattering Measurements	66
3.2.7	Electric Field Poling and EO Property Measurements	66
3.3	Conclusions	69
3.4	Experimental Section	69
3.5	References	74

## **CHAPTER 4**

### **Photostable Nonlinear Optical Polycarbonates**

4.1	Introduction	80
4.2	Results and Discussion	81
4.2.1	Synthesis	81

---

4.2.2	Thermal Analysis	84
4.2.3	Linear Optical Properties	86
4.2.4	Photobleaching Test	86
4.2.5	Electric Field Poling and EO Property Measurements	88
4.3	Conclusions	91
4.4	Experimental Section	92
4.5	References	97

## **CHAPTER 5**

### **Facile Attachment of Nonlinear Optical Chromophores to Polycarbonates**

5.1	Introduction	100
5.2	Results and Discussion	102
5.2.1	Synthesis	102
5.2.2	Polymer Physical Properties and Processing	106
5.3	Conclusions	108
5.4	Experimental Section	108
5.5	References	114

## **CHAPTER 6**

### **Fabrication of Polymeric Microring Resonators Using Photolithography and Nanoimprint Lithography**

6.1	Introduction	118
6.2	Results and Discussion	120
6.2.1	Synthesis	120
6.2.2	Optical Properties	120
6.2.3	Simultaneous Cross-linking and Poling	121

6.2.4	Microring Resonator Fabrication by Photodefinition.	125
6.2.5	Microring Resonator Fabrication by NIL.	128
6.3	Conclusions	129
6.4	Experimental Section	130
6.5	References	132
<b>CHAPTER 7</b>		
<b>Electro-optic Active Cyclodextrin-based Rotaxanes</b>		
7.1	Introduction	136
7.2	Results and Discussion	138
7.2.1	Synthesis	138
7.2.4	Photobleaching Test	145
7.3	Conclusions	146
7.4	Experimental Section	146
7.5	References	148
	<b>Summary</b>	151
	<b>Samenvatting</b>	155
	<b>Thanks</b>	159



# Chapter 1

## General Introduction

As internet and multimedia applications become an integral part of everyday home and business life, the demand for multimedia connectivity and services will continuously grow and accelerate.<sup>1</sup> Optical fiber networks currently form the backbone of the telecom, internet, and telephone networks. Transmitting signals by using infrared light through an optical fiber is the most effective way to move large amounts of data rapidly over long distances (Figure 1). As result of this bandwidth need, optical fiber networks are expanding, moving closer to the end user, allowing the highly desired fiber to the home (FTTH) networks to become reality. Fiber-based access networks will allow providers to provide real-time multimedia services such as video, voice, and data services.

The need for increased capacity and speed in transporting and processing information is driving the development of advanced optical components for applications in broadband communication and high speed computing. In general, advanced optical components should operate at high frequency with a broad bandwidth, consume less power, and be integrated with other optical components.<sup>2</sup>

The electro-optic (EO) modulator is a key device in optical communication, because it allows the translation of an electrical signal into an optical signal.<sup>3</sup> One way to accomplish this electrical-to-optical translation is by exploiting the EO effect, which is the change in the refractive index of a material in response to an applied electric field.

In present technology, lithium niobate ( $\text{LiNbO}_3$ ) is the most widely used EO material in high-speed optical modulators. These devices, however, operate well at frequencies below 20 GHz (~20 billion bits per second), but their performance degrades quickly

above 40 GHz. This restriction is mainly due to the crystalline nature of lithium niobate, which has discrete properties that cannot be changed substantially, limiting operational speed and integration of lithium niobate devices with other components.

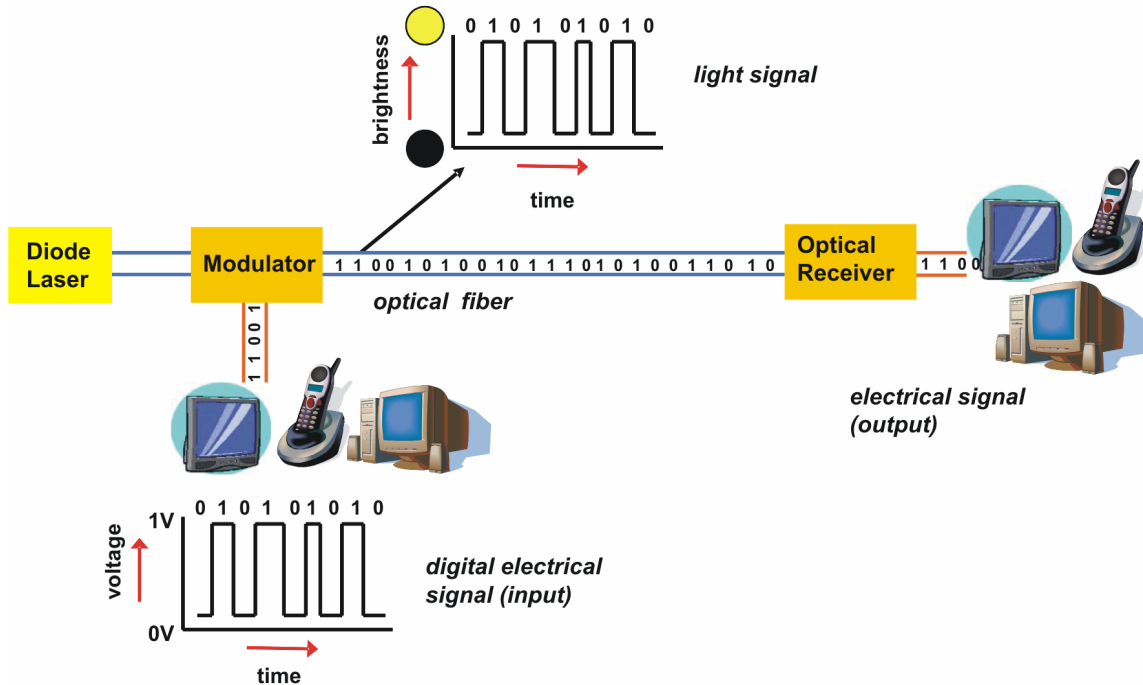


**Figure 1.** Schematic representation of the optical communication.

To surpass the current frequency limitations, employment of new EO materials and devices is necessary. Electro-optic polymers have several distinct advantages that enable high data rate operation, low operating voltages (low power consumption), and an extremely broad bandwidth.<sup>4,5</sup> These beneficial properties, along with the ease of processing and integration with conventional semi-conductor fabrication techniques, have driven the development and demonstration of optical components made from EO polymers such as Mach-Zehnder modulators,<sup>6</sup> micro-ring resonators (useful as both modulators and optical filters),<sup>7</sup> digital optical switches, phase modulators,<sup>8</sup> linear analog modulators for cable TV deployment, and directional couplers.

Although questions about the long-term reliability of polymeric devices remain to be answered, polymeric optical waveguides and EO materials clearly provide excellent tools for the high-speed photonic applications important to next-generation optical communications.

This thesis aims to contribute toward long-lifetime device-quality materials with the synthesis and study of new, thermal and photostable EO polymeric materials. Their chemical, photochemical, and optical properties are described, together with the fabrication of prototype EO devices derived there from.

Chapter 2 first gives an introduction to the theory and concepts of nonlinear optics (NLO). Then it describes the recent developments in the field of second-order NLO polymers, including chromophore design, and the different approaches for their incorporation in noncentrosymmetric materials. The different architectures are compared, together with the requirements for their incorporation into practical EO devices.

Chapter 3 describes the synthesis of a series of highly photostable NLO chromophores, and the thermal and optical properties of the polymeric materials obtained by incorporating them as a guest at high loading in a polymer host.

Chapter 4 deals with the synthesis and the properties of thermally and photochemically stable NLO polycarbonates in which the chromophore is covalently attached to the polymer backbone. Moreover, the effect of the attachment mode and the flexibility on the EO properties is studied, together with a comparison with a guest-host system incorporating the same chromophore as described in Chapter 3.

Chapter 5 describes a versatile, generally applicable approach for the covalent incorporation of NLO chromophores to a pre-polymerized polycarbonate backbone. In addition to the synthesis, the characterization, the thermal properties, as well as the second-order nonlinearity of the synthesized polymeric materials are described.

Chapter 6 deals with the fabrication of microring resonator devices either by direct photodefinition of the negative photoresist SU8, incorporating a NLO chromophore, or by nano imprint lithography.

Chapter 7 describes the preliminary results of the synthesis of NLO chromophores of which the  $\pi$ -electron bridge is encapsulated by a cyclodextrin, to form an EO active rotaxane. This encapsulation is expected not only to provide a protection from photochemical attack of the vulnerable NLO chromophore, elongating its lifetime, but also to efficiently reduce the unfavorable intermolecular interactions among dipoles.

## 1.1 References

- 1 D. Cotter, R. J. Manning, K. J. Blow, A. D. Ellis, A. E. Kelly, D. Nesses, I. D. Phillips, A. J. Poustie, D. C. Rogers, *Science*, **1999**, 286, 1523-1528.
- 2 A. J. Seeds, *IEEE Trans. Microw. Theory*, **2002**, 50, 877-887.
- 3 M. Lee, H. E. Katz, C. Erben, D. M. Gill, P. Gopalan, J. D. Heber, D. J. McGee, *Science*, **2002**, 298, 1401-1403.
- 4 Y. Q. Shi, C. Zhang, H. Zhang, J. H. Bechtel, L. R. Dalton, B. H. Robinson, W. H. Steier, *Science*, **2000**, 288, 119-122.
- 5 L. R. Dalton, W. H. Steier, B. H. Robinson, C. Zhang, A. Ren, S. Garner, A. Chen, T. Londergan, L. Irwin, B. Carlson, L. Fifield, G. Phelan, C. Kincaid, J. Amend, A. Jen, *J. Mater. Chem.*, **1999**, 9, 1905-1920.
- 6 Y. Enami, C. T. Derose, D. Mathine, C. Loychik, C. Greenlee, R. A. Norwood, T. D. Kim, J. Luo, Y. Tian, A. K. Y. Jen, N. Peyghambarian, *Nature Photonics*, **2007**, 1, 180-185.
- 7 P. Rabiei, W. H. Steier, C. Zhang, L. R. Dalton, *J. Lightwave Technol.*, **2002**, 20, 1968-1975.
- 8 D. T. Chen, H. R. Fetterman, A. T. Chen, W. H. Steier, L. R. Dalton, W. S. Wang, Y. Q. Shi, *Appl. Phys. Lett.*, **1997**, 70, 3335-3337.

# Chapter 2

## Nonlinear Optical Polymeric Materials

*This Chapter reviews the theory and the current state of the art of nonlinear optical (NLO) active molecules and materials. Focus is on the synthesis of NLO polymers including chromophore design, the comparison among comprehensive electro-optical (EO) polymer systems, and the requirements for their incorporation into practical EO devices.*

## 2.1 Introduction

Polymeric electro-optic (EO) materials incorporating nonlinear optical (NLO) chromophores have shown commercial potential as active media in high speed broadband waveguides for optical switches, optical sensors, and information processors. Meanwhile, several reviews appeared describing the different aspects of this topic. Some of them focus more on the different classes of chromophores<sup>1</sup> (such as charge-transfer molecules, octopolar compounds, ionic materials, multichromophore systems, and organometallics), on their design and synthesis, and on the optimization of their intermolecular interactions to obtain large macroscopic EO activities.<sup>2,3</sup> Other describe chromophore orientation techniques<sup>4</sup> (such as static field poling, photoassisted poling, all optical poling, contact and corona poling), or materials characterization and the steps and techniques required for EO device fabrication and operation.<sup>5,6</sup>

This Chapter deals with the design of efficient dipolar NLO chromophores and the different approaches for their incorporation in noncentrosymmetric materials, including guest-host polymer systems, chromophore-functionalized polymers (side-chain and main-chain), crosslinked chromophore-macromolecule matrices, dendrimers, and intrinsically acentric self-assembled chromophoric superlattices. The different architectures will be compared, together with the requirements (such as large EO coefficient, low optical absorption, high stability, and processability) for their incorporation into practical EO devices. First, a brief introduction to nonlinear optics is presented.

## 2.2 General Background

Nonlinear optics originates from the ability of matter to respond in a nonlinear way to the interaction with external electromagnetic fields (such as that associated with light).<sup>7,8</sup> When an external forcing field is applied to a material, it causes a displacement of the charges in molecules and atoms. In case of a low intensity field, this induced polarization ( $P$ ) is linearly proportional to the field strength ( $E$ ). However, under sufficiently intense fields (such as laser light), the relationship is no longer linear, and the polarization can be

expressed as a power series expansion. Thus, the molecular polarization  $p$  can be written as (neglecting quadrupolar terms):

$$p = \alpha E + \beta EE + \gamma EEE + \dots \quad \text{Eq. 1}$$

where  $\alpha$  is the molecular polarizability, while  $\beta$ ,  $\gamma$ , etc. are molecular hyperpolarizabilities of first order, second order, etc. corresponding to second-, third-, and higher-order nonlinearities, respectively. On a macroscopic scale, the polarizability can be expressed as:

$$P = \chi^{(1)}E + \chi^{(2)}EE + \chi^{(3)}EEE + \dots \quad \text{Eq. 2}$$

where  $\chi$ s are the macroscopic susceptibilities.

Unlike the first- and third-order terms of the above equations, a requirement to induce second-order nonlinear optical activity is the non-centrosymmetry, or acentric symmetry both at the molecular and macroscopic level.<sup>9</sup> At the molecular level, highly polarizable materials with absence of symmetry can be easily obtained by connecting strong electron donors and acceptors by a conjugated  $\pi$  bridge, giving strong charge-transfer molecules. The application of an electric field will effect the mixing of a neutral ground state and a charge-separated excited state, thus changing the molecular polarization of the dipole.

In order to achieve electro-optic activity at the macroscopic level, chromophores must display non-centrosymmetry. To achieve this condition, dipolar molecules should be oriented to yield acentric chromophore lattices. The most commonly used method is electric field poling (corona poling or contact poling) of NLO polymers.<sup>9</sup> The polymer containing NLO chromophores must first be converted into thin films by spincoating on conductive substrates. Then, by heating the film close to its glass transition temperature ( $T_g$ ), the material becomes softer, allowing dipoles to increase their mobility. Subsequently, an electric field is applied and the chromophores in the matrix can reorient towards the electric field. After some time the temperature can be decreased until below the  $T_g$  of the material, while keeping the orienting field applied, eventually resulting in an acentric ordered lattice. Other used orientation methods include non-centrosymmetric

crystallization,<sup>10</sup> Langmuir-Blodgett-film formation,<sup>11</sup> layer-by-layer growth on solid supports,<sup>12-14</sup> liquid crystals,<sup>15</sup> and incorporation of chromophores into inclusion compounds (supramolecular alignment).<sup>16</sup>

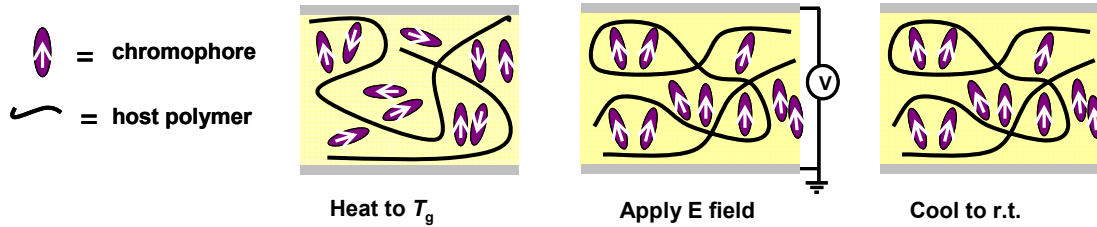


**Figure 1.** Schematic representation of the electric field poling process.

Electro-optic activity arises from the ability of a material to change its refractive index upon application of an external electric field. Since the refractive index relates with the speed of the light transiting a material, electro-optic activity can be defined as a voltage-controlled phase shift of light. Therefore, the application of an electric field will cause a change in the charge distribution in the material (change of mixing of ground and excited forms) and thus alter the speed of light propagating through the material. In case of Boltzmann distributed chromophores, the macroscopic electro-optic activity ( $r_{33}$ ) of the material is given by:

$$r_{33} = \frac{2N\beta f(\omega)\langle \cos^3 \theta \rangle}{n^4} \quad \text{Eq. 3}$$

where  $N$  is the chromophore number density,  $f(\omega)$  is a local optical field correction factor from the dielectric nature of the environment surrounding the chromophore,  $n$  is the refractive index, and  $\langle \cos^3 \theta \rangle$  is the order parameter. If electrostatic interactions between chromophores are neglected, the order parameter in eq. 3 can be expressed as:

$$\langle \cos^3 \theta \rangle = \frac{\mu F}{5kT} \quad \text{Eq. 4}$$



where  $k$  is the Boltzmann's constant,  $T$  the poling temperature,  $\mu$  the dipole moment of the chromophore, and  $F (= f_0 E_p)$  the electric poling field felt by the chromophore. By combining eqs. 3 and 4, the EO coefficient becomes:

$$r_{33} = \frac{2N\mu\beta f(\omega)f(o)E_p}{5kTn^4} \quad \text{Eq. 5}$$

A variety of techniques is being employed to measure the EO activity,  $r_{33}$ , including ellipsometry,<sup>17,18</sup> attenuated total reflection (ATR),<sup>19</sup> and two-slit interference modulation.<sup>20</sup>

From eq. 5 it is clear that for a given  $\mu\beta$  chromophore the EO activity can be maximized either by increasing the poling field strength  $E_p$ , or by increasing the chromophore loading (concentration) in the polymer matrix. However, this linear relationship is only valid at low chromophore concentration, where  $\langle \cos^3 \theta \rangle$  and  $N$  are independent. Differently, at higher concentrations, intermolecular electrostatic interactions among dipoles cannot be neglected, and the relationship between  $\langle \cos^3 \theta \rangle$ ,  $N$ , and  $E_p$  becomes more complex. Therefore, in order to achieve the maximum EO activity the product  $\langle \cos^3 \theta \rangle N$  has to be optimized.

### 2.3 Applications of EO Materials

During the past two decades, great efforts have led to a good fundamental knowledge of the relationship between chemical structure and NLO properties, and thus to the production of materials with ever increasing performances. Based on these advances, several devices incorporating polymeric electro-optic materials have been fabricated for different types of applications including electrical to optical signal transduction, optical switching in local area networks (LANs), millimeter wave signal generation, optical beam steering (for addressing phosphors in flat panel displays), backplane interconnections for high speed personal computers or wavelength division multiplexing (WDM).<sup>3,5</sup> Among all these devices, electro-optic modulators play a fundamental role in

many growing areas of broadband telecommunication and increase the diffusion of multimedia services such as high quality cable television, telephone, real-time video conferencing, telemedicine, distance learning, video-on-demand, and ultra fast internet.

A simple device configuration for light modulation based on a second-order NLO phenomenon is the Mach-Zehnder interferometer (MZ), which acts as an electrical to optical switch (Figure 2).

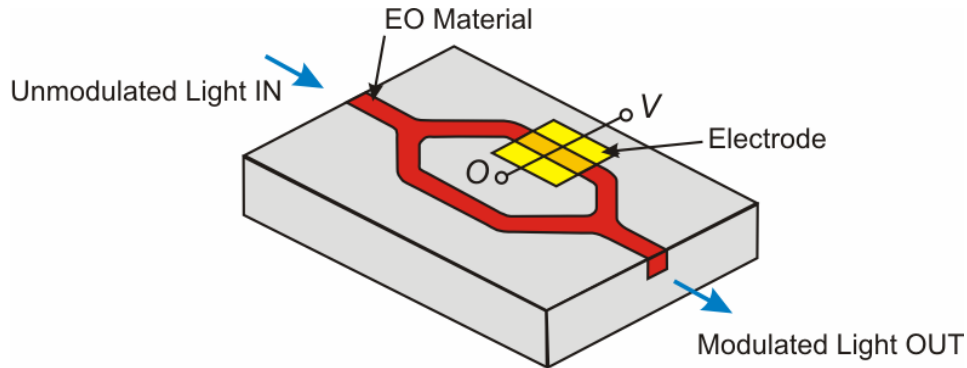


**Figure 2.** Schematic representation of a Mach-Zehnder (MZ) modulator.

If no electric field is applied, the input light is split into two beams propagating in separate arms of the MZ modulator to then recombine at the end of the Y-junction ('on'-position). By applying an electric field of a proper intensity to one arm, the refractive index of this channel will change, resulting in a phase retardation of  $\pi$  relative to the signal traversing the other arm and thus to destructive interference ('off'-position). Using this principle, the MZ modulator can transduce the applied electrical signal onto the optical beam as an amplitude modulation.

The relative phase shift  $\Delta\phi$  of light passing through an electro-optic material when an electric field is applied is given by eq. 6, where  $n$  is the material refractive index,  $r$  its EO coefficient,  $L$  the propagation length (waveguide length),  $E$  the strength of the applied electric field, and  $\lambda$  is the operation wavelength.

$$\Delta\phi = \frac{\pi^3 r L E}{\lambda} \quad \text{Eq. 6}$$

The minimum voltage required for a  $\pi$  phase shift, called half-wave voltage  $V_\pi$ , can be expressed as:

$$V_\pi = \frac{\lambda h}{n^3 r L \Gamma} \quad \text{Eq. 7}$$

where  $h$  is the electrode spacing and  $\Gamma$  the overlap integral of the electrical and optical wave (close to 1).

## 2.4 Material Requirements

In 2000, an encouragingly low half-wave voltage  $V_\pi$  of 0.8 V has been achieved in a polymer waveguide modulator using highly nonlinear organic chromophores.<sup>21</sup> This breakthrough, together with a more recent demonstration of a device with exceptional bandwidths (up to 200 GHz)<sup>22</sup>, has provided a solid foundation for applying polymeric EO materials in the future generations of telecommunication networks.

However, apart from large nonlinearities, many other essential parameters, including a good thermal and photochemical stability, low optical loss (high transparency) and good processability, need to be simultaneously optimized in order for the active material to be incorporated in a practical device.

In order for the non-linear optical response to be stable during processing and operation of chromophore/polymer materials, the chromophores need to be chemically stable at all temperatures that the system encounters in electric field poling, and should withstand the fabrication steps needed for device fabrication. Usually, during device processing the temperature can rise up to 250 °C, while during operation the material is subject to temperatures around 100 °C for long periods of time.

Moreover, after removal of the poling field, the electro-optical response of the material should be stable over time. For this reason the glass transition temperature ( $T_g$ ) of the polymer should be high enough in order for the chromophore acentric order to be kept frozen over device operation.

EO devices are expected to be operational for several years. Therefore chromophores should possess a sufficient photostability to withstand a high intensity illumination for long periods of time, without structural degradation, resulting in a loss of non-linearity.

Optical loss of chromophore-containing materials is a key performance parameter in EO devices. In general, EO polymers must possess a good optical transparency at datacom wavelengths (840 nm) and telecom wavelengths (1310 and 1550 nm). Optical loss can be due either to vibrational absorption or to electronic absorption. Vibrational absorption is mainly due to the C-H overtones coming from the polymer backbone (especially at low chromophore loadings), while electronic absorption is mainly caused by the charge transfer (HOMO-LUMO) band of the chromophores. High- $\beta$  red-shifted chromophores could cause some long-wavelength tailing at operative wavelength.<sup>23</sup> In general, the optical loss due to chromophore absorption should remain below 1 dB/cm.<sup>24</sup> Moreover, both the chromophores and the host polymer must exhibit a good solubility in spin-casting solvents in order to be converted in optical quality thin films.

## 2.5 Chromophore Design

In general, second-order NLO materials can be considered as dipolar chromophores non-centrosymmetrically aligned in poled polymers. Therefore, the most intuitive way of achieving a large bulk EO response is by optimizing the molecular first hyperpolarizability  $\beta$  of the active component. For organic molecules,  $\beta$  is generally determined in solution, using methods such as electric-field induced second harmonic generation (EFISH)<sup>25,26</sup> or hyper-Rayleigh scattering (HRS).<sup>27,28</sup> Commonly used figures of merit for comparing chromophores are  $\mu\beta$  or  $\mu\beta/M_w$  ( $M_w$  is the chromophore molecular weight).

Oudar and Chemla proposed a simple two-state quantum mechanical model as a powerful tool to predict the molecular first hyperpolarizability  $\beta$  in the design of second-order NLO chromophores<sup>29</sup>:

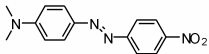
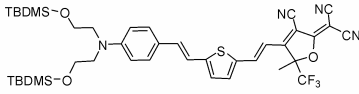
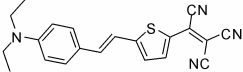
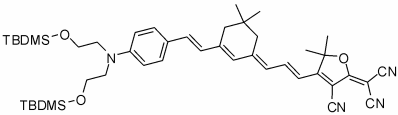
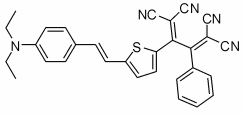
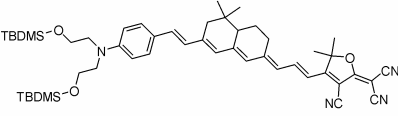
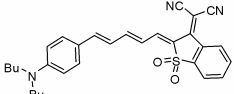
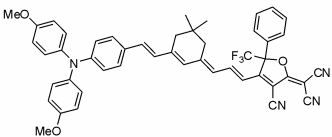
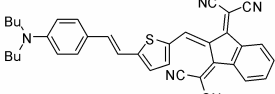
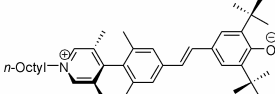
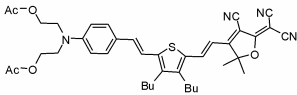
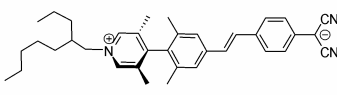
$$\beta = (\mu_{ee} - \mu_{gg})(\mu_{ge})^2 / (\Delta E_{ge})^2 \quad \text{Eq. 8}$$

where  $(\mu_{ee} - \mu_{gg})$  is the difference between the dipole moments of excited and ground state,  $\mu_{ge}$  the transition dipole moment (transition matrix element between ground and excited state), and  $\Delta E_{ge}$  the HOMO-LUMO energy gap. In the early 1990's, based on this model, Marder *et al.* developed a structure-function relationship that illustrates how  $\beta$ , for a given conjugation bridge, can be maximized through an optimal combination of donor and acceptor strengths, which can be viewed as tuning the degree of mixing between the neutral and the charge separated form.<sup>30,31</sup> They have shown that, by structural modifications of donor-acceptor polyenes,  $\beta$  increases in a sinusoidal manner with molecular parameters like the bond length alternation (BLA), which is defined as the average of the difference between carbon single and double bond lengths in the conjugated chromophore core. For a given conjugation bridge there is an optimal combination of donor and acceptor strengths to maximize the molecular first hyperpolarizability, and a further increment of the strength will only reduce  $\beta$ .

Quantum mechanical analysis based on these theories has resulted in an incredibly useful tool for designing chromophores with a large molecular hyperpolarizability. Some representative examples of chromophores with an ever improved molecular optical nonlinearity developed over the last decade are reported in Table 1.

The search for new chromophores has focused on the development of various types of acceptor moieties and conjugated bridges. Mainly, all chromophores developed for EO applications contain invariably amine-based donors.<sup>32</sup> Structural modifications have been explored to improve the solubility, and the thermal or photostability of the chromophores. It has been noted that the use of a 4-(diarylamino)phenyl electron donor results in a significant improvement in thermal stability compared to the 4-(dialkylamino)phenyl substituted derivatives.<sup>33-37</sup> A theoretical comparison on aminophenyl and aminothieryl donor systems reported recently, provides a useful guideline for the design of improved NLO chromophores.<sup>32</sup>

**Table 1.**  $\mu\beta$  Values for representative NLO chromophores<sup>a</sup> and  $r_{33}$  values for their guest-host polymers.<sup>b</sup>

NLO chromophore	$\lambda_{max}$ (nm)	$\mu\beta$ ( $10^{-48}$ esu)	NLO chromophore	$\lambda_{max}$ (nm)	$\mu\beta$ ( $10^{-48}$ esu)
	475	580		711	N/A
<b>DR</b>		$r_{33} = 13$ pm/V (30% in PMMA)	<b>AJL-8</b>		$r_{33} = 42$ pm/V (25% in APC)
	640	6200		695	35000
		$r_{33} = 30$ pm/V (25% in PI)	<b>CLD</b>		$r_{33} = 92$ pm/V (25% in APC at 1.06 $\mu$ m)
	604	N/A		N/A	N/A
<b>Ph-TCBD</b>		$r_{33} = 36$ pm/V (25% in PQ100)	<b>GLD</b>		$r_{33} = 105$ pm/V (17.5% in PMMA)
	770	13500		770	N/A
		$r_{33} = 55$ pm/V (20% in PC)			$r_{33} = 106$ pm/V (25% in APC)
	770	6100		462	-315000
<b>TCI</b>			<b>TM-2</b>		
	650	18000		540	-488000
		$r_{33} = 57$ pm/V (20% in PMMA at 1.06 $\mu$ m)	<b>TMC-3</b>		$r_{33} = 330$ pm/V (10% in PVP)

<sup>a</sup> Measured at 1907 nm; <sup>b</sup> Measured at 1,3  $\mu$ m, otherwise indicated)

Although very large hyperpolarizabilities have been obtained with long and unprotected polyene bridges, these materials are chemically and photochemically unstable or it is impossible to prepare them in adequate yield and purity, and therefore they are not suitable for practical applications. On the other hand, chromophores based on fused ring systems, like naphthalene benzimidazoles,<sup>38</sup> or phthalocyanines<sup>39,40</sup> possess a good nonlinearity and thermal stabilities over 350 °C, but they are poorly soluble in spincoating solvents and they cannot be effectively poled.

Improvements in thermal and photochemical stability have been achieved by using conformationally locked polyenes<sup>41,42</sup> by incorporating the polyene chain into ring systems like isophorone<sup>43</sup> or by introducing heterocyclic conjugating units such as thiazole,<sup>44</sup> furan, and thiophene.<sup>45</sup> Many studies have investigated the role of heteroaromatics and clarified the effect of the nature and the location of the heterocyclic ring on the charge-transfer (CT) transitional energies of the chromophores, leading to the development of the ‘auxiliary donor and acceptor’ model.<sup>46-48</sup> This theory correlates the molecular hyperpolarizability  $\beta$  with the electron density of the  $\pi$  conjugation, arguing that electron-excessive/deficient heterocyclic bridges act as auxiliary donors/acceptors giving larger  $\beta$  values.

Many different acceptor groups have been investigated. Very large nonlinearities have been achieved using for instance, nitro, cyanovinyl, thiobarbituric acid moieties<sup>49</sup>, or strong multicyano-containing heterocyclic electron acceptors.<sup>35,50-52</sup>

Highly hyperpolarizable chromophores have been reported using the tricyanovinyl (TCV) moiety as electron acceptor and various conjugating moieties ( $\mu\beta$ , as high as  $9800 \times 10^{-48}$  esu).<sup>53</sup> However, the TCV group is very sensitive to chemical attack. To overcome this, Jen *et al.*<sup>54</sup> prepared a series of thermally and chemically stable chromophores containing a 2-phenyl-tetracyanobutadienyl acceptor (Ph-TCBD), which have been demonstrated to be much more stable toward amine nucleophiles than their tricyanovinyl counterparts. An enormous progress has been achieved since the introduction of the tricyano-derivatized furan (TCF) acceptor in the late 90’s.<sup>55-57</sup> Its incorporation in chromophores such as **FTC**, **CLD**, and **GLD** (Table 1) resulted in chromophore figures-of-merit,  $\mu\beta$ , as high as  $35\,000 \times 10^{-48}$  esu.<sup>21</sup> Moreover, these

chromophores display a good solubility in spin casting solvents, a good processability, and a thermal stability of approximately 300 °C.

More recently, Marks *et al.* developed a totally different approach for obtaining very high  $\beta$  values. Their strategy does not focus on extensive planar  $\pi$  conjugation, which is prone to chemical, thermal and photochemical instabilities,<sup>58</sup> but on twisted  $\pi$ -electron system chromophores. Such unconventional twisted  $\pi$  zwitterionic structures (**TM** and **TMC**) exhibit unprecedented hyperpolarizabilities as large as  $15 \times$  higher than reported previously ( $\mu\beta$  as high as  $-488\,000 \times 10^{-48}$  esu).<sup>59,60</sup>

## 2.6 Guest-Host Systems

Guest-host systems have been the first NLO polymer systems investigated, since they can be easily obtained by simply dissolving an EO chromophore in a compatible amorphous polymeric matrix, to form a solid solution. The selection of polymer host should be based on a good optical transparency, high thermal stability, and good solubility in spin casting solvents. In order to obtain a high EO response, the chromophore should be able to dissolve in the polymer matrix at high loadings, without phase separation to occur. A high  $T_g$  polymer is desirable in order to maintain the electrical induced noncentrosymmetric order stable over time at device operating temperatures. Although the  $T_g$  of commonly used host polymers is 150-250 °C, the incorporation of a chromophore will induce plasticization, considerably lowering the  $T_g$  of the composite material, and therefore reducing the temporal stability of the EO response.

A number of different chromophores has been investigated in various low- $T_g$  polymer lattices, such as polycarbonate (PC) or poly(methyl methacrylate) (PMMA), obtaining very large EO coefficients. An  $r_{33}$  value of 21 pm/V at 1.06  $\mu\text{m}$  was achieved by Sun *et al.* in PMMA thin films doped at 30-40 wt% with a strong heteroaromatic electron-acceptor chromophore.<sup>51</sup> A polycarbonate film, containing 20 wt% of a highly NLO-active compound yielded a very large  $r_{33}$  value of 55 pm/V at 1.06  $\mu\text{m}$ .<sup>50</sup> However, the limited thermal stability of these materials, suggested the use of high- $T_g$  polymers such as



polyimides<sup>61,62</sup> and polyquinolines.<sup>63,64</sup> On the other hand, since the chromophore is not covalently connected to the polymer backbone, it can sublime out of the blend when high poling and processing temperatures are required. Much improved long-term stabilities at elevated temperatures have been obtained using highly thermally stable chromophores such as **Ph-TCBD**, incorporated as a guest (20 wt%) in the rigid-rod polyquinoline PQ-100 ( $T_g = 265$  °C). An  $r_{33}$  value of 36 pm/V was recorded at 1.3  $\mu\text{m}$  after poling, which remained at ~80% of its original value at 85 °C for over 1000 h.<sup>54</sup>

Recently, a very large EO coefficient ( $r_{33} = 169$  pm/V at 1.3  $\mu\text{m}$ ) and an excellent long-term alignment stability at 85 °C under vacuum for more than 500 h have been demonstrated by incorporating a large  $\mu\beta$  chromophore bearing a 2-dicyanomethylidene-3-cyano-4,5-dimethyl-5-trifluoromethyl-2,5-dihydrofuran ( $\text{CF}_3$ -TCF) electron acceptor into PQ-100 as a guest (25 wt%).<sup>64</sup>

Together with the development of highly NLO active molecules like **CLD** and **FTC**, amorphous polycarbonate (APC) has been extensively investigated as a host polymer, due to its low crystallization tendency, good solubility in halogenated solvents and high glass transition temperature ( $T_g = 205$  °C). Its good compatibility with large  $\mu\beta$  chromophores, and its high dielectric constant allow EO coefficients as large as 92 pm/V (25 % **CLD-1**/APC composite, at 1.06  $\mu\text{m}$ ) to be routinely obtained. Mach-Zehnder (MZ) modulators fabricated from **CLD-1**/APC showed a good thermal stability at 50 °C, an optical loss of 1.7 dB/cm, and a low modulation voltage ( $V_\pi$ ) of 3.7 V.<sup>65,66</sup> EO modulators have also been fabricated from 30% **CLD-1**/PMMA material, demonstrating a  $V_\pi$  value of 0.8 V.<sup>21</sup> However, due to the low  $T_g$  of this composite, the dynamic thermal stability of poling induced alignment was only 75 °C, 40 °C lower than for the corresponding APC material. More recently, really large  $r_{33}$  values (as high as 169 pm/V at 1.31  $\mu\text{m}$ ) have been recorded for a series of thermally stable chromophores with a 4-(diaryl-amino)phenyl donor and a strong  $\text{CF}_3$ -TCF electron acceptor incorporated at 25 wt% in APC.<sup>67</sup>

Furthermore, Garner *et al.*<sup>68</sup> demonstrated the practicality of using polysulfone as a novel host material. A chromophore-polysulfone system showed a similarly high EO performance and a lower  $V_\pi$  value, compared to the analogous polycarbonate system.

Moreover, this material combines a reasonably high  $T_g$  of 190 °C and a high refractive index of 1.63 and is a better host than polycarbonate with respect to the photostability.<sup>69</sup>

Very recently, it has been reported that a guest-host system, consisting of twisted  $\pi$ -zwitterionic chromophores **TM** and **TMC** in polyvinylphenol (PVP), provided very large EO responses ( $r_{33}$  as high as 330 pm/V at 1.31  $\mu\text{m}$ ; 10 wt% ), 3-5  $\times$  greater than ever reported.<sup>59</sup>

## 2.7 Side-Chain Systems

Differently than for guest-host systems, in side-chain polymers the NLO chromophores are covalently attached to the polymer backbone, rather than being simply dissolved into it. These systems have the advantage that high chromophore loadings (and therefore high NLO responses) can be obtained, without phase separation, crystallization or chromophore sublimation. In general, the glass transition temperatures of side-chain polymers are considerably higher than of a guest-host system with comparable chromophore loading (no plasticization effect occurs).<sup>70</sup> Therefore an improved thermal and temporal stability of the poled order is observed, since the chromophore rotational freedom is restricted by the chemical connection to the polymer.

Many different NLO chromophore-functionalized polymers have been investigated, including polymethacrylates, polystyrenes, poly(acrylamides), polyurethanes, polyquinolines, polyesters, polyethers, and polyamides.<sup>4,70,71</sup> In the next sections, more attention will be paid to high- $T_g$  polyimides.

### 2.7.1 Polyimides

NLO chromophore-functionalized polyimides have attracted a lot of interest thanks to their high  $T_g$  and excellent temporal stability. Verbiest<sup>72,73</sup> and Miller<sup>74</sup> *et al.* reported several highly stable aromatic polyimides (Figure 3) including the synthesis of the **PI-1** polymer, which is the first reported example of a processable “donor-embedded” side-chain polyimide having a very high  $T_g$  of 350 °C, and a chemical stability at temperatures as high as 350 °C. Poled samples of polymer **PI-1** have an EO coefficient of 4-7 pm/V (at

1.3  $\mu\text{m}$ ) and a much higher orientational stability (up to 225  $^{\circ}\text{C}$ ) compared with a true side-chain polyimide (**PI-2**) in which a similar chromophore is covalently linked to the polymer backbone by a flexible spacer.

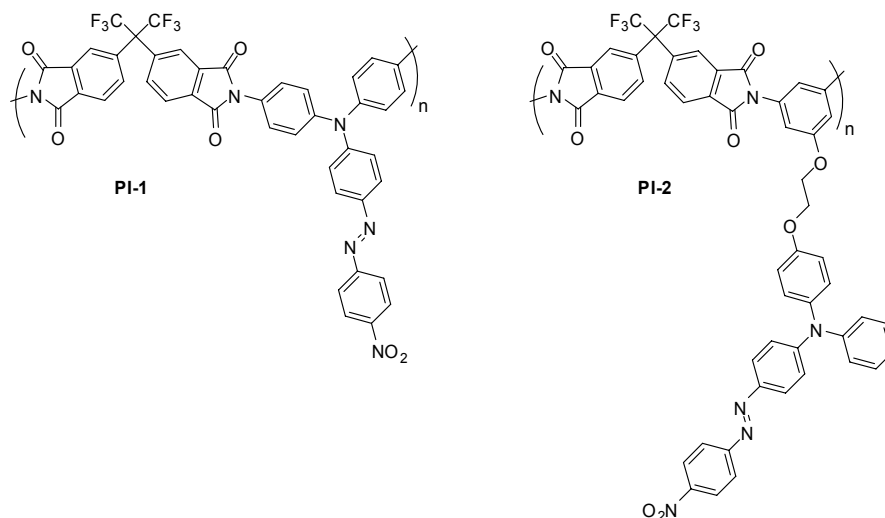


**Figure 3.** Processable polyimides **PI-1** and **PI-2**.

Davey *et al.* reported a general, convergent approach for the synthesis of protected diamine NLO chromophores, which allows of both acid- and base-sensitive chromophores to be incorporated, using either alkaline or acidic deprotection, into polyimide backbones.<sup>75</sup> The obtained chromophores have been condensed into two types of high- $T_g$ /high thermal stability polyimide chain structures (Figure 4). The polymers based on the more rigid 6F-subunit (**PI-3a-c**), exhibit  $T_g$  values in excess of 300  $^{\circ}\text{C}$ , however, due to the lower inherent mobility, they do not show high nonlinearities ( $\chi^{(2)} = 16\text{-}48$  pm/V). In contrast, polyimides based on the more flexible TMEG-DA subunit (**PI-4a-c**), containing the same chromophore, have lower  $T_g$ s (225-265  $^{\circ}\text{C}$ ), but an increased NLO response ( $\chi^{(2)} = 44\text{-}82$  pm/V), due to the greater structural mobility and poling efficiency.

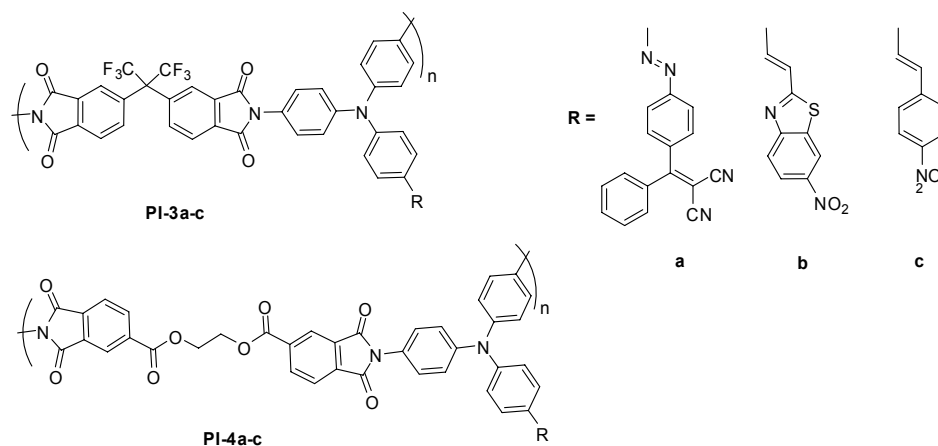


**Figure 4.** Polyimides **PI-3a-c** and **PI-4a-c**.

However, the synthetic methods for aromatic side-chain polyimides include tedious procedures and the fact that not all chromophores can survive to the harsh imidization conditions limits their application. To alleviate this problem, Chen *et al.* developed a two-step, generally applicable synthetic approach for the synthesis of NLO side-chain aromatic polyimides, which consists of a one-pot preparation of a preimidized, hydroxyl-containing polyimide, followed by covalent attachment of a chromophore onto the backbone of the polyimide via a post-Mitsunobu reaction.<sup>76</sup> Using this facile methodology, NLO side-chain polyimides with a wide variety of pendant NLO chromophores have been synthesized (**PI-5a-c**, Figure 5) with fine control of the chromophore loading. The resulting NLO polyimides possess high  $T_g$ s ( $> 200$  °C), large EO coefficients (up to 34 pm/V at 0.63  $\mu\text{m}$  and 11 pm/V at 0.83  $\mu\text{m}$ ), and a long term stability of the dipole alignment ( $> 500$  h at 100 °C).

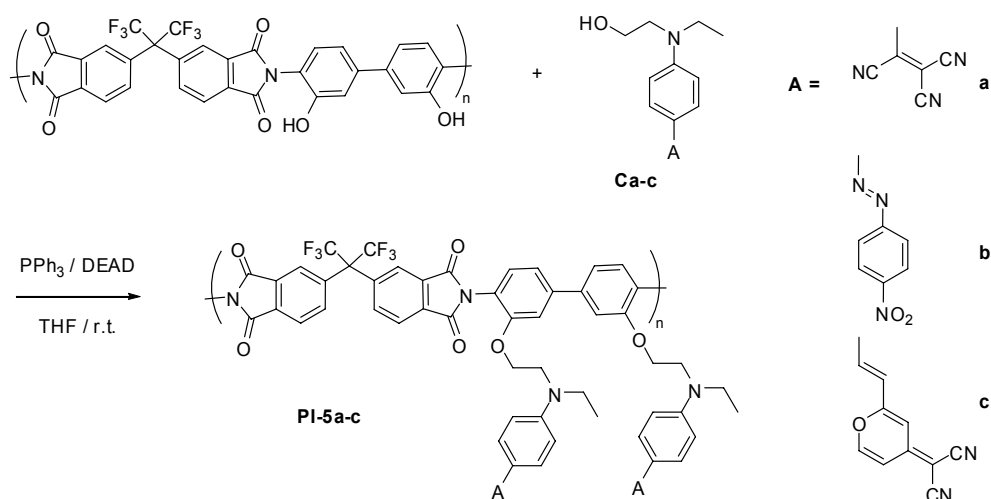


**Figure 5.** Synthesis and structures of polyimides **PI-5a-c**.

A new synthetic method for the effective attachment of a wide variety of chromophores, even highly active ones such as **FTC** and **CLD**, to polyimide backbones has recently been developed by Wright<sup>77</sup> and Guenther *et al.*<sup>78</sup> They have shown that the benzyl alcohol pendant group in the polymers can be chemically modified with a bis-functional linking agent, like bis(isocyanates) or bis(acid chlorides), to afford reactive side-chain polyimides. The reactive isocyanate or acid chloride pendant group can then be easily linked to an alcohol-containing dye (Figure 6). The resulting materials possess  $r_{33}$  values as high as those achieved in guest-host systems (e.g. 60 pm/V at 1300 nm, for a **FTC** functionalized polyimide), whereas having substantially higher  $T_g$ s ( $> 170$  °C), and an enhanced stability of the poling induced order. Mach-Zehnder optical interferometers have been fabricated with polymers that contained **CLD**- and **FTC**-type of chromophores. Their long-term aging performance (for months at four temperatures ranging from ambient to 110 °C) has been determined from the increase of the  $V_\pi$  value of the modulator.<sup>79</sup> Multi-year high-temperature stability was predicted by fitting the data to a newly developed aging model.

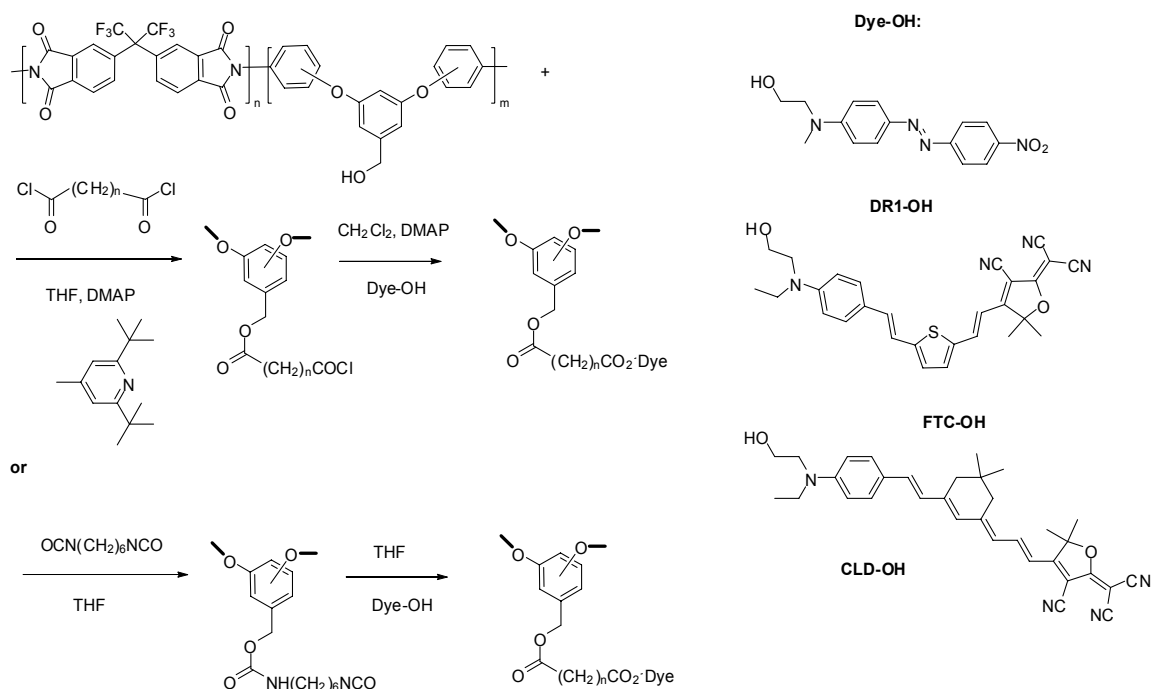


**Figure 6.** Synthesis of high- $\mu\beta$  chromophore functionalized polyimides.

## 2.8 Main-Chain Systems

Another approach to attenuate the poled-order relaxation comprises the use of main-chain polymer systems, in which the chromophores are chemically incorporated in the polymer backbone itself, rather than being attached as pendant groups. The main difference between the main-chain and the side chain approach is that large segmental motion of the polymer backbone is needed for poling and relaxation.<sup>80</sup> Main chain NLO polymers can be divided into three categories (Figure 7): (i) head-to-tail,<sup>81</sup> and (ii) random,<sup>82</sup> where the chromophore dipole moments are pointing along the polymer backbone, and (iii) accordion polymers,<sup>83</sup> where the dipole moments are nearly perpendicular to the main chain.

With the purpose of improving processability, thermal stability, and alignment stability, a wide variety of main-chain chromophoric polymers have been investigated, including polyurethanes,<sup>84</sup> polyimides,<sup>85</sup> polyamides,<sup>86</sup> carbazoles,<sup>87</sup> and polyesters.<sup>88</sup> However, to date most main-chain polymers show relatively poor processabilities (including solubility, poling efficiency, etc) and/or low NLO responses. In addition, the

choice of the chromophores suitable for main-chain incorporation is limited and high loadings are difficult to achieve. For these reasons, the current researches in the NLO polymer field are mainly focused on the side chain and cross-linked type. Therefore, main-chain systems will not be discussed in detail in this review.

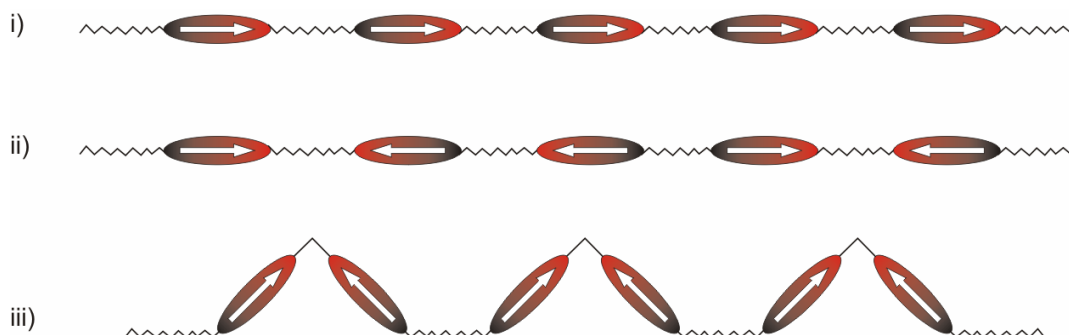


**Figure 7.** Different types of main-chain NLO polymers: (i) Head-to-tail; (ii) random; and (iii) accordion.

## 2.9 Cross-linked Systems

Covalently attaching chromophores to the polymer backbone or incorporating them into the backbone, as described in the sections 7 and 8, can effectively increase the chromophore loading, and prevent phase separation, and thermal relaxation of the chromophore dipole moment. However, such high- $T_g$  materials require high temperature poling, where chromophore decomposition may occur. Moreover, this process lacks in flexibility, since to screen potential host polymers and to vary the polymer/chromophore compositions require tedious batch-to-batch production, which makes it difficult to precisely control the composition and the properties of the final material.

The use of low- $T_g$  cross-linkable materials offers the advantage that the poling process can be conducted at relatively low temperatures during the hardening process, ending up with a high- $T_g$  noncentrosymmetric material. In general, the cross-linking process must not degrade the optical quality of the films, like causing defects and poor uniformity, which could increase the optical loss. The general approaches to lattice hardening are: (i) photo-induced crosslinking, and (ii) thermally-induced crosslinking.<sup>89</sup> Photo-induced crosslinking has the advantage that the lattice hardening process can be

completely separated from the temperature-dependent poling process. However, the UV or visible light applied to activate the photo-initiator could be preferably absorbed by the NLO chromophore, making the exposure ineffective and promoting chromophore degradation. This drawback has so far limited this development, hence thermally-induced cross-linking has been applied more widely.<sup>9</sup>

Since lattice hardening and poling are both temperature dependent processes, fine tuning of the conditions should be done to simultaneously achieve a high poling efficiency and a high  $T_g$ . Increasing the temperature permits a higher chromophore mobility to reorient along the poling field. It also antagonistically drives the hardening process, hence reducing the mobility. On the other hand, the application of a too high electric field to a soft film can result in material breakdown. This often leads to a trade-off between poling efficiency and material stability. Thus optimum conditions can be achieved using stepped poling protocols (where temperature and electric field are increased in a series of steps).<sup>90</sup>

Different thermally-induced cross-linking approaches have been investigated, like the formation of sol-gel networks,<sup>91,92</sup> or reactions resulting in polyimides<sup>93</sup> and maleimides.<sup>94</sup> Thermoset polyurethanes (PU) have been widely studied for EO applications.<sup>90,95</sup> Zhang *et al.* synthesized a high  $\mu\beta$  derived isophorone-derived phenyltetraene chromophore (**CLD-5**) modified with a hexyl group at the middle of the  $\pi$ -conjugate bridge to improve the solubility and two hydroxyl terminal groups for covalent incorporation into cross-linked PU polymer systems.<sup>96</sup> The chromophore was incorporated into a PU matrix based on triethanolamine (TEA) and toluene-2,4-diisocyanate (TDI) and, after curing and poling, an EO coefficient of 57.6 pm/V at 1.06  $\mu\text{m}$  and a dynamic stability till about 80 °C was obtained for the resulting material. By using more rigid monomeric cross-linkers, the thermal stability could be enhanced up to 133 °C. This gain, however, does not come without a sacrifice in the EO activity. In addition, from a study on the cross-linking density it is clear that excessive cross-linking is harmful to electrical poling of a polyurethane material and that cross-linking by itself is not enough to provide a very high thermal stability of electrical field-induced chromophore alignment.



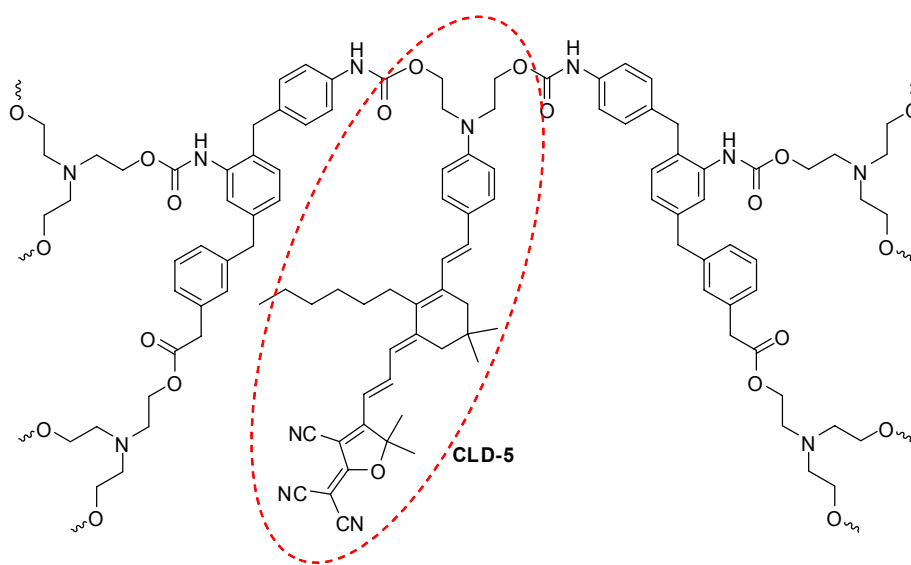


**Figure 8.** Example of a CLD-5 containing polyurethane.

Sol-gel and PU oligomerization reactions require a strict control of the reaction conditions, since atmospheric moisture can negatively influence the reaction, causing phase separation and optical loss. To tackle this problem, a new cross-linking unit, trifluorovinyl ether (TFVE), has been introduced. TFVE-containing monomeric units can be converted into perfluorocyclobutane (PFCB) containing polymers by a radical-mediated thermal cyclopolymerization reaction. These polymers have excellent properties such as a low dielectric constant, good thermal stability, and optical transparency.<sup>97</sup>

A new synthetic strategy for incorporating a wide variety of NLO chromophores into PFCB polymers has been developed by Ma *et al.*<sup>98</sup> The chromophore loading can be tuned by varying the ratio of chromophore-substituted di-TFVE monomer and the tri-TFVE inert monomer. The obtained mixture is then pre-polymerized at 150 °C, spincoated to obtain high quality films, and efficiently cross-linked at 180-250 °C. All resulting NLO PFCB (Figure 9) thermosets possess excellent solvent resistance, large  $r_{33}$  values, and can retain ~80% of their original values at 85 °C for more than 1000 h.

PFCB chemistry, thanks to its versatility, has been applied to different kinds of material architectures including side-chain polymers, NLO-dendrimers, and dendronized polymers, as will be described in the next section.

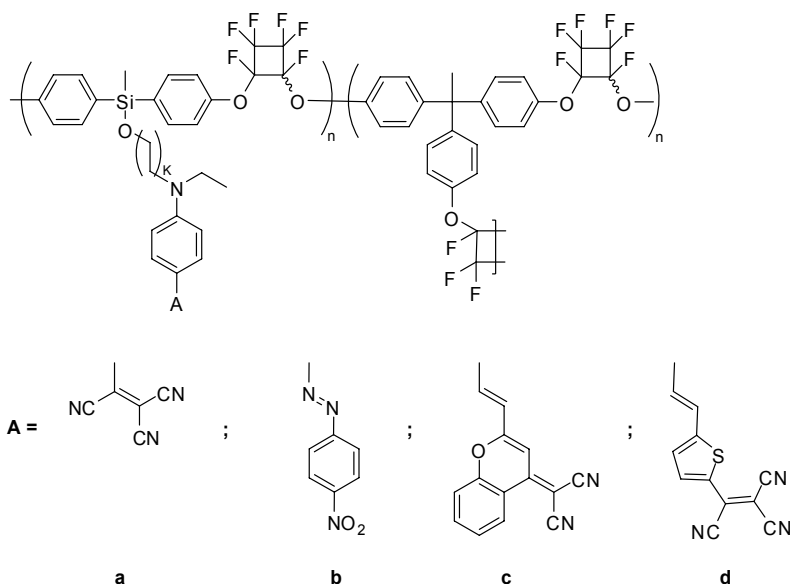


**Figure 9.** Structures of the PFCB polymers.

More recently, another lattice hardening approach has been demonstrated using the thermally-reversible Diels-Alder [4+2] cycloaddition reaction (Figure 10) to provide significant advantages over the conventional NLO thermosets, such as high poling efficiency and fine-tuning of the processing temperatures.<sup>99,100</sup> This procedure has mainly been applied to obtain NLO dendrimers and dendritic polymers, which are described in the next sections.

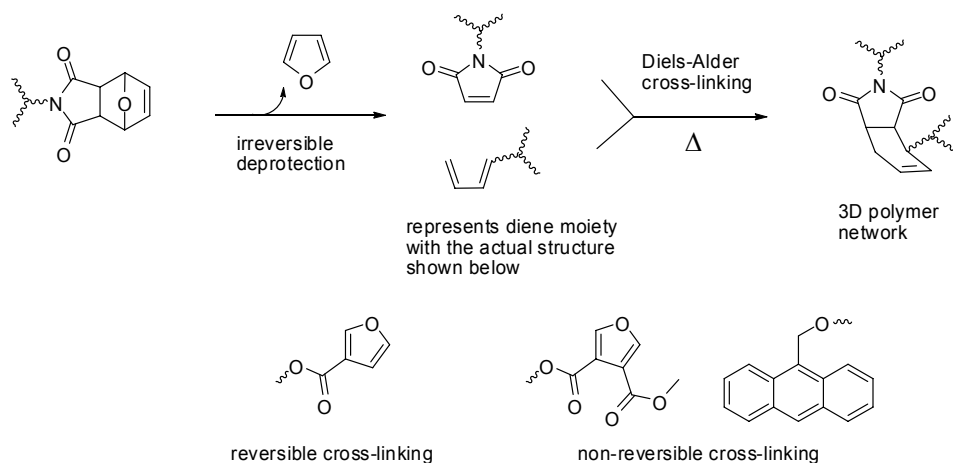


**Figure 10.** Representation of the Diels Alder cross-linking reactions.

## 2.10 Dendritic Systems

In the past decade, much effort has been made to develop polymeric materials possessing simultaneously large EO coefficients, high thermal and photostabilities, and low optical losses, which could be suitable for incorporation into practical EO devices. One major obstacle that limits the development in this area is to efficiently translate high non-linearities into large macroscopic EO activities. In fact, although the  $\mu\beta$  values of chromophores have been improved more than 250-fold, only several times of enhancement of the  $r_{33}$  value could be achieved. From the ideal-gas model, the EO coefficient should increase linearly with the chromophore number density (loading) in the polymer matrix, making a  $r_{33}$  of several hundreds of pm/V theoretically obtainable.<sup>101</sup> However, molecules with large dipole moments, cannot be treated as non-interacting, and strong intermolecular dipole-dipole interactions, especially at high chromophore loading levels, become competitive with the poling induced non-centrosymmetric alignment.<sup>102-</sup>  
104

Recently, theoretical and experimental results by Robinson *et al.* demonstrated that a logical approach to improve the maximum achievable EO activity is to modify the shape of the chromophores by introducing bulky substituents.<sup>105</sup> Derivatization of chromophores with these inert groups makes them more spherically shaped, limiting intermolecular electrostatic interactions and hence antiparallel clustering, therefore enabling higher poling efficiency. Disappointingly, only a slight increase of the  $r_{33}$  could be achieved using this method.

Chromophore-containing dendritic structures have emerged as an alternative solution to achieve spherical shape modification of chromophores.<sup>106</sup> In spite of any conventional EO polymer, the void containing structure of dendrimers provides the site isolation needed for chromophores to independently reorient under the external poling field.<sup>107</sup> Moreover, these dendritic materials possess a monodisperse and well defined globular geometry. Their structure is synthetically controllable in size and shape, allowing wide control over solubility, processability, viscosity, and stability.

### 2.10.1 3D-shaped Dendritic NLO Chromophores

One of the very first examples of the spontaneous, non-centrosymmetric organization of NLO chromophores in dendritic structures has been reported by Yokoyama *et al.*<sup>108</sup> They studied the conformational and NLO properties of a series of azobenzene-containing dendrons, synthesized by introducing 1-15 azobenzene branching units and by placing aliphatic functionalities at the end of the dendritic chains (Figure 11). HRS measurements showed that the synthesized dendrons had a cone-shaped conformation, with each chromophore contributing coherently to the macroscopic EO activity with no need of application of an external field. In fact the  $\beta$  measured for the azobenzene dendron **D1** with 15 chromophoric units was  $3010 \times 10^{-30}$  esu, a value which is more than 20 times larger than that of the individual azobenzene monomer ( $150 \times 10^{-30}$  esu).

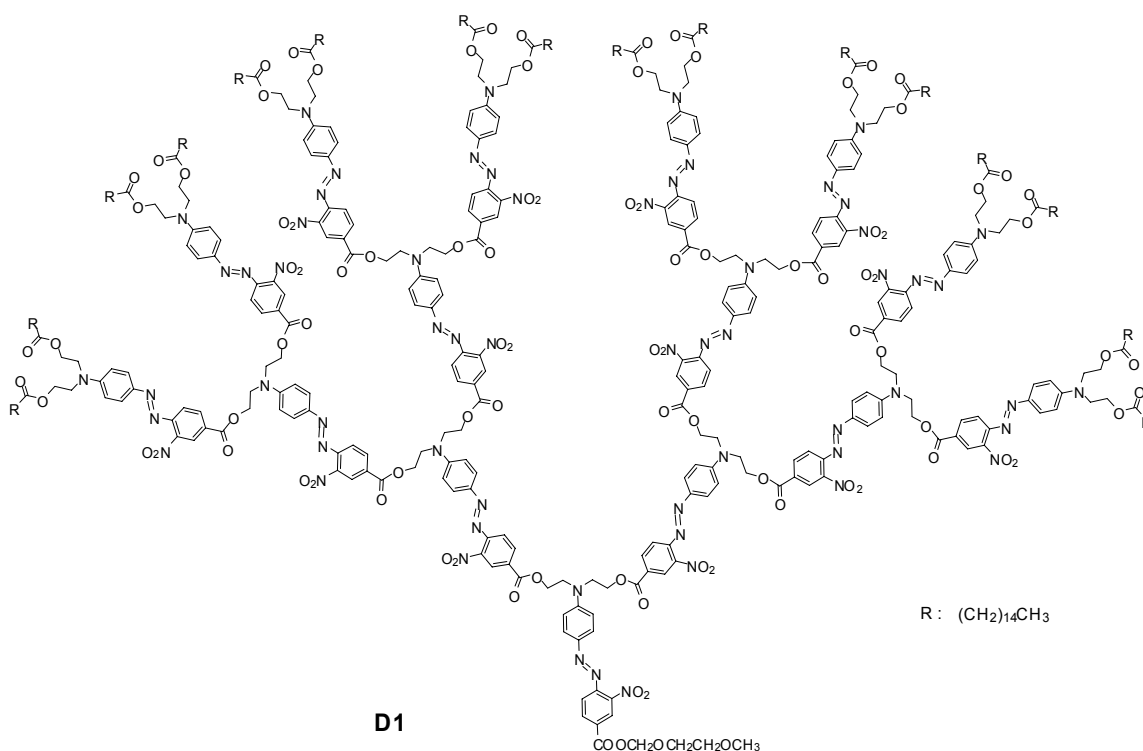


**Figure 11.** Structure of the azobenzene dendron **D1**.

In order to explore the dendritic effect on the poling efficiency of dipolar NLO chromophores, Ma *et al.*<sup>109</sup> modified the highly stable **Ph-TCBD** chromophore with three highly fluorinated aromatic dendrons (Figure 12). In comparison with the pristine

analogue, the resulting dendritic chromophore **D2** exhibits a 20 °C higher decomposition temperature and a large blue shift (29 to 42 nm) of the charge-transfer absorption maximum ( $\lambda_{\text{max}}$ ), indicating the influence of the fluoro-rich dendrons on the microenvironment of the core chromophore in solid films. When **D2** and **Ph-TCBD** were incorporated with the same amount of active component into APC (12 wt%), the poled films of **D2** showed a three times larger EO coefficient (30 pm/V at 1.3  $\mu\text{m}$ ) than the pristine chromophore, providing a clear evidence of the improved poling efficiency due to the dendrons.

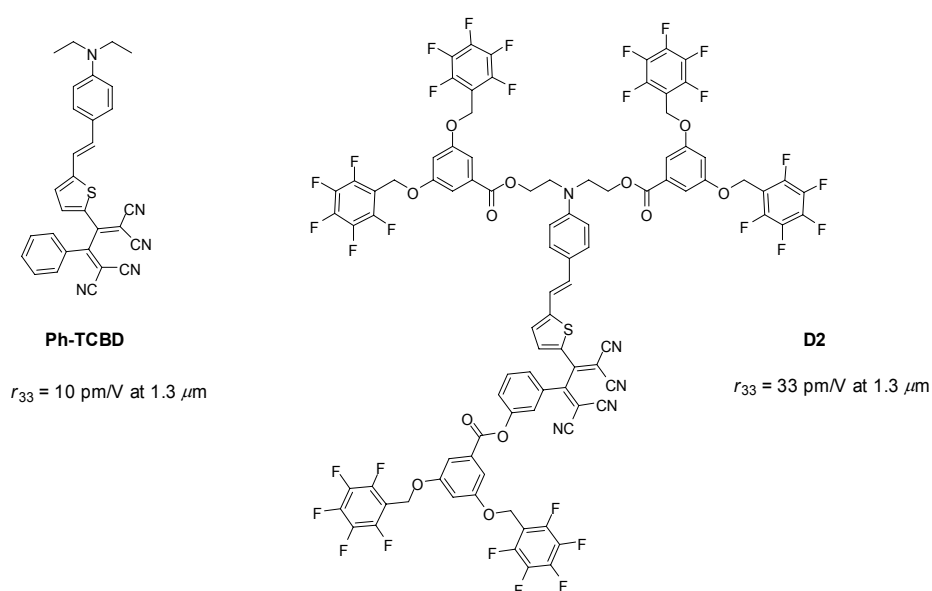


**Figure 12.** Comparison between dendritic chromophore **D2** and its pristine NLO chromophore **Ph-TCBD**.

More recently, Dalton *et al.* investigated the EO properties of tri-functional dendritic chromophores and the effectiveness of theoretical analysis as a guide in the bottom-up design of such molecular architectures.<sup>110</sup> The analyzed structures consisted of three thiophene-containing **FTC**-type chromophores, connected to the tri-branched inert core through flexible spacers. Four tri-arm EO dendrimers were prepared and evaluated to explore the effects on the EO behavior of end-on relative to side-on chromophore attachment geometry as well as varying chromophore-to-dendrimer core tether groups (Figure 13).

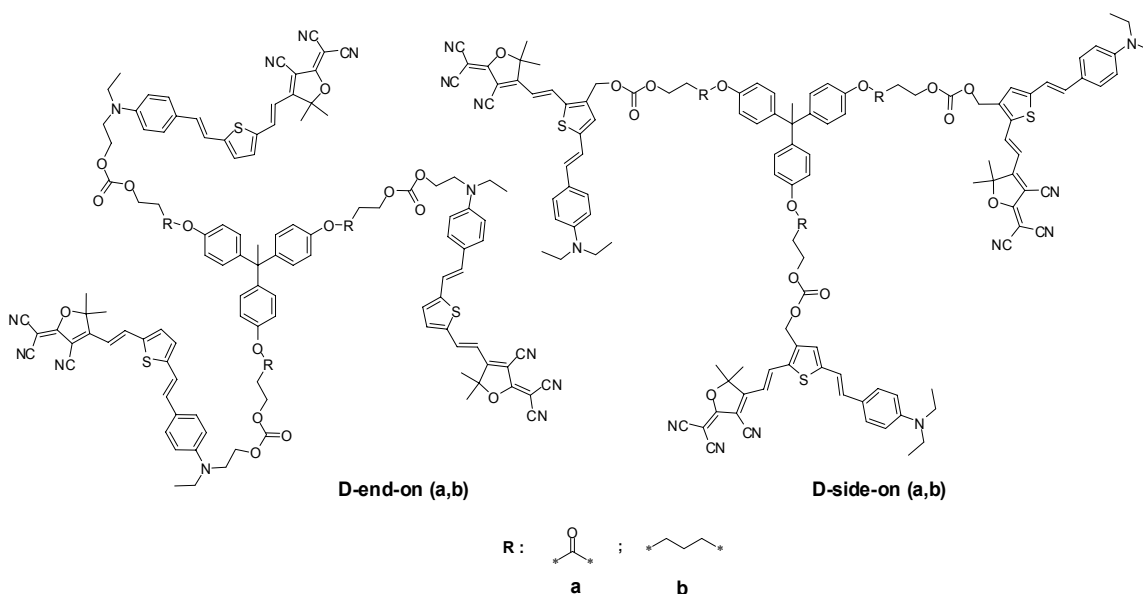


**Figure 13.** Structures of the *FTC*-containing dendrimers.

These dendritic materials were dispersed into APC and tested as thin film composites. The side-on geometry provided a more stable EO signal, requiring larger activation energies to induce dipole randomization than the end-on type. The differences in average  $r_{33}$  between side-on and end-on geometries were small but consistent. The EO behavior depended heavily on the length and rigidity of the moieties used to covalently anchor the chromophore to the inert host or core. A nearly 3-fold enhancement in EO coefficient was noted when the short di-ester tether was replaced by a longer, more aliphatic system, however, a faster thermal decay of  $r_{33}$  was observed.

These experimental findings, together with quantum mechanical modeling, were then employed to guide the design and synthesis of tri-arm dendritic structures with extended outer peripheral functionalities.<sup>111</sup> The resulting materials were used to fabricate stand-alone thin films, without the addition of an inert polymer host. These all-dendrimer films exhibit a high poling efficiency ( $r_{33}/E_p$ ) and a stunning linear relationship between  $r_{33}$  and  $N$ . The linear dependence holds even at very high chromophore concentrations ( $N = 6.45 \times 10^{20}$  chromophores/cm<sup>3</sup>), yielding a maximum EO coefficient of 140 pm/V (at 1.31  $\mu\text{m}$ ).

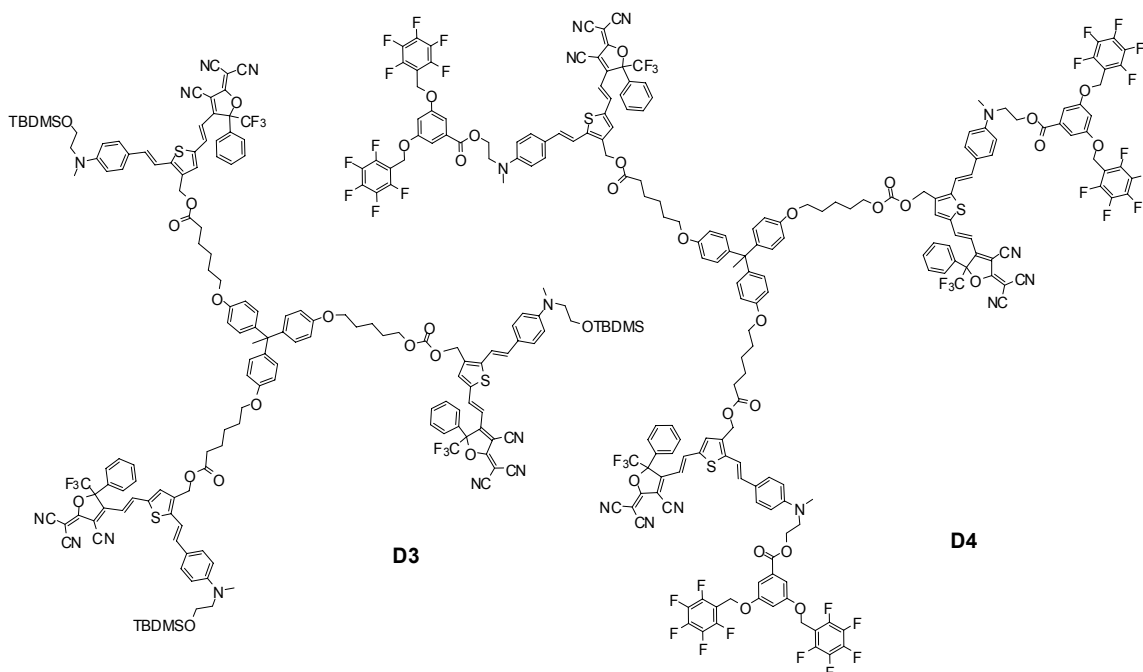


**Figure 14.** Structures of tri-arm EO dendrimers **D3** and **D4**.

### 2.10.2 Crosslinkable NLO Dendrimers

Low molecular weight multichromophore containing dendrimers (described in the previous section) have very large  $r_{33}$  values, which is very promising for next generation EO materials. However, the materials obtained with this approach, have intrinsically low  $T_g$ s, which translates into a poor thermal stability of the poling order, and a low solvent resistance (high solubility in spincoating solvents), which limits their incorporation in multi-layer polymer optical devices.

To alleviate this problem, Ma *et al.* developed a NLO dendrimer, having the center core connected to a **Ph-TCBD**-containing chromophore and thermally cross-linkable TFVE-containing dendrons at the periphery (Figure 15).<sup>112</sup> The resulting dendrimer **D5**, thanks to its relatively high molecular weight (4664 Da), can be directly spin-coated, with no need of a pre-polymerization process. Moreover, this approach offers the advantage that the sequential hardening/crosslinking process can be efficiently conducted during electric field poling, making it possible that large EO coefficients ( $r_{33} = 60$  pm/V at 1.55  $\mu\text{m}$ ) and long-term alignment stability (over 90% at 85 °C for more than 1000 h) can be simultaneously obtained.

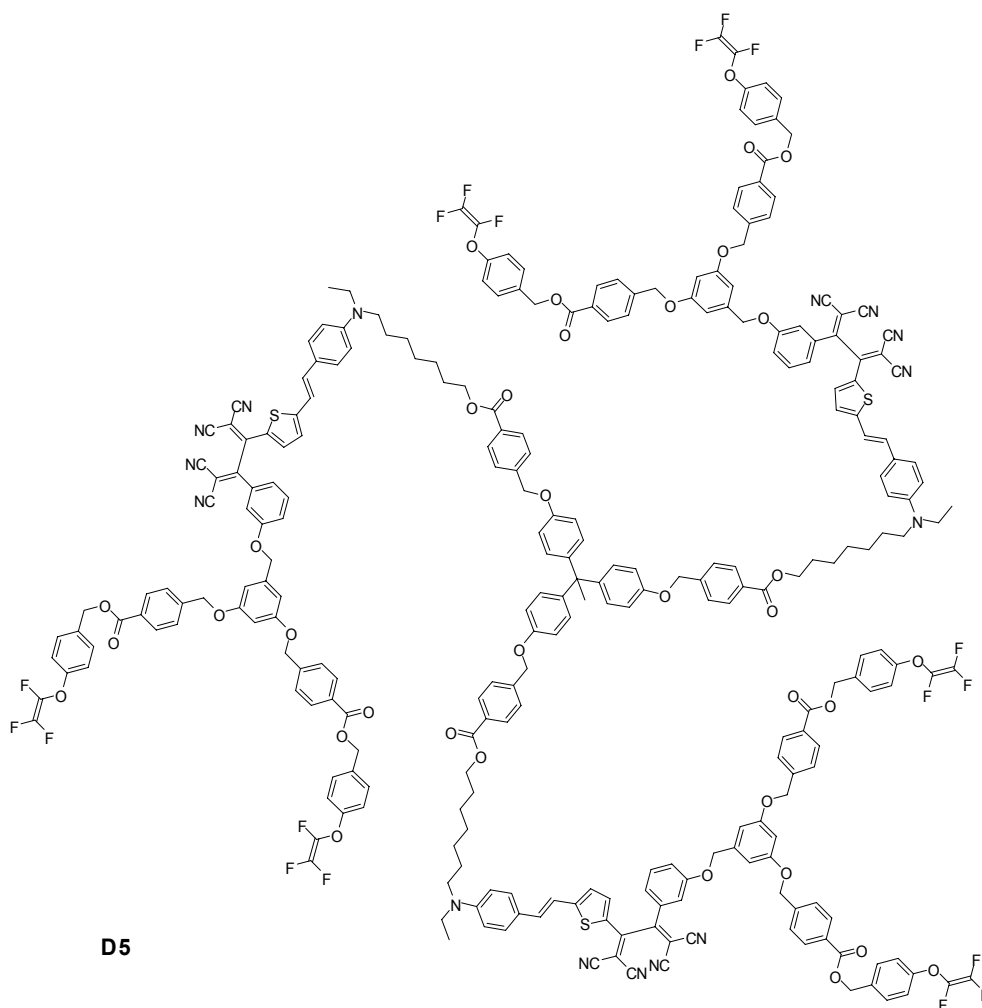


**Figure 15.** Structure of the tri-arm cross-linkable NLO dendrimer **D5**.

Recently, Sullivan *et al.* introduced a novel, thermally curable, tri-component dendrimer glass, which takes advantage of the Diels-Alder cycloaddition reaction to achieve efficient crosslinking during poling.<sup>113</sup> This tri-component material consists of a multichromophore dendrimer functionalized with a diene-containing outer periphery (**D6**), a guest chromophore that is bis-functionalized with a furan-protected dienophile (**GC**), and an optically inert maleimide-based dienophile cross-linking agent (**MD**) (Figure 16).



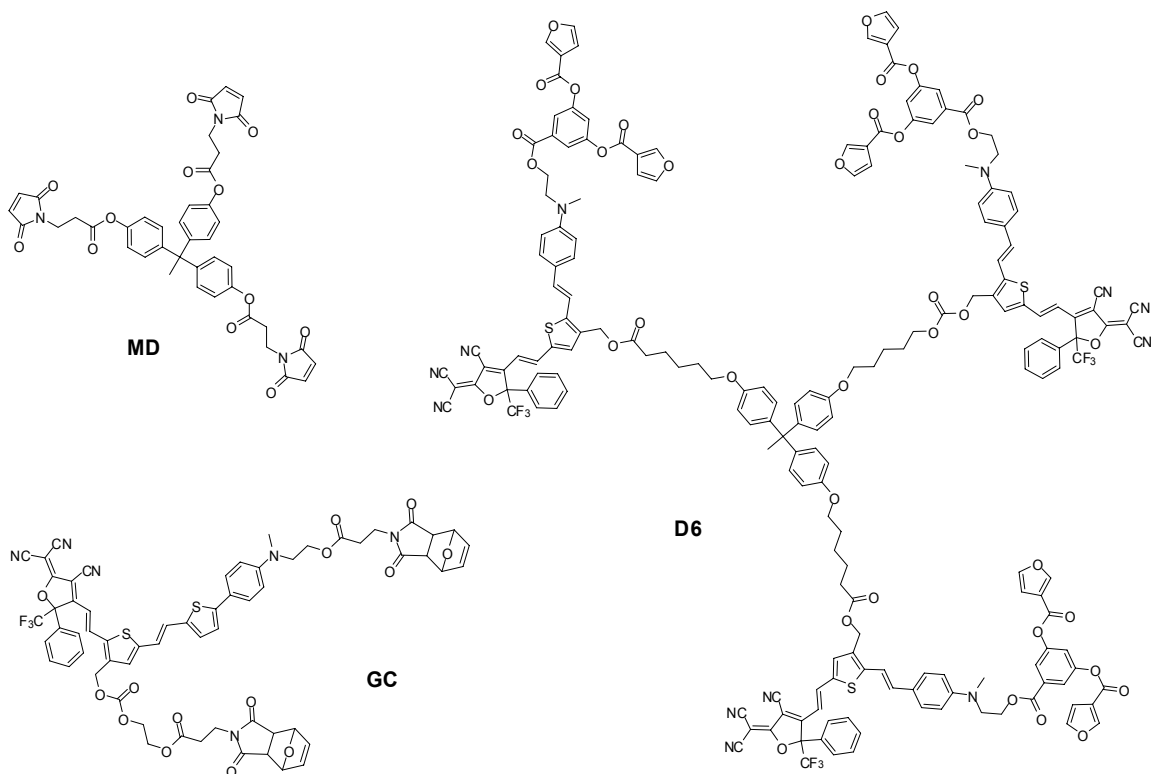


**Figure 16.** Structures of the cross-linkable dendrimer **D6**, the chromophore **GC**, and optically inert pre-cross-linker **MD**.

The optimized tri-component mixture has an  $r_{33}$  of 150 pm/V (at 1.31  $\mu\text{m}$ ) and a thermal stability up to 130  $^{\circ}\text{C}$  (a 48  $^{\circ}\text{C}$  improvement over similar uncross-linked materials). The materials were insoluble in acetone and retained 90% of their original  $r_{33}$  value after 15 months at room temperature.

Using a similar Diels-Alder cycloaddition based approach, Jen *et al.* developed a series of cross-linkable dendrimers by functionalization of the **AJL8**-type chromophore with diene-containing dendrons which could be cross-linked at a later stage by using a trismaleimide dienophile (Figure 17).<sup>114</sup>

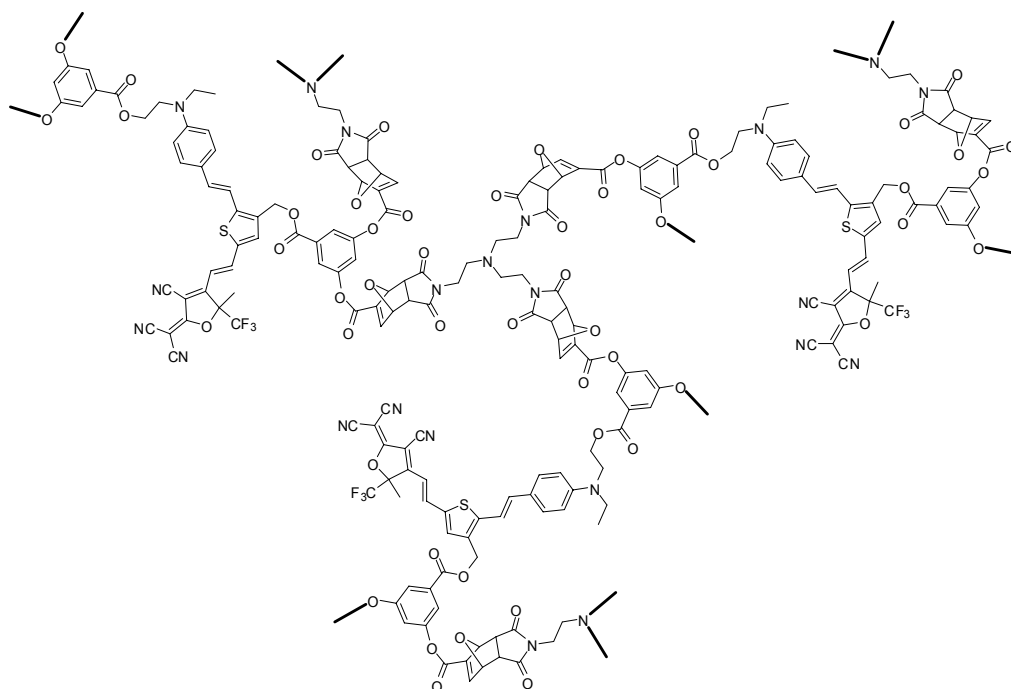


**Figure 17.** Example of a **AJL-8**-containing crosslinked EO dendrimer.

The high EO activity and solvent resistance allowed these materials to be processed through multiple lithographic and etching steps to fabricate a race-track-shaped micro-ring resonator. By coupling this resonator with a side polished optical fiber a broadband electric-field sensor with a high sensitivity of 100 mV/m at 55 MHz has been demonstrated.<sup>114</sup>

### 2.10.3 Side-chain Dendronized NLO Polymers

Although stand alone EO dendritic glasses with high, ever improving poling efficiencies (EO activities) can be obtained, a drawback is the long and tedious synthesis needed to produce sufficiently high molecular weight dendrimers with good film forming properties.

Another approach is to produce dendron-substituted polymers (or dendronized polymers) by combining the site-isolation effect of dendrimers with the good processability of linear polymers. This strategy provides a greater flexibility in designing suitable molecular structures for realizing high performance EO materials.

Making use of this principle, Jen *et al.* synthesized the first side-chain dendronized polymer by attaching TFVE-containing dendritic moieties to a chromophore-functionalized polystyrene based backbone **DP1-a** (Figure 18).<sup>115</sup> The poled films of this polymer showed an  $r_{33}$  of 81 pm/V (at 1.31  $\mu\text{m}$ ), a value that is about 2.5 times larger than that of the corresponding pristine side-chain NLO polymer. A similar modification has also been applied to high  $\mu\beta$  CLD type of chromophores, obtaining dendronized polymers **DP1-b** and **DP2** with  $r_{33}$  values of 97 and 111 pm/V (at 1.31  $\mu\text{m}$ ), respectively.<sup>116</sup> Polymer **DP2** assembles in a pseudo-cylindrical rigid rod conformation, which may explain the high poling efficiency. In fact, in such a rigid polymer the chain entanglement may be reduced, allowing the chromophores a higher freedom to reorient in the channels of such a cylindrical structure.

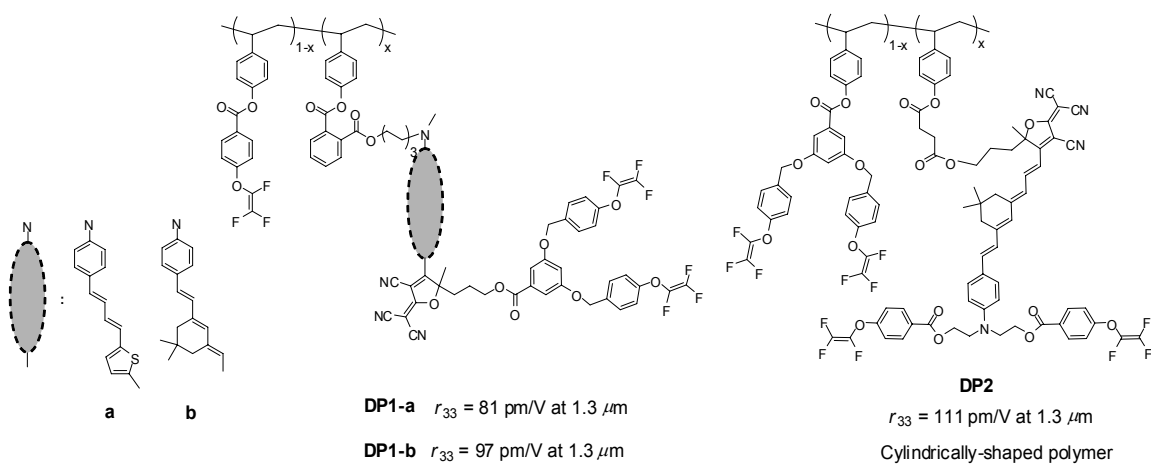


**Figure 18.** Side-chain dendronized polymers with thermoset TFVE groups.

In order to improve the thermal stability a high- $T_g$  cardo-type polyimide with a dendronized CLD-type chromophore has been developed.<sup>117</sup> A high poling efficiency was achieved to afford a very large EO coefficient (71 pm/V at 1.3  $\mu\text{m}$ ); more than 90% of this value can be retained at 85  $^\circ\text{C}$  for more than 650 h.

The synthetic/processing scheme based on the Diels-Alder cycloaddition reaction described in the previous section has also been employed to generate chromophore-functionalized side-chain EO polymers in situ during the poling process.<sup>99</sup> The advantages of using this approach are the very mild heating conditions, the specificity, and the absence of ionic species and catalysts. A series of highly efficient EO materials

has been produced by covalent attachment of maleimide-containing NLO chromophores onto PMMA-based polymers substituted with pendant anthracene diene groups (PMMA-AMA).<sup>118</sup> Different macromolecular architectures were created by changing the attaching mode of the chromophore onto the polymer and onto the fluorinated dendritic units. The obtained polymers showed a good optical quality and processability, fairly high  $T_g$ s ( $\sim 150$  °C), and large  $r_{33}$  values (as high as 60 pm/V at 1.31  $\mu\text{m}$ ). Addition of a bismaleimide crosslinker (BMI) to the polymer blend resulted in an increase of the temporal stability and the solvent resistance, without a significant decrease of the poling efficiency.

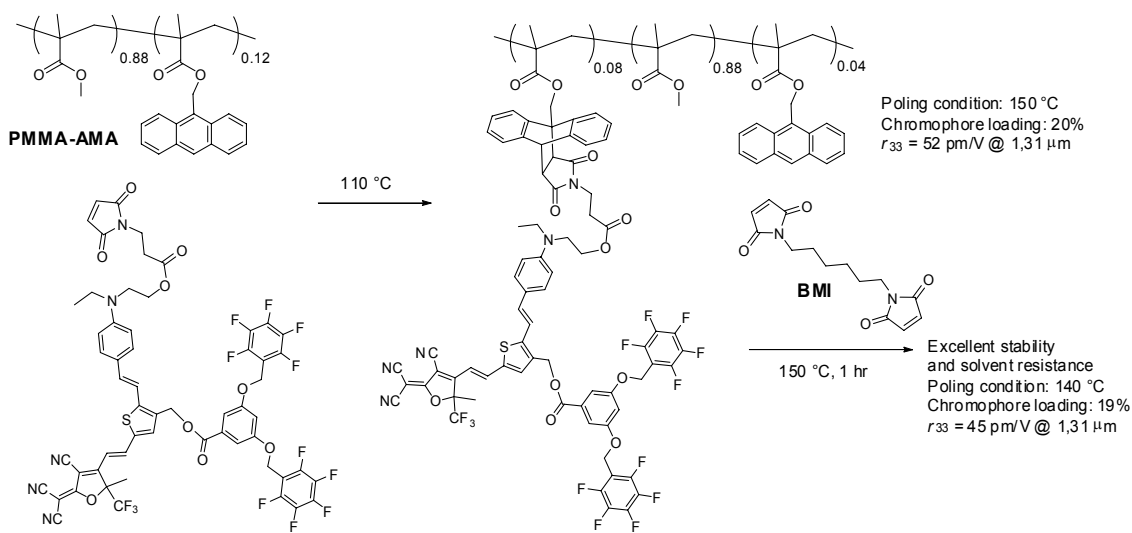


**Figure 19.** Example of the synthesis of a side chain polymer using Diels-Alder post-functionalization.

## 2.11 Self-assembled Systems

The main requirement for molecule-based second order NLO materials is a non-centrosymmetric organization of the constituent active species. Furthermore, organic materials should be effectively fabricated in device-applicable (waveguiding) films of micrometers scale thickness, good optical quality and homogeneity over areas as large as centimeters squares.

Electric field poling of polymers, as described in the previous sections, is the most commonly used methodology to achieve polar order of chromophores within the selected

matrixes. Although this method makes use of strong external forces, it does not take full advantage of the large nonlinear optical properties ( $\beta$ ) of organic chromophores. Therefore the preparation of bulk materials in which the dipoles are well aligned is still a hard challenge.

A totally different strategy to achieve acentric film architectures is by self-assembly. Self-assembled chromophore multilayer structures tend to have an intrinsic molecular dipolar alignment. It does not require electric field poling to achieve a highly acentric film, thus eliminating a possible cause of surface damage and defects. Based on this principle many design strategies have been explored. The most prominent examples are: liquid crystals,<sup>15</sup> chirality,<sup>119,120</sup> Langmuir-Blodgett (LB) film growth, head-to-tail hydrogen bonding, covalent layer-by-layer chemisorption from solution, and vapor deposition.

### **2.11.1 Langmuir-Blodgett (LB) Films**

The LB technique takes advantage of amphiphilic molecules, having a hydrophilic head and a hydrophobic tail, to achieve alignment at the air/water interface. This technique allows films to be deposited with great control at the molecular level, obtaining well ordered structures with high chromophore number densities and homogeneous thicknesses.<sup>11</sup> Since during deposition, the majority of amphiphilic molecules tend to adopt a head-to-head or a tail-to tail arrangement (Y-type), which is centrosymmetric, it is necessary to manipulate the molecular structure in order to impose non-centrosymmetric arrangements (X-type or Z-type) (Figure 20). This issue has been overcome in several ways: alternating optically active layers with inactive spacers, using complementary dyes with chromophores hydrophobically substituted at opposite ends, the tail attached to the donor ( $C_nH_{2n+1}-D-\pi-A$ ) and acceptor ( $D-\pi-A-C_nH_{2n+1}$ ) in adjacent layers, or chromophores with two hydrophobic end-groups.<sup>121</sup> Some molecules show a particular non-centrosymmetric Y-type structure called herringbone arrangement, in which the dipoles are arranged in a plane parallel to the substrate and the alignment is retained in all subsequent layers.<sup>122</sup> The second harmonic intensity increases quadratically with the number of bylayers. Despite the LB technique has been successful

in providing waveguiding NLO active thin films consisting of more than 100 monolayers, several important drawbacks are related to the fragility of the films, such as the low temporal stability of the dipole order (even at room temperature), the scattering from microdomains, and the tedious thick films growth. Recently, the use of alternative approaches to the reduction of molecular mobility, such as polyelectrolyte complexation,<sup>123,124</sup> hydrogen-bonding,<sup>125</sup> and photopolymerization<sup>126</sup> have led to LB films with improved thermal stabilities.

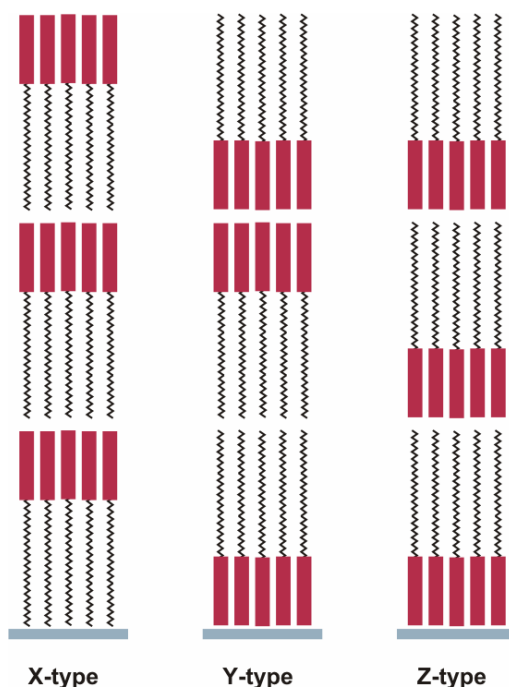


**Figure 20.** Schematic representation of centrosymmetric (Y-type) and non-centrosymmetric (X-type and Z-type) LB structures.

### 2.11.2 Covalent Layer-by-Layer Assemblies

Another approach to make thin-film NLO materials is based on the sequential construction of covalently self-assembled chromophore-containing multilayer structures as first introduced by Marks.<sup>127,128</sup> The general strategy for superlattice construction employs three steps (Figure 21-a). Chemisorption of alkyl or benzyl halide containing trichlorosilane coupling agents (step i) onto flat, hydroxy-terminated surfaces (e.g. glass, silicon, organic polymers) provides functionalized surfaces for the polar anchoring of a

bifunctional chromophore precursor. The quaternization/anchoring process (step ii) converts the NLO-inactive precursor into the NLO active chromophore. It also creates surface hydroxyalkyl functionalities that are subsequently used to “lock in” the polar structure with a capping agent via three-dimensional siloxane network formation. This “capping” reaction (step iii) planarizes the structure, exposes silanol functionalities mimicking the original SiO<sub>2</sub> interface, and thus allows superlattice construction by iteration of steps i-iii.

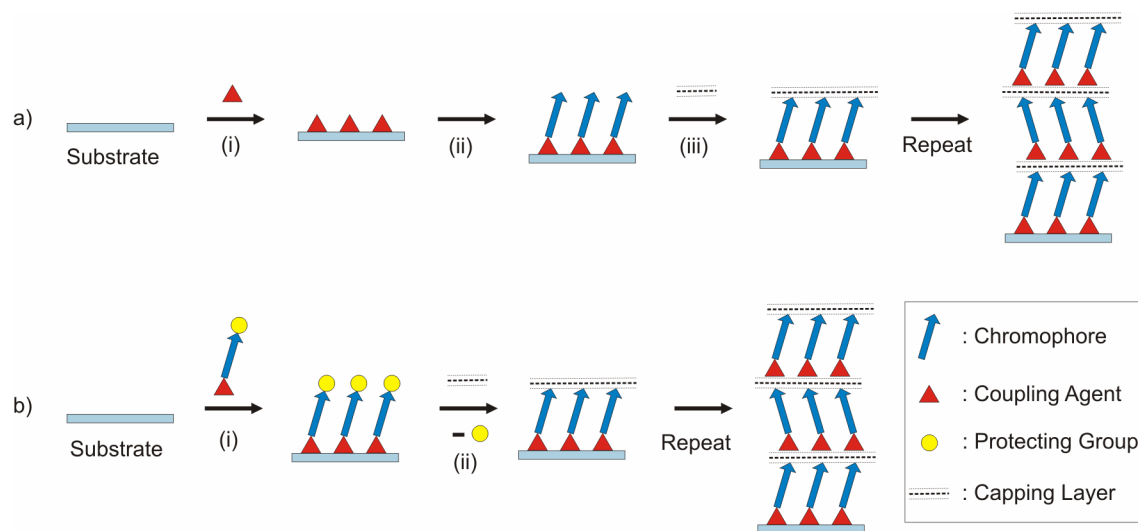


**Figure 21.** Schematic representation of the three-step (a) and the two-step (b) LbL assembly processes for chromophoric superlattices.

This layer-by-layer chemisorptive siloxane-based self-assembly approach is particularly attractive because it offers a greater net chromophore alignment and number densities than poled films and a much better structural control and stability than LB films. Molecular orientation is intrinsically acentric. In fact chromophores are covalently linked to the substrates, and further locked into place with strong covalent cross-links. Hence, the microstructural orientation is very stable and the films are closely packed and robust.

This three-step assembly method is suitable for a wide range of donor-acceptor chromophore precursors, such as stilbazole-, acetylenic-, azobenzene,<sup>129,130</sup> or pyrrole-based<sup>131</sup> chromophores resulting in films with very large NLO/EO responses ( $\chi^{(2)}$  of 150-220 pm/V and  $r_{33}$  values as high as  $\sim 80$  pm/V).

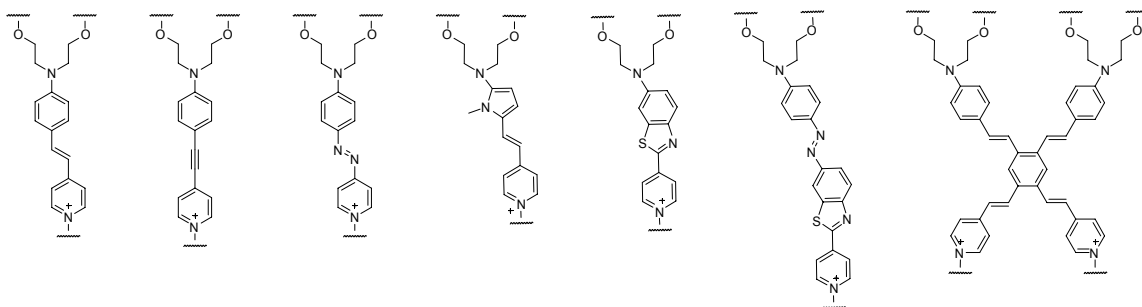


**Figure 22.** High- $\beta$  chromophoric building blocks used in self-assembled superlattices.

Very recently, a novel type of X-shaped 2D chromophore with extended conjugation has been used. The resulting self-assembled chromophoric films exhibit a dramatically blue-shifted optical maximum (325 nm), while maintaining a large EO response ( $\chi^{(2)} \sim 232$  pm/V at 1064 nm;  $r_{33} \sim 45$  pm/V at 1310 nm).<sup>14,132</sup>

However, this three-step process is very time consuming and tedious, especially due to the quaternization reaction which involves inefficient spin-coating followed by vacuum treatment in an oven at 110 °C, to obtain full chromophore coverage. To enhance the process efficiency and speed, a greatly improved all-“wet-chemical” two-step approach has been introduced.<sup>133</sup> Specifically, the deposition technique (Figure 21-b) employs the iterative combination of only two steps: (i) self-limiting polar chemisorption of a protected high- $\beta$  chromophore monolayer ( $t \sim 15$  min) and (ii) in situ selective trialkylsilyl protecting group removal, plus capping of each “deprotected” chromophore layer using octachlorotrisiloxane ( $t \sim 25$  min).

This all-“wet-chemical” two-step process can be efficiently implemented in a vertical dipping procedure to yield polar films consisting of more than 80 alternating chromophore and capping layers. Each nanoscale bilayer (chromophore + polysiloxane layer are  $\sim 3.26$  nm thick) can be grown at least one order of magnitude more rapidly than using previous siloxane-based solution deposition methodologies.<sup>134</sup> The thermally and photochemically robust superlattices exhibit very large EO responses (up to ( $\chi^{(2)}$ ) 370 pm/V and  $r_{33} \sim 120$  pm/V determined by SHG measurements at  $\lambda = 1064$  nm)<sup>135</sup> and high chromophore surface densities and have been integrated in frequency doubling devices,<sup>136</sup> ultrafast optical switches,<sup>137</sup> and EO phase modulators.<sup>138,139</sup>



Several, alternative self-assembly approaches for producing thermally stable, acentric chromophoric multilayers have been reported.<sup>140-142</sup> The most prominent example is that developed by Katz *et al.*,<sup>143,144</sup> which is taking advantage of the zirconium phosphonate/phosphate coordinative bonding to fix layers of a dye to one another producing films with a good structural regularity and stability to orientational randomization up to 150 °C. Another example utilizes the electric-field induced LbL assembly technique of ionic species, followed by UV irradiation to convert the ionic bonds between layers into covalent bonds.<sup>145</sup>

### 2.11.3 Hydrogen Bonded and Supramolecular Assemblies

An attractive way of self-assembling, highly EO active organic materials is by using supramolecular interactions, such as intermolecular hydrogen bonding, to achieve highly ordered, non-covalently bound, acentric structures under mild conditions.<sup>146-148</sup>

Saadeh *et al.* successfully applied this approach to generate a series of polymer-like materials exhibiting large optical nonlinearities.<sup>149</sup> These assemblies were built up through the spontaneous formation of three parallel hydrogen bonds between a NLO chromophore bearing two 2,6-diacetamido-4-pyridone moieties (**D1-3**) and a monomer with a diimide group or two uracil groups (**A1-3**) (Figure 23). These NLO supramolecular self-assemblies can form amorphous films with a good optical quality,  $r_{33}$  as high as 70 pm/V, and a long-term stability (4000 h) of the second harmonic generation (SHG) signal at room temperature.

Generally, self-assembled organic thin films are formed in solution. However, the solution techniques have the disadvantage of being time consuming and limited by the diffusion and aggregation of molecules that interferes with the deposition process. To tackle this problem, Gunther *et al.* have developed a novel vapor phase deposition technique, to produce supramolecular assemblies with well defined polar ordering.<sup>150</sup>

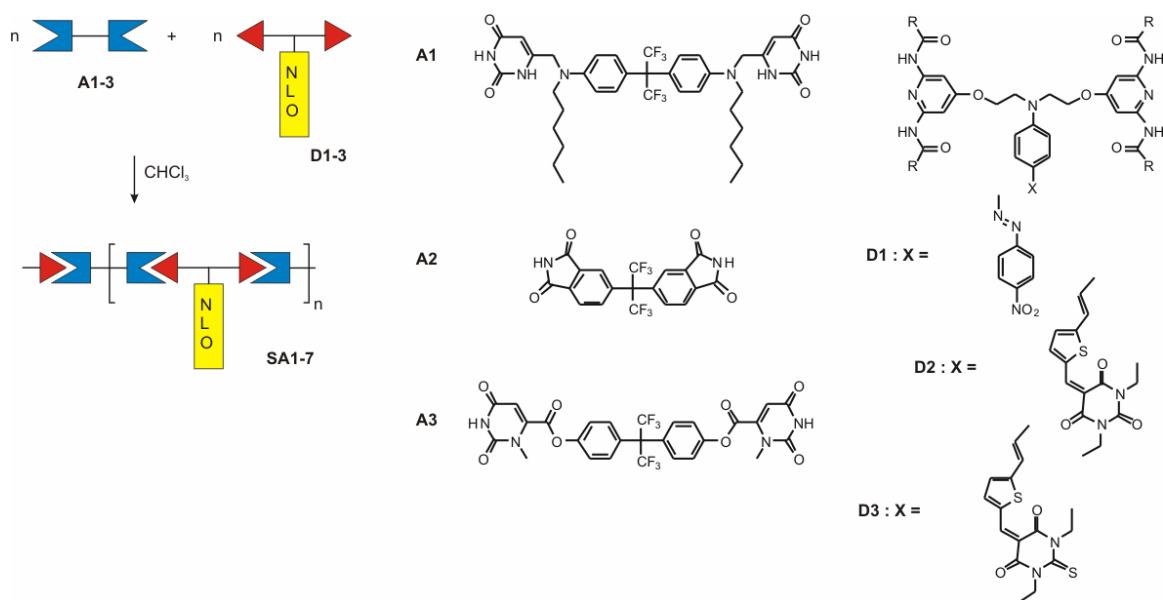


**Figure 23.** Structures of monomers *A1-3* and *D1-3* and synthesis of their supramolecular self-assemblies *SA1-7*.

This technique, the so-called organic molecular beam deposition (OMBD), consists of evaporation of chromophores onto a substrate under high or ultra high vacuum (UHV) conditions. Suitable molecules must be strongly hydrogen-bonded to one another in a head-to-tail fashion to form linear supramolecular assemblies in the solid state. The vapor phase approach offers many advantages over the solution phase one, such as high chemical purity, faster growing rates, and superior control over growth parameters. Films can be grown homogeneously over large areas and with a high degree of molecular ordering and tight molecular packing over thicknesses of about 1  $\mu\text{m}$ . However, only low nonlinearities ( $d_{11} = 5 \text{ pm/V}$ ) could be obtained so far.<sup>151</sup>

Significantly larger EO responses have been achieved by Facchetti *et al.* applying a similar vapor deposition process to heteroaromatic-based chromophores.<sup>152</sup> Those high-response molecules contain one pyridine ring as hydrogen-bond acceptor at one end and at the opposite end either a hydrazobenzoic acid or hydrazophenyl group as hydrogen-bond donor, making them capable to self-organize in a head-to-tail fashion from the vapor phase (Figure 24). High quality films, as thick as 700 nm, could be grown in a few hours either on siloxane-modified substrates or hydroxyl functionalized substrates. The

EO responses at 1.30 and 1.55  $\mu\text{m}$  ( $r_{33} \sim 14\text{-}26 \text{ pm/V}$ ,  $(\chi^{(2)}) 136\text{-}320 \text{ pm/V}$ ) are exceeding by about two orders of magnitude those of previously reported H-bonded EO films.<sup>153</sup>

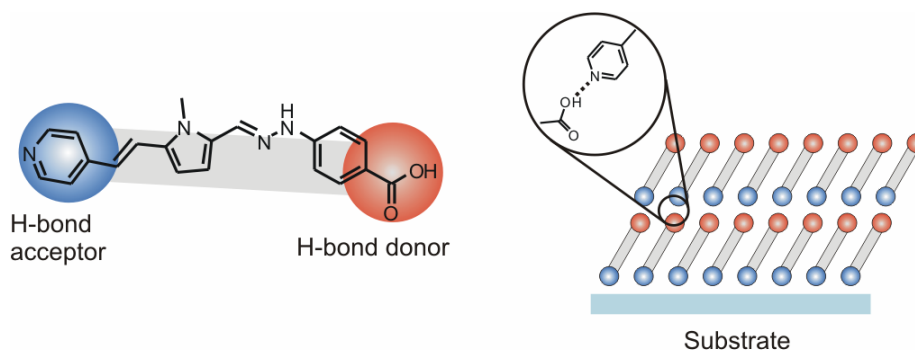


**Figure 24.** Graphical illustration of the head-to-tail self-assembly of chromophores by vapor deposition.

Recently, Jen *et al.* developed a new class of molecular glasses based on the reversible self-assembly of aromatic/perfluoroaromatic ( $\text{Ar-Ar}^{\text{F}}$ ) dendron-substituted nonlinear high- $\mu\beta$  chromophores.<sup>154</sup> In these molecules (Figure 25) both phenyl and pentafluorophenyl rings are incorporated as peripheral dendrons on the  $\pi$ -bridge and the donor-end of the chromophores **C1**, **C2**, and **C3**.

Despite of being not directional and therefore needing an external electric field to achieve acentric order, complementary  $\text{Ar-Ar}^{\text{F}}$  interactions have been demonstrated to improve the poling efficiency of the self-organized molecular glasses. In fact, chromophore **C3** gave the highest  $r_{33}$  value (108 pm/V at 1310 nm) among all monolithic molecular glasses, due to the favorable  $\text{Ar-Ar}^{\text{F}}$  interactions. This value is more than two times larger than those obtained for chromophores **C1** or **C2** that do not have such interactions. Moreover, the binary 1:1 composite of **C1** and **C2** showed an  $r_{33}$  value of 130 pm/V. These poled thin films could retain over 90% of their original  $r_{33}$  values at room temperature for more than 2 years. On the contrary, the temporal stability of the glasses without the  $\text{Ar-Ar}^{\text{F}}$  interactions deteriorated dramatically within 1 month. Although the chromophore number density in these molecular glasses are already very high ( $\sim 2\times$  that of the typical guest-host polymers), it is still possible to further enhance the  $r_{33}$  values of these materials by doping a second chromophore with higher  $\beta$  in these glasses, obtaining stunning  $r_{33}$  values (up to 327 pm/V).

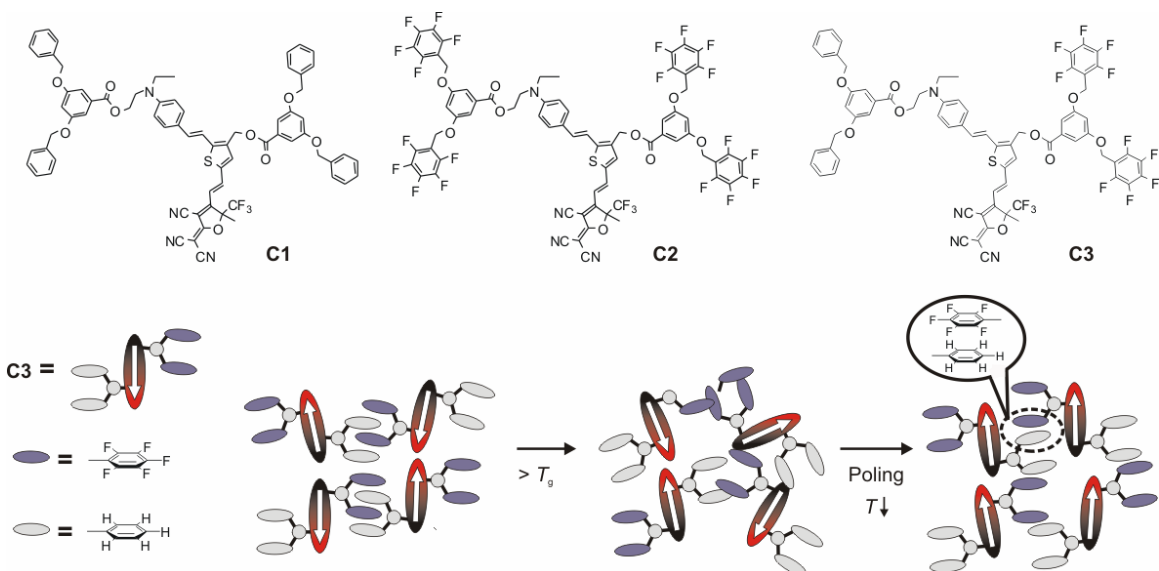


**Figure 25.** Structures of the glass forming chromophores and a graphical illustration of the alignment of self-assembled chromophore C3 by  $Ar-Ar^F$  interactions.

## 2.12 Conclusions and Outlook

In this Chapter, an overview of the state-of-the-art of polymeric NLO materials is given. The great effort made during the past 20 years has led to a better knowledge of the influence of chromophore design on material structure-function relationships. In particular, the theories developed by Dalton and Robinson have provided a better fundamental understanding of the role of chromophore shape and structure in defining the maximum achievable EO activity.<sup>105</sup> This has led to the development of a new generation of chromophores, with improved acceptors and conjugated bridges giving better stabilities, reduced dipole-dipole interactions, and large nonlinearities. Recently, an alternative approach for obtaining high  $\beta$  values, based on twisted  $\pi$ -zwitterionic structures, instead of on extensive planar conjugation, has been reported by Marks *et al.*<sup>60</sup> This new molecular design resulted in unprecedented molecular hyperpolarizabilities, and thus provides new paradigms for the future molecule-based EO materials.<sup>59</sup>

Several diverse synthetic approaches to obtain EO materials with acentric symmetry have been pursued. Among them, poling of guest-host polymers and chromophore-functionalized polymers have been investigated most intensely. Nevertheless, innovative

designs like that involving the development of multichromophore-containing dendritic materials investigated by Dalton and Jen have been introduced.<sup>111</sup> Such dendritic materials are of particular interest because of the opportunities for molecular-scale architectural control.<sup>107</sup> Moreover, a polymer host is not required and stand-alone thin films can be fabricated with extremely higher loading densities and larger EO activities than those that have been found in conventional EO materials. These properties, in combination with a good processability, high stability, and solvent resistance, makes NLO dendrimers a good candidate for next generation high-performance EO devices.<sup>114</sup>

Self-assembly methods proceeding from substrates, such as layer-by-layer chemisorptive siloxane-based self assembly<sup>14</sup> and vapor deposition techniques<sup>152</sup> have experienced a substantial growth in the past five years. Thanks to intrinsic molecular dipolar alignment, thermally robust and highly EO active films can be achieved without the use of external forces. Although prototype devices integrating self-assembly superlattices have been fabricated, some crucial aspects, such as the ability of growing optical quality films in the order of micrometers thickness, still needs to be optimized.

While the state-of-the-art in organic electro-optics has advanced considerably during the past five years in terms of getting materials with large NLO responses and induced temporal stabilities of the polar order, the problem of chemical (aging) and photochemical stability (light induced chromophore degradation) requires more systematic study and better understanding to be solved. The solution of this issue is critical for organic EO modulators and other devices to become reality. Therefore more intensive research efforts will be required to realize the full potential of organic EO materials.

This thesis aims to contribute in this direction with the synthesis and the study of new thermally and photostable NLO chromophores and polymers. The chemical, photochemical and optical properties of the EO materials derived therefrom are described.

## 2.13 References

- 1 T. Verbiest, S. Houbrechts, M. Kauranen, K. Clays, A. Persoons, *J. Mater. Chem.*, **1997**, *7*, 2175-2189.
- 2 L. R. Dalton, *J. Phys.: Condens. Matter*, **2003**, *15*, R897-R934.
- 3 L. R. Dalton, W. H. Steier, B. H. Robinson, C. Zhang, A. Ren, S. Garner, A. Chen, T. Londergan, L. Irwin, B. Carlson, L. Fifield, G. Phelan, C. Kincaid, J. Amend, A. Jen, *J. Mater. Chem.*, **1999**, *9*, 1905-1920.
- 4 F. Kajzar, K. S. Lee, A. K. Y. Jen, *Adv. Polym. Sci.*, **2003**, *161*, 1-85.
- 5 L. R. Dalton, *Adv. Polym. Sci.*, **2002**, *158*, 1-86.
- 6 L. Dalton, A. Harper, A. Ren, F. Wang, G. Todorova, J. Chen, C. Zhang, M. Lee, *Ind. Eng. Chem. Res.*, **1999**, *38*, 8-33.
- 7 P. N. Prasad, D. J. Williams, *"Introduction to Nonlinear Optical Effects in Molecules and Polymers"*, John Wiley and Sons, N. Y., **1991**.
- 8 R. W. Boyd, *"Nonlinear Optics"*, Academic Press, SanDiego, CA, **1992**.
- 9 D. M. Burland, R. D. Miller, C. A. Walsh, *Chem. Rev.*, **1994**, *94*, 31-75.
- 10 O. R. Evans, W. Lin, *Acc. Chem. Res.*, **2002**, *35*, 511-522.
- 11 G. J. Ashwell, *J. Mater. Chem.*, **1999**, *9*, 1991-2003.
- 12 J. R. Heflin, M. T. Guzy, P. J. Neyman, K. J. Gaskins, C. Brands, Z. Wang, H. W. Gibson, R. M. Davis, K. E. VanCott, *Langmuir*, **2006**, *22*, 5723-5727.
- 13 E. H. Kang, T. Bu, P. Jin, J. Sun, Y. Yang, J. Shen, *Langmuir*, **2007**, *23*, 7594-7601.
- 14 H. Kang, G. Evmenenko, P. Dutta, K. Clays, K. Song, T. J. Marks, *J. Am. Chem. Soc.*, **2006**, *128*, 6194-6205.
- 15 G. Hennrich, A. Omenat, I. Asselberghs, S. Foerier, K. Clays, T. Verbiest, J. L. Serrano, *Angew. Chem., Int. Ed.*, **2006**, *45*, 4203-4206.
- 16 L. Wang, J. Yoshida, N. Ogata, S. Sasaki, T. Kajiyama, *Chem. Mater.*, **2001**, *13*, 1273-1281.
- 17 C. C. Teng, H. T. Man, *Appl. Phys. Lett.*, **1990**, *56*, 1734-1736.
- 18 F. Michelotti, G. Nicolao, F. Tesi, M. Bertolotti, *Chem. Phys.*, **1999**, *245*, 311-326.
- 19 V. Dentan, Y. Levy, M. Dumont, P. Robin, E. Chastaing, *Opt. Commun.*, **1989**, *69*, 379-383.
- 20 S. Kalluri, S. Garner, M. Ziari, W. H. Steier, Y. Shi, L. R. Dalton, *Appl. Phys. Lett.*, **1996**, *69*, 275-277.

- 21 Y. Q. Shi, C. Zhang, H. Zhang, J. H. Bechtel, L. R. Dalton, B. H. Robinson, W. H. Steier, *Science*, **2000**, *288*, 119-122.
- 22 M. Lee, H. E. Katz, C. Erben, D. M. Gill, P. Gopalan, J. D. Heber, D. J. McGee, *Science*, **2002**, *298*, 1401-1403.
- 23 R. R. Barto, C. W. Frank, P. V. Bedworth, S. Ermer, R. E. Taylor, *J. Phys. Chem. B*, **2004**, *108*, 8702-8715.
- 24 H. Ma, A. K. Y. Jen, L. R. Dalton, *Adv. Mater.*, **2002**, *14*, 1339-1365.
- 25 B. F. Levine, C. G. Bethea, *J. Chem. Phys.*, **1975**, *63*, 2666-2682.
- 26 A. Willetts, J. E. Rice, D. M. Burland, D. P. Shelton, *J. Chem. Phys.*, **1992**, *97*, 7590-7599.
- 27 K. Clays, A. Persoons, *Phys. Rev. Lett.*, **1991**, *66*, 2980-2983.
- 28 K. Clays, A. Persoons, *Rev. Sci. Instrum.*, **1992**, *63*, 3285-3289.
- 29 J. L. Oudar, D. S. Chemla, *J. Chem. Phys.*, **1977**, *66*, 2664-2668.
- 30 S. R. Marder, D. N. Beratan, L. T. Cheng, *Science*, **1991**, *252*, 103-106.
- 31 C. B. Gorman, S. R. Marder, *Proc. Natl. Acad. Sci. U. S. A.*, **1993**, *90*, 11297-11301.
- 32 O. Kwon, S. Barlow, S. A. Odom, L. Beverina, N. J. Thompson, E. Zojer, J. L. Bredas, S. R. Marder, *J. Phys. Chem. A*, **2005**, *109*, 9346-9352.
- 33 C. R. Moylan, R. J. Twieg, V. Y. Lee, S. A. Swanson, K. M. Betterton, R. D. Miller, *J. Am. Chem. Soc.*, **1993**, *115*, 12599-12600.
- 34 P. V. Bedworth, Y. Cai, A. Jen, S. R. Marder, *J. Org. Chem.*, **1996**, *61*, 2242-2246.
- 35 C. R. Moylan, S. Ermer, S. M. Lovejoy, I. H. McComb, D. S. Leung, R. Wortmann, P. Krdmer, R. J. Twieg, *J. Am. Chem. Soc.*, **1996**, *118*, 12950-12955.
- 36 S. Thayumanavan, J. Mendez, S. R. Marder, *J. Org. Chem.*, **1999**, *64*, 4289-4297.
- 37 G. Koeckelberghs, T. Verbiest, M. Vangheluwe, L. De Groof, I. Asselberghs, I. Picard, K. Clays, A. Persoons, C. Samyn, *Chem. Mater.*, **2005**, *17*, 118-121.
- 38 R. F. Shi, M. H. Wu, S. Yamada, Y. M. Cai, A. F. Garito, *Appl. Phys. Lett.*, **1993**, *63*, 1173-1175.
- 39 G. Rojo, G. De La Torre, J. Garcia-Ruiz, I. Ledoux, T. Torres, J. Zyss, F. Agullo-Lopez, *Chem. Phys.*, **1999**, *245*, 27-34.
- 40 M. O. Senge, M. Fazekas, E. G. A. Notaras, W. J. Blau, M. Zawadzka, O. B. Locos, E. M. N. Mhuirheartaigh, *Adv. Mater.*, **2007**, *19*, 2737-2774.
- 41 B. Kippelen, S. R. Marder, E. Hendrickx, J. L. Maldonado, G. Guillemet, B. L. Volodin, D. D. Steele, Y. Enami, Sandalphon, Y. J. Yao, J. F. Wang, H. Rockel, L. Erskine, N. Peyghambarian, *Science*, **1998**, *279*, 54-57.

- 42 Y. C. Shu, Z. H. Gong, C. F. Shu, E. M. Breitung, R. J. McMahon, G. H. Lee, A. K. Y. Jen, *Chem. Mater.*, **1999**, *11*, 1628-1632.
- 43 C. Zhang, A. S. Ren, F. Wang, J. Zhu, L. R. Dalton, J. N. Woodford, C. H. Wang, *Chem. Mater.*, **1999**, *11*, 1966-1968.
- 44 C. W. Dirk, H. E. Katz, M. L. Schilling, L. A. King, *Chem. Mater.*, **1990**, *2*, 700-705.
- 45 S. Gilmour, S. R. Marder, J. W. Perry, L. T. Cheng, *Adv. Mater.*, **1994**, *6*, 494-496.
- 46 P. R. Varanasi, A. K. Y. Jen, J. Chandrasekhar, I. N. N. Namboothiri, A. Rathna, *J. Am. Chem. Soc.*, **1996**, *118*, 12443-12448.
- 47 I. D. L. Albert, T. J. Marks, M. A. Ratner, *J. Am. Chem. Soc.*, **1997**, *119*, 6575-6582.
- 48 C. F. Shu, Y. K. Wang, *J. Mater. Chem.*, **1998**, *8*, 833-835.
- 49 S. Gilmour, R. A. Montgomery, S. R. Marder, L. T. Cheng, A. K. Y. Jen, C. Yongming, J. W. Perry, L. R. Dalton, *Chem. Mater.*, **1994**, *6*, 1603-1604.
- 50 M. Ahlheim, M. Barzoukas, P. V. Bedworth, M. Blanchard-Desce, A. Fort, Z. Y. Hu, S. R. Marder, J. W. Perry, C. Runser, M. Staehelin, B. Zysset, *Science*, **1996**, *271*, 335-337.
- 51 S. S. Sun, C. Zhang, L. R. Dalton, S. M. Garner, A. Chen, W. H. Steier, *Chem. Mater.*, **1996**, *8*, 2539-2541.
- 52 Z. Y. Hu, A. Fort, M. Barzoukas, A. K. Y. Jen, S. Barlow, S. R. Marder, *J. Phys. Chem. B*, **2004**, *108*, 8626-8630.
- 53 A. K. Y. Jen, Y. Cai, P. V. Bedworth, S. R. Marder, *Adv. Mater.*, **1997**, *9*, 132-135.
- 54 X. Wu, J. Wu, Y. Liu, A. K. Y. Jen, *J. Am. Chem. Soc.*, **1999**, *121*, 472-473.
- 55 F. Wang, A. S. Ren, M. He, A. W. Harper, L. R. Dalton, S. M. Garner, H. Zhang, A. Chen, W. H. Steier, *Polym. Mater. Sci. Eng.*, **1998**, *78*, 42.
- 56 M. He, T. M. Leslie, J. A. Sinicropi, *Chem. Mater.*, **2002**, *14*, 2393-2400.
- 57 M. He, T. M. Leslie, J. A. Sinicropi, S. M. Garner, L. D. Reed, *Chem. Mater.*, **2002**, *14*, 4669-4675.
- 58 A. Galvan-Gonzalez, K. D. Belfield, G. I. Stegeman, M. Canva, S. R. Marder, K. Staub, G. Levina, R. J. Twieg, *J. Appl. Phys.*, **2003**, *94*, 756-763.
- 59 H. Kang, A. Facchetti, H. Jiang, E. Cariati, S. Righetto, R. Ugo, C. Zuccaccia, A. Macchioni, C. L. Stern, Z. F. Liu, S. T. Ho, E. C. Brown, M. A. Ratner, T. J. Marks, *J. Am. Chem. Soc.*, **2007**, *129*, 3267-3286.
- 60 H. Kang, A. Facchetti, P. W. Zhu, H. Jiang, Y. Yang, E. Cariati, S. Righetto, R. Ugo, C. Zuccaccia, A. Macchioni, C. L. Stern, Z. F. Liu, S. T. Ho, T. J. Marks, *Angew. Chem., Int. Ed.*, **2005**, *44*, 7922-7925.



- 61 J. W. Wu, J. F. Valley, S. Ermer, E. S. Binkley, J. T. Kenney, G. F. Lipscomb, R. Lytel, *Appl. Phys. Lett.*, **1991**, *58*, 225.
- 62 K. Y. Wong, A. K. Y. Jen, *J. Appl. Phys.*, **1994**, *75*, 3308-3310.
- 63 Y. M. Cai, A. K. Y. Jen, *Appl. Phys. Lett.*, **1995**, *117*, 7295.
- 64 S. Liu, M. A. Haller, H. Ma, L. R. Dalton, S. H. Jang, A. K. Y. Jen, *Adv. Mater.*, **2003**, *15*, 603-607.
- 65 C. Zhang, L. R. Dalton, M. C. Oh, H. Zhang, W. H. Steier, *Chem. Mater.*, **2001**, *13*, 3043-3050.
- 66 M. C. Oh, H. Zhang, C. Zhang, H. Erlig, Y. Chang, B. Tsap, D. Chang, A. Szep, W. H. Steier, H. R. Fetterman, L. R. Dalton, *IEEE J. Sel. Top. Quantum Electron.*, **2001**, *7*, 826-835.
- 67 Y. J. Cheng, J. Luo, S. Hau, D. H. Bale, T. D. Kim, Z. Shi, D. B. Lao, N. M. Tucker, Y. Tian, L. R. Dalton, P. J. Reid, A. K. Y. Jen, *Chem. Mater.*, **2007**, *19*, 1154-1163.
- 68 S. M. Garner, J. S. Cites, M. He, J. Wang, *Appl. Phys. Lett.*, **2004**, *84*, 1049-1051.
- 69 M. He, T. Leslie, S. Garner, M. DeRosa, J. Cites, *J. Phys. Chem. B*, **2004**, *108*, 8731-8736.
- 70 C. Samyn, T. Verbiest, A. Persoons, *Macromol. Rapid Commun.*, **2000**, *21*, 1-15.
- 71 C. C. Chang, C. P. Chen, C. C. Chou, W. J. Kuo, R. J. Jeng, *J. Macromol. Sci., Polym. Rev.*, **2005**, *45*, 125-170.
- 72 T. Verbiest, D. M. Burland, M. C. Jurich, V. Y. Lee, R. D. Miller, W. Volksen, *Science*, **1995**, *268*, 1604-1606.
- 73 T. Verbiest, D. M. Burland, M. C. Jurich, V. Y. Lee, R. D. Miller, W. Volksen, *Macromolecules*, **1995**, *28*, 3005-3007.
- 74 R. D. Miller, D. M. Burland, M. Jurich, V. Y. Lee, C. R. Moylan, J. I. Thackara, R. J. Twieg, T. Verbiest, W. Volksen, *Macromolecules*, **1995**, *28*, 4970-4974.
- 75 M. H. Davey, V. Y. Lee, L. M. Wu, C. R. Moylan, W. Volksen, A. Knoesen, R. D. Miller, T. J. Marks, *Chem. Mater.*, **2000**, *12*, 1679-1693.
- 76 T. A. Chen, A. K. Y. Jen, Y. Cai, *Macromolecules*, **1996**, *29*, 535-539.
- 77 M. E. Wright, S. Fallis, A. J. Guenther, L. C. Baldwin, *Macromolecules*, **2005**, *38*, 10014-10021.
- 78 A. J. Guenther, M. E. Wright, S. Fallis, G. A. Lindsay, B. J. Petteys, G. R. Yandek, D. Y. Zang, M. Sanghadasa, P. R. Ashley, in *Proc. SPIE-Int. Soc. Opt. Eng., Vol. 6331*, **2006**.
- 79 G. A. Lindsay, A. J. Guenther, M. E. Wright, M. Sanghadasa, P. R. Ashley, *Polymer*, **2007**, *48*, 6605-6616.
- 80 M. E. Wright, S. Mullick, H. S. Lackritz, L. Y. Liu, *Macromolecules*, **1994**, *27*, 3009-3015.

- 81 F. Fuso, A. B. Padias, H. K. Hall Jr, *Macromolecules*, **1991**, *24*, 1710-1713.
- 82 C. Xu, B. Wu, L. R. Dalton, P. M. Ranon, Y. Shi, W. H. Steier, *Macromolecules*, **1992**, *25*, 6716-6718.
- 83 G. A. Lindsay, J. D. Stenger-Smith, R. A. Henry, J. M. Hoover, R. A. Nissan, K. J. Wynne, *Macromolecules*, **1992**, *25*, 6075-6077.
- 84 Z. Li, S. Dong, G. Yu, Z. Li, Y. Liu, C. Ye, J. Qin, *Polymer*, **2007**, *48*, 5520-5529.
- 85 N. Tsutsumi, M. Morishima, W. Sakai, *Macromolecules*, **1998**, *31*, 7764-7769.
- 86 M. Dobler, C. Weder, O. Ahumada, P. Neuenschwander, U. W. Suter, S. Follonier, C. Bosshard, P. Gunter, *Macromolecules*, **1998**, *31*, 7676-7681.
- 87 Y. D. Zhang, L. M. Wang, T. Wada, H. Sasabe, *Macromolecules*, **1996**, *29*, 1569-1573.
- 88 G. Sheeren, A. Persoons, H. Bolink, M. Heylen, M. Vanbeylen, C. Samyn, *Eur. Polym. J.*, **1993**, *29*, 981-986.
- 89 L. R. Dalton, A. W. Harper, R. Ghosn, W. H. Steier, M. Ziari, H. Fetterman, Y. Shi, R. V. Mustacich, A. K. Y. Jen, K. J. Shea, *Chem. Mater.*, **1995**, *7*, 1060-1081.
- 90 S. S. H. Mao, Y. Ra, L. Guo, C. Zhang, L. R. Dalton, A. Chen, S. Garner, W. H. Steier, *Chem. Mater.*, **1998**, *10*, 146-155.
- 91 L. Chen, G. Qian, X. Jin, Y. Cui, J. Gao, Z. Wang, M. Wang, *J. Phys. Chem. B*, **2007**, *111*, 3115-3121.
- 92 M. Guglielmi, G. Brusatin, G. Della Giustina, *J. Non-Cryst. Solids*, **2007**, *353*, 1681-1687.
- 93 Y. Bai, N. Song, J. P. Gao, X. Sun, X. Wang, G. Yu, Z. Y. Wang, *J. Am. Chem. Soc.*, **2005**, *127*, 2060-2061.
- 94 R.-J. Jeng, C.-C. Chang, C.-P. Chen, C.-T. Chen, W.-C. Su, *Polymer*, **2003**, *44*, 143-155.
- 95 C. Zhang, C. Wang, L. R. Dalton, H. Zhang, W. H. Steier, *Macromolecules*, **2001**, *34*, 253-261.
- 96 C. Zhang, C. Wang, J. Yang, L. R. Dalton, G. Sun, H. Zhang, W. H. Steier, *Macromolecules*, **2001**, *34*, 235-243.
- 97 D. W. Smith, D. A. Babb, *Macromolecules*, **1996**, *29*, 852-860.
- 98 H. Ma, J. Wu, P. Herguth, B. Chen, A. K. Y. Jen, *Chem. Mater.*, **2000**, *12*, 1187-1189.
- 99 M. Haller, J. Luo, H. Li, T. D. Kim, Y. Liao, B. H. Robinson, L. R. Dalton, A. K. Y. Jen, *Macromolecules*, **2004**, *37*, 688-690.
- 100 J. Luo, M. Haller, H. Li, T. D. Kim, A. K. Y. Jen, *Adv. Mater.*, **2003**, *15*, 1635-1638.
- 101 R. D. Nielsen, H. L. Rommel, B. H. Robinson, *J. Phys. Chem. B*, **2004**, *108*, 8659-8667.
- 102 S. D. Bella, M. A. Ratner, T. J. Marks, *J. Am. Chem. Soc.*, **1992**, *114*, 5842-5849.

- 103 L. R. Dalton, A. W. Harper, B. H. Robinson, *Proc. Natl. Acad. Sci. U. S. A.*, **1997**, *94*, 4842-4847.
- 104 I. Liakatas, C. Cai, M. Bösch, M. Jäger, C. Bosshard, P. Günter, C. Zhang, L. R. Dalton, *Appl. Phys. Lett.*, **2000**, *76*, 1368-1370.
- 105 A. W. Harper, S. Sun, L. R. Dalton, S. M. Garner, A. Chen, S. Kalluri, W. H. Steier, B. H. Robinson, *J. Opt. Soc. Am. B*, **1998**, *15*, 329-337.
- 106 H. Ma, S. Liu, J. D. Luo, S. Suresh, L. Liu, S. H. Kang, M. Haller, T. Sassa, L. R. Dalton, A. K. Y. Jen, *Adv. Funct. Mater.*, **2002**, *12*, 565-574.
- 107 Y. V. Pereverzev, O. V. Prezhdo, L. R. Dalton, *Chem. Phys. Lett.*, **2003**, *373*, 207-212.
- 108 S. Yokoyama, T. Nakahama, A. Otomo, S. Mashiko, *J. Am. Chem. Soc.*, **2000**, *122*, 3174-3181.
- 109 J. D. Luo, H. Ma, M. Haller, A. K. Y. Jen, R. R. Barto, *Chem. Commun.*, **2002**, 888-889.
- 110 P. A. Sullivan, A. J. P. Akelaitis, S. K. Lee, G. McGrew, S. K. Lee, D. H. Choi, L. R. Dalton, *Chem. Mater.*, **2006**, *18*, 344-351.
- 111 P. A. Sullivan, H. Rommel, Y. Liao, B. C. Olbricht, A. J. P. Akelaitis, K. A. Firestone, J. W. Kang, J. Luo, J. A. Davies, D. H. Choi, B. E. Eichinger, P. J. Reid, A. Chen, A. K. Y. Jen, B. H. Robinson, L. R. Dalton, *J. Am. Chem. Soc.*, **2007**, *129*, 7523-7530.
- 112 H. Ma, B. Chen, T. Sassa, L. R. Dalton, A. K. Y. Jen, *J. Am. Chem. Soc.*, **2001**, *123*, 986-987.
- 113 P. A. Sullivan, B. C. Olbricht, A. J. P. Akelaitis, A. A. Mistry, Y. Liao, L. R. Dalton, *J. Mater. Chem.*, **2007**, *17*, 2899-2903.
- 114 Z. Shi, S. Hau, J. Luo, T. D. Kim, N. M. Tucker, J. W. Ka, H. Sun, A. Pyajt, L. Dalton, A. Chen, A. K. Y. Jen, *Adv. Funct. Mater.*, **2007**, *17*, 2557-2563.
- 115 A. K. Y. Jen, J. Luo, S. Liu, M. Haller, L. Liu, H. Ma, *Adv. Mater.*, **2002**, *14*, 1763-1768.
- 116 J. Luo, M. Haller, H. Ma, S. Liu, T. D. Kim, Y. Tian, B. Chen, S. H. Jang, L. R. Dalton, A. K. Y. Jen, *J. Phys. Chem. B*, **2004**, *108*, 8523-8530.
- 117 J. Luo, M. Haller, H. Li, H. Z. Tang, A. K. Y. Jen, K. Jakka, C. H. Chou, C. F. Shu, *Macromolecules*, **2004**, *37*, 248-250.
- 118 T. D. Kim, J. Luo, Y. Tian, J. W. Ka, N. M. Tucker, M. Haller, J. W. Kang, A. K. Y. Jen, *Macromolecules*, **2006**, *39*, 1676-1680.
- 119 S. Sioncke, T. Verbiest, A. Persoons, *Mater. Sci. Eng., R*, **2003**, *42*, 115-155.
- 120 T. Verbiest, S. Van Elshocht, M. Kauranen, L. Helleman, J. Snauwaert, C. Nuckolls, T. J. Katz, A. Persoons, *Science*, **1998**, *282*, 913-915.
- 121 G. J. Ashwell, P. D. Jackson, W. A. Crossland, *Nature*, **1994**, *368*, 438-440.

- 122 T. L. Penner, H. R. Motschmann, N. J. Armstrong, M. C. Ezenyilimba, D. J. Williams, *Nature*, **1994**, *367*, 49-50.
- 123 K. Rajesh, M. S. Chandra, S. Hirakawa, J. Kawamata, T. P. Radhakrishnan, *Langmuir*, **2007**, *23*, 8560-8568.
- 124 G. Panambur, Y. Zhang, A. Yesayan, T. Galstian, C. G. Bazuin, A. M. Ritcey, *Langmuir*, **2004**, *20*, 3606-3615.
- 125 Q. Huo, S. Russev, T. Hasegawa, J. Nishijo, J. Umemura, G. Puccetti, K. C. Russell, R. M. Leblanc, *J. Am. Chem. Soc.*, **2000**, *122*, 7890-7897.
- 126 Y. Wang, C. Wang, X. Wang, Y. Guo, B. Xie, Z. Cui, L. Liu, L. Xu, D. Zhang, B. Yang, *Chem. Mater.*, **2005**, *17*, 1265-1268.
- 127 D. Li, M. A. Ratner, T. J. Marks, C. Zhang, J. Yang, G. K. Wong, *J. Am. Chem. Soc.*, **1990**, *112*, 7389-7390.
- 128 A. K. Kakkar, S. Yitzchaik, S. B. Roscoe, F. Kubota, D. S. Allan, T. J. Marks, W. Lin, G. K. Wong, *Langmuir*, **1993**, *9*, 388-390.
- 129 T. J. Marks, M. A. Ratner, *Angew. Chem., Int. Ed.*, **1995**, *34*, 155-173.
- 130 S. Yitzchaik, T. J. Marks, *Acc. Chem. Res.*, **1996**, *29*, 197-202.
- 131 A. Facchetti, A. Abbotto, L. Beverina, M. E. van der Boom, P. Dutta, G. Evmenenko, G. A. Pagani, T. J. Marks, *Chem. Mater.*, **2003**, *15*, 1064-1072.
- 132 H. Kang, P. Zhu, Y. Yang, A. Facchetti, T. J. Marks, *J. Am. Chem. Soc.*, **2004**, *126*, 15974-15975.
- 133 M. E. van der Boom, A. G. Richter, J. E. Malinsky, P. A. Lee, N. R. Armstrong, P. Dutta, T. J. Marks, *Chem. Mater.*, **2001**, *13*, 15-17.
- 134 P. Zhu, M. E. van der Boom, H. Kang, G. Evmenenko, P. Dutta, T. J. Marks, *Chem. Mater.*, **2002**, *14*, 4982-4989.
- 135 M. E. van der Boom, G. Evmenenko, C. Yu, P. Dutta, T. J. Marks, *Langmuir*, **2003**, *19*, 10531-10537.
- 136 P. M. Lundquist, W. Lin, H. Zhou, D. N. Hahn, S. Yitzchaik, T. J. Marks, G. K. Wong, *Appl. Phys. Lett.*, **1997**, *70*, 1941-1943.
- 137 G. Wang, P. Zhu, T. J. Marks, J. B. Ketterson, *Appl. Phys. Lett.*, **2002**, *81*, 2169.
- 138 Y. G. Zhao, S. Chang, A. Wu, H. L. Lu, S. T. Ho, M. E. van der Boom, T. J. Marks, *Opt. Eng.*, **2003**, *42*, 298-299.
- 139 Y. G. Zhao, A. Wu, H. L. Lu, S. Chang, W. K. Lu, S. T. Ho, M. E. van der Boom, T. J. Marks, *Appl. Phys. Lett.*, **2001**, *79*, 587-589.

- 140 J. R. Heflin, M. T. Guzy, P. J. Neyman, K. J. Gaskins, C. Brands, Z. Wang, H. W. Gibson, R. M. Davis, K. E. Van Cott, *Langmuir*, **2006**, *22*, 5723-5727.
- 141 W. C. Flory, S. M. Mehrens, G. J. Blanchard, *J. Am. Chem. Soc.*, **2000**, *122*, 7976-7985.
- 142 G. A. Neff, M. R. Helfrich, M. C. Clifton, C. J. Page, *Chem. Mater.*, **2000**, *12*, 2363-2371.
- 143 H. E. Katz, G. Scheller, T. M. Putvinski, M. L. Schilling, W. L. Wilson, C. E. D. Chidsey, *Science*, **1991**, *254*, 1485-1487.
- 144 H. E. Katz, W. L. Wilson, G. Scheller, *J. Am. Chem. Soc.*, **1994**, *116*, 6636-6640.
- 145 Y. Wang, X. Wang, Y. Guo, Z. Cui, Q. Lin, W. Yu, L. Liu, L. Xu, D. Zhang, B. Yang, *Langmuir*, **2004**, *20*, 8952-8954.
- 146 F. Wuerthner, J. Schmidt, M. Stolte, R. Wortmann, *Angew. Chem., Int. Ed.*, **2006**, *45*, 3842-3846.
- 147 M. S. Johal, Y. W. Cao, X. D. Chai, L. B. Smilowitz, J. M. Robinson, T. J. Li, D. McBranch, D. Q. Li, *Chem. Mater.*, **1999**, *11*, 1962-1965.
- 148 Y. W. Cao, X. D. Chai, W. S. Yang, R. Lu, Y. S. Jiang, T. J. Li, M. Blanchard-Desce, J. M. Lehn, *Thin Solid Films*, **1996**, *284-285*, 859-862.
- 149 H. Saadeh, L. Wang, L. Yu, *J. Am. Chem. Soc.*, **2000**, *122*, 546-547.
- 150 C. Cai, M. M. Bosch, Y. Tao, B. Muller, Z. Gan, A. Kundig, C. Bosshard, I. Liakatas, M. Jager, P. Gunter, *J. Am. Chem. Soc.*, **1998**, *120*, 8563-8564.
- 151 A. N. Rashid, C. Erny, P. Gunter, *Adv. Mater.*, **2003**, *15*, 2024-2027.
- 152 A. Facchetti, E. Annoni, L. Beverina, M. Morone, P. Zhu, T. J. Marks, G. A. Pagani, *Nature Materials*, **2004**, *3*, 910-917.
- 153 P. Zhu, H. Kang, A. Facchetti, G. Evmenenko, P. Dutta, T. J. Marks, *J. Am. Chem. Soc.*, **2003**, *125*, 11496-11497.
- 154 T. D. Kim, J. W. Kang, J. Luo, S. H. Jang, J. W. Ka, N. Tucker, J. B. Benedict, L. R. Dalton, T. Gray, R. M. Overney, D. H. Park, W. N. Herman, A. K. Y. Jen, *J. Am. Chem. Soc.*, **2007**, *129*, 488-489.



# Chapter 3

## Enhanced Poling Efficiency in Highly Thermal and Photostable Nonlinear Optical Chromophores\*

*A series of nonlinear optical chromophores based on the highly thermal and photostable tricyanovinylidenediphenylaminobenzene (TCVDPA) was synthesized and their thermal and optical properties were investigated. Modification of the TCVDPA chromophore with bulky groups provides reduction of dipole–dipole interactions and thus great improvement of the macroscopic electro-optic (EO) response of the polymeric materials obtained by incorporating these derivatives as a guest at high loading in polysulfone. The best result was obtained with chromophore 5, bearing fluorinated aromatic substituents, which shows a doubling of the EO activity at 30 wt% (25 pm/V at 830 nm) compared with the pristine TCVDPA. The bulkier the chromophore, the lower the induced plasticization effect (as much as 50 °C difference on the T<sub>g</sub> attenuation). Furthermore, all chromophores in this study possess good processability and exhibit high thermal decomposition temperatures (highest T<sub>d</sub> = 360 °C).*

---

\* This chapter has been published in: M. Faccini, M. Balakrishnan, M. B. J. Diemeer, Z. P. Hu, K. Clays, I. Asselberghs, A. Leinse, A. Driessen, D. N. Reinhoudt, W. Verboom, *J. Mater. Chem.*, **2008**, *18*, 2141-2149.

M. Balakrishnan, M. Faccini, M. B. J. Diemeer, W. Verboom, A. Driessen, D. N. Reinhoudt, A. Leinse, *Electron. Lett.*, **2006**, *42*, 51-52.

### 3.1 Introduction

As outlined in Chapter 2, organic materials exhibiting large electro-optic (EO) responses ( $r_{33}$ ) have attracted considerable attention over the past two decades.<sup>1-7</sup> However, high nonlinearity is not enough to ensure widescale commercial utilization of polymeric electro-optic devices. Other essential properties, such as good thermal, mechanical and photochemical stability, low optical loss (high transparency) and good processability, need to be simultaneously optimized in order for the active material to be successfully implemented in a practical device.

Several classes of compounds exhibiting very high thermal stability (over 300 °C) have been reported.<sup>8-10</sup> From these studies it emerges that the use of a 4-(diarylamino)phenyl electron donor results in a significant improvement in thermal stability compared to the 4-(dialkylamino)phenyl substituted derivatives.<sup>11-15</sup>

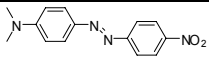
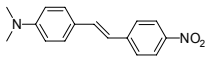
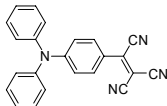
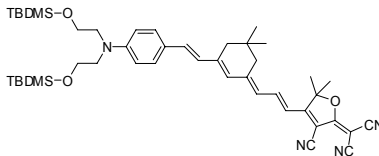
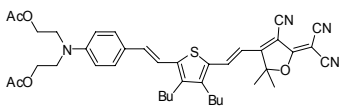
One of the most crucial parameters for the long term efficiency of EO devices is photostability, since they are expected to last years without significant degradation under high photon flux. The absorption of photons by molecules under illumination can lead to changes in their chemical structure and consequent loss of nonlinearity. Several research groups have done extensive work examining the photostability of EO polymers, taking into account the influence on the photodegradation of factors such as chromophore structure,<sup>16,17</sup> wavelength and intensity,<sup>18-20</sup> and the presence of oxygen.<sup>17,21</sup>

The general conclusion that can be drawn from these studies is that the most photostable compounds have a simple benzene  $\pi$ -bridge and a tricyanovinyl electron-acceptor group. More elongated conjugated bridges between the electron-donor and electron-acceptor groups lead to faster photobleaching. Galvan-Gonzalez et al.<sup>20</sup> identified tricyanovinylidenediphenylaminobenzene (**TCVDPA**) as the most photostable structure: it is about two orders of magnitude more stable than the **DANS** (4-*N,N*-dimethylamino-4'-nitrostilbene) chromophore and one order of magnitude more stable than the azo chromophore **DR1** (4-[*N*-ethyl-*N*-2-hydroxyethyl]amino]-4'-nitroazobenzene). In fact, it shows no degradation upon irradiation at the absorption maxima ( $\lambda_{\text{max}}$ ), nor it is acting as a sensitizer for the formation of singlet oxygen upon



radiation with UV. On the other hand, the price to pay for this higher stability is a shorter conjugation path and therefore a lower second-order nonlinearity compared to extremely large  $\mu\beta$  chromophores like **CLD** or **FTC** (Table 1).<sup>16</sup> However, it has been reported that the photostability of such chromophores is quite poor in air,<sup>22</sup> and a high-cost packaging is necessary for shielding the oxygen in the air, which is responsible for the photodegradation of the chromophore by the formation of singlet oxygen. Given that photostability is of key importance to the long-term reliability of devices, we strongly believe that **TCVDPA** (**1**) holds a strong competitiveness for EO applications, particularly for the fabrication of low-cost devices (like EO-based sensors)<sup>23</sup> operating at 850 nm, where cheap laser sources are available.

**Table 1.** Comparison of  $\lambda_{max}$  and  $\mu\beta$  values of known NLO chromophores<sup>a</sup>

NLO chromophore	$\lambda_{max}$ (nm)	$\mu\beta$ ( $10^{-48}$ esu)	$\mu\beta/M_w$	$B^d$	
	<b>DR1</b>	475	800 <sup>b,24</sup>	3.0	$5 \times 10^6$
	<b>DANS</b>	438	580 <sup>25</sup>	2.1	$2 \times 10^4$
	<b>TCVDPA</b>	531	584 <sup>c</sup>	1.7	$2 \times 10^7$
	<b>CLD</b>	695	35000 <sup>26</sup>	45.7	N/A <sup>e</sup>
	<b>FTC</b>	650	18000 <sup>27</sup>	25.9	N/A <sup>e</sup>

<sup>a</sup> Measured at 1907 nm unless otherwise indicated; <sup>b</sup> Measured at 1580 nm; <sup>c</sup>  $\mu\beta_0$ , <sup>d</sup>  $B$  is the number absorption events needed, on average, to photodegrade a single chromophore molecule; Data taken from ref.<sup>20</sup>; <sup>e</sup> Data not available.

Moreover, the **TCVDPA** chromophore possesses the unique feature of having a low absorption window in the UV region (blue window), where most of the chromophores absorb, which allows UV-crosslinking to be used for photodefinition.<sup>28</sup> It has been demonstrated that the direct waveguide photodefinition of the negative photoresist SU8 containing **TCVDPA**, using a conventional (I, H, G-line) mask aligner.<sup>29</sup> In addition, this system has the advantage that low temperature poling can be done in the uncrosslinked state, because the uncured SU8 is a low- $T_g$  solid.

A major obstacle impeding the development and employment of organic electro-optic materials is the difficulty of translating a high hyperpolarizability ( $\beta$ ) into macroscopic EO coefficient ( $r_{33}$ ). This is because, in particular at high chromophore number density ( $N$ ), dipole–dipole interactions start to become competitive with chromophore dipole–applied poling field interactions, favoring centrosymmetric arrangements of chromophores. From both theoretical and experimental analyses the Dalton group has shown that the maximum achievable EO activity of a chromophore can be greatly enhanced by modification of its shape. In fact, the derivatization of chromophores with bulky substituents will make them more spherically shaped and hence limit intermolecular electrostatic interactions.<sup>30-35</sup> These added side groups are only expected to contribute in minimizing the tendency of the dipoles to cluster in an anti-parallel fashion, positively affecting the poling efficiency and the macroscopic EO response of polymeric materials in which these chromophores are incorporated, without having any influence on the molecular hyperpolarizability.

In this Chapter we describe how the EO response and the poling efficiency of a series of thermally and photochemically stable **TCVDPA**-based chromophores (**2-6**) considerably improve by shape modification. The chromophores are incorporated as guests in a high  $T_g$  (190 °C) polysulfone (PS) polymer host matrix. The chemical, photochemical, thermal, linear optical, and non-linear optical (NLO) characterization of these chromophores and the polymeric materials derived therefrom are described.

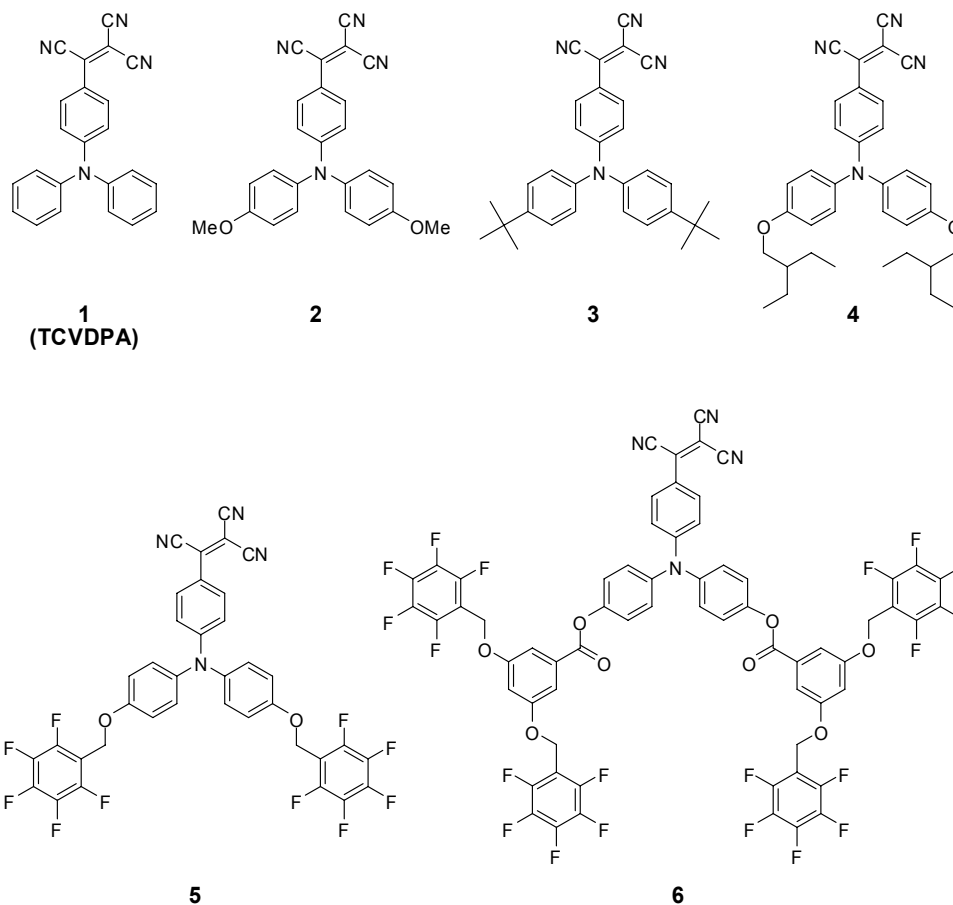


**Chart 1.** Chemical structures of chromophores 1-6.

## 3.2 Results and Discussion

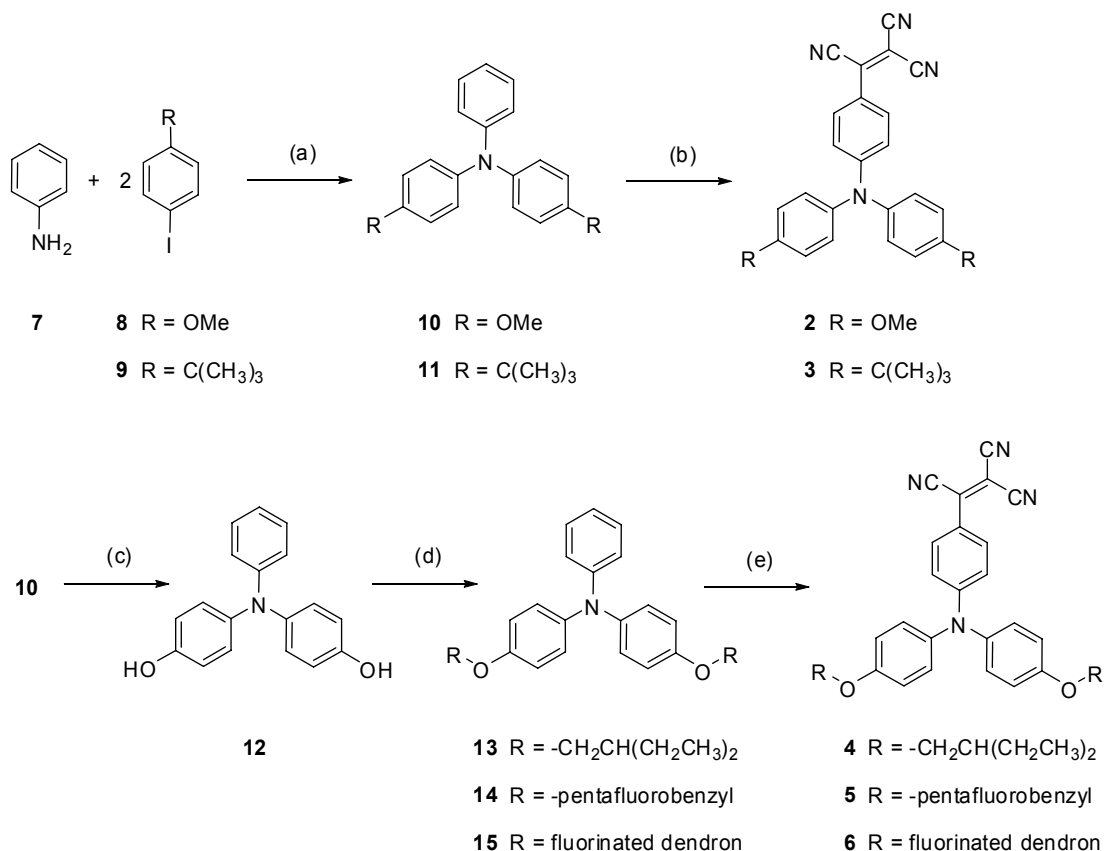
### 3.2.1 Synthesis

The synthesis of the chromophores **2-6** is depicted in Scheme 1. All chromophores were synthesized using a similar approach: first the formation of the triphenylamine donor part, substituted with the desired group, followed by tricyanovinylolation of the unsubstituted aryl ring.

The triarylamines were assembled using a copper-catalyzed amination of aryl iodides following a recently reported procedure.<sup>36,37</sup> Aniline (**7**) was reacted with 4-iodoanisole (**8**) and 1-*tert*-butyl-4-iodobenzene (**9**), respectively, in the presence of potassium *tert*-butoxide and a catalytic amount of CuI/P(But)<sub>3</sub> complex, to afford the triarylamines **10**

and **11**. Demethylation of dimethoxytriphenylamine **10** with  $\text{BBr}_3$  gave the corresponding bisphenol **12**. Subsequent functionalization of the hydroxyl groups in **12** with 1-bromo-2-ethylbutane and 2,3,4,5,6-pentafluorobenzyl bromide under Finkelstein conditions gave the dialkoxytriarylamines **13** and **14**, respectively.

*Scheme 1. Synthesis of chromophores 2-6.<sup>a</sup>*

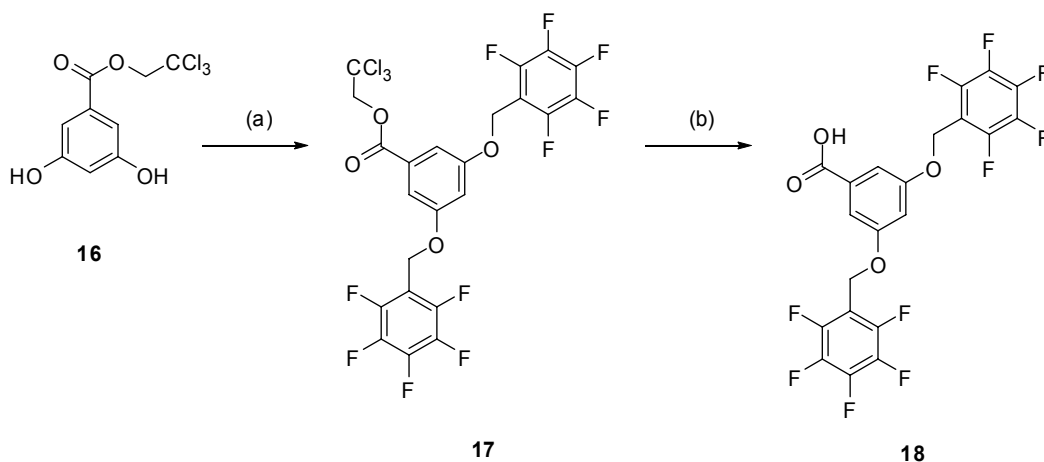


<sup>a</sup> Reagents and conditions: (a)  $\text{P}(\text{But})_3$ ,  $\text{CuI}$ ,  $\text{KOtBu}$ , toluene, reflux; (b) TCNE, DMF, rt (c)  $\text{BBr}_3$ ,  $\text{CHCl}_3$ , rt, then  $\text{CH}_3\text{OH}$ ; (d) for **13** and **14**:  $\text{K}_2\text{CO}_3$ ,  $\text{KI}$ , THF, reflux; for **15**: DCC, DMAP, THF,  $\text{CH}_2\text{Cl}_2$ , rt; (e) TCNE, DMF, rt.

Derivatization of EO chromophores with highly fluorinated dendrons has been demonstrated to be an efficient way to provide the spatial isolation needed for more efficient orientation of the chromophores.<sup>38</sup> Fluorinated dendron **18** was synthesized by reaction of protected dihydroxybenzoic acid **17**<sup>39</sup> with 2,3,4,5,6-pentafluorobenzyl bromide to give **17**, followed by deprotection of the carboxylic acid by treatment with zinc dust in glacial acetic acid (Scheme 2). Esterification of the carboxylic acid in

fluorinated dendron **19** with bisphenol **12** afforded the triarylamine diester **15**. Reaction of the disubstituted triarylamines **10**, **11**, **13-15** with tetracyanoethylene (TCNE) in DMF gave the corresponding chromophores **2-6**, respectively.

**Scheme 2.** Synthesis of dendron **18**.<sup>a</sup>



<sup>a</sup> Reagents and conditions: (a) pentafluorobenzyl bromide,  $K_2CO_3$ , KI, THF, reflux; (b) glacial acetic acid, Zn dust, THF, rt.

### 3.2.2 Linear Optical Properties

UV spectra of chromophores **1-6** were recorded in  $CH_2Cl_2$  and the  $\lambda_{max}$  values are reported in Table 2.

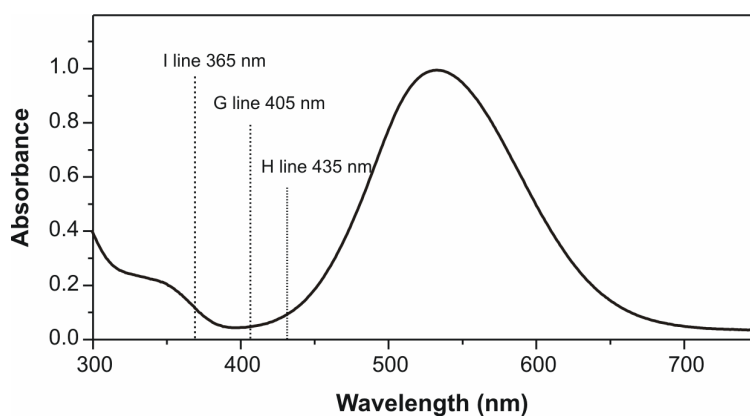


**Figure 1.** Absorption spectrum of chromophore **6** in  $CH_2Cl_2$ .

All chromophores studied have a strong charge-transfer band (450-650 nm) in the visible region of the spectrum. In general, no significant change in the spectrum was caused by the modification, with  $\lambda_{max}$  lying between 529 and 545 nm. A typical spectrum is shown in Figure 1. Moreover, all derivatives preserve the lower minimum in the absorption spectra (around 400 nm), between the charge-transfer band and the higher-energy aromatic electronic transitions. This blue window allows photo-induced crosslinking to be used for lattice hardening.

**Table 2.** Summary of thermal and optical properties of chromophores 1-6

	$T_d^{5\%}$ <sup>a</sup> (°C)	$T_d$ onset <sup>b</sup> (°C)	$\lambda_{max}$ <sup>c</sup> (nm)	$E$ <sup>d</sup> (M <sup>-1</sup> cm <sup>-1</sup> )	$\beta_{zzz}$ <sup>e</sup> (10 <sup>-30</sup> esu)
<b>1</b>	286	335	539	38500	425 +/- 80
<b>2</b>	296	331	530	24000	428 +/-16
<b>3</b>	292	323	537	30000	424 +/- 25
<b>4</b>	350	360	545	31000	418 +/- 42
<b>5</b>	308	326	536	31000	409 +/- 18
<b>6</b>	355	365	529	33500	275 +/- 17

<sup>a</sup> The weight loss decomposition temperature,  $T_d^{5\%}$ , is defined as the point at which 5% weight loss has occurred in the chromophore; <sup>b</sup> The onset temperature of degradation ( $T_d$  onset) can be calculated from the intersection of the tangent to the slope of the curve corresponding to the first weight loss event; <sup>c</sup>  $\lambda_{max}$  was measured in CH<sub>2</sub>Cl<sub>2</sub>; <sup>d</sup> Molar absorptivity in CH<sub>2</sub>Cl<sub>2</sub>; <sup>e</sup>  $\beta$  values were measured at 800 nm.

### 3.2.3 Optical Loss Measurements

Optical losses were measured by the prism coupling method and they are shown in Figure 2. Slab waveguides were made on 8  $\mu$ m thick silicon oxide on silicon wafers by spincoating PS and 1 20 % w/w in PS. The resulting film thickness was about 4  $\mu$ m and it sustains three modes at 1550 nm. As the surface of the spin coated film is extremely smooth, the loss mechanism is mainly due to material absorption. White light from a broadband source is coupled into the polymer slab using a prism. After propagating a certain distance it is out-coupled using another prism and sent to a spectrum analyzer.

The experiment is repeated varying the distance between the in-coupling and the out-coupling prisms. By plotting the out-coupled power as a function of the distance of propagation it is possible to obtain the absorption loss spectra.

In general, device-quality EO materials should possess good optical transparency (low optical loss), in particular at the main telecom wavelengths (1310 and 1550 nm) and datacom wavelengths (840 nm). For the PS host polymer the optical loss remains relatively low (around 1 dB/cm) either at 840, 1310, or at 1550 nm. This retained loss could probably be addressed to light scattering from particles or roughness due to polymer processing. When 20 wt % of chromophore **1** is incorporated as guest into a PS host matrix, the long-wavelength tail of the main absorption peak of the chromophore is appearing, extending further into the near-IR and therefore causing a high loss of 7.2 dB/cm at 840 nm. Although the high chromophore loading causes big vibrational C-H overtone absorptions to appear, this does not have a detrimental effect on the optical transparency at telecom wavelength, which only increases to 1.7 and 1.5 at 1310 and 1550 nm, respectively, making the material well suitable for telecom waveguide applications.

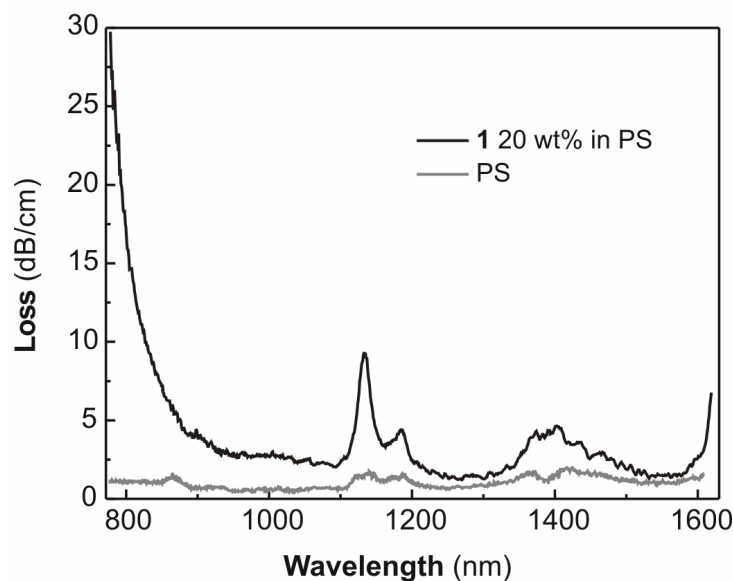


**Figure 2.** Optical loss spectrum of PS and chromophore **1** at 20 wt. % in PS slab waveguides.

### 3.2.4 Thermal Analysis

The thermal properties of the chromophores are reported in Table 2. TGA data were recorded at a heating rate of 20 °C/min. It should be noted that weight loss in these experiments may be due to sublimation and/or decomposition of the substance.

Thermal stability is a critical parameter for long term efficiency of EO devices. Since the NLO response has to be stable during processing and operation of the chromophore/polymer materials, the chromophores need to be chemically stable at all temperatures that the system encounters in electric field poling, and they should withstand all fabrication steps needed for device fabrication.

The decomposition temperature of chromophores **1-6** is really high, being above 320 °C for all of them. The highest value, 365 °C, which has been recorded for **6**, is among the highest ever reported for NLO chromophores.

### 3.2.5 Photobleaching Test

Several research groups have done extensive work examining the photostability of EO polymers. Previous studies clearly show that the presence of oxygen can greatly increase the degradation rate of organic chromophores.<sup>17,40</sup> The photodegradation of various chromophore families has been reported, including stilbenes and azobenzenes. In these studies the photobleaching measurements were made by using lasers as a light source on film samples of guest-host polymeric materials.

Here we introduce a straightforward and low-cost qualitative method for the fast screening of the photostability of new chromophores. These simple photobleaching tests are carried out by monitoring the decrease in absorbance during irradiation of oxygen-saturated solutions of chromophores in CDCl<sub>3</sub> with visible white light. The experiments were conducted in CDCl<sub>3</sub> because the singlet oxygen (<sup>1</sup>O<sub>2</sub>) has a very long lifetime in this solvent, so that its effect can be established with greater sensitivity.<sup>41</sup> Although being qualitative, thus producing relative results instead of absolute values, this technique can give good estimation of the photostability, particularly, when a direct comparison with chromophores of known photostability *B* is performed.



Photobleaching tests were carried out for chromophores **1**, **3**, and **5**, and for the commercially available NLO chromophores **DANS** and **DR1** (Table 1). In fact, our measurements are in good relative agreement with the reported data (see Table 1), showing that the stilbene chromophore **DANS** degrades very rapidly due to the attack on the central carbon double bond by oxygen. The most photostable compounds are characterized by benzene bridges and tricyanovinyl electron-acceptor groups. From the results reported in Figure 3 it can be noticed that chromophores **1**, **3**, and **5**, are photostable under our experimental conditions, showing hardly any degradation upon exposure to white light for 120 min. Moreover, comparing the decay curves of chromophores **3** and **5** with that of **1**, no significant difference can be noticed. More than 95% of the initial absorbance is retained after 100 min of exposure, showing that functionalization with bulky side groups does not have a detrimental influence on the photostability. From these data it can be concluded that chromophores **1-6** possess among the highest photostabilities reported for D- $\pi$ -A chromophores.

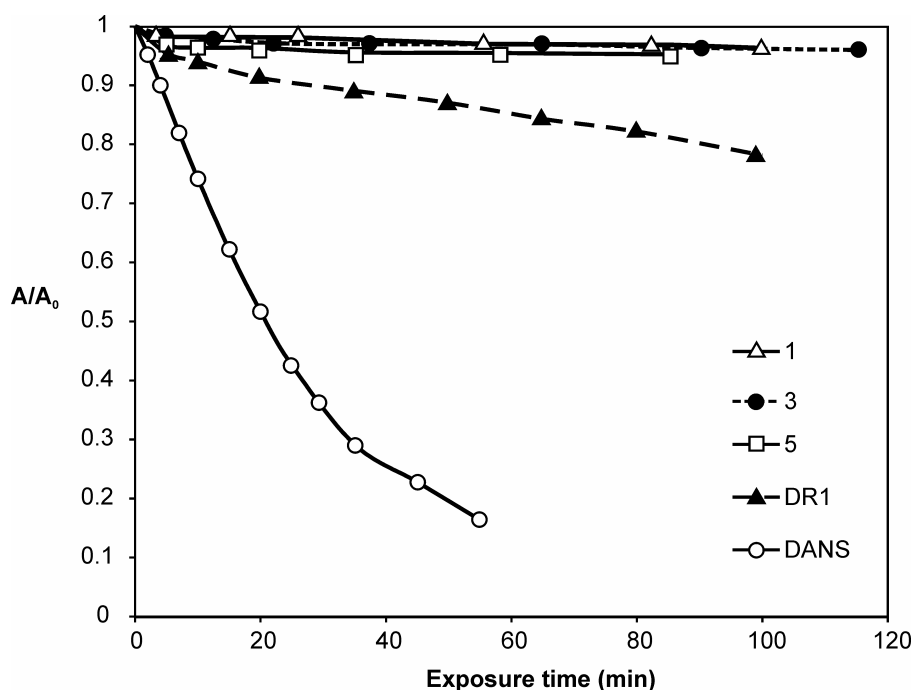


**Figure 3.** Photo-bleaching curves of chromophores **1**, **3**, **5**, **DR1**, and **DANS** in  $\text{CDCl}_3$ .  $A$  is the absorbance at time  $t$  and  $A_0$  is the initial absorbance. Photolyses were carried out in 10 mm quartz cuvettes with light from a 75 Watt halogen lamp. The samples were irradiated at a distance of 10 cm from the light source and were shielded from daylight.

### 3.2.6 Hyper-Rayleigh Scattering Measurements

The Hyper-Rayleigh scattering (HRS) technique was employed to measure  $\beta_{zzz}$  for all chromophores at 800 nm (Table 2). Crystal violet chloride (CV) was used as an external reference. In most of the cases, the hyperpolarizability is quite constant, slightly above  $400 \times 10^{-30}$  esu. Apparently, the functionalization at the donor site of the chromophores, does not have a big influence on  $\beta_{zzz}$ . However, the sensibly lower value found for chromophore **6** may be due to the ester bond directly connected to the diphenylamine moiety, reducing its electron donating ability.

### 3.2.7 Electric Field Poling and EO Property Measurements

In order to study the substituent effect on the poling efficiency, EO measurements were performed in PS doped with chromophores **1-6** at different concentrations using cyclopentanone as a solvent. The resulting solutions were filtered through a 0.2- $\mu\text{m}$  filter and spin-coated onto indium tin oxide (ITO) coated glass wafers. The obtained films were then baked on a hot plate at 95 °C for 1 hour and in a vacuum oven at 95 °C for 8 hours to completely remove the solvent. A 100 nm layer of gold was then sputtered onto the films as a top electrode to perform electric-field poling. The films were contact-poled at the respective  $T_g$  for 40 min with DC electric field of 100 V/ $\mu\text{m}$ . The  $r_{33}$  values were measured using a Teng-Man simple reflection technique at a wavelength of 830 nm.<sup>42</sup>

The chromophore loading could be varied over a wide range without phase separation occurring and the resulting materials could easily be processed into films with high optical quality. As shown in Figure 4, for unmodified chromophore **1**, the EO activity increases linearly with loading up to 15 wt %, after which the curve starts to deviate from linearity, showing evidence of chromophore-chromophore electrostatic interactions starting to take place. A similar behavior was noticed for chromophore **2**, in which the methoxy groups are not big enough to significantly affect the interactions, but only providing a small improvement of about 2 pm/V with respect to **1**. Moreover, **1** and **2** remain at lower  $r_{33}$  values compared with other bulky substituted chromophores, like **3**, **4**, and **5** (Figures 4), suggesting a significantly higher dipole-dipole interaction already at low loadings. However, the increment in poling efficiency provided by the *tert*-butyl

groups of **3** and the branched alkoxy moieties of **4** is clearly visible already at low chromophore loadings, whereas at larger concentrations the shape modification is even more effective showing a nearly doubling of  $r_{33}$  at 35 wt % with respect to **1** (from 12.5 pm/V to 25 pm/V). The best result was obtained with chromophore **5**, that provides a more significant enhancement of the EO response reaching its maximum  $r_{33}$  of 25 pm/V at already 30 wt %. Probably, the very bulky pentafluorobenzyl groups provide the site isolation needed for free chromophore reorientation under electric field poling conditions. In the case of the dendritic chromophore **6**, an EO coefficient of only 5.5 pm/V was obtained at 10 wt %. Even though this chromophore is the bulkiest of the whole series and thus it is expected to induce the highest poling efficiency, its  $r_{33}$  value recorded at 10 wt % does not even follow the linear slope observed for the smaller fluorinated aromatic derivative **5**. The increment of  $r_{33}$  compared with **1** is only 20% at low loading. This result suggests that a good compromise has to be found for a given chromophore in order to achieve the site isolation needed for maximizing the poling efficiency.

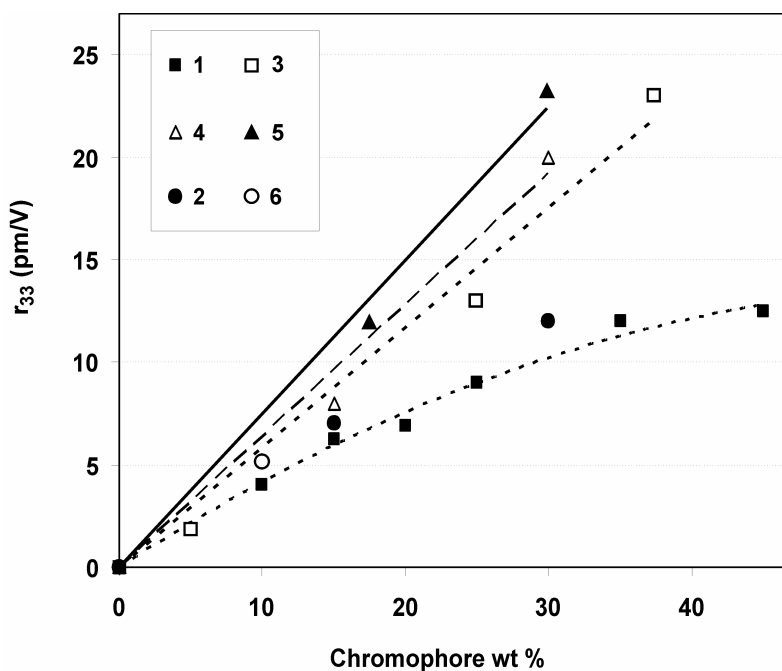


**Figure 4.**  $r_{33}$  at 830 nm as function of the effective concentrations of **1-6** in PS.

It can be concluded that, since the hyperpolarizability is similar for all chromophores, the enhancements in  $r_{33}$  for the shape modified chromophores are not due to

improvements at the molecular level, but indeed to reduced electrostatic interactions between chromophores and hence to a better poling efficiency.

For comparison,  $T_g$  has been plotted against the loading density for films made with chromophores **1**, **3**, and **6**. From the curves shown in Figure 5, a clear decay of the  $T_g$  of the material can be seen upon increasing the chromophore concentration. This is a common behavior in guest-host systems in which the NLO chromophore, being simply dissolved in a polymer matrix, can act as a plasticizer and consequently decreases the  $T_g$  of the polymeric material.<sup>3</sup> An interesting trend can be noticed in the decay: the bulkier the chromophore ( $\mathbf{1} < \mathbf{3} < \mathbf{6}$ ), the lower its plasticization effect is. In fact, when **1** is incorporated in PS at 45 wt%, the  $T_g$  of the resulting blend drops to 80 °C. Such a low  $T_g$  is detrimental for the long term efficiency of a device, causing serious relaxation of the molecular alignment. Differently, dendritic chromophore **6** at 50 wt % loading displays a much improved  $T_g$  of 130 °C, resulting in a better material for long term device applications.

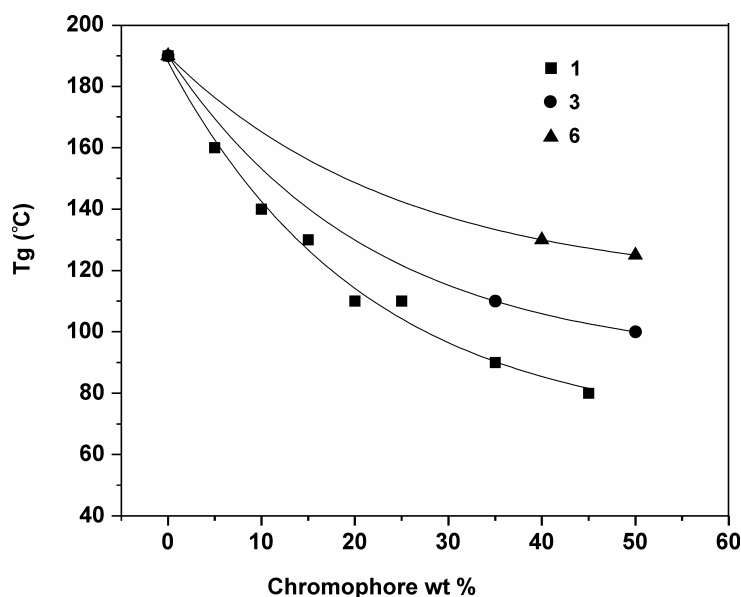


**Figure 5.** Comparison of the  $T_g$  for chromophores **1**, **3**, and **6** incorporated in PS at different concentrations.

### 3.3 Conclusions

A series of nonlinear optical chromophores was synthesized by applying a shape modification to the TCVDPA chromophore. These changes have led to a decrease of the chromophore induced plasticization effect and to a great reduction of intermolecular interactions. Consequently, improved poling efficiencies were observed for most of the derivatives when incorporated at high loadings in PS host polymer. A doubling of the EO activity was even obtained for chromophore **5**, compared with the pristine TCVDPA, showing an EO coefficient of 25 pm/V at 830 nm. Moreover, all chromophores exhibit a good processability and possess among the highest thermal and photochemical stabilities reported in literature.

### 3.4 Experimental Section

**General Procedures.** All chemicals were of reagent grade and used without further purification. THF was freshly distilled from Na/benzophenone, and CH<sub>2</sub>Cl<sub>2</sub> from CaCl<sub>2</sub>. All chromatography associated with product purification was performed by flash column techniques using Merck Kieselgel 600 (230-400 mesh). All reactions were carried out under an inert argon atmosphere. Melting points (uncorrected) of all compounds were obtained with a Reichert melting point apparatus and a Kofler stage. <sup>1</sup>H and <sup>13</sup>C NMR spectra were recorded on a Varian Unity 300 using tetramethylsilane (TMS) or the corresponding residual solvent signal as internal standard. FAB-MS spectra were recorded on a Finningan MAT 90 spectrometer with *m*-nitrobenzyl alcohol (NBA) as a matrix. Thermogravimetric analyses were conducted using a Perkin-Elmer TGA-7 thermogravimetric analyzer (scanning rate: 20 °C min<sup>-1</sup>). UV-Vis measurements were carried out on a Varian Cary 3E UV-spectrophotometer.

HRS measurements were performed using the 800 nm fundamental wavelength of a regenerative mode-locked Ti<sup>3+</sup> sapphire laser.<sup>43</sup> Measurements were carried out in CH<sub>2</sub>Cl<sub>2</sub>, with CV as an external reference ( $\beta_{xxx}$ ),  $338 \times 10^{-30}$  esu in methanol at 800 nm, taking into account the difference in symmetry (octopolar for CV and dipolar for the

chromophores). The sample was dissolved in CH<sub>2</sub>Cl<sub>2</sub> and passed through 0.2 μm filters. Dilute solutions (10<sup>-5</sup>-10<sup>-6</sup> M) were used to ensure a linear dependence of  $I_{2\omega}/I_{\omega}^2$  on solute concentration, precluding the need for a Lambert-Beer correction for self-absorption of the second harmonic generation (SHG) signal. High-frequency femtosecond HRS was used to assess any multiphoton fluorescence contribution at 400 nm. No fluorescence effects were observed at 400 nm for all chromophores.

For poled films, the  $T_g$  is defined as the temperature at which a change in the reflection of the top gold electrode is first noticed, by heating the sample is on a heating chuck, raising the temperature in steps of 10 °C and holding for 5 min at each step. The change of mobility in the material at the  $T_g$  causes the gold to buckle, hence losing perfect light reflectivity.

Compounds **10**<sup>44</sup> and **16**<sup>39</sup> were prepared according to procedures reported in literature.

**Compound 2.** To a solution of **10** (960 mg, 3.14 mmol) in dry DMF (30 mL) was added tetracyanoethylene (805 mg, 6.28 mmol) and the resulting mixture was stirred at rt for 12 h. The solvent was removed under reduced pressure and the residue dissolved in CH<sub>2</sub>Cl<sub>2</sub> (100 mL) and then washed with water (3 × 50 mL). The organic layer was dried over MgSO<sub>4</sub> and the resulting solid was purified by chromatography (hexane/ CH<sub>2</sub>Cl<sub>2</sub> 1/1) to give **2** as a purple solid (1.2 g, 93%): mp 157-160 °C. <sup>1</sup>H NMR (CDCl<sub>3</sub>) δ 3.84 (s, 6H, OCH<sub>3</sub>), 6.84 (d,  $J = 9.3$  Hz, 2H, ar-H), 6.95 (d,  $J = 9.0$  Hz, 4H, ar-H), 7.15 (d,  $J = 9.0$  Hz, 4H, ar-H), 7.95 (d,  $J = 9.6$  Hz, 2H, ar-H); <sup>13</sup>C NMR (CDCl<sub>3</sub>) δ 55.5, 100.4, 114.2, 115.3, 116.7, 119.51, 121.9, 128.1, 132.4, 136.8, 155.0, 158.5; MS FAB<sup>+</sup>  $m/z$  406.1 ([M<sup>+</sup>], calcd for C<sub>25</sub>H<sub>18</sub>N<sub>4</sub>O<sub>2</sub> 406.1), FAB<sup>-</sup>  $m/z$  405.9 ([M<sup>-</sup>], calcd 406.1).

**4-4'-Di-tert-butyltriarylamine (11)** was prepared analogously to compound **10**, starting from aniline (**7**) (0.48 mL, 5.24 mmol), 1-tert-butyl-4-iodobenzene (**9**) (2.0 mL, 11.53 mmol), CuI (40 mg, 0.21 mmol), tributyl phosphine (0.10 mL, 0.42 mmol), and KOtBu (1.9 g, 15.72 mmol). Compound **11** was obtained as a white solid (1.16 g, 62%): mp 100-102 °C. <sup>1</sup>H NMR (CDCl<sub>3</sub>) δ 1.39 (s, 18H, C(CH<sub>3</sub>)<sub>3</sub>), 7.01 (t,  $J = 6.9$  Hz, 1H, ar-H), 7.09 (d,  $J = 8.4$  Hz, 4H, ar-H), 7.14 (d,  $J = 7.8$  Hz, 2H, ar-H), 7.29 (t,  $J = 7.8$  Hz, 2H, ar-H), 7.32 (d,  $J = 8.4$  Hz, 4H, ar-H); <sup>13</sup>C NMR (CDCl<sub>3</sub>) δ 31.4, 34.2, 121.8, 123.3, 123.7,

125.9, 129.0, 145.1, 145.3, 148.1; MS MALDI-TOF  $m/z$  357.5 ( $[M^+]$ , calcd for  $C_{26}H_{31}N$  357.5).

**Compound 3.** Triarylamine **11** (550 mg, 1.54 mmol) was reacted with tetracyanoethylene (790 mg, 6.16 mmol) following a procedure similar to that used for **2**, giving **3** as a purple solid (0.57 g, 80%): mp  $>230$  °C;  $^1H$  NMR ( $CDCl_3$ )  $\delta$  1.36 (s, 18H,  $C(CH_3)_3$ ), 6.91 (d,  $J = 9.0$  Hz, 2H, ar-H), 7.16 (d,  $J = 8.4$  Hz, 4H, ar-H), 7.44 (d,  $J = 8.4$  Hz, 4H, ar-H), 7.97 (d,  $J = 9.0$  Hz, 2H, ar-H);  $^{13}C$  NMR ( $CDCl_3$ )  $\delta$  31.2, 34.4, 113.2, 113.4, 114.2, 117.4, 126.40, 127.0, 132.3, 139.2, 141.3, 150.3, 154.8; MS MALDI-TOF  $m/z$  458.1 ( $[M^+]$ , calcd for  $C_{31}H_{30}N_4$  458.2),  $FAB^-$   $m/z$  458.2 ( $[M^-]$ , 458.1).

**Bisphenol 12.** A solution of **10** (7.5 g, 24.6 mmol) in dry chloroform (100 mL) was cooled to 0 °C, and  $BBr_3$  (98.4 mL 1 M-solution in  $CH_2Cl_2$ , 94.8 mmol) was added dropwise. After stirring for 1 h at this temperature, the reaction mixture was allowed to warm up to rt and stirred for 5 h. The reaction was carefully quenched with methanol using an ice bath. The solvent was removed under reduced pressure and the residue dissolved in ethyl acetate (200 mL). The resulting solution was washed with a saturated solution of  $NaHCO_3$  ( $2 \times 100$  mL) and water ( $2 \times 100$  mL), dried over  $MgSO_4$ , and evaporated to give **12** as a grey solid (6.8 g, 100%): mp 220-222 °C;  $^1H$  NMR ( $DMSO-d_6$ )  $\delta$  6.64 (d,  $J = 8.4$  Hz, 2H, ar-H), 6.70 (d,  $J = 8.3$  Hz, 4H, ar-H), 6.50-6.75 (m, 1H, ar-H), 6.88 (d,  $J = 8.3$  Hz, 4H, ar-H), 7.09 (t,  $J = 7.2$  Hz, 2H, ar-H), 9.22 (s, 2H, OH);  $^{13}C$  NMR ( $DMSO-d_6$ )  $\delta$  116.8, 119.0, 119.8, 127.7, 129.5, 139.4, 149.6, 154.61; MS  $FAB^+$   $m/z$  277.1 ( $[M^+]$ , calcd for  $C_{18}H_{15}NO_2$  277.1),  $FAB^-$   $m/z$  276.0 ( $[M-H^-]$ , calcd 276.0).

**Dialkoxytriarylamine 13.** To a solution of **12** (1.5 g, 5.4 mmol) in dry DMF (15 mL) was added  $K_2CO_3$  (5.9 g, 43.3 mmol) and the mixture was stirred at rt for 30 min. After the addition of 1-bromo-2-ethylbutane (6.6 mL, 32.5 mmol) and KI (5.4 g, 32.4 mmol), the reaction mixture was allowed to warm up to 70 °C and stirred for 24 h. After evaporating the solvent, the residue was dissolved in  $CH_2Cl_2$  (100 mL) and then washed with a 10% HCl solution until neutral pH and water ( $3 \times 50$  mL). The organic phase was dried over  $MgSO_4$ , concentrated under reduced pressure and the residue further purified

by chromatography (hexane/CH<sub>2</sub>Cl<sub>2</sub> 4/1) to afford **13** as a colorless oil (1.9 g, 85%): <sup>1</sup>H NMR (CDCl<sub>3</sub>) δ 0.94 (t, *J* = 7.2 Hz, 12H, CH<sub>3</sub>), 1.42-1.53 (m, 8H, CH<sub>2</sub>), 1.68-1.62 (m, 2H, CH), 3.82 (d, *J* = 5.4 Hz, 4H, OCH<sub>2</sub>), 6.75-6.86 (m, 5H, ar-H), 6.40 (d, *J* = 7.8 Hz, 2H, ar-H), 7.03 (d, *J* = 7.5 Hz, 4H, ar-H), 7.13 (t, *J* = 7.0 Hz, 2H, ar-H); <sup>13</sup>C NMR (CDCl<sub>3</sub>) δ 11.4, 23.6, 41.2, 70.6, 115.4, 120.6, 120.9, 126.6, 129.1, 141.1, 149.1, 155.8; MS FAB<sup>+</sup> *m/z* 445.3 ([M<sup>+</sup>], calcd for C<sub>30</sub>H<sub>39</sub>NO<sub>2</sub> 445.3).

**Compound 4.** Reaction of **13** (780 mg, 1.75 mmol) with tetracyanoethylene (1.3 g, 10.5 mmol) following a procedure similar to that for **2**, yielded **4** as a purple solid (717 mg, 75%): mp 130 °C; <sup>1</sup>H NMR (CDCl<sub>3</sub>) δ 0.96 (t, *J* = 7.5 Hz, 12H, CH<sub>3</sub>), 1.42-1.50 (m, 8H, CH<sub>2</sub>), 1.61-1.71 (m, 2H, CH), 3.85 (d, *J* = 6.0 Hz, 4H, OCH<sub>2</sub>), 6.84 (d, *J* = 9.0 Hz, 2H, ar-H), 6.92 (d, *J* = 8.7 Hz, 4H, ar-H), 7.12 (d, *J* = 8.7 Hz, 4H, ar-H), 7.93 (d, *J* = 9.6 Hz, 2H, ar-H); <sup>13</sup>C NMR (CDCl<sub>3</sub>) δ 11.4, 23.6, 41.1, 70.6, 79.9, 113.6, 113.8, 114.5, 116.1, 116.9, 119.7, 128.3, 132.6, 137.7, 155.4, 158.6; MS FAB<sup>+</sup> *m/z* 546.0 ([M<sup>+</sup>], calcd for C<sub>35</sub>H<sub>38</sub>F<sub>10</sub>N<sub>4</sub>O<sub>2</sub> 546.3).

**Dialkoxytriarylamine 14.** To a solution of **12** (700 mg, 2.52 mmol) in dry DMF (15 mL) was added K<sub>2</sub>CO<sub>3</sub> (3.5 g, 25.2 mmol) and the mixture was stirred at rt for 30 min. After the addition of 2,3,4,5,6-pentafluorobenzyl bromide (1.53 mL, 10.1 mmol) and KI (1.68 g, 10.1 mmol), the reaction mixture was allowed to warm up to 70 °C and stirred for 24 h. After evaporating the solvent, the residue was dissolved in CH<sub>2</sub>Cl<sub>2</sub> (100 mL) and then washed with a 10% HCl solution until neutral pH and water (3 × 50 mL). The organic phase was dried over MgSO<sub>4</sub>, concentrated under reduced pressure and the residue further purified by chromatography (hexane/CH<sub>2</sub>Cl<sub>2</sub> 6/4) to afford **14** as a white off solid (1.40 g, 88%): mp 103-105 °C; <sup>1</sup>H NMR (CDCl<sub>3</sub>) δ 5.02 (s, 4H, OCH<sub>2</sub>), 6.80 (d, *J* = 9.3 Hz, 4H, ar-H), 6.70-6.98 (m, 1H, ar-H), 6.90 (d, *J* = 8.4 Hz, 2H, ar-H), 6.97 (d, *J* = 9.3 Hz, 4H, ar-H), 7.12 (t, *J* = 8.4 Hz, 2H, ar-H); <sup>13</sup>C NMR (CDCl<sub>3</sub>) δ 57.8, 110.2, 115.8, 121.4, 121.9, 126.0, 129.0, 138.8, 140.4, 142.3, 142.9, 144.5, 146.9, 148.3, 153.8; MS FAB<sup>+</sup> *m/z* 637.2 ([M<sup>+</sup>], calcd for C<sub>32</sub>H<sub>17</sub>F<sub>10</sub>NO<sub>2</sub> 637.1).



**Compound 5.** Reaction of **14** (1.36 g, 2.14 mmol) with tetracyanoethylene (823 mg, 6.42 mmol) following a procedure similar to that for **2**, gave **5** as a purple solid (1.10 g, 68%): mp 207-209 °C;  $^1\text{H}$  NMR ( $\text{CDCl}_3$ )  $\delta$  5.14 (s, 4H,  $\text{OCH}_2$ ), 6.86 (d,  $J = 9.0$  Hz, 2H, ar-H), 7.01 (d,  $J = 9.3$  Hz, 4H, ar-H), 7.18 (d,  $J = 9.3$  Hz, 4H, ar-H), 7.95 (d,  $J = 9.0$  Hz, 2H, ar-H);  $^{13}\text{C}$  NMR ( $\text{CDCl}_3$ )  $\delta$  57.6, 81.0, 113.0, 113.3, 114.2, 116.3, 117.0, 119.80, 128.3, 132.3, 137.9, 147.0, 154.7, 156.7; MS  $\text{FAB}^+$   $m/z$  738.8 ( $[\text{M}^+]$ , calcd for  $\text{C}_{37}\text{H}_{16}\text{F}_{10}\text{N}_4\text{O}_2$  738.1,  $\text{FAB}^-$   $m/z$  738.5 ( $[\text{M}^-]$ , calcd 738.1).

**2,2,2-Trichloroethyl 3,5-bis(perfluorobenzoyloxy)benzoate (17)** was prepared analogously to **14** starting from **16** (1.6 g, 5.60 mmol), pentafluorobenzyl bromide (2.03 mL, 13.4 mmol),  $\text{K}_2\text{CO}_3$  (7.7 g, 56.0 mmol) and KI (3.7 g, 22.4 mmol) in dry THF (30 mL) instead of dry DMF. Compound **17** was obtained as a colorless oil (1.18 g, 33%).  $^1\text{H}$  NMR ( $\text{CDCl}_3$ ),  $\delta$  4.97 (s, 2H,  $\text{COOCH}_2$ ), 5.17 (s, 4H,  $\text{OCH}_2$ ), 6.82 (t,  $J = 2.1$  Hz, 1H, ar-H), 7.41 (d,  $J = 2.1$  Hz, 2H, ar-H); MS  $\text{FAB}^+$   $m/z$  645.4, calcd for  $\text{C}_{23}\text{H}_9\text{Cl}_3\text{F}_{10}\text{O}_4$  645.6.

**3,5-Bis(perfluorobenzoyloxy)benzoic acid (18).** To a solution of **17** (1.18 g, 1.82 mmol) in dry THF (6 mL) was added glacial acetic acid (6 mL), and the mixture was stirred at rt for 10 min. Zn dust (0.74 g, 11.5 mmol) was then added and the resulting mixture was stirred vigorously for 1.5 h. The reaction mixture was filtered and the filtrate was poured into water (100 mL). After extracting with diethyl ether, ( $2 \times 50$  mL) the combined extracts were dried over  $\text{MgSO}_4$  and the solvent removed under reduced pressure to afford **18** as a white solid (0.94 g, 100%): mp 158-159 °C;  $^1\text{H}$  NMR ( $\text{CDCl}_3$ )  $\delta$  5.16 (s, 4H,  $\text{CH}_2$ ), 6.79 (t,  $J = 3.0$  Hz, 1H, ar-H), 7.40 (d,  $J = 3.0$  Hz, 2H, ar-H);  $^{13}\text{C}$  NMR ( $\text{CDCl}_3$ )  $\delta$  58.0, 108.5, 109.6, 131.7, 136.1, 144.3, 147.6, 159.3, 170.7; MS  $\text{FAB}^+$   $m/z$  514.1 ( $[\text{M}^+]$ , calcd 514.0); MS  $\text{FAB}^+$   $m/z$  514.1 ( $[\text{M}^+]$ , calcd for  $\text{C}_{21}\text{H}_8\text{F}_{10}\text{O}_4$  514.0),  $\text{FAB}^-$   $m/z$  512.8 ( $[\text{M} - \text{H}^-]$ , calcd 513.0).

**Fluorinated Dendron (15).** To a solution of **18** (600 mg, 1.17 mmol) in a mixture of dry  $\text{CH}_2\text{Cl}_2$  (4 mL) and dry THF (8 mL) was added **13** (147 mg, 0.53 mmol) followed by 4-dimethylaminopyridine (DMAP) (65 mg, 0.53 mmol), and the mixture was stirred at rt for 15 min.  $N,N'$ -dicyclohexylcarbodiimide (DCC) (264 mg, 1.28 mmol) was then added,

and the mixture was stirred for 48 h. The reaction mixture was filtered, and the filtrate was evaporated to dryness under reduced pressure. The crude product was purified by silica gel column chromatography (hexane/ CH<sub>2</sub>Cl<sub>2</sub> 1/1) to afford **15** as a yellow solid (347 mg, 52%): mp 69-71 °C; <sup>1</sup>H NMR (CDCl<sub>3</sub>) δ 5.18 (s, 8H, OCH<sub>2</sub>), 6.81-6.83 (m, 2H, ar-H), 7.02-7.07 (m, 1H, ar-H), 7.07-7.12 (m, 4H, ar-H), 7.12-7.15 (m, 2H, ar-H), 7.16-7.18 (m, 4H, ar-H), 7.28-7.30 (m, 2H, ar-H), 7.48-7.49 (m, 4H); <sup>13</sup>C NMR (CDCl<sub>3</sub>) δ 58.0, 108.2, 109.6, 122.5, 123.4, 124.5, 125.1, 129.6, 132.2, 136.1, 139.5, 144.3, 145.8, 146.2, 147.8, 159.4, 164.7; MS MALDI-TOF *m/z* 1269.1 ([M<sup>+</sup>], calcd for C<sub>60</sub>H<sub>27</sub>F<sub>20</sub>NO<sub>8</sub> 1269.0).

**Compound 6.** To a solution of **15** (300 mg, 0.24 mmol ) in DMF (10 mL) was added tetracyanoethylene (605 mg, 4.72 mmol), followed by heating at 90 °C for 48 h. The solvent was removed under reduced pressure and the residue dissolved in CH<sub>2</sub>Cl<sub>2</sub> (50 mL). The solution was washed with a saturated brine solution (4 × 100 mL). The organic layer was dried over MgSO<sub>4</sub> and the resulting solid was purified by chromatography (hexane/CH<sub>2</sub>Cl<sub>2</sub> 3/7) to give **6** as a purple solid (279 mg, 86%): mp 103-105 °C ; <sup>1</sup>H NMR (CDCl<sub>3</sub>) δ 5.20 (s, 8H, OCH<sub>2</sub>), 6.86 (t, *J* = 2.1 Hz, 2H, ar-H), 7.04 (d, *J* = 9.3 Hz, 2H, ar-H), 7.26 (d, *J* = 9.0 Hz, 4H, ar-H), 7.33 (d, *J* = 9.0 Hz, 4H, ar-H), 7.49 (d, *J* = 2.1 Hz, 4H, ar-H), 8.00 (d, *J* = 9.3 Hz, 2H, ar-H); <sup>13</sup>C NMR (CDCl<sub>3</sub>) δ 58.0, 108.3, 109.6, 113.1, 114.2, 118.5, 120.8, 123.7, 128.1, 131.6, 132.5, 138.6, 142.06, 149.4, 154.3, 159.4, 164.3; MS MALDI-TOF *m/z* 1369.4 ([M<sup>+</sup>], calcd for C<sub>65</sub>H<sub>26</sub>F<sub>20</sub>N<sub>4</sub>O<sub>8</sub> 1370.0)

### 3.5 References

- 1 L. R. Dalton, *Adv. Polym. Sci.*, **2002**, *158*, 1-86.
- 2 L. R. Dalton, A. W. Harper, R. Ghosn, W. H. Steier, M. Ziari, H. Fetterman, Y. Shi, R. V. Mustacich, A. K. Y. Jen, K. J. Shea, *Chem. Mater.*, **1995**, *7*, 1060-1081.
- 3 C. Samyn, T. Verbiest, A. Persoons, *Macromol. Rapid Commun.*, **2000**, *21*, 1-15.
- 4 Y. Q. Shi, C. Zhang, H. Zhang, J. H. Bechtel, L. R. Dalton, B. H. Robinson, W. H. Steier, *Science*, **2000**, *288*, 119-122.

- 5 A. M. Sinyukov, M. R. Leahy, L. M. Hayden, M. Haller, J. D. Luo, A. K. Y. Jen, L. R. Dalton, *Appl. Phys. Lett.*, **2004**, *85*, 5827-5829.
- 6 M. Lee, H. E. Katz, C. Erben, D. M. Gill, P. Gopalan, J. D. Heber, D. J. McGee, *Science*, **2002**, *298*, 1401-1403.
- 7 F. Kajzar, K. S. Lee, A. K. Y. Jen, *Adv. Polym. Sci.*, **2003**, *161*, 1-85.
- 8 S. Suresh, H. Zengin, B. K. Spraul, T. Sassa, T. Wada, J. D. W. Smith, *Tetrahedron Lett.*, **2005**, *46*, 3913-3916.
- 9 B. K. Spraul, S. Suresh, T. Sassa, M. Angeles Herranz, L. Echegoyen, T. Wada, D. Perahia, D. W. Smith, *Tetrahedron Lett.*, **2004**, *45*, 3253-3256.
- 10 Y. J. Cheng, J. Luo, S. Hau, D. H. Bale, T. D. Kim, Z. Shi, D. B. Lao, N. M. Tucker, Y. Tian, L. R. Dalton, P. J. Reid, A. K. Y. Jen, *Chem. Mater.*, **2007**, *19*, 1154-1163.
- 11 C. R. Moylan, R. J. Twieg, V. Y. Lee, S. A. Swanson, K. M. Betterton, R. D. Miller, *J. Am. Chem. Soc.*, **1993**, *115*, 12599-12600.
- 12 P. V. Bedworth, Y. Cai, A. K. Y. Jen, S. R. Marder, *J. Org. Chem.*, **1996**, *61*, 2242-2246.
- 13 C. R. Moylan, S. Ermer, S. M. Lovejoy, I. H. McComb, D. S. Leung, R. Wortmann, P. Krdmer, R. J. Twieg, *J. Am. Chem. Soc.*, **1996**, *118*, 12950-12955.
- 14 S. Thayumanavan, J. Mendez, S. R. Marder, *J. Org. Chem.*, **1999**, *64*, 4289-4297.
- 15 G. Koeckelberghs, T. Verbiest, M. Vangheluwe, L. De Groof, I. Asselberghs, I. Picard, K. Clays, A. Persoons, C. Samyn, *Chem. Mater.*, **2005**, *17*, 118-121.
- 16 A. Galvan-Gonzalez, G. I. Stegeman, A. K. Y. Jen, X. Wu, M. Canva, A. C. Kowalczyk, X. Q. Zhang, H. S. Lackritz, S. R. Marder, S. Thayumanavan, G. Levina, *J. Opt. Soc. Am. B*, **2001**, *18*, 1846-1853.
- 17 A. Galvan-Gonzalez, M. Canva, G. I. Stegeman, R. Twieg, T. C. Kowalczyk, H. S. Lackritz, *Opt. Lett.*, **1999**, *24*, 1741-1743.
- 18 R. S. Moshrefzadeh, D. K. Misemer, M. D. Radcliffe, C. V. Francis, S. K. Mohapatra, *Appl. Phys. Lett.*, **1993**, *62*, 16-18.
- 19 M. A. Mortazavi, H. N. Yoon, C. C. Teng, *J. Appl. Phys.*, **1993**, *74*, 4871-4876.
- 20 A. Galvan-Gonzalez, M. Canva, G. I. Stegeman, R. Twieg, K. P. Chan, T. C. Kowalczyk, X. Q. Zhang, H. S. Lackritz, S. R. Marder, S. Thayumanavan, *Opt. Lett.*, **2000**, *25*, 332-334.
- 21 M. E. DeRosa, M. He, J. S. Cites, S. M. Garner, Y. R. Tang, *J. Phys. Chem. B*, **2004**, *108*, 8725-8730.
- 22 M. C. Oh, H. Zhang, C. Zhang, H. Erlich, Y. Chang, B. Tsap, D. Chang, A. Szep, W. H. Steier, H. R. Fetterman, L. R. Dalton, *IEEE J. Sel. Top. Quantum Electron.*, **2001**, *7*, 826-835.

- 23 P. V. Lambeck, *Meas. Sci. Technol.*, **2006**, *17*, R93-R116.
- 24 C. W. Dirk, H. E. Katz, M. L. Schilling, L. A. King, *Chem. Mater.*, **1990**, *2*, 700-705.
- 25 H. E. Katz, K. D. Singer, J. E. Sohn, C. W. Dirk, L. A. King, H. M. Gordon, *J. Am. Chem. Soc.*, **1987**, *109*, 6561-6563.
- 26 L. R. Dalton, A. Harper, A. Ren, F. Wang, G. Todorova, J. Chen, C. Zhang, M. Lee, *Ind. Eng. Chem. Res.*, **1999**, *38*, 8-33.
- 27 C. H. Wang, J. N. Woodford, C. Zhang, L. R. Dalton, *J. Appl. Phys.*, **2001**, *89*, 4209-4217.
- 28 T. H. Dai, K. D. Singer, R. J. Twieg, T. C. Kowalczyk, *J. Opt. Soc. Am. B*, **2000**, *17*, 412-421.
- 29 M. Balakrishnan, M. Faccini, M. B. J. Diemeer, W. Verboom, A. Driessen, D. N. Reinhoudt, A. Leinse, *Electron. Lett.*, **2006**, *42*, 51-52.
- 30 L. R. Dalton, W. H. Steier, B. H. Robinson, C. Zhang, A. Ren, S. Garner, A. Chen, T. Londergan, L. Irwin, B. Carlson, L. Fifield, G. Phelan, C. Kincaid, J. Amend, A. K. Y. Jen, *J. Mater. Chem.*, **1999**, *9*, 1905-1920.
- 31 A. W. Harper, S. Sun, L. R. Dalton, S. M. Garner, A. Chen, S. Kalluri, W. H. Steier, B. H. Robinson, *J. Opt. Soc. Am. B*, **1998**, *15*, 329-337.
- 32 I. Liakatas, C. Cai, M. Bösch, M. Jäger, C. Bosshard, P. Günter, C. Zhang, L. R. Dalton, *Appl. Phys. Lett.*, **2000**, *76*, 1368-1370.
- 33 L. R. Dalton, A. W. Harper, B. H. Robinson, *Proc. Natl. Acad. Sci. U. S. A.*, **1997**, *94*, 4842-4847.
- 34 R. D. Nielsen, H. L. Rommel, B. H. Robinson, *J. Phys. Chem. B*, **2004**, *108*, 8659-8667.
- 35 B. H. Robinson, L. R. Dalton, *J. Phys. Chem. A*, **2000**, *104*, 4785-4795.
- 36 N. M. Patil, A. A. Kelkar, Z. Nabi, R. V. Chaudhari, *Chem. Commun.*, **2003**, 2460-2461.
- 37 A. A. Kelkar, N. M. Patil, R. V. Chaudhari, *Tetrahedron Lett.*, **2002**, *43*, 7143-7146.
- 38 H. Ma, S. Liu, J. D. Luo, S. Suresh, L. Liu, S. H. Kang, M. Haller, T. Sassa, L. R. Dalton, A. K. Y. Jen, *Adv. Funct. Mater.*, **2002**, *12*, 565-574.
- 39 S. H. Kang, J. Luo, H. Ma, R. R. Barto, C. W. Frank, L. R. Dalton, A. K. Y. Jen, *Macromolecules*, **2003**, *36*, 4355-4359.
- 40 A. Galvan-Gonzalez, M. Canva, G. I. Stegeman, L. Sukhomlinova, R. J. Twieg, K. P. Chan, T. C. Kowalczyk, H. S. Lackritz, *J. Opt. Soc. Am. B*, **2000**, *17*, 1992-2000.
- 41 J. R. Hurst, J. D. McDonald, G. B. Schuster, *J. Am. Chem. Soc.*, **1982**, *104*, 2065-2067.
- 42 C. C. Teng, H. T. Man, *Appl. Phys. Lett.*, **1990**, *56*, 1734-1736.
- 43 G. Olbrechts, R. Strobbe, K. Clays, A. Persoons, *Rev. Sci. Instrum.*, **1998**, *69*, 2233-2241.

- 44 R. J. Bushby, D. R. McGill, K. M. Ng, N. Taylor, *J. Chem. Soc., Perkin Trans. 2*, **1997**, 1405-1414.



# Chapter 4

## Photostable Nonlinear Optical Polycarbonates

*Highly thermal and photostable NLO polymers were obtained by covalently incorporating the tricyanovinylidenediphenylaminobenzene (TCVDPA) chromophore to a polycarbonate backbone. NLO polycarbonates with different chromophore attachment modes and flexibilities were synthesized. In spite of the high loading levels (ranging from 33.1 to 39.8 wt%), the polymers exhibit  $T_g$ s as high as 215 °C, representing a significant improvement of over 100 °C of the material  $T_g$  compared with that of the guest-host system containing the same chromophore at similar high loadings. EO coefficients up to 33 pm/V at 830 nm were achieved, and good temporal stability of the dipole alignment at 50 °C was observed.*

## 4.1 Introduction

In the past decade, a large number of NLO chromophores has been synthesized and incorporated as a guest in a wide variety of host polymers.<sup>1-12</sup> In particular, amorphous polycarbonate (APC) has been extensively investigated as a host polymer, due to its low crystallization tendency, good solubility in spin-casting solvents and high glass transition temperature ( $T_g = 205$  °C).<sup>13,14</sup> Moreover, its compatibility with large  $\mu\beta$  chromophores and its high dielectric constant allow a good poling efficiency.<sup>15</sup>

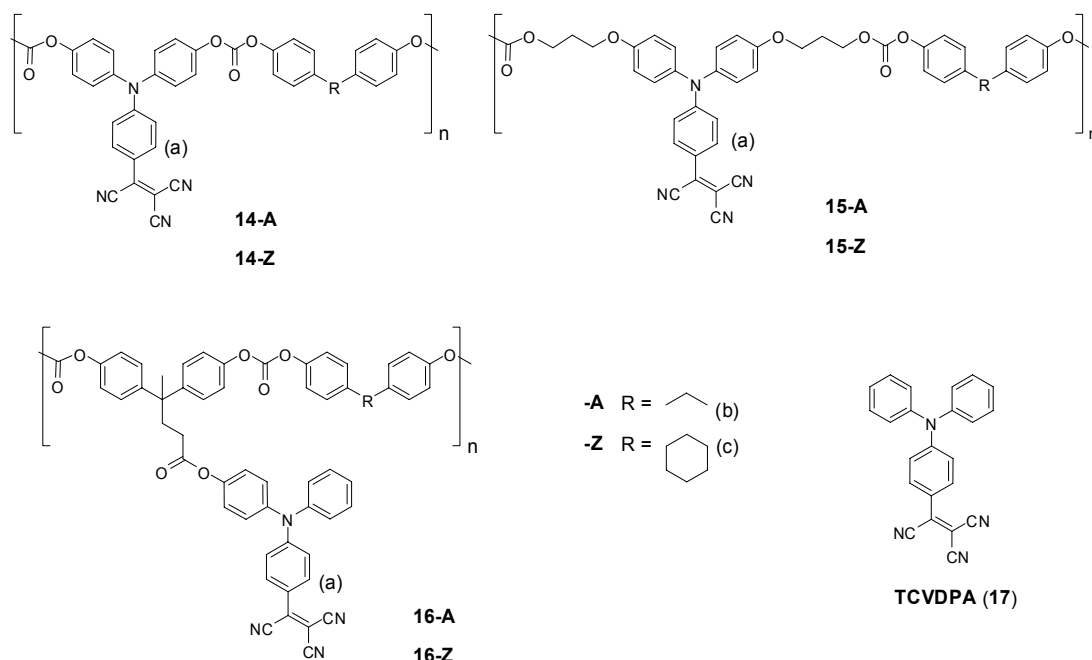
Although the  $T_g$  of APC polymers is high, the incorporation of a chromophore will induce plasticization, considerably lowering the  $T_g$  of the composite material, and therefore reducing the temporal stability of the poling induced alignment.<sup>16</sup> Moreover chromophores can sublime out of the matrix at high processing temperatures, or could be dissolved by organic solvents used in fabrication of multilayer devices. One way to solve these problems is by covalently incorporating the chromophores into high- $T_g$  polymers.<sup>17</sup> Surprisingly, in spite of the exceptional properties of polycarbonates when employed as host, there are only a few reports about the incorporation of chromophores as a side-chain in a polycarbonate backbone.<sup>18</sup>

In the previous Chapter we have described a series of chromophores based on the highly thermal and photostable tricyanovinylidenediphenylaminobenzene (TCVDPA)<sup>19,20</sup> which were incorporated as a guest at high loading in polysulfone. Although the increase of the chromophore concentration led to higher EO coefficients, it also resulted in a dramatic decrease of the  $T_g$  of the polymeric material, which might be detrimental for the long term efficiency of a device.

To provide EO materials with improved stability, in this Chapter the TCVDPA chromophore (17) (Chart 1) is incorporated into a polycarbonate backbone, combining the good properties of polycarbonates with the improved temporal stability given by chromophore attachment. The synthesis and the properties of six novel thermally and photochemically stable NLO polycarbonates in which the TCVDPA chromophore (17) is either “donor-embedded” into the polymer backbone or linked to it through flexible spacers is described. Moreover, the effect of the attachment mode and the flexibility on



the poling efficiency and alignment stability is studied, together with a comparison with a guest-host system incorporating the same chromophore.

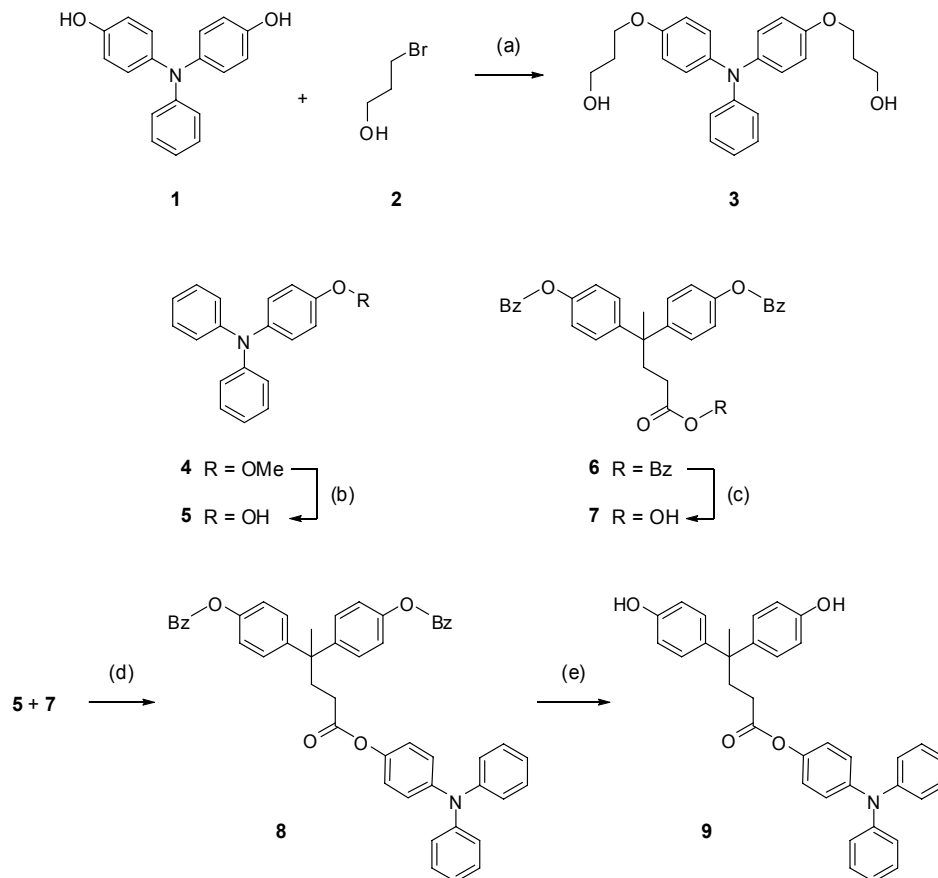


**Chart 1.** Structures of NLO polycarbonates.

## 4.2 Results and Discussion

### 4.2.1 Synthesis

The synthesis of the necessary dihydroxy-functionalized monomers **3** and **9** containing the triphenyl amine donor group is given in Scheme 1. Monomer **3**, having flexible alkyl chains, was synthesized by reaction of bisphenol **1** with 2-bromo-1-propanol (**2**) under Finkelstein conditions. The synthesis of bisphenol monomer **9** starts with the demethylation of 4-methoxy-triphenylamine (**4**) with  $\text{BBr}_3$  to give 4-hydroxy-triphenylamine **5**. Saponification of the ester in diarylmethane derivative **6** with KOH gave **7** having a free valeric acid moiety, which was then reacted with 4-hydroxy-triphenylamine **5** under DCC coupling conditions to afford ester **8**. Cleavage of the benzyl ether bonds by Pd/C catalyzed reduction with hydrogen gave bisphenol monomer **9**.

**Scheme 1.** Synthesis of monomers **3** and **9**.<sup>a</sup>

<sup>a</sup> Reagents and conditions: (a)  $K_2CO_3$ , KI, THF, reflux; (b)  $BBr_3$ ,  $CH_2Cl_2$ , rt; (c) KOH, ethanol, water, reflux; (d) dicyclohexylcarbodiimide (DCC), 4-(Dimethylamino)pyridinium-4-toluenesulfonate (DPTS),  $CH_2Cl_2$ , rt; (e)  $H_2$ , Pd/C,  $Na_2CO_3$ , THF, rt.

The general synthetic route for the NLO active polymers is depicted in Scheme 2. Condensation polymerization of equimolar amounts of the dihydroxy-functionalized triphenyl amine group containing monomers (**1**, **3**, or **9**) with the corresponding bisphenol (A or Z) bis(chloroformate) (**10-A** or **10-Z**) in solution using pyridine as a base, afforded the donor containing polycarbonates. Subsequent post-tricyanovinylolation by treatment with tetracyanoethylene (TCNE) gave the corresponding NLO active polymers. The tricyanovinyl (TCV) groups were introduced in the last stage of the polymer preparation to prevent the exposure of the chromophores to the harsh reaction conditions.



the donor embedded **14-A** and **14-Z** polymers functionalization proceeded for 73 and 75%, respectively. For the **15-A** and **15-Z** polymers, having a three-carbon spacer connecting the triphenylamine donor unit to the polycarbonate backbone, over 80% tricyanovinylation was obtained. However, for the **16-A** and **16-Z** polymers, having the donor attached as side chain, the highest degrees of functionalization were obtained, namely 92 and 88%, respectively.

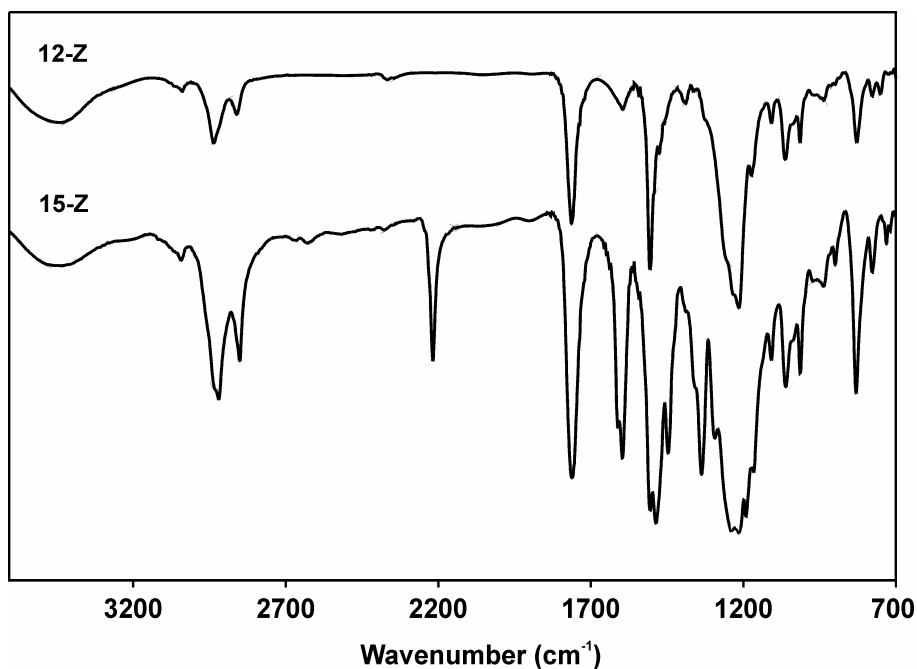


*Figure 1. Infrared spectra of 12-Z and 15-Z.*

#### **4.2.2 Thermal Analysis**

The thermal properties of the NLO polymers (Chart 1) are reported in Table 1. The decomposition temperature ( $T_d$ ) of all chromophore-containing polycarbonates is in the range between 329 and 380 °C, being the donor-embedded polycarbonates **14-A** and **14-Z** the most stable structures. Due to their more rigid structure, these two polymers, in spite of the high chromophore loading of over 38 wt%, possess the highest  $T_g$ s of the whole series, being 206 and 215 °C, respectively. This result represents a significant improvement of over 100 °C of the material  $T_g$  compared with that of a guest-host system

incorporating the **TCVDPA** chromophore (**17**) at similar high loadings, as reported in Chapter 3.

While the introduction of flexible alkyl chromophore-polymer tethers can enhance the chromophore mobility, facilitating the poling process, it is known that it will reduce the  $T_g$  of the material.<sup>21</sup> For the **16-A** and **16-Z** polycarbonates, having the chromophore anchored as side-chain through a valeric acid tether, the  $T_g$  drops to 178 and 184 °C, respectively. However, this drop is even more pronounced when three-carbon spacers are introduced between the chromophore and the bisphenol moieties, leading to a  $T_g$  of 166 °C for polymer **15-A** and 172 °C for polymer **15-Z**. The higher intrinsic structural rigidity induced by the cyclohexyl group<sup>22</sup> in the bisphenol Z monomer, generally results in polymers with substantially higher  $T_g$ s (6 to 9 °C increment) with respect to those containing a bisphenol A monomer, having two methyl groups instead.

**Table 1.** Summary of the thermal, physical, and optical properties the NLO polycarbonates.<sup>a</sup>

	$\lambda_{max}^b$ (nm)	$T_d^c$ (°C)	$T_g$ (°C)	$M_w$	$M_w/M_n$	Chrom. content (wt%)	$r_{33}$ (pm/V) <sup>d</sup>
<b>TCVDPA (17)</b>	531	360	85 <sup>c</sup>	-	-	35 in PS <sup>e</sup>	12
<b>14-A</b>	523	371	206	12700	2.3	39.8	15
<b>14-Z</b>	523	380	215	14600	1.9	38,6	15
<b>15-A</b>	524	351	166	12400	1.7	37.0	33
<b>15-Z</b>	524	359	172	8300	1.9	36.2	31
<b>16-A</b>	526	329	178	12400	1.8	35.3	13
<b>16-Z</b>	526	341	184	10900	1.8	33.1	12

<sup>a</sup> For structures see Chart 1; <sup>b</sup>  $\lambda_{max}$  was measured in CH<sub>2</sub>Cl<sub>2</sub>; <sup>c</sup> the onset temperature of degradation ( $T_d$  onset) can be calculated from the intersection of the tangent to the slope of the curve corresponding to the first weight loss event; <sup>d</sup> measured at 830 nm; <sup>e</sup> as guest in polysulfone host (data taken from Chapter 3).

### 4.2.3 Linear Optical Properties

UV spectra of the NLO polymers were recorded in  $\text{CH}_2\text{Cl}_2$  and the  $\lambda_{\text{max}}$  values are reported in Table 1. All NLO polycarbonates studied have a strong charge-transfer band (450-650 nm) in the visible region of the spectrum, with  $\lambda_{\text{max}}$  lying between 523 and 526 nm. A typical spectrum is shown in Figure 2. In general a small but consistent blue shift (5-8 nm) compared with that of the **TCVDPA** chromophore (**17**) is noticeable for all polymers. This can be attributed to the fact that, in the polymer, the chromophore is more crowdedly surrounded by a low dielectric constant environment. Moreover, all derivatives have a minimum in the absorption spectra (around 400 nm) between the charge-transfer band and the higher-energy aromatic electronic transitions.

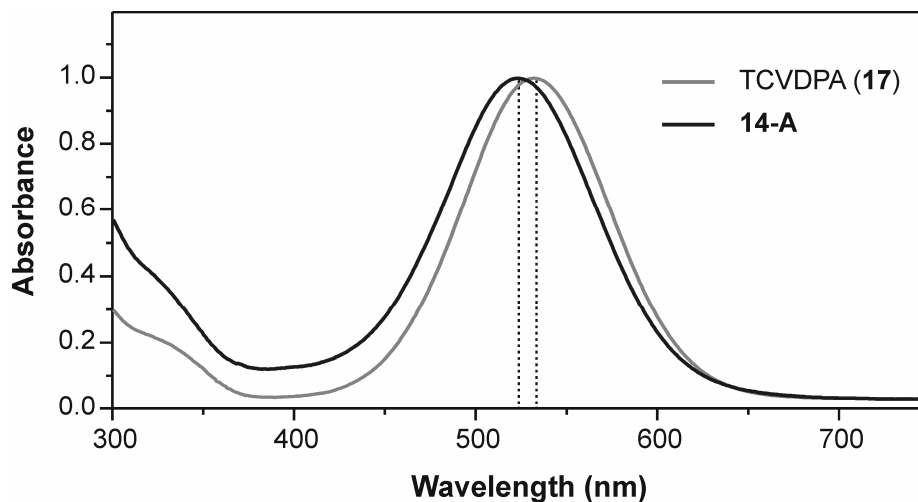


**Figure 2.** Absorption spectrum of the **TCVDPA** chromophore (**17**) and the **14-A** polymer in  $\text{CH}_2\text{Cl}_2$ .

### 4.2.4 Photobleaching Test

To obtain an estimation of the photostability of the NLO polycarbonates, the straightforward and low-cost qualitative method described in Chapter 3 was used. It concerns the monitoring of the decrease in absorbance during irradiation of oxygen-saturated solutions of chromophore-containing polymers in  $\text{CDCl}_3$  with visible white light.

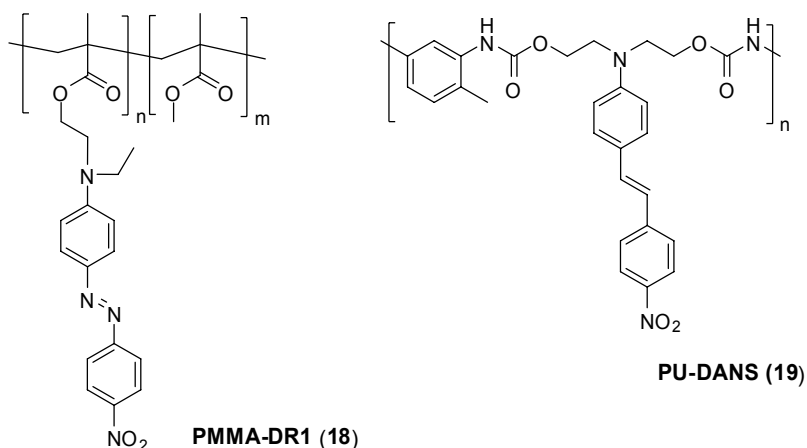


**Chart 2.** Structures of **PMMA-DR1 (18)** and **PU-DANS (19)** polymers.

Photobleaching tests were carried out for the chromophore-containing **14-A**, **15-A**, polymethylmethacrylate-DR1 (**PMMA-DR1**), and polyurethane-DANS (**PU-DANS**) polymers (Chart 2). From Figure 3 it can be seen that the **14-A** and **15-A** polycarbonates, containing the highly photostable **TCVDPA** chromophore, have an exceptional stability under the experimental condition used. In fact, only 5% decay of the original adsorbance was noticed after irradiation for 130 min. There is no significant difference in the photobleaching behavior between the two polycarbonate polymers, indicating the minor influence of the polycarbonate backbone on the photobleaching process. In comparison, the **PMMA-DR1 (18)** and **PU-DANS (19)** polymers, containing stilbene-based and azo-based chromophores, show significantly faster degradation rates. This trend reflects the behavior obtained for the monomeric chromophores (reported in Chapter 3) suggesting that, for solution experiments, there is little or neglectable influence of the nature of the polymeric structure on the chromophore degradation rate. This parameter is known to play a fundamental role in photostability experiments conducted on thin films.<sup>23</sup> From these results it can be concluded that the NLO polycarbonates described in this Chapter are among the most photostable structures ever reported in literature.

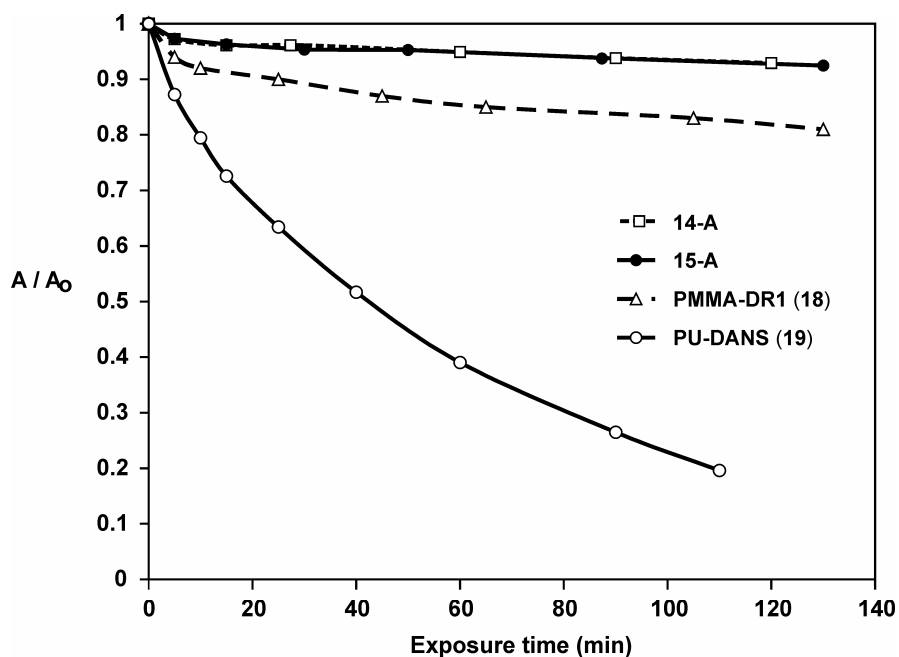


**Figure 3.** Photo-bleaching curves of the **14-A**, **15-A**, **PMMA-DR1 (18)**, and **PU-DANS (19)** polymers in  $\text{CDCl}_3$ .  $A$  is the absorbance at time  $t$  and  $A_0$  is the initial absorbance. Photolyses were carried out in 10 mm quartz cuvettes with light from a 75 Watt halogen lamp. The samples were irradiated at a distance of 10 cm from the light source and were shielded from daylight.

#### 4.2.5 Electric Field Poling and EO Property Measurements

All polymers described have a good solubility in common organic solvents, such as THF and  $\text{CH}_2\text{Cl}_2$ . Thin films for EO measurements were prepared as described in Chapter 3, starting from solutions of the NLO polycarbonates at 10-15 wt% in cyclopentanone. The  $r_{33}$  values, reported in Table 1, were measured using a Teng-Man simple reflection technique at a wavelength of 830 nm.<sup>24</sup>

As an example, Figure 4 shows the poling curve of the **14-A** polymer. The poling curves of all polycarbonates show as a general trend the strong dependence of the EO coefficient on the poling temperature. The measured  $r_{33}$  value increases linearly with the poling temperature, reaching a maximum at 10-15 °C below the  $T_g$  of the material. After this point, no further increase or even a decrease of the EO coefficient is observed. Therefore these temperatures were chosen as the poling temperatures.



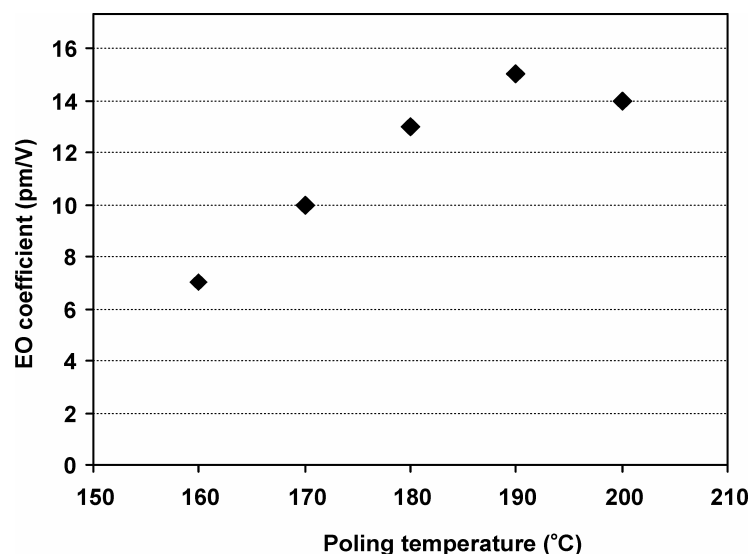


*Figure 4. Poling curve of the 14-A polymer.*

The **14-A** and **14-Z** polymers, having the highest chromophore loading density of the series (being 39.8 and 38.6 wt%, respectively), have an  $r_{33}$  value of 15 pm/V. In comparison, the **15-A** and **15-Z** polymers exhibit a more efficient poling, with  $r_{33}$  values of 33 and 31 pm/V, respectively. This probably reflects the intrinsically lower  $T_g$  values, caused by the higher degree of chain flexibility, enabling the chromophore a higher degree of freedom to reorient under the electric field. These high EO coefficients significantly outperform that of the **17-polysulfone** guest-host system (12 pm/V at 35 wt%), as reported in the previous Chapter. This result can possibly be explained by a combination of the good poling efficiency provided by the polycarbonate and the improved shielding of chromophores by the attached polymer backbone.

For the **16-A** and **16-Z** polymers a higher EO response was expected, due to a possibly higher poling efficiency provided by the chromophore-to-polymer tethers. However, disappointing  $r_{33}$  values of 12 and 13 pm/V, respectively, were recorded. From other studies it is known that the degree of dipolar ordering within a covalently attached chromophore-host matrix heavily depends on subtle differences in architectural design, including polymer backbone rigidity, degree of branching, free volume, chromophore binding mode, and chromophore electrostatic interactions.<sup>25-28</sup>

To study the effect of the chromophore-to-polymer binding mode and the attachment flexibility on the temporal stability of the dipole alignment, the decay of the EO

coefficient at 50 °C was followed over time for poled samples of the **14-A**, **15-A**, and **16-A** polycarbonates. From Figure 5 it is clear that **14-A** and **15-A** have the highest temporal stability, retaining over 90% of their original EO response after 300 h. Differently, for **16-A** a faster decay was observed, retaining only 74% of the starting value. These trends might be understood considering the two factors that contribute to the decay: (i) the  $T_g$  of the polymer, which is related to the energy needed for the whole backbone to increase its mobility and (ii) the chromophore binding mode, which is related to its degree of freedom and therefore with the energy needed for the single chromophore to reorient. While the first factor is predominant at high temperatures (less than 50 °C to the  $T_g$ ), the latter has a big influence at lower temperatures. Since all polycarbonates in this study have a  $T_g$  higher than 160 °C it is assumed that at 50 °C the observed decay is due to differences in the chromophore binding mode.

In case of the **14-A** and **15-A** polymers the chromophore is part of the polymer main-chain being covalently bound at two positions. Therefore it requires more energy to relax back to the centrosymmetric state. However, in case of **16-A** the NLO chromophore is attached as a side appendage to the backbone, giving to it a greater degree of freedom to reorient independently, without requiring the additional energy needed for the polycarbonate structure to move with it.

Furthermore, a temporal stability experiment at the same temperature was conducted with a poled sample of the chromophore **7** at 25 wt% as guest in polysulfone, resulting in a material with a  $T_g$  of 110 °C. A much steeper decay was observed during the first 24 hours after poling, after which a constant but slow decrease took place, resulting in a loss of 32% of the original EO signal after 250 h.

From these results it can be concluded that the stability of the dipole alignment increases with the number of chromophore-to-polymer attachment points. Moreover, direct incorporation of the **TCVDPA** chromophore into the polymer backbone gives a higher temporal stability than being attached through a tether.

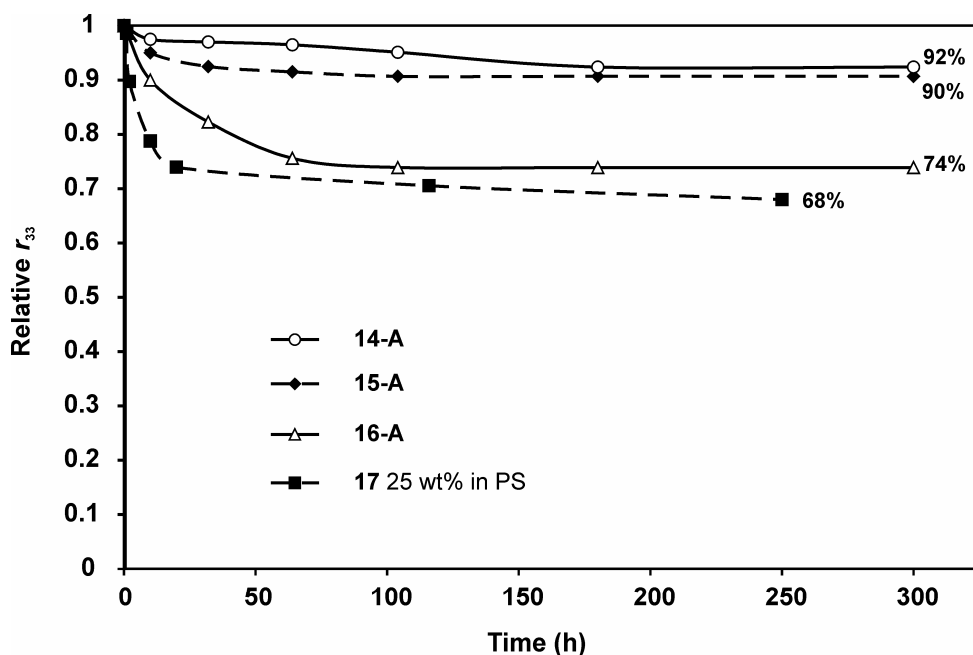


**Figure 5.** Comparison of the thermal decay curves at 50 °C for different EO polymer systems.

### 4.3 Conclusions

NLO polycarbonates incorporating the **TCVDPA** chromophore (**17**) with different attachment modes and flexibility were synthesized. Chemical bonding of the chromophore to the backbone allowed high loading levels (ranging from 33.1 to 39.8 wt%) without any plasticization effect.  $T_g$  values as high as 215 °C were obtained, representing a significant improvement of over 100 °C of the material  $T_g$  compared with that of the guest-host system containing the same chromophore at similar high loadings reported in Chapter 3. Higher poling efficiencies were achieved when a larger degree of chain flexibility was introduced, with EO coefficients (up to 33 pm/V at 830 nm) that significantly outperform that of the **17**-polysulfone guest-host system. The temporal stability at 50 °C increases with the number of chromophore-to-polymer attachment points, retaining up to 92 % of the original  $r_{33}$  value after 300 h of isothermal heating. Thanks to their excellent photostabilities, combined with their thermal stabilities up to 380 °C, these NLO polycarbonates could represent a step forward toward long-lifetime device-quality materials.

## 4.4 Experimental Section

**General Procedures.** All chemicals were obtained from commercial sources and used without further purification. THF was freshly distilled from Na/benzophenone, and CH<sub>2</sub>Cl<sub>2</sub> from CaCl<sub>2</sub>. All chromatography associated with product purification was performed by flash column techniques using Merck Kieselgel 600 (230-400 mesh). All reactions were carried out under an inert argon atmosphere. Melting points of all compounds were obtained with a Reichert melting point apparatus and a Kofler stage. <sup>1</sup>H and <sup>13</sup>C NMR spectra were recorded on a Varian Unity 300 using tetramethylsilane (TMS) or the corresponding residual solvent signal as internal standard. FAB-MS spectra were recorded on a Finningan MAT 90 spectrometer with *m*-nitrobenzyl alcohol (NBA) as a matrix. Thermogravimetric (TGA) analyses were conducted using a Perkin-Elmer TGA-7 thermogravimetric analyzer (heating rate: 20 °C/min). Differential scanning calorimetry (DSC) was performed using a Perkin-Elmer DSC-7 instrument at a heating rate of 20 °C/min. The molecular weights and polydispersities (relative to polystyrene standards) were determined by PL-GPC-120 (gel permeation chromatograph (GPC) using THF as eluent. Infrared spectra were taken on a Perkin-Elmer BX FT-IR spectrometer by incorporating samples in KBr disks. UV-Vis measurements were carried out on a Varian Cary 3E UV-spectrophotometer.

The synthesis of compound **1** is reported in Chapter 3. Compound **6**<sup>29</sup> and DPTS<sup>30</sup> was prepared according to literature procedures.

**4,4'-Bis[(3-propanoyl)oxy]tryphenylamine (3).** A suspension of **1** (300 mg, 1.08 mmol), KI (718 mg, 3.25 mmol), K<sub>2</sub>CO<sub>3</sub> (598 mg, 3.25 mmol) in dry THF (20 mL) was stirred for 10 min. Subsequently, 2-bromo-1-propanol (**2**) (0.211 mL, 2.6 mmol) was added and the mixture was refluxed over night. After cooling to rt, water was added (50 mL). The mixture was extracted with CHCl<sub>3</sub> (3 x 50 mL) and then purified with column chromatography: hexane/ethyl acetate 2/8 to give **3** as a grey solid (60%): mp 63-65 °C; <sup>1</sup>H NMR (CDCl<sub>3</sub>), δ 1.78-1.97 (m, 4H, CH<sub>2</sub>), 3.67-3.78 (m, 4H, OCH<sub>2</sub>), 3.98-4.02 (m, 4H, OCH<sub>2</sub>), 6.70-6.85 (m, 7H, ar-H), 6.94 (d, *J* = 8.7 Hz, 4H, ar-H), 7.06 (t, *J* = 7.7 Hz, 2H,

ar-H);  $^{13}\text{C}$  NMR ( $\text{CDCl}_3$ ),  $\delta$  32.3, 60.8, 66.3, 115.5, 120.9, 121.4, 126.5, 129.1, 141.6, 148.9, 155.0; MS MALDI-ESI  $m/z$  393.1 ( $[\text{M}^+]$ ), calcd for  $\text{C}_{24}\text{H}_{27}\text{NO}_4$  393.4).

**4,4-Bis[4'-(benzyloxy)phenyl]valeric Acid (7).** A mixture of compound **6** (9.71 g, 17.46 mmol) and potassium hydroxide (5.4 g) in a mixture of ethanol (26 mL) and water (8 mL) was heated at reflux for 24 h, cooled, and concentrated. Water (400 mL) was added to the residue and the mixture acidified with glacial acetic acid and then extracted with  $\text{CH}_2\text{Cl}_2$  (6 x 100 mL). The combined extracts were dried with  $\text{MgSO}_4$  and evaporated to dryness to give **7** as a white-yellow powder (70%): mp 80-82 °C;  $^1\text{H}$  NMR ( $\text{CDCl}_3$ ),  $\delta$  1.61 (s, 3H,  $\text{CH}_3$ ), 2.18 (t,  $J = 7.8$  Hz, 2H,  $\text{CH}_2$ ), 2.45 (t,  $J = 7.8$  Hz, 2H,  $\text{CH}_2$ ), 5.05 (s, 4H,  $\text{OCH}_2$ ), 6.92 (d,  $J = 7.9$  Hz, 4H, ar-H), 7.14 (d,  $J = 7.95$  Hz, 4H, ar-H), 7.32-7.47 (m, 10 H, ar-H);  $^{13}\text{C}$  NMR ( $\text{CDCl}_3$ ),  $\delta$  28.1, 30.7, 36.7, 44.7, 70.2, 114.6, 127.2, 127.7, 128.8, 133.9, 137.4, 141.3, 157.1, 179.9; MS MALDI-ESI  $m/z$  466.5 ( $[\text{M}^+]$ ), 489.4 ( $[\text{M}+\text{Na}^+]$ ), 505.4 ( $[\text{M}+\text{K}^+]$ ), calcd for  $\text{C}_{31}\text{H}_{30}\text{O}_4$  466.2.

**4-Hydroxytriphenylamine (5).**  $\text{BBr}_3$  (98.4 mL of a 1M-solution in  $\text{CH}_2\text{Cl}_2$ ) was added dropwise to a solution of 4-methoxytriphenylamine (**4**) (7.5 g, 24.6 mmol) in dry chloroform (100 mL) at 0 °C. After stirring for 1 h at this temperature, the mixture was allowed to warm up to rt and stirred for 5 h. The reaction was carefully quenched with methanol using an ice bath. The solvent was evaporated and the residue dissolved in ethyl acetate (150 mL). The resulting solution was washed with a saturated solution of  $\text{NaHCO}_3$  (2 x 50 mL) and water (2 x 50 mL), dried over  $\text{MgSO}_4$ , and evaporated to give **5** as a green solid in a quantitative yield: mp 108 °C;  $^1\text{H}$  NMR ( $\text{CDCl}_3$ ),  $\delta$  6.77-6.89 (m, 2H, ar-H), 6.90-7.06 (m, 8H, ar-H), 7.13-7.35 (m, 4H, ar-H);  $^{13}\text{C}$  NMR ( $\text{CDCl}_3$ ),  $\delta$  117.4, 125.8, 127.1, 130.3, 133.7, 139.4, 146.7, 153.5; MS MALDI-ESI  $m/z$  261.1 ( $[\text{M}^+]$ ), 262.1 ( $[\text{M}+\text{H}^+]$ ), calcd for  $\text{C}_{18}\text{H}_{15}\text{NO}$  261.11.

**4,4-Bis[4'-(benzyloxy)phenyl]-1-[4-(triphenylamine)] Valerate (8).** To a solution of **7** (1.96 g, 4.21 mmol) in dry  $\text{CH}_2\text{Cl}_2$  (25 mL) was added **5** (1.0 g, 3.83 mmol), followed by DPTS (250 mg, 4.21 mmol), and the mixture was stirred at rt for 15 min. DCC (888 mg, 4.21 mmol) was then added and the mixture was stirred for 12 h. The

reaction mixture was filtered, and the filtrate was evaporated to dryness under reduced pressure. The crude product was purified by flash chromatography eluting with 7/3 CH<sub>2</sub>Cl<sub>2</sub>/hexane, to give **8** as a white solid (70%): mp 90-93 °C; <sup>1</sup>H NMR (CDCl<sub>3</sub>), δ 1.71 (s, 3H, CH<sub>3</sub>), 2.43 (t, *J* = 7.8 Hz, 2H, CH<sub>2</sub>), 2.61 (t, *J* = 7.8 Hz, 2H, CH<sub>2</sub>), 5.09 (s, 4H, OCH<sub>2</sub>), 6.98 (d, *J* = 8.8 Hz, 6H, ar-H), 7.03-7.15 (m, 8 H, ar-H), 7.22 (d, *J* = 8.6 Hz, 4H, ar-H), 7.26-7.50 (m, 14H, ar-H); <sup>13</sup>C NMR (CDCl<sub>3</sub>), δ 28.1, 30.7, 36.7, 44.7, 70.2, 114.6, 122.3, 123.0, 124.3, 125.0, 127.2, 127.7, 128.7, 129.5, 133.9, 137.4, 141.3, 145.7, 145.9, 157.1, 173.8; MS MALDI-ESI *m/z* 709.3 ([M<sup>+</sup>]), 732.3 ([M+Na<sup>+</sup>]), 748.3 ([M+K<sup>+</sup>]), calcd for C<sub>49</sub>H<sub>43</sub>NO<sub>4</sub> 709.32.

**4,4-Bis(4'-hydroxyphenyl)-1-[4-(triphenylamine)] Valerate (9).** A mixture of **8** (1.0 g, 1.4 mmol), 10% Pd/C (100 mg), and sodium carbonate (86 mg) in dry THF (8.6 mL) was vigorously stirred under an atmosphere of hydrogen until the theoretical amount of hydrogen was consumed. The reaction mixture was then filtered and evaporated to dryness, to give **9** as a white solid in quantitative yield: mp 92-94 °C; <sup>1</sup>H NMR (CDCl<sub>3</sub>), δ 1.60 (s, 3H, CH<sub>3</sub>), 2.35 (t, *J* = 7.7 Hz, 2H, CH<sub>2</sub>), 2.51 (t, *J* = 7.7 Hz, 2H, CH<sub>2</sub>), 6.77 (d, *J* = 8.5 Hz, 4H, ar-H), 6.91 (d, *J* = 8.8 Hz, 2H, ar-H), 6.88-7.08 (m, 12H, ar-H), 7.23 (t, *J* = 7.9 Hz, 4H, ar-H); <sup>13</sup>C NMR (CDCl<sub>3</sub>), δ 28.1, 30.7, 36.7, 44.8, 115.2, 122.3, 123.0, 124.3, 125.0, 128.7, 129.5, 141.2, 145.7, 145.9, 147.9, 153.8, 173.4; MS MALDI-ESI *m/z* 530.2 ([M]<sup>+</sup>), 531.2 ([M+H<sup>+</sup>]), 570.2 ([M+K<sup>+</sup>]), calcd for C<sub>35</sub>H<sub>31</sub>NO<sub>4</sub> 529.63.

**Polycarbonate 11-A.** To a mixture of **1** (2.0 g, 7.21 mmol) and bisphenol A bis(chloroformate) (**10-A**) (2.55 g, 7.21 mmol) in a mixture of dry CH<sub>2</sub>Cl<sub>2</sub> (20 mL) and dry THF (15 mL) was added dropwise a solution of pyridine (1.23 mL, 15.14 mmol) in dry THF (5 mL) at 0 °C. Subsequently, the polymer was stirred overnight at rt. The mixture was precipitated in methanol (350 mL), filtered and washed with methanol. Drying at 60 °C for 24 h yielded **11-A** as a white solid (81%): <sup>1</sup>H NMR (CDCl<sub>3</sub>) δ 1.69 (s, 6H, CH<sub>3</sub>); 6.95-7.07 (m, 1H, ar-H), 7.09-7.17 (m, 14H, ar-H), 7.19-7.26 (m, 6H, ar-H); IR 1774 (s, C=O), 1225 and 1189 (s, C-O).

**Polycarbonate 12-A** was prepared in a similar way from **3** and bisphenol A bis(chloroformate) (**10-A**) as a white solid (76%):  $^1\text{H NMR}$  ( $\text{CDCl}_3$ )  $\delta$  1.65 (s, 6H,  $\text{CH}_3$ ), 2.13 (m, 4H,  $\text{CH}_2$ ), 3.96-4.21 (m, 4H,  $\text{OCH}_2$ ), 4.44 (t,  $J = 6.1$  Hz, 4H,  $\text{OCH}_2$ ), 6.77-6.87 (m, 4H, ar-H), 7.06 (d,  $J = 8.7$  Hz, 5H, ar-H), 7.16-7.24 (m, 12 H, ar-H); IR 1165 (s, C-O), 1596 (s, C=C aromatic), 1760 (s, O-COO), 2920 (s, C-H), 3043 (s, C-H, aromatic).

**Polycarbonate 13-A** was prepared in a similar way from **9** and bisphenol A bis(chloroformate) (**10-A**) as a white solid (75%):  $^1\text{H NMR}$  ( $\text{CDCl}_3$ )  $\delta$  1.64 (s, 3H,  $\text{CH}_3$ ), 1.68 (s, 6H,  $\text{CH}_3$ ), 2.32-2.37 (m, 2H,  $\text{CH}_2$ ), 2.53 (t,  $J = 8.6$ , 2H,  $\text{CH}_2$ ), 6.77 (d,  $J = 9.1$  Hz, 2H, ar-H), 6.91 (d,  $J = 8.7$  Hz, 2H, ar-H), 6.97-7.08 (m, 6H, ar-H), 7.15-7.23 (m, 20H, ar-H); IR 1162 (s, C-O), 1365 (s, C-H), 1590 (s, C=C aromatic), 1775 (s, O-COO broad), 2976 (s, C-H), 3038 (s, C-H, aromatic).

**Polycarbonate 11-Z** was prepared in a similar way from **1** and bisphenol Z bis(chloroformate) (**10-Z**) as a white solid (82%):  $^1\text{H NMR}$  ( $\text{CDCl}_3$ )  $\delta$  1.55 (s, 6H,  $\text{CH}_2$ ), 2.27 (s, 4H,  $\text{CH}_2$ ), 7.03 (br, 1H, ar-H), 7.08-7.17 (m, 14H, ar-H), 7.23-7.29 (br, m, 6H, ar-H); IR 1774 (s, C=O), 1225 and 1189 (s, C-O).

**Polycarbonate 12-Z** was prepared in a similar way from **3** and bisphenol Z bis(chloroformate) (**10-Z**) as a white solid (78%):  $^1\text{H NMR}$  ( $\text{CDCl}_3$ )  $\delta$  1.43 (s, 6H,  $\text{CH}_2$ ), 2.12-2.42 (m, 8H,  $\text{CH}_2$ ), 3.96-4.20 (m, 4H,  $\text{OCH}_2$ ), 4.38-4.53 (m, 4H,  $\text{OCH}_2$ ), 7.10 (d,  $J = 8.5$  Hz, 5H, ar-H), 7.16-7.24 (m, 12H, ar-H); IR 1164 (s, C-O), 1597 (s, C=C aromatic), 1760 (s, O-COO), 2923 (s, C-H), 3043 (s, C-H aromatic).

**Polycarbonate 13-Z** was prepared in a similar way from **9** and bisphenol Z bis(chloroformate) (**10-Z**) as a white solid (75%):  $^1\text{H NMR}$  ( $\text{CDCl}_3$ )  $\delta$  1.39-1.67 (m, 9H,  $\text{CH}_2$ ), 2.21-2.36 (m, 6H,  $\text{CH}_2$ ), 2.52-2.58 (m, 2H,  $\text{CH}_2$ ), 6.91 (d,  $J = 8.8$  Hz, 2H, ar-H), 6.96-7.30 (m, 28H, ar-H); IR 1181 (s, C-O), 1590 (s, C=C aromatic), 1775 (s, O-COO broad), 2936 (s, C-H), 3040 (s, C-H, aromatic).

**Polycarbonate 14-A.** A solution of **11-A** (3.0 g) and TCNE (11.7 g, 91.3 mmol) in DMF (10 mL) was heated at 90 °C for 4 h. After cooling, the polymer was precipitated in methanol (400 mL). The precipitate was filtered and washed with methanol. Drying yielded **14-A** as a purple solid (90%):  $^1\text{H NMR}$  ( $\text{CDCl}_3$ )  $\delta$  1.62 (s, 6H,  $\text{CH}_2$ ), 6.92 (d, 2H, ar-H), 7.11 (d, 4H, ar-H), 7.14-7.29 (m, 12H, ar-H), 7.89 (d, 2H, ar-H); IR 2219 (s,  $\text{C}\equiv\text{N}$ ), 1774 (s,  $\text{C}=\text{O}$ ), 1654 (w,  $\text{C}=\text{C}$ ), 1185 (s,  $\text{C}-\text{O}$ ).

**Polycarbonate 15-A** was prepared in a similar way from **12-A** and TCNE as a purple solid (83%):  $^1\text{H NMR}$  ( $\text{CDCl}_3$ )  $\delta$  1.65 (s, 6H,  $\text{CH}_3$ ), 2.02-2.32 (m, 4H,  $\text{CH}_2$ ), 3.97-4.21 (m, 4H,  $\text{OCH}_2$ ), 4.38-4.53 (m, 4H,  $\text{OCH}_2$ ), 6.83 (d,  $J = 8.7$  Hz, 2H, ar-H), 6.94 (d,  $J = 8.3$  Hz, 4H, ar-H), 7.05-7.23 (m, 12H, ar-H), 7.92 (d,  $J = 9.4$  Hz, 2H, ar-H); IR 1165 (s,  $\text{C}-\text{O}$ ), 1596 (s,  $\text{C}=\text{C}$  aromatic), 1760 (s,  $\text{O}-\text{COO}$ ), 2218 (s,  $\text{C}\equiv\text{N}$ ), 2920 (s,  $\text{C}-\text{H}$ ), 3043 (s,  $\text{C}-\text{H}$ , aromatic).

**Polycarbonate 16-A** was prepared in a similar way from **13-A** and TCNE as a purple solid (80%):  $^1\text{H NMR}$  ( $\text{CDCl}_3$ )  $\delta$  1.59 (s, 3H,  $\text{CH}_3$ ), 1.68 (s, 6H,  $\text{CH}_3$ ), 2.33-2.45 (m, 2H,  $\text{CH}_2$ ), 2.50-2.63 (m, 2H,  $\text{CH}_2$ ), 6.95 (d,  $J = 9.1$  Hz, 2H, ar-H), 7.07-7.41 (m, 25H, ar-H), 7.96 (d,  $J = 9.3$  Hz, 2H, ar-H); IR 1162 (s,  $\text{C}-\text{O}$ ), 1365 (s,  $\text{C}-\text{H}$ ), 1590 (s,  $\text{C}=\text{C}$  aromatic), 1776 (s,  $\text{O}-\text{COO}$  broad), 2220 (s,  $\text{C}\equiv\text{N}$ ), 2977 (s,  $\text{C}-\text{H}$ ), 3038 (s,  $\text{C}-\text{H}$ , aromatic).

**Polycarbonate 14-Z** was prepared in a similar way from **11-Z** and TCNE as a purple solid (85%):  $^1\text{H NMR}$  ( $\text{CDCl}_3$ )  $\delta$  1.55 (s, 6H,  $\text{CH}_2$ ), 2.27 (s, 4H,  $\text{CH}_2$ ), 6.98 (d, 2H, ar-H), 7.17 (d, 4H, ar-H), 7.35-7.21 (m, 12H, ar-H), 7.95 (d, 2H, ar-H); IR 2219 (s,  $\text{C}\equiv\text{N}$ ), 1774 (s,  $\text{C}=\text{O}$ ), 1654 (w,  $\text{C}=\text{C}$ ), 1156 (s,  $\text{C}-\text{O}$ ).

**Polycarbonate 15-Z** was prepared in a similar way from **12-Z** and TCNE as a purple solid (90%):  $^1\text{H NMR}$  ( $\text{CDCl}_3$ )  $\delta$  1.43 (s, 6H,  $\text{CH}_3$ ), 2.03-2.20 (m, 8H,  $\text{CH}_2$ ), 3.96-4.20 (m, 4H,  $\text{OCH}_2$ ), 4.38 (t,  $J = 6.0$  Hz, 4H,  $\text{OCH}_2$ ), 6.80 (d,  $J = 8.7$  Hz, 2H, ar-H), 6.91 (d,  $J = 8.3$  Hz, 4H, ar-H), 7.23 (m, 12 H, ar-H), 7.93 (d,  $J = 9.4$  Hz, 2H, ar-H); IR 1165 (s,  $\text{C}-\text{O}$ ), 1596 (s,  $\text{C}=\text{C}$ , aromatic), 1760 (s,  $\text{O}-\text{COO}$ ), 2219 (s,  $\text{C}\equiv\text{N}$ ), 2920 (s,  $\text{C}-\text{H}$ ), 3043 (s,  $\text{C}-\text{H}$ , aromatic).



**Polycarbonate 16-Z** was prepared in a similar way from **13-Z** and TCNE as a purple solid (82%):  $^1\text{H NMR}$  ( $\text{CDCl}_3$ )  $\delta$  1.42-1.69 (m, 9H,  $\text{CH}_2$ ), 2.17-2.31 (m, 4H,  $\text{CH}_2$ ), 2.33-2.43 (m, 2H,  $\text{CH}_2$ ), 2.48-2.61 (m, 2H,  $\text{CH}_2$ ), 6.96 (d,  $J = 9.0$  Hz, 2H, ar-H), 7.01-7.48 (m, 25H, ar-H), 7.94 (d,  $J = 8.4$  Hz, 2H, ar-H); IR 1181 (s, C-O), 1591 (s, C=C aromatic), 1775 (s, O-COO, broad), 2220 (s,  $\text{C}\equiv\text{N}$ ), 2936 (s, C-H), 3040 (s, C-H, aromatic).

## 4.5 References

- 1 L. R. Dalton, A. Harper, A. Ren, F. Wang, G. Todorova, J. Chen, C. Zhang, M. Lee, *Ind. Eng. Chem. Res.*, **1999**, *38*, 8-33.
- 2 L. R. Dalton, *J. Phys.: Condens. Matter*, **2003**, *15*, R897-R934.
- 3 F. Kajzar, K. S. Lee, A. K. Y. Jen, *Adv. Polym. Sci.*, **2003**, *161*, 1-85.
- 4 L. R. Dalton, *Adv. Polym. Sci.*, **2002**, *158*, 1-86.
- 5 T. Verbiest, S. Houbrechts, M. Kauranen, K. Clays, A. Persoons, *J. Mater. Chem.*, **1997**, *7*, 2175-2189.
- 6 M. Ahlheim, M. Barzoukas, P. V. Bedworth, M. Blanchard-Desce, A. Fort, Z. Y. Hu, S. R. Marder, J. W. Perry, C. Runser, M. Staehelin, B. Zysset, *Science*, **1996**, *271*, 335-337.
- 7 S. Liu, M. A. Haller, H. Ma, L. R. Dalton, S. H. Jang, A. K. Y. Jen, *Adv. Mater.*, **2003**, *15*, 603-607.
- 8 H. Kang, A. Facchetti, H. Jiang, E. Cariati, S. Righetto, R. Ugo, C. Zuccaccia, A. Macchioni, C. L. Stern, Z. F. Liu, S. T. Ho, E. C. Brown, M. A. Ratner, T. J. Marks, *J. Am. Chem. Soc.*, **2007**, *129*, 3267-3286.
- 9 M. E. Wright, S. Fallis, A. J. Guenther, L. C. Baldwin, *Macromolecules*, **2005**, *38*, 10014-10021.
- 10 D. Briers, G. Koeckelberghs, I. Picard, T. Verbiest, A. Persoons, C. Samyn, *Macromol. Rapid Commun.*, **2003**, *24*, 841-846.
- 11 H. Ma, A. K. Y. Jen, J. Wu, X. Wu, S. Liu, C. F. Shu, L. R. Dalton, S. R. Marder, S. Thayumanavan, *Chem. Mater.*, **1999**, *11*, 2218-2225.
- 12 Y. Liao, C. A. Anderson, P. A. Sullivan, A. J. P. Akelaitis, B. H. Robinson, L. R. Dalton, *Chem. Mater.*, **2006**, *18*, 1062-1067.
- 13 C. Zhang, L. R. Dalton, M. C. Oh, H. Zhang, W. H. Steier, *Chem. Mater.*, **2001**, *13*, 3043-3050.

- 14 M. C. Oh, H. Zhang, C. Zhang, H. Erlig, Y. Chang, B. Tsap, D. Chang, A. Szep, W. H. Steier, H. R. Fetterman, L. R. Dalton, *IEEE J. Sel. Top. Quantum Electron.*, **2001**, *7*, 826-835.
- 15 Y. J. Cheng, J. Luo, S. Hau, D. H. Bale, T. D. Kim, Z. Shi, D. B. Lao, N. M. Tucker, Y. Tian, L. R. Dalton, P. J. Reid, A. K. Y. Jen, *Chem. Mater.*, **2007**, *19*, 1154-1163.
- 16 C. C. Chang, C. P. Chen, C. C. Chou, W. J. Kuo, R. J. Jeng, *J. Macromol. Sci., Polym. Rev.*, **2005**, *45*, 125-170.
- 17 C. Samyn, T. Verbiest, A. Persoons, *Macromol. Rapid Commun.*, **2000**, *21*, 1-15.
- 18 R. H. Woudenberg, T. O. Boonstra, J. W. Ladage, U. E. Wiersum, *Vol. WO96/28493*, **1999**.
- 19 A. Galvan-Gonzalez, M. Canva, G. I. Stegeman, R. Twieg, K. P. Chan, T. C. Kowalczyk, X. Q. Zhang, H. S. Lackritz, S. Marder, S. Thayumanavan, *Opt. Lett.*, **2000**, *25*, 332-334.
- 20 A. Galvan-Gonzalez, M. Canva, G. I. Stegeman, L. Sukhomlinova, R. J. Twieg, K. P. Chan, T. C. Kowalczyk, H. S. Lackritz, *J. Opt. Soc. Am. B*, **2000**, *17*, 1992-2000.
- 21 M. H. Davey, V. Y. Lee, L. M. Wu, C. R. Moylan, W. Volksen, A. Knoesen, R. D. Miller, T. J. Marks, *Chem. Mater.*, **2000**, *12*, 1679-1693.
- 22 X. Li, A. F. Yee, *Macromolecules*, **2003**, *36*, 9421-9429.
- 23 M. He, T. Leslie, S. Garner, M. DeRosa, J. Cites, *J. Phys. Chem. B*, **2004**, *108*, 8731-8736.
- 24 C. C. Teng, H. T. Man, *Appl. Phys. Lett.*, **1990**, *56*, 1734-1736.
- 25 P. A. Sullivan, A. J. P. Akelaitis, S. K. Lee, G. McGrew, S. K. Lee, D. H. Choi, L. R. Dalton, *Chem. Mater.*, **2006**, *18*, 344-351.
- 26 D. Briers, L. De Cremer, G. Koeckelberghs, S. Foerier, T. Verbiest, C. Samyn, *Macromol. Rapid Commun.*, **2007**, *28*, 942-947.
- 27 I. Bahar, B. Erman, G. Fytas, W. Steffen, *Macromolecules*, **1994**, *27*, 5200-5205.
- 28 M. D. Ediger, *Annu. Rev. Phys. Chem.*, **2000**, *51*, 99-128.
- 29 K. Y. Chen, C. B. Gorman, *J. Org. Chem.*, **1996**, *61*, 9229-9235.
- 30 J. S. Moore, S. I. Stupp, *Macromolecules*, **1990**, *23*, 65-70.

# Chapter 5

## Facile Attachment of Nonlinear Optical Chromophores to Polycarbonates

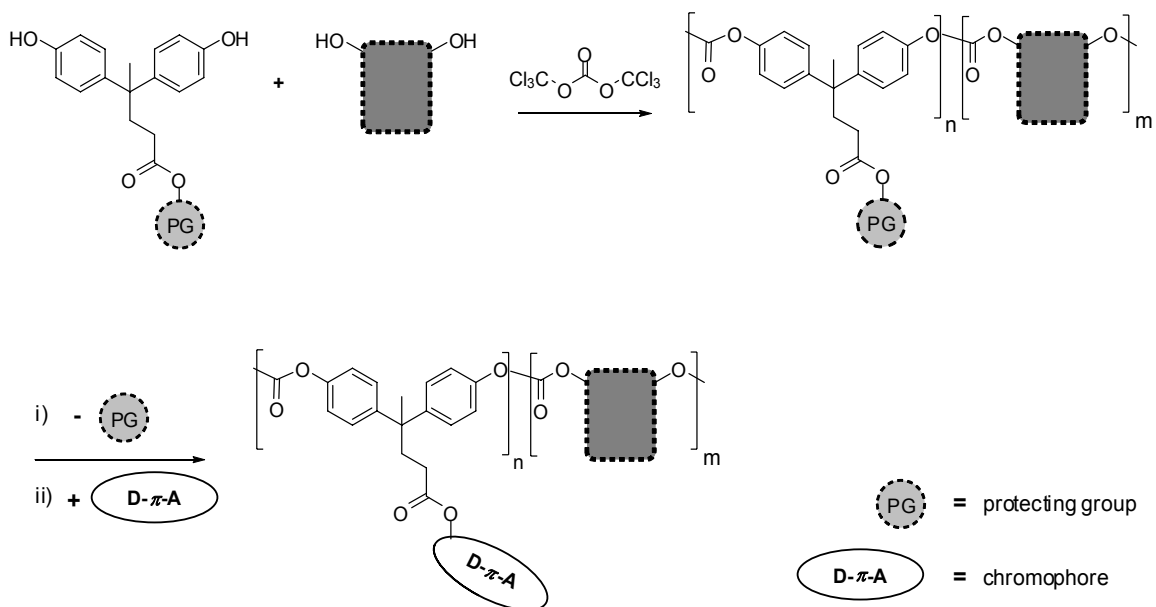
*The first example of covalent incorporation of NLO chromophores to a pre-polymerized polycarbonate backbone is presented. It is based on the versatile synthesis of a polycarbonate backbone, followed by chromophore attachment as the last reaction step. This generally applicable synthetic methodology allows a fine-tuning of the physico-chemical properties of the resulting material both by modifying the polymer backbone structure and by varying the chromophore loading level. Chromophores with different structures and NLO activities were incorporated to give polymers with  $T_g$ s as high as 213 °C, good solubilities, and thermal stabilities. Moreover, when a FTC type of chromophore was incorporated EO coefficients as high as 38 pm/V (at 1300 nm) were achieved.*

## 5.1 Introduction

There are two major ways to achieve chemical incorporation of a chromophore into a polymer.<sup>1-3</sup> One method is to functionalize the chromophore with suitable chemical groups, to give a monomer that can eventually react to form a co-polymer.<sup>4-6</sup> Although the so obtained side-chain NLO polymers have shown several advantages, such as a high temperature alignment stability and good mechanical properties, this approach often requires tedious procedures for the synthesis of the appropriate chromophore-containing monomers. The other method is to covalently connect the chromophore, either directly or using a linker or spacer, to a pre-polymerized macromolecule possessing a suitable pendent functionality for the attachment.<sup>7-9</sup> This procedure is particularly attractive for high NLO dyes, which are often prone to chemical degradation under the polymerization conditions.<sup>10,11</sup>

In the previous Chapter, a synthetic methodology to side-chain NLO polycarbonates is reported, requiring the synthesis of donor-containing dihydroxy monomers, followed by co-polymerization and post-tricyanovinilation. In this procedure, the polycarbonate backbones were achieved by condensation polymerization of equimolar amounts of a dihydroxy-containing monomer with the commercially available bis(chloroformates) of bisphenol A or Z. This class of compounds, however, is expensive and not many derivatives are readily attainable, requiring the prior laboratory preparation in case monomers with different properties are needed. Furthermore, the general applicability of this procedure is limited by the small availability of post-functionalization reactions, which restricts the selection of chromophores.<sup>6</sup>

In this Chapter, a recently developed procedure to synthesize polycarbonates is used. It concerns the polycondensation polymerization of bisphenol derivatives with triphosgene (bis(trichloromethyl)carbonate).<sup>12,13</sup> This methodology has two main advantages over the former one: (i) virtually any dihydroxy-containing monomer can be used; (ii) the monomer-to-monomer ratio is not limited to equimolarity, but can easily be varied over a wide range, or even more than two different dihydroxy monomers can be employed. This results in a greatly improved versatility in tuning the physico-chemical properties (i.e. rigidity,  $T_g$ , thermal stability) of the final material.

**Scheme 1.** General strategy for the synthesis of side-chain NLO polycarbonates.

To the best of our knowledge, there are no synthetic procedures that provide a convenient modular approach to attach NLO chromophores to the polycarbonate backbone. This Chapter deals with a versatile synthesis of NLO side-chain polycarbonates as depicted in Scheme 1. It is based on the reaction of a carboxylic acid-containing polycarbonate with appropriately functionalized chromophores. The introduction of the chromophore in the final reaction step also allows a great flexibility, both in forming the polymer backbone, and controlling the amount of chromophore incorporated. In addition to the synthesis, the characterization, the thermal properties as well as the second-order nonlinearity of the synthesized polymeric materials is described.

## 5.2 Results and Discussion

### 5.2.1 Synthesis

To synthesize a polycarbonate with a pendent anchoring group 4,4-bis(4-hydroxyphenyl)valeric acid (**1**) was chosen as diphenolic monomer. It is known that its carboxylic acid group causes cross-linking and branching when directly polymerized with phosgene.<sup>14</sup> Therefore to obtain well-defined, linear polycarbonates, the carboxylic group was first protected by esterification with *tert*-butanol (Scheme 2). The obtained bisphenol **2** was then condensed with bisphenol Z (**4**) using triphosgene and pyridine as a base in the presence of a few mol % of phenol as chain terminator to give polymer **5** with  $M_n$  in the range of ~10000 to ~15000 and a polydispersity of ~ 2, and a good solubility.<sup>15</sup> Subsequently, the *tert*-butyl groups in polymer **5** were quantitatively cleaved with trifluoroacetic acid at room temperature, achieving polycarbonate **7** with free pendent carboxylic acid groups. The completion of the reaction was checked by the consistent reduction of the C-H stretching band at around 2900 nm in the IR spectrum, and the complete disappearance of the singlet of the *tert*-butyl group at 1.41 ppm in the <sup>1</sup>H NMR spectrum.

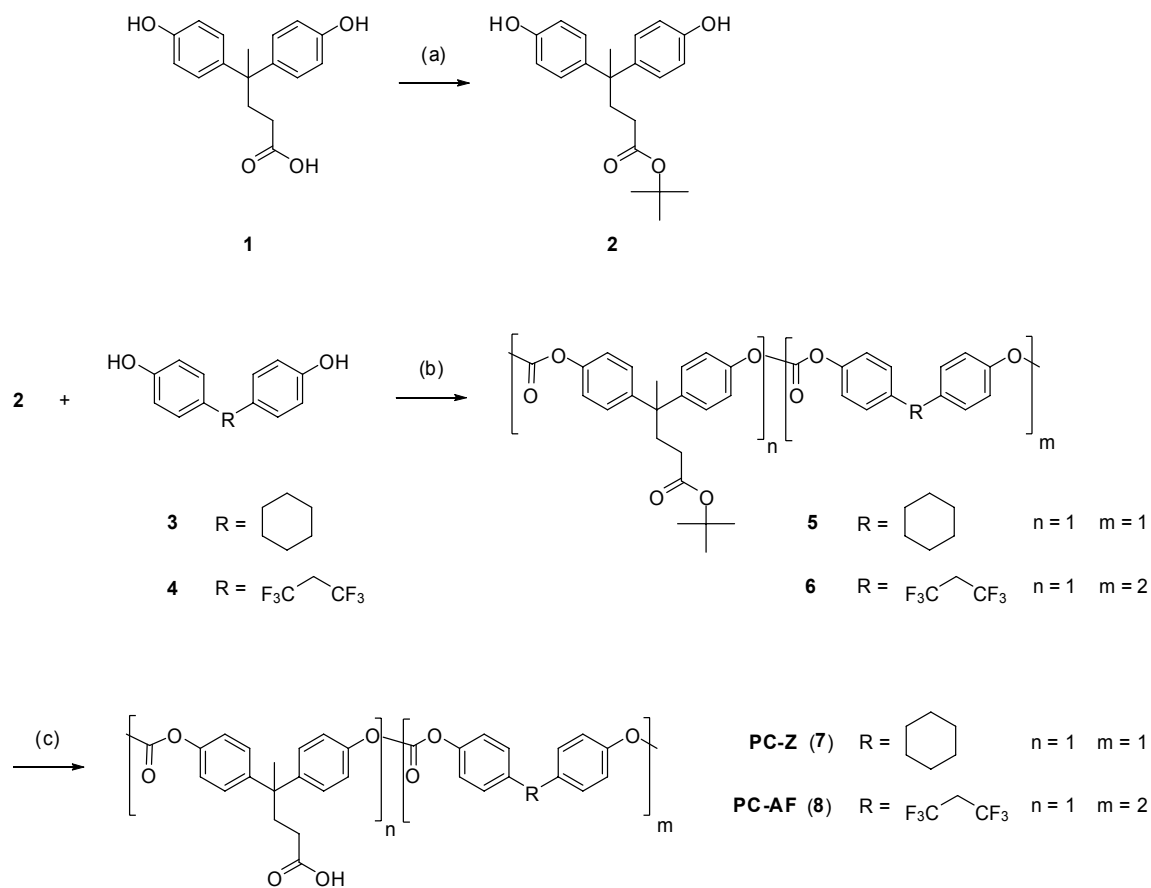
Polymers that contain fluorine in or along the backbone possess many desirable physical properties. In general, fluoropolymers exhibit high thermal stabilities, enhanced chemical resistance, and decreased intermolecular attractive forces (which turns in a better solubility) compared to their hydrocarbon analogs.<sup>16,17</sup> The optical loss by absorption due to the vibration overtones of the polymer at the key telecommunication wavelength of 1.3  $\mu\text{m}$  is also minimized by substituting hydrogen with fluorine.<sup>18</sup>

To obtain a polycarbonate with high fluorine content, bisphenol AF (**4**) was used, containing two CF<sub>3</sub> groups instead of the cyclohexyl moiety in bisphenol Z (**3**). Following the same procedure described above, monomer **2** was copolymerized in a 1:2 ratio with bisphenol AF (**4**) to obtain polycarbonate **PC-AF** (**8**) (Scheme 2).

The polycarbonates **PC-Z** (**7**) and **PC-AF** (**8**) are soluble in polar solvents, such as THF, DMF, and cyclopentanone, with polymer **PC-AF** (**8**) showing the best solubility. This

might be explained either by the presence of the hexafluoropropylidene moiety reducing intermolecular packing, or by the smaller content of carboxylic acid groups.

**Scheme 2.** Synthesis of the **PC-Z (7)** and **PC-AF (8)** polycarbonates.<sup>a</sup>

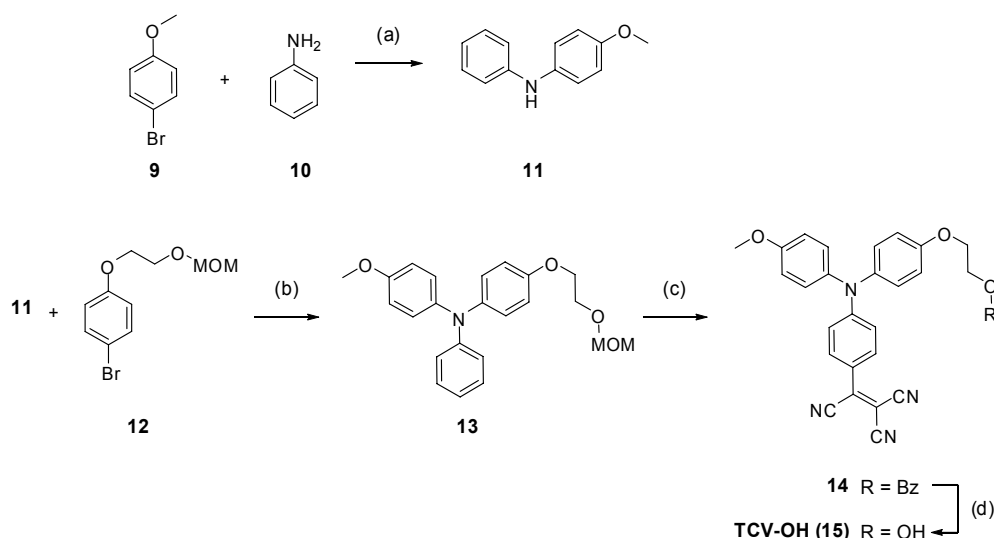


<sup>a</sup> Reagents and conditions: (a) trifluoroacetic anhydride, *tert*-butanol, THF, rt; (b) triphosgene, pyridine, THF, CH<sub>2</sub>Cl<sub>2</sub>, rt; (c) CF<sub>3</sub>COOH, CH<sub>2</sub>Cl<sub>2</sub>, rt.

The synthesis of monohydroxyalkyl **TCVDPA** type chromophore **TCV-OH (15)** is depicted in Scheme 3. In a sequential Hartwig-Buchwald Pd-catalyzed amination, 4-bromoanisole (**9**) was first reacted with aniline (**10**) to give diarylamine **11**, which was then reacted with arylbromide **12** to afford triarylamine **13** having a methoxymethyl (MOM)-protected hydroxyl group. Subsequent reaction of triarylamine **13** with tetracyanoethylene (TCNE) in DMF gave chromophore **14**. Its MOM protecting group was then cleaved with bromotrimethylsilane to give chromophore **TCV-OH (15)**. The

completion of the reaction was proven by the complete disappearance in the  $^1\text{H}$  NMR spectrum of the peaks at 3.40 and 3.88 ppm corresponding to the methoxymethyl protons.

**Scheme 3.** Synthesis of the **TCV-OH (15)** chromophore.<sup>a</sup>



<sup>a</sup> Reagents and conditions: (a, b)  $\text{Pd}_2(\text{dba})_3$ , 1,1'-bis-(diphenylphosphino)ferrocene (DPPF), *t*-BuONa, toluene, reflux; (c) TCNE, DMF, rt; (d) bromotrimethylsilane,  $\text{CH}_2\text{Cl}_2$ , 0 °C.

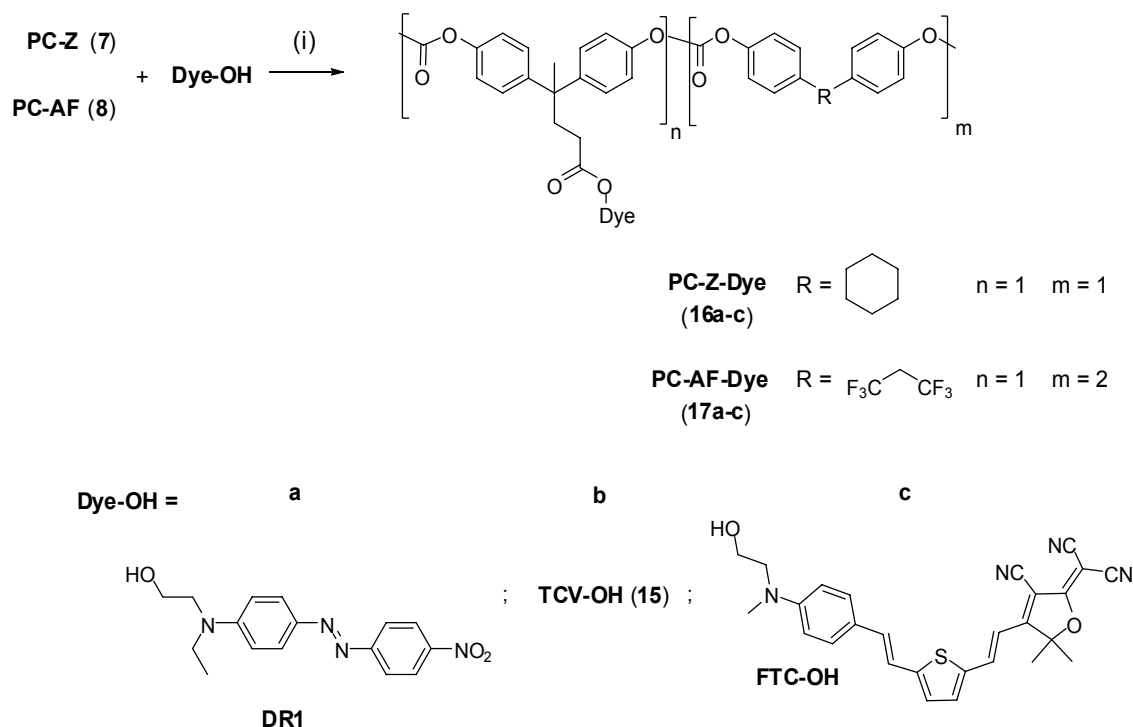
The hydroxyethyl-group containing chromophores **DR1**, **TCV-OH**, and **FTC-OH** (Scheme 4) were attached to the polycarbonate backbones using 1,3-dicyclohexylcarbodiimide (DCC) and 4-(dimethylamino)pyridium-4-toluenesulfonate (DPTS) as the coupling agents.<sup>19</sup> This methodology has been reported to provide efficient anchoring of high- $\mu\beta$  dyes, such as the **CLD** and **FTC** type (see Chapter 2), to a wide variety of polymers and dendrimers.<sup>20-23</sup> After attaching the chromophores a new peak appeared in the  $^1\text{H}$  NMR spectra at about 4.18 ppm, that was assigned to the oxymethylene protons ( $-\text{OCH}_2-$ ) of the ester linkage with the dye. The degree of functionalization was determined either on the basis of the peak area of the methylene protons of the pendent group (at 2.0-2.3 ppm) and the area at 4.2 ppm that corresponds to the  $-\text{OCH}_2-$  protons, or by quantitative analysis of the UV spectra of their solution in THF. In all cases, attachment efficiencies of over 70% were obtained (Table 1).

All NLO polymers containing the **DR1** and **FTC** chromophores have a good solubility in high boiling solvents, such as cyclopentanone. Disappointingly, the **PC-Z-**



**TCV (16b)** and **PC-AF-TCV (17b)** polymers show a poor solubility. This might be explained by the chemical sensitivity of the tricyanovinyl (TCV) moiety to nucleophiles, which may have caused a certain degree of crosslinking under the conditions of the attachment. This hypothesis is supported by the increase in the  $M_w$  of the polymer determined by gel permeation chromatography (GPC). This deficiency may be overcome either by using a 2-phenyl-tetracyanobutadienyl (Ph-TCBD) moiety having an aryl group instead of the most reactive CN group in the TCV moiety, resulting in a better stability to amine nucleophiles<sup>24</sup> or by employing even milder conditions, such as the Mitsunobu reaction.<sup>25,26</sup>

**Scheme 4.** Dye attachment to the polycarbonates **PC-Z (7)** and **PC-AF (8)**.<sup>a</sup>



<sup>a</sup> Reagents and conditions: (i) DCC, DPTS,  $\text{CH}_2\text{Cl}_2$ , THF, rt.

**Table 1.** Summary of the thermal, physical, and optical properties the NLO polycarbonates.

	$\lambda_{\max}^a$ (nm)	$T_d^{5b}$ (°C)	$T_g$ (°C)	$M_w$	$M_w/M_n$	Chrom. density (wt%)	$r_{33}$ (pm/V)
<b>PC-Z-DR1 (16a)</b>	476	347	202	14500	2.3	29	22 <sup>c</sup>
<b>PC-Z-TCV (16b)</b>	526	352	213	36400	4.1	32	-
<b>PC-Z-FTC (16c)</b>	624	282	186	16200	2.1	35	26 <sup>d</sup>
<b>PC-AF-DR1 (17a)</b>	475	385	189	16800	2.0	20	16 <sup>c</sup>
<b>PC-AF-TCV (17b)</b>	525	384	198	38900	4.4	22	-
<b>PC-AF-FTC (17c)</b>	629	303	174	19300	2.4	24	38 <sup>d</sup>

<sup>a</sup>  $\lambda_{\max}$  was measured in THF; <sup>b</sup>  $T_d^{5}$  is defined as the point at which 5% weight loss has occurred in the polymer; <sup>c</sup> measured at 830 nm; <sup>d</sup> measured at 1300 nm

### 5.2.2 Polymer Physical Properties and Processing

The thermal properties of the polymers were determined by DSC and TGA measurements. All NLO side-chain polycarbonates have a high  $T_g$  (>174 °C) and excellent thermal stabilities (Table 1). The  $T_g$  of these polymers varied from 174-213 °C, depending on the structure and the density of the attached chromophores. Weight losses of less than 5% were observed up to 280 °C. In general, the NLO polymers containing the bisphenol Z monomer show sensibly higher  $T_g$  values (11-15 °C) compared with the corresponding polymers containing the bisphenol AF monomer, while the former ones possess higher decomposition temperatures  $T_d^{5}$  (21-38 °C). Moreover, the fact that polymers containing the thermally most stable **TCV-OH (15)** chromophore ( $T_d > 350$  °C) also possess the highest  $T_d^{5}$  of the NLO polymers, suggests that the thermal properties of NLO polycarbonates can be further improved if thermally more stable chromophores are chosen.

UV spectra of the NLO polymers were recorded in CH<sub>2</sub>Cl<sub>2</sub> and the  $\lambda_{\max}$  values are reported in Table 1. All polymers exhibit strong absorption maxima in the visible region attributed to the  $\pi$ - $\pi^*$  charge-transfer band of NLO chromophores and show colors ranging from red to blue (Figure 1).

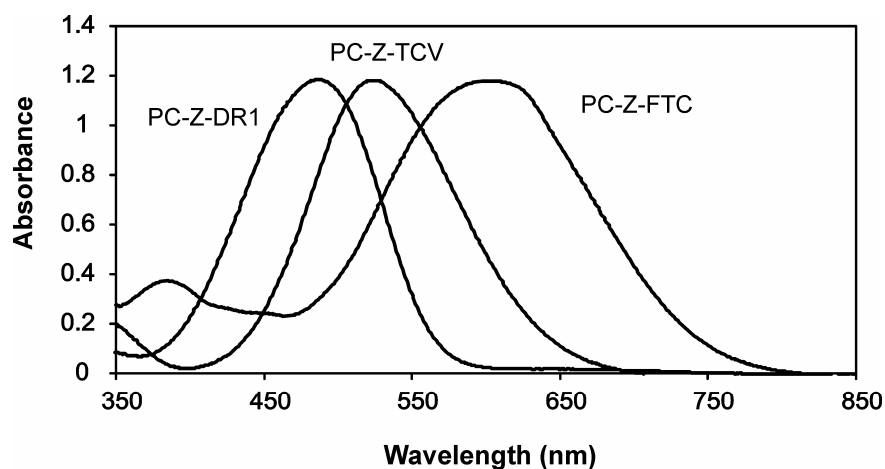


**Figure 1.** Absorption spectrum of the **PC-Z-DR1 (16a)**, **PC-Z-TCV (16b)**, and **PC-Z-FTC (16c)** polymers in THF.

To minimize the optical loss contributed from absorption, it is important to have the material with its absorption band edge far away from the operating wavelength of EO devices. Therefore, the **PC-Z-FTC (16c)** and **PC-AF-FTC (17c)** polymers are suitable for use at 1300 nm, while the polymers containing the **DR1** and **TCV** chromophores are more appropriate to be used at 830 nm. Accordingly, the measurements of the EO coefficient ( $r_{33}$ ) were carried out at two different wavelengths, and the results are reported in Table 1.

Thin films for EO measurements were prepared as described in Chapter 3, starting from solutions of the NLO polycarbonates at 10-15 wt% in cyclopentanone. The  $r_{33}$  values, reported in Table 1, were measured using a Teng-Man simple reflection technique.<sup>27</sup>

For the **PC-Z-TCV (16b)** and **PC-AF-TCV (17b)** polymers it was not possible to obtain optical-quality thin films, due to the poor solubility in spin-coating solvents, making any EO coefficient measurement impossible to be performed. For the **PC-Z-DR1 (16a)** and **PC-AF-DR1 (17a)** polymers, containing 29 and 20 wt% of **DR1** chromophore,  $r_{33}$  values of 22 and 16 pm/V (at 830 nm) were measured, respectively.

It has been reported that the  $r_{33}$  values for **FTC**-based guest-host systems increase up to 55 pm/V upon chromophore loading, but decrease again when more than  $\sim 25$  wt% is added.<sup>4,28</sup> For **PC-Z-FTC (16c)**, containing 36 wt% of the highly active **FTC-OH** dye,

an EO coefficient of 26 pm/V (at 1300 nm) was recorded. This can be attributed to the detrimental aggregation effects between the highly polar chromophores, which decreases the EO response at high chromophore loading levels. This hypothesis is in part supported by the fact that the highest  $r_{33}$  value, being 37 pm/V, was obtained for **PC-AF-FTC (17c)** containing only 24 wt% of chromophore. A similar behavior has been observed for other polymer systems containing highly active dyes.<sup>29,30</sup>

This problem may be avoided by incorporation of bulky structures into the polymer backbone or directly into the chromophore that can ensure site isolation, consequently avoiding chromophore aggregation at high loading densities.<sup>4,31,32</sup>

### 5.3 Conclusions

A versatile, generally applicable synthetic methodology for side-chain NLO polycarbonates was developed. This represents the first example of covalent incorporation of NLO chromophores to a pre-polymerized polycarbonate backbone. This methodology allows to adjust the polymer backbone structure and to vary the chromophore loading level in order to fine-tune the physical properties of the resulting material. The resulting NLO polycarbonates possess a high thermal stability, good solubility and can be easily processed into films of excellent quality. In spite of the high chromophore concentrations, fairly high glass transition temperatures were obtained ( $T_g$ s as high as 213 °C). Moreover, when a **FTC** type of chromophore was incorporated EO coefficients as high as 38 pm/V (at 1300 nm) were achieved. The combination of these properties provides a great promise for the development of EO devices. Attachment of bulky spacers or cross-linkable units to the pendent carboxylic acid groups may further enhance both the poling efficiency and the temporal stability of these materials.

### 5.4 Experimental Section

**General Procedures.** All chemicals were obtained from commercial sources and used without further purification. THF was freshly distilled from Na/benzophenone, and

CH<sub>2</sub>Cl<sub>2</sub> from CaCl<sub>2</sub>. All chromatography associated with product purification was performed by flash column techniques using Merck Kieselgel 600 (230-400 mesh). All reactions were carried out under an inert argon atmosphere. Melting points of all compounds were obtained with a Reichert melting point apparatus and a Kofler stage. <sup>1</sup>H and <sup>13</sup>C NMR spectra were recorded on a Varian Unity 300 spectrometer using tetramethylsilane (TMS) or the corresponding residual solvent signal as internal standard. FAB-MS spectra were recorded on a Finningan MAT 90 spectrometer with *m*-nitrobenzyl alcohol (NBA) as a matrix. Thermogravimetric (TGA) analyses were conducted using a Perkin-Elmer TGA-7 thermogravimetric analyzer (heating rate: 20 °C/min). Differential scanning calorimetry (DSC) was performed using a Perkin-Elmer DSC-7 instrument at a heating rate of 20 °C/min. The molecular weights and polydispersities (relative to polystyrene standards) were determined by PL-GPC-120 gel permeation chromatograph (GPC) using THF as eluent. Infrared spectra were taken on Perkin-Elmer BX FT-IR spectrometer by incorporating samples in KBr disks. UV-Vis measurements were carried out on a Varian Cary 3E UV-spectrophotometer.

DPTS<sup>19</sup>, CLD-OH<sup>29</sup>, and compound **12**<sup>33</sup> were prepared according to literature procedures.

**Bisphenol derivative 2.** To a solution of diphenolic acid (**1**) (30.1 g, 0.1 mol) in THF (100 mL) was added dropwise trifluoroacetic anhydride (50 mL) at 0 °C. Subsequently, the mixture and stirred for 3 h at rt. *Tert*-butanol (80 mL) was then added dropwise to the reaction mixture at 0 °C. Subsequently, the mixture was stirred overnight at rt. A 10% aqueous K<sub>2</sub>CO<sub>3</sub> solution was added until neutral pH. The oil-like product was extracted with CH<sub>2</sub>Cl<sub>2</sub> (2 × 250 mL). The combined organic layers were dried over MgSO<sub>4</sub> and evaporated to dryness. The crude product was purified by column chromatography (diethyl ether/hexane v/v 6/4) to give **2** as a white solid (80%): mp 131-132 °C; <sup>1</sup>H NMR (acetone-*d*<sub>6</sub>), δ 1.41 (s, 9H, CH<sub>3</sub>), 1.52 (s, 3H CH<sub>3</sub>), 2.02 (t, *J* = 8.2 Hz, 2H, CH<sub>2</sub>), 2.34 (t, *J* = 8.3 Hz, 2H, CH<sub>2</sub>), 6.78 (d, *J* = 8.6 Hz, 4H, ar-H), 7.06 (d, *J* = 8.6 Hz, 4H, ar-H), 8.18 (s, 2H, OH); <sup>13</sup>C NMR (acetone-*d*<sub>6</sub>), δ 13.4, 27.6, 33.8, 44.4, 79.5, 114.9, 128.3, 140.4, 155.4, 177.4; IR ν 831, 1014, 1163, 1195, 1229 (C-O), 1504, 1709 (COOH), 1773 (O-COO), 2971.

**4-Methoxydiphenylamine (11).** A mixture of aniline (2.0 g, 21.5 mmol), 4-bromoanisole (2.3 mL, 18.1 mmol), Pd<sub>2</sub>(dba)<sub>3</sub> (311 mg, 0.34 mmol), DPPF (295 mg, 0.53 mmol), *t*-BuONa (2.9 g, 29.6 mmol) in toluene (50 mL) was refluxed for 24 h. The toluene was removed in vacuo and the residue was purified by column chromatography (hexane/ethyl acetate v/v 9/1) to give **11** as a yellow solid (60%): mp 100-104 °C; <sup>1</sup>H NMR (CDCl<sub>3</sub>), δ 3.83 (s, 3H, CH<sub>3</sub>), 5.51 (s, 1H, NH), 6.81-6.93 (m, 6H, Ar-H), 7.07 (d, *J* = 9.1 Hz, 2H, ar-H), 7.21 (t, *J* = 7.95 Hz, 1H, ar-H); <sup>13</sup>C NMR (CDCl<sub>3</sub>), δ 55.8, 114.9, 116.1, 120.1, 122.5, 129.5, 135.9, 145.4, 155.9; MS MALDI-ESI *m/z* 199.1 ([M]<sup>+</sup>), 200.1 ([M+H]<sup>+</sup>) calcd for C<sub>13</sub>H<sub>13</sub>NO 199.1.

**Triarylamine 13.** A mixture of 4-methoxydiphenylamine **11** (2.3 g, 11.6 mmol), **12** (3.0 g, 11.6 mmol), Pd<sub>2</sub>(dba)<sub>3</sub> (168 mg, 0.18 mmol), DPPF (160 mg, 0.29 mmol), *t*-BuONa (1.6 g, 16.3 mmol) in toluene (50 mL) was refluxed for 24 h. The toluene was removed in vacuo and the residue was purified by column chromatography (hexane/ethyl acetate v/v 8/2) to give **13** as a yellow oil (80%): <sup>1</sup>H NMR (CDCl<sub>3</sub>), δ 3.40 (s, 3H, OCH<sub>3</sub>), 3.78 (s, 3H, OCH<sub>3</sub>), 3.88 (t, *J* = 4.8 Hz, 2H, OCH<sub>2</sub>), 4.12 (t, *J* = 4.8 Hz, 2H, OCH<sub>2</sub>), 4.71 (s, 3H, OCH<sub>3</sub>), 6.79-6.85 (m, 6H, ar-H), 6.93 (d, *J* = 8.6 Hz, 2H, ar-H), 7.01-7.04 (m, 4H, ar-H), 7.16 (t, *J* = 7.95 Hz, 1H, ar-H); <sup>13</sup>C NMR (CDCl<sub>3</sub>), δ 55.4, 55.5, 55.7, 66.2, 67.8, 96.8, 114.8, 120.8, 121.2, 126.4, 126.6, 129.1, 141.3, 141.6, 148.9, 155.0, 155.9; MS MALDI-ESI *m/z* 379.1 [M]<sup>+</sup>, 402.1 [M+Na]<sup>+</sup> calcd for C<sub>23</sub>H<sub>25</sub>NO<sub>4</sub> 379.18.

**Chromophore TCV-O-MOM (14).** To a solution of **13** (1.5 g, 4.0 mmol) in DMF (20 mL) was added tetracyanoethylene (2.1 g, 16.0 mmol). The resulting mixture was stirred at rt for 12 h, and then extracted with a saturated solution of NaHCO<sub>3</sub> (3 x 100 mL) and CHCl<sub>3</sub> (250 mL). The combined organic layers were dried, evaporated to dryness and the residue was washed with methanol to give **14** as a purple solid (78%): mp 68-70 °C; <sup>1</sup>H NMR (CDCl<sub>3</sub>), δ 3.40 (s, 3H, OCH<sub>3</sub>), 3.88 (s, 3H, OCH<sub>3</sub>), 3.91 (t, *J* = 4.7 Hz, 2H, OCH<sub>2</sub>), 4.14 (t, *J* = 4.7 Hz, 2H, OCH<sub>2</sub>), 6.82 (d, *J* = 9.3 Hz, 2H, ar-H), 6.94 (t, *J* = 8.8 Hz, 4H, ar-H), 7.13 (d, *J* = 8.8 Hz, 4H, ar-H), 7.92 (d, *J* = 9.3 Hz, 2H, ar-H); <sup>13</sup>C

NMR (CDCl<sub>3</sub>),  $\delta$  55.4, 55.6, 66.0, 67.9, 96.7, 96.8, 96.9, 113.6, 113.7, 114.5, 115.6, 116.9, 119.7, 128.3, 132.6, 137.0, 137.3, 137.7, 155.3, 157.9, 158.7; MS MALDI-ESI  $m/z$  480.2 ([M]<sup>+</sup>), 481.2 ([M+H]<sup>+</sup>) calcd for C<sub>28</sub>H<sub>24</sub>N<sub>4</sub>O<sub>4</sub> 480.18.

**Chromophore TCV-OH (15).** To a cooled solution of **14** (1.0 g, 2.1 mmol) in CH<sub>2</sub>Cl<sub>2</sub> (50 mL) was added dropwise bromotrimethylsilane (6 mL). The reaction mixture was stirred at -20 °C for 2.5 h, and then neutralized with a saturated solution of NaHCO<sub>3</sub> (200 mL). After layer separation, the aqueous layer was extracted with CH<sub>2</sub>Cl<sub>2</sub> (50 mL). The combined organic layers were dried over MgSO<sub>4</sub> and evaporated to dryness. Recrystallization from ethanol gave **TCV-OH (15)** as a purple powder (85%): mp 60-63 °C; <sup>1</sup>H NMR (CDCl<sub>3</sub>),  $\delta$  3.67 (s, 3H, OCH<sub>3</sub>), 3.79-3.83 (m, 4H, OCH<sub>2</sub>), 3.92-4.01 (m, 4H, OCH<sub>3</sub>), 6.67 (d,  $J$  = 9.3 Hz, 2H, ar-H), 6.78 (t,  $J$  = 8.8 Hz, 4H, ar-H), 6.96-7.00 (m, 4H, ar-H), 7.77 (d,  $J$  = 9.2 Hz, 2H, ar-H); <sup>13</sup>C NMR (CDCl<sub>3</sub>),  $\delta$  55.7, 55.8, 61.5, 69.8, 113.4, 113.7, 114.4, 115.6, 116.2, 116.9, 119.8, 128.3, 132.6, 137.0, 137.5, 137.8, 155.2, 157.7, 158.7; MS MALDI-ESI  $m/z$  436.4 [M]<sup>+</sup>, 437.4 [M+H]<sup>+</sup>, 459.4 [M+Na]<sup>+</sup> calcd for C<sub>26</sub>H<sub>20</sub>N<sub>4</sub>O<sub>3</sub> 436.15.

**Polymer 5.** To a mixture of **2** (1.52 g, 4.5 mmol) and bisphenol Z (**3**) (1.50 g, 4.5 mmol) in a mixture of CH<sub>2</sub>Cl<sub>2</sub> (40 mL) and THF (30 mL) was added triphosgene (925 mg, 3.12 mmol). After stirring for 10 min at rt, the mixture was cooled at 0 °C and a solution of pyridine (2.4 mL, 29.7 mmol) in dry THF (10 mL) was added dropwise. Subsequently, the mixture was stirred overnight at rt. The polymer was precipitated in methanol (500 mL), filtered, washed with methanol, and dried in a vacuum oven for 24 h at 60 °C (90%): <sup>1</sup>H NMR (CDCl<sub>3</sub>),  $\delta$  1.33 (s, 9H, CH<sub>3</sub>), 1.41-1.52 (m, 6H, CH<sub>2</sub>), 1.94 (t,  $J$  = 7.5 Hz, 2H, CH<sub>2</sub>), 2.15-2.22 (m, 5H, CH<sub>2</sub>), 2.32 (t,  $J$  = 7.5 Hz, 2H, CH<sub>2</sub>), 7.08-7.22 (m, 16H, ar-H); IR  $\nu$  1162 (C-O), 1506 (C=C aromatic), 1727 ((CH<sub>3</sub>)<sub>3</sub>), 1777 (O-COO), 2937 (C-H), 3043 (C-H, aromatic).

**Polymer PC-Z (7).** To a solution of polymer **5** (3.0 g) in CH<sub>2</sub>Cl<sub>2</sub> (30 mL) was added trifluoroacetic acid (2 mL), and the reaction mixture was stirred at rt for 3 h. Subsequently, CH<sub>2</sub>Cl<sub>2</sub> was evaporated and the residual liquid was treated with a large

amount of water. The precipitated polymer was filtered, washed with distilled water several times, and then dried in a vacuum oven for 5 h at 50 °C (95%):  $^1\text{H}$  NMR (DMSO- $d_6$ ),  $\delta$  1.42-1.57 (m, 9H, CH<sub>2</sub>), 1.87-1.99 (m, 2H, CH<sub>2</sub>), 2.18-2.39 (m, 6H, CH<sub>2</sub>), 7.20-7.24 (m, 10H, ar-H), 7.36-7.39 (m, 6H, ar-H); IR  $\nu$  1192 (C-O), 1507 (C=C, aromatic), 1705 (COOH), 1774 (O-COO), 2937 (C-H), 3043 (C-H, aromatic).

**Polymer 6.** To a mixture of **2** (318 mg, 0.93 mmol) and bisphenol AF (**4**) (934.7 mg, 2.78 mmol) in a mixture of CH<sub>2</sub>Cl<sub>2</sub> (20 mL) and THF (15 mL) was added triphosgene (386 mg, 1.30 mmol). After stirring for 10 min at rt, the mixture was cooled at 0 °C and a solution of pyridine (1.05 mL, 13.0 mmol) in dry THF (5 mL) was added dropwise. Subsequently, the mixture was stirred overnight at rt. The polymer was precipitated in methanol (350 mL), filtered, washed with methanol, and dried in a vacuum oven for 24 h at 60 °C (86%):  $^1\text{H}$  NMR (CDCl<sub>3</sub>),  $\delta$  1.41 (s, 9H, CH<sub>3</sub>), 1.63 (s, 3H, CH<sub>3</sub>), 2.02 (t,  $J$  = 8.1 Hz, 2H, CH<sub>2</sub>), 2.42 (t,  $J$  = 8.1 Hz, 2H, CH<sub>2</sub>), 7.17-7.25 (m, 4H, ar-H), 7.32 (d,  $J$  = 9.0 Hz, 6H, ar-H), 7.46 (d,  $J$  = 8.5 Hz, 6H, ar-H); IR  $\nu$  1162 (C-O), 1244 (C-F), 1508 (C=C aromatic), 1727 ((CH<sub>3</sub>)<sub>3</sub>), 1776 (O-COO), 2936 (C-H), 3042 (C-H, aromatic).

**Polymer PC-AF (8).** To a solution of polymer **6** (3.0 g) in CH<sub>2</sub>Cl<sub>2</sub> (30 mL) was added trifluoroacetic acid (2 mL), and the reaction mixture was stirred at rt for 3 h. Subsequently, CH<sub>2</sub>Cl<sub>2</sub> was evaporated and the residual liquid was treated with a large amount of water. The precipitated polymer was filtered, washed with distilled water several times, and then dried in a vacuum oven for 5 h at 50 °C (96%):  $^1\text{H}$  NMR (DMSO- $d_6$ ),  $\delta$  1.62 (s, 3H, CH<sub>3</sub>), 2.03-2.20 (m, 2H, CH<sub>2</sub>), 2.37-2.51 (m, 2H, CH<sub>2</sub>), 7.20-7.30 (m, 10H, ar-H), 7.45 (d,  $J$  = 8.0 Hz, 6H, ar-H); IR  $\nu$  1192 (C-O), 1244 (C-F), 1507 (C=C, aromatic), 1706 (COOH), 1774 (O-COO), 2937 (s, C-H), 3043 (C-H aromatic).

**Attachment of dyes to PC-Z.** A typical procedure is as follows: To a solution of **PC-Z (7)** (300 mg) in a mixture of THF (10 mL) and CH<sub>2</sub>Cl<sub>2</sub> (10 mL) was added the chromophore **Dye-OH** (0.495 mmol) followed by DPTS (29 mg), and the mixture was stirred at rt for 15 min. DCC (115 mg) was then added, and the mixture was stirred for 12 h. The precipitated urea was filtered off, and the polymer was isolated by precipitation



into methanol (250 mL) followed by filtration. This procedure was repeated until the filtrate was colorless. Drying typically yielded 80-85% of the **PC-Z-Dye (16a-c)** polymers as powders.

**Polymer PC-Z-DR1 (16a).**  $^1\text{H}$  NMR ( $\text{CDCl}_3$ ),  $\delta$  1.18-1.38 (m,  $\text{CH}_3$ ), 1.40-1.98 (m,  $\text{CH}_2$ ), 2.03-2.15 (br m,  $\text{CH}_2$ ), 2.21-2.30 (br m,  $\text{CH}_2$ ), 2.37-2.43 (br m,  $\text{CH}_2$ ), 3.41-3.55 (m,  $\text{NCH}_2$ ), 3.60-3.65 (m,  $\text{NCH}_2$ ), 4.18-4.28 (m,  $\text{OCH}_2$ ), 6.76 (d,  $J = 9.5$  Hz, ar-H), 7.06-7.36 (m, ar-H), 7.39-7.41 (m, ar-H), 7.82-8.00 (m, ar-H), 8.20 (d,  $J = 9.3$  Hz, ar-H).

**Polymer PC-Z-TCV (16b).**  $^1\text{H}$  NMR ( $\text{DMSO}-d_6$ )  $\delta$  1.42-1.69 (m,  $\text{CH}_2$ ), 1.61 (s,  $\text{CH}_3$ ), 2.10-2.25 (m,  $\text{CH}_2$ ), 2.33-2.43 (br m,  $\text{CH}_2$ ), 2.48-2.61 (br m,  $\text{CH}_2$ ), 3.60 (s,  $\text{OCH}_3$ ), 3.84-3.90 (br m,  $\text{OCH}_2$ ), 4.10-4.18 (br m,  $\text{OCH}_2$ ) 6.76 (d,  $J = 8.9$  Hz, ar-H), 6.96-7.45 (m, ar-H), 7.80 (d,  $J = 8.7$  Hz, ar-H).

**Polymer PC-Z-FTC (16c).**  $^1\text{H}$  NMR ( $\text{CDCl}_3$ ),  $\delta$  1.38-1.52 (m,  $\text{CH}_2$ ), 1.56 (s,  $\text{CH}_3$ ), 1.96-2.19 (br m,  $\text{CH}_2$ ), 2.28-2.39 (br m,  $\text{CH}_2$ ), 2.99 (s,  $\text{CH}_3$ ), 3.48-3.54 (br m,  $\text{CH}_2$ ), 4.06-4.16 (br m,  $\text{OCH}_2$ ), 6.44 (d,  $J = 12$  Hz, ar-H), 6.54-6.72 (br m, ar-H), 6.75-6.95 (br m, ar-H), 7.04-7.43 (m, ar-H), 7.66 (d,  $J = 12$  Hz, ar-H).

**Attachment of dyes to the polymer PC-AF (8).** A typical procedure is as follows: To a solution of **PC-AF (8)** (500 mg) in a mixture of THF (15 mL) and  $\text{CH}_2\text{Cl}_2$  (15 mL) was added the chromophore **Dye-OH (15)** (0.482 mmol) followed by DPTS (28 mg), and the mixture was stirred at rt for 15 min. DCC (102 mg) was then added, and the mixture was stirred for 12 h. The precipitated urea was filtered off, and the polymer was isolated by precipitation into methanol (400 mL) followed by filtration. This procedure was repeated until the filtrate was colorless. Drying typically yielded 80-85% of the **PC-AF-Dye (17a-c)** polymers as powders.

**Polymer PC-AF-DR1 (17a).**  $^1\text{H}$  NMR ( $\text{CDCl}_3$ ),  $\delta$  1.15 (t,  $J = 7.2$  Hz,  $\text{CH}_3$ ), 1.52 (s,  $\text{CH}_3$ ), 1.98-2.05 (br m,  $\text{CH}_2$ ), 2.26-2.37 (br m,  $\text{CH}_2$ ), 3.38-3.44 (m,  $\text{NCH}_2$ ), 3.54-3.61 (m,

NCH<sub>2</sub>), 4.14-4.22 (m, OCH<sub>2</sub>), 6.71 (d,  $J = 8.7$  Hz, ar-H), 7.11-7.27 (m, ar-H), 7.39-7.41 (m, ar-H), 7.83 (m, ar-H), 7.22 (d,  $J = 8.7$  Hz, ar-H).

**Polymer PC-AF-TCV (17b).** <sup>1</sup>H NMR (DMSO-*d*<sub>6</sub>)  $\delta$  1.62 (s, CH<sub>3</sub>), 1.96-2.11 (br m, CH<sub>2</sub>), 2.25-2.39 (br m, CH<sub>2</sub>), 3.62 (s, OCH<sub>3</sub>), 3.82-3.88 (br m, OCH<sub>2</sub>), 4.12-4.19 (br m, OCH<sub>2</sub>) 6.76 (d,  $J = 9.0$  Hz, ar-H), 6.96-7.45 (m, ar-H), 7.77 (d,  $J = 8.9$  Hz, ar-H).

**Polymer PC-AF-FTC (17c).** <sup>1</sup>H NMR (CDCl<sub>3</sub>),  $\delta$  1.45 (s, CH<sub>3</sub>), 1.56 (s, CH<sub>3</sub>), 1.95-2.10 (br m, CH<sub>2</sub>), 2.24-2.35 (br m, CH<sub>2</sub>), 2.93 (s, CH<sub>3</sub>), 3.52-3.57 (br m, CH<sub>2</sub>), 4.08-4.16 (br m, OCH<sub>2</sub>), 6.50 (d,  $J = 12$  Hz, ar-H), 6.60-6.72 (br m, Ar-H), 6.90-6.95 (br m, ar-H), 7.11-7.38 (m, ar-H), 7.66 (d,  $J = 12$  Hz, ar-H).

## 5.5 References

- 1 C. C. Chang, C. P. Chen, C. C. Chou, W. J. Kuo, R. J. Jeng, *J. Macromol. Sci., Polym. Rev.*, **2005**, *45*, 125-170.
- 2 C. Samyn, T. Verbiest, A. Persoons, *Macromol. Rapid Commun.*, **2000**, *21*, 1-15.
- 3 F. Kajzar, K. S. Lee, A. K. Y. Jen, *Adv. Polym. Sci.*, **2003**, *161*, 1-85.
- 4 Y. Liao, C. A. Anderson, P. A. Sullivan, A. J. P. Akelaitis, B. H. Robinson, L. R. Dalton, *Chem. Mater.*, **2006**, *18*, 1062-1067.
- 5 M. H. Davey, V. Y. Lee, L. M. Wu, C. R. Moylan, W. Volksen, A. Knoesen, R. D. Miller, T. J. Marks, *Chem. Mater.*, **2000**, *12*, 1679-1693.
- 6 E. Gubbelmans, T. Verbiest, M. Van Beylen, A. Persoons, C. Samyn, *Polymer*, **2002**, *43*, 1581-1585.
- 7 M. E. Wright, S. Fallis, A. J. Guenther, L. C. Baldwin, *Macromolecules*, **2005**, *38*, 10014-10021.
- 8 H. Ma, A. K. Y. Jen, J. Y. Wu, X. M. Wu, S. Liu, C. F. Shu, L. R. Dalton, S. R. Marder, S. Thayumanavan, *Chem. Mater.*, **1999**, *11*, 2218-2225.
- 9 T. D. Kim, J. Luo, Y. Tian, J. W. Ka, N. M. Tucker, M. Haller, J. W. Kang, A. K. Y. Jen, *Macromolecules*, **2006**, *39*, 1676-1680.
- 10 G. A. Lindsay, A. J. Guenther, M. E. Wright, M. Sanghadasa, P. R. Ashley, *Polymer*, **2007**, *48*, 6605-6616.

- 11 D. Briers, I. Picard, T. Verbiest, A. Persoons, C. Samyn, *Polymer*, **2004**, *45*, 19-24.
- 12 H. Eckert, B. Forster, *Angew. Chem., Int. Ed. Engl.*, **1987**, *26*, 894-895.
- 13 H. R. Kricheldorf, S. Bohme, G. Schwarz, *Macromol. Chem. Phys.*, **2005**, *206*, 432-438.
- 14 R. Zhang, J. A. Moore, *Macromolecular Symposia*, **2003**, *199*, 375-390.
- 15 It has been reported that polymerization with triphosgene leads to high molar mass polycarbonates with number-average molecular weights ( $M_n$ ) above  $10^5$  Da. In general this gives rise to a poor solubility in common organic solvents, which is detrimental for the formation of optical quality thin films.
- 16 J. J. Reisinger, M. A. Hillmyer, *Prog. Polym. Sci.*, **2002**, *27*, 971-1005.
- 17 S. H. Kang, J. Luo, H. Ma, R. R. Barto, C. W. Frank, L. R. Dalton, A. K. Y. Jen, *Macromolecules*, **2003**, *36*, 4355-4359.
- 18 H. Ma, A. K. Y. Jen, L. R. Dalton, *Adv. Mater.*, **2002**, *14*, 1339-1365.
- 19 J. S. Moore, S. I. Stupp, *Macromolecules*, **1990**, *23*, 65-70.
- 20 J. D. Luo, H. Ma, M. Haller, A. K. Y. Jen, R. R. Barto, *Chem. Commun.*, **2002**, 888-889.
- 21 P. A. Sullivan, H. Rommel, Y. Liao, B. C. Olbricht, A. J. P. Akelaitis, K. A. Firestone, J. W. Kang, J. Luo, J. A. Davies, D. H. Choi, B. E. Eichinger, P. J. Reid, A. Chen, A. K. Y. Jen, B. H. Robinson, L. R. Dalton, *J. Am. Chem. Soc.*, **2007**, *129*, 7523-7530.
- 22 A. K. Y. Jen, J. Luo, S. Liu, M. Haller, L. Liu, H. Ma, *Adv. Mater.*, **2002**, *14*, 1763-1768.
- 23 J. Luo, M. Haller, H. Li, H. Z. Tang, A. K. Y. Jen, K. Jakka, C. H. Chou, C. F. Shu, *Macromolecules*, **2004**, *37*, 248-250.
- 24 X. Wu, J. Wu, Y. Liu, A. K. Y. Jen, *J. Am. Chem. Soc.*, **1999**, *121*, 472-473.
- 25 O. Mitsunobu, *Synthesis*, **1981**, 1-28.
- 26 W. Ballet, I. Picard, T. Verbiest, A. Persoons, C. Samyn, *Macromol. Chem. Phys.*, **2004**, *205*, 13-18.
- 27 C. C. Teng, H. T. Man, *Appl. Phys. Lett.*, **1990**, *56*, 1734-1736.
- 28 B. H. Robinson, L. R. Dalton, *J. Phys. Chem. A*, **2000**, *104*, 4785-4795.
- 29 D. Briers, G. Koeckelberghs, I. Picard, T. Verbiest, A. Persoons, C. Samyn, *Macromol. Rapid Commun.*, **2003**, *24*, 841-846.
- 30 L. R. Dalton, W. H. Steier, B. H. Robinson, C. Zhang, A. Ren, S. Garner, A. Chen, T. Londergan, L. Irwin, B. Carlson, L. Fifield, G. Phelan, C. Kincaid, J. Amend, A. Jen, *J. Mater. Chem.*, **1999**, *9*, 1905-1920.
- 31 H. Ma, S. Liu, J. D. Luo, S. Suresh, L. Liu, S. H. Kang, M. Haller, T. Sassa, L. R. Dalton, A. K. Y. Jen, *Adv. Funct. Mater.*, **2002**, *12*, 565-574.

- 32 A. W. Harper, S. Sun, L. R. Dalton, S. M. Garner, A. Chen, S. Kalluri, W. H. Steier, B. H. Robinson, *J. Opt. Soc. Am. B*, **1998**, *15*, 329-337.
- 33 C. Y. Chen, Y. Tian, Y. J. Cheng, A. C. Young, J. W. Ka, A. K. Y. Jen, *J. Am. Chem. Soc.*, **2007**, *129*, 7220-7221.

# Chapter 6

## **Fabrication of Polymeric Microring Resonators Using Photolithography and Nanoimprint Lithography\***

*This Chapter describes the fabrication of a prototype integrated optical device, namely an EO microring resonator, by direct photodefinition on negative photoresist SU8, incorporating the TCVDPA chromophore as guest. The high photostability of TCVDPA in combination with its low absorption window in the UV region enables UV-crosslinking to be used for photodefinition. The resulting device showed EO modulation at 10 MHz and an excellent photostability. TCVDPA functionalized with epoxy groups allowed covalent insertion of the chromophore by photopolymerization, resulting in a material with a 40 °C higher  $T_g$ . The low  $T_g$  of the SU8-TCVDPA-epoxy system in the uncross-linked state enables UV-nanoimprint lithography (NIL) to be used as alternative technique for the fabrication and replication of devices based on EO polymeric materials.*

---

\* Part of this chapter has been published in: M. Balakrishnan, M. Faccini, M. B. J. Diemeer, E. J. Klein, G. Sengo, A. Driessen, W. Verboom, D. N. Reinhoudt, *Appl. Phys. Lett.*, **2008**, 92.

## 6.1 Introduction

Semiconductor and inorganic materials have been extensively investigated to serve as both passive and active materials in integrated optical devices. Recently, however, polymers have attracted more attention because their properties can be easily tuned by chemical modification of the structure or by doping with materials with different functions and properties.<sup>1</sup> In addition, their good processability, low optical loss, and ease of integration with existing fabrication technologies make organic polymeric materials the most promising candidate for the low-cost fabrication of optical devices.<sup>2</sup>

Among integrated optical circuits, the microring optical resonator (MR) is a key device, because it is a highly compact device that allows electrical/optical field interaction lengths while conserving space.<sup>3</sup> Moreover, MRs permit multiple functions such as electro-optical (EO) modulation,<sup>4</sup> wavelength selective filtering,<sup>5</sup> and sensing<sup>6,7</sup> to be performed in the same device. The typical fabrication procedure for polymeric guiding structures uses reactive ion etching (RIE).<sup>4</sup> RIE, however, being a dry etching process, gives rise to a high sidewall roughness, which results in undesired waveguide scattering losses.

UV photolithography has been extensively used for the fabrication of passive waveguide structures.<sup>8,9</sup> Using this technique, differently than with RIE, it is possible to achieve the high resolution structures required for laterally coupled waveguides such as in MRs. Moreover, the sidewall roughness is dramatically reduced compared with RIE.

Despite these advantages, photodefinition has hardly been applied for the fabrication of devices containing EO active polymers due to the poor stability of most of the EO chromophores to UV light. In fact, the long exposure times required during the photodefinition process causes photodegradation of the chromophores, which is detrimental for the device performances.

The highly photostable **TCVDPA** chromophore (**1**), however, as described in Chapter 3, possesses the unique feature of having a low absorption window in the UV region (blue window), where most of the chromophores absorb, which allows to use UV-crosslinking for photodefinition.<sup>10</sup> Direct waveguide photodefinition of the negative photoresist SU8 containing **TCVDPA**, using a conventional (I, H, G-line) mask aligner

has been demonstrated.<sup>11</sup> In addition, this system has the advantage that low temperature poling can be done in the uncrosslinked state, because the uncured SU8 is a low- $T_g$  solid.

However, in the resulting cross-linked material the chromophore is not chemically attached to the polymer matrix, but it is simply incorporated as in a guest-host system, causing plasticization and therefore lowering the  $T_g$  of the material.

In this Chapter the **TCVDPA** chromophore will be functionalized with epoxy groups. This modification allows the covalent insertion of the chromophore in the polymer matrix by a photopolymerization reaction. The resulting SU8-**TCVDPA**-epoxy (**2**) system is a versatile material that can be applied to other microfabrication techniques such as UV-nanoimprint lithography (UV-NIL). NIL utilizes a master device to reproduce identical replicas by embossing in a photocurable film.<sup>12</sup> The replica device is then cured by UV light. This fast, low-cost fabrication technique provides the nanometer precision, which is required for integrated optical device manufacturing.<sup>13</sup>

In this Chapter, the fabrication of laterally coupled microring resonator devices by direct photodefinition of SU8 doped with the **TCVDPA** chromophore (**1**) is described. The active performances of the resulting device are also tested. Moreover, the possibility of fabricating devices with the SU8-**TCVDPA**-epoxy (**2**) system by UV-NIL is explored.

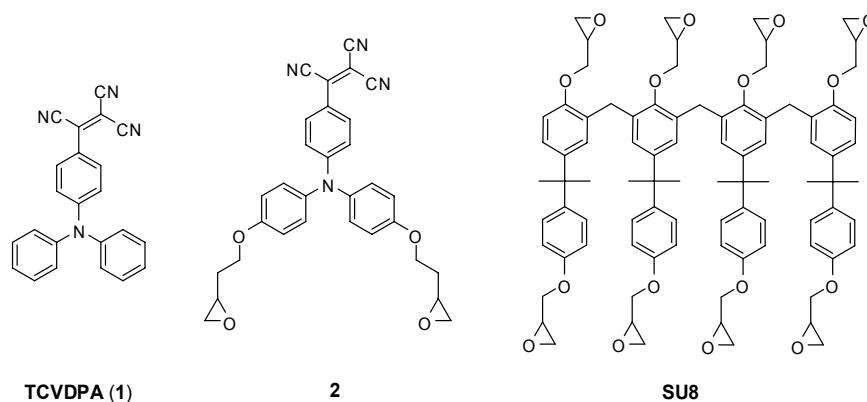


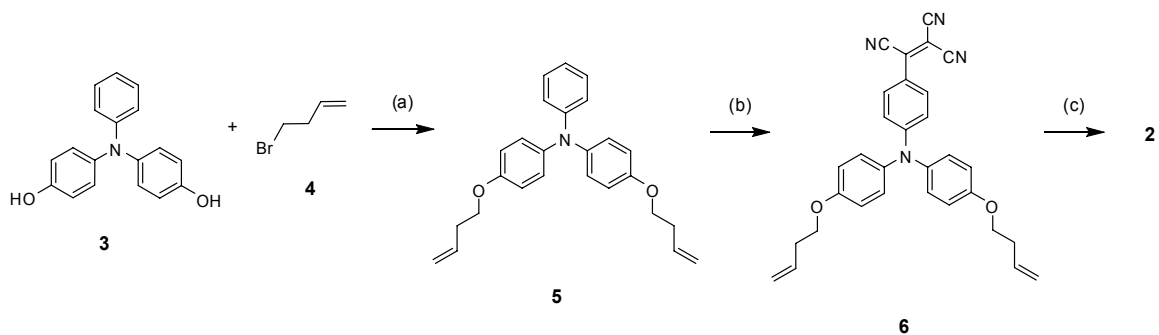
**Figure 1.** Chemical structures of chromophores **TCVDPA (1)**, **2**, and epoxy resin **SU8**.

## 6.2 Results and Discussion

### 6.2.1 Synthesis

The synthesis of the epoxy-functionalized chromophore **2** is depicted in Scheme 1. Functionalization of the hydroxyl groups in triarylamine **3** with 4-bromo-1-butene (**4**) under Finkelstein conditions gave the bis(but-3-enyloxy)-triarylamine **5**. Subsequent electrophilic aromatic substitution of **5** with tetracyanoethylene (TCNE) in DMF gave chromophore **6**. The final epoxidation step was performed by treatment of **6** with an excess of *m*-chloroperbenzoic acid (*m*-CPBA) to give **TCVDPA**-epoxy chromophore (**2**). The formation of **2** was confirmed by the appearance of the characteristic multiplets of a terminal epoxyde moiety between 1.82 and 3.11 ppm in the <sup>1</sup>H NMR spectrum.

*Scheme 1. Synthesis of chromophore 2.<sup>a</sup>*



<sup>a</sup> Reagents and conditions: (a) K<sub>2</sub>CO<sub>3</sub>, KI, THF, CH<sub>3</sub>CN, reflux; (b) TCNE, DMF, rt (c) *m*-CPBA, CH<sub>2</sub>Cl<sub>2</sub>, rt.

### 6.2.2 Optical Properties

UV spectra of the chromophores **1** and **2** were recorded in CH<sub>2</sub>Cl<sub>2</sub> and the  $\lambda_{max}$  values are reported in Table 1. As expected, the introduction of epoxy groups to the **TCVDPA** chromophore (**1**) did not cause significant changes in the UV spectrum (Figure 2). Chromophore **2** preserves the lower minimum in the absorption spectrum (around 400 nm), between the charge-transfer band and the higher-energy aromatic electronic transitions that is necessary for photo-induced crosslinking to be applied for lattice hardening.



The Hyper-Rayleigh scattering (HRS) technique was employed to measure  $\beta_{zzz}$  for chromophores **1** and **2** at 800 nm (Table 2). The functionalization at the donor site of the chromophores, has a small influence on  $\beta_{zzz}$ . However, a slightly higher value was found for the epoxy-functionalized chromophore **2**, compared to **1**, probably due to the ether bond directly connected to the diphenylamine moiety, slightly increasing its electron donating ability.

**Table 1.** Summary of the optical properties of chromophores **1** and **2**.

	$\lambda_{max}^a$ (nm)	$E^b$ ( $M^{-1}cm^{-1}$ )	$\beta_{zzz}^c$ ( $10^{-30}$ esu)
<b>1</b>	539	38500	425 +/- 80
<b>2</b>	536	25000	492 +/- 23

<sup>a</sup>  $\lambda_{max}$  was measured in  $CH_2Cl_2$ ; <sup>b</sup> Molar absorptivity in  $CH_2Cl_2$ ; <sup>c</sup>  $\beta$  values were measured at 800 nm.

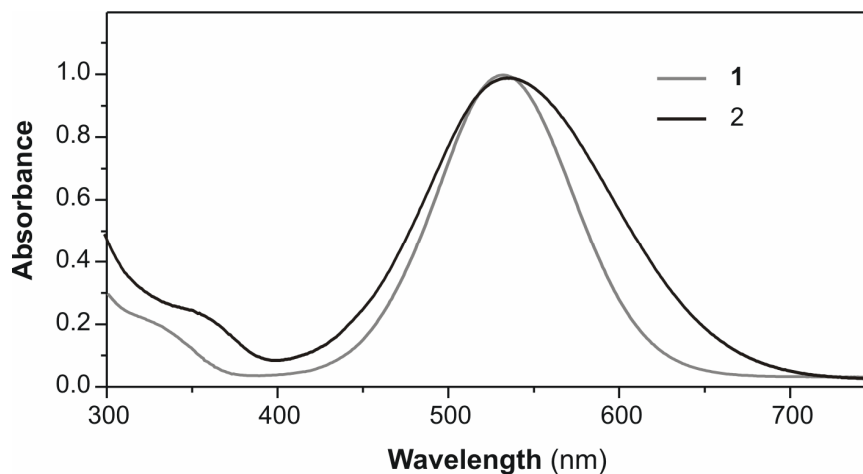


**Figure 2.** Absorption spectrum of the chromophores **1** and **2** in  $CH_2Cl_2$ .

### 6.2.3 Simultaneous Cross-linking and Poling

The typical UV lithography process of a negative photoresist, such as SU8, is shown in Figure 3. The application of UV light through a contact mask to a spin coated polymer

thin film, activates the photo-initiator in the resist. The released photoacid causes ring opening of the epoxy groups, hence cross-linking to start. However, this process is slow at room temperature and a post-exposure bake step is needed to complete the curing process. A final development step is required to remove the unexposed regions, which are not cross-linked, and reveal the fabricated structures. In order to explore the possibility of obtaining EO-active structures through UV-photodefinition, simultaneous poling and lattice hardening experiments were carried out in the SU8-TCVDPA (**1**) system. This system has a low  $T_g$ , thus offers the advantage that low-temperature poling can be conducted in the uncrosslinked state.

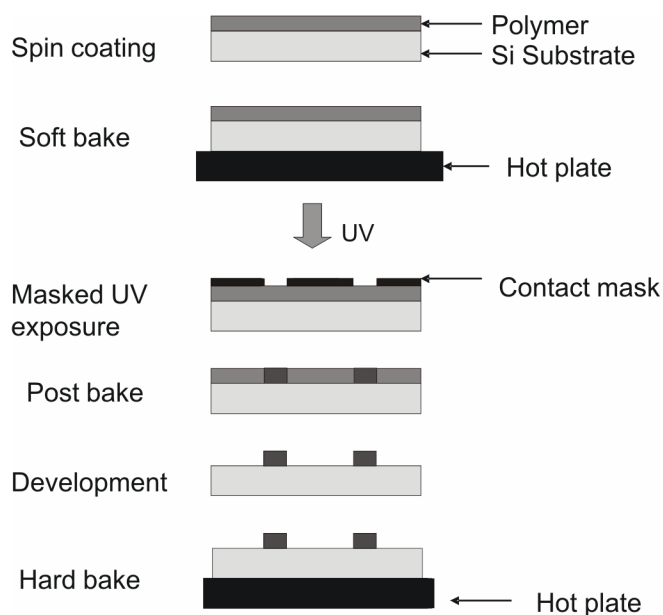


**Figure 3.** UV lithography process of the negative photoresist SU8.

Samples were prepared by doping chromophores **1** and **2** into a commercially available SU8 solution in  $\gamma$ -butyrolactone. The resulting solutions were filtered through a 0.2- $\mu\text{m}$  filter and spin-coated onto indium tin oxide (ITO) coated glass wafers. A 100 nm layer of gold was then sputtered onto the films as a top electrode to perform electric-field poling. The films were exposed to UV light before being contact-poled with a DC electric field of 100 V/ $\mu\text{m}$ . The  $r_{33}$  values were measured using a Teng-Man simple reflection technique at a wavelength of 830 nm.<sup>14</sup>

Since lattice hardening and poling are both temperature dependent processes, fine tuning of the conditions should be done to simultaneously achieve a high poling efficiency and a high  $T_g$ . Increasing the temperature permits a higher chromophore mobility to reorient along the poling field. It also antagonistically drives the hardening process, hence reducing the mobility.<sup>15</sup> On the other hand, the application of a too high electric field to a soft film can result in material breakdown. This often leads to a trade-off between poling efficiency and material stability. Thus optimum conditions can be achieved using stepped poling protocols (where temperature and electric field are increased in a series of steps).<sup>16</sup>

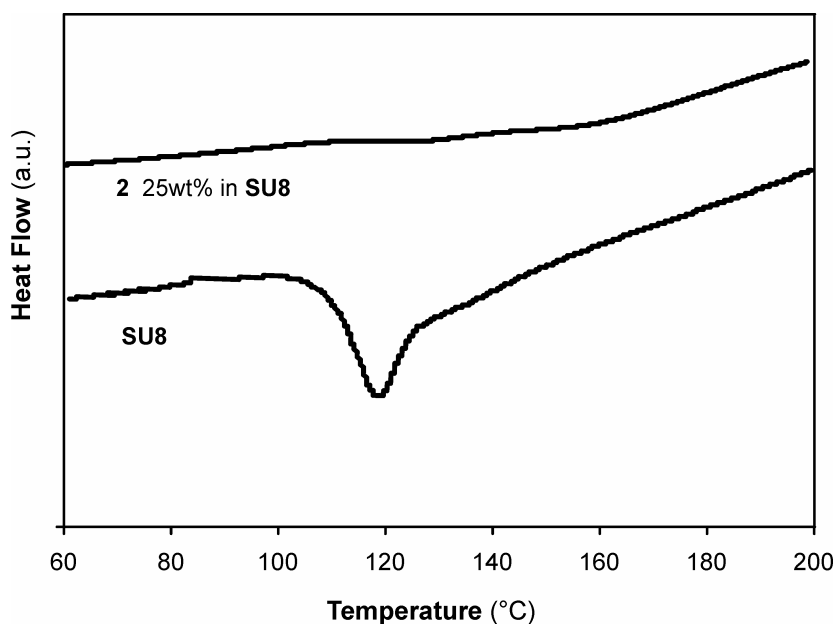


**Figure 4.** DSC thermograms for SU8 and chromophore **2** at 25 wt% in SU8.

The simultaneous cross-linking and poling process was first studied on a SU8-chromophore **2** film. The film was UV exposed and stepwise poling was applied. However, an EO coefficient of only 1.2 pm/V was measured and the  $T_g$  of the material was only slightly increased to 70 °C, suggesting that chromophore **2** acts as a plasticizer inhibiting the completion of the crosslinking process under such experimental conditions. DSC experiments were carried out to better understand the reasons of such a behavior. SU8 containing 1% w/w of thermal initiator (Nacure XC7321) was scanned between 50 and 250 °C at a scanning rate of 10 °C/min. The graph in Figure 4 shows a large

exothermic band around 100 °C, that can be attributed to the cross-linking process of the SU8. Using similar experimental conditions a sample containing 25 wt% of epoxy-functionalized **TCVDPA** chromophore (**2**) added to the SU8 matrix was scanned, but the resulting DSC curve shows no peak corresponding to the cross-linking process, probably due to the presence of the N-containing chromophore into the matrix that inhibits the completion of the polymerization, neutralizing the photoacid.

To support this hypothesis, as basic initiator imidazole was added to a 25% solution of **2** in SU8 and cured by DSC at 100 °C for 15 min and then scanned from 25 to 300 °C. The resulting DSC curve shows a  $C_p$  change at around 150 °C that can be attributed to the  $T_g$  of the resulting SU8-**2** cross-linked polymer, demonstrating the ability of chromophore **2** to cross-link with SU8 using basic initiators.

Since the thermal curing agent used in the DSC experiments, cannot be used in the UV cross-linking process, as alternative an extra amount of photoinitiator was added to compensate the neutralization induced by the chromophore.

A film containing 15 wt% of **TCVDPA** chromophore (**1**) in SU8 with 3 wt% extra photoinitiator, was prepared as described above and UV exposed before poling. The poling voltage was first applied to the sample and the temperature was slowly raised from room temperature to 90° C in 30 min and maintained at that temperature for 5 min. An  $r_{33}$  of 5 pm/V was measured after poling, which is in good agreement with the results obtained for the same chromophore as a guest in PS at a similar loading density (see Chapter 3). The glass transition raised to about 150 °C after simultaneous cross-linking and poling. However, the glass transition of fully cross-linked SU8 is about 200° C. This reduction may be due to the plasticizing effect of the chromophore which reduces the glass transition temperature. A parallel experiment was carried out under similar experimental conditions, but using epoxy-functionalized chromophore **2** (15 wt% in SU8) in stead of **TCVDPA 1**. After simultaneous cross-linking and poling the material  $T_g$  increased to 190 °C. This value is 40 °C higher than that of **TCVDPA 1**, clearly demonstrating the reduced plasticization effect provided by the introduction of a certain degree of cross-linking between chromophore and host polymer. This results in the formation of a **TCVDPA (2)** side-chain polymer. Moreover, an almost double  $r_{33}$  value

of 9 pm/V was measured. This might be explained by a better poling efficiency induced by the epoxy side groups.

#### 6.2.4 Microring Resonator Fabrication by Photodefinition.

A schematic drawing of a microring resonator (MR) is shown in Figure 5. It consists of a ring waveguide and two straight port waveguides which serve as optical input and output for the device. The ring and the waveguides are evanescently coupled, therefore a fraction of the incoming light is coupled to the ring. When the optical path-length of a roundtrip is a multiple of the effective wavelength, light ‘builds up’ inside the ring and constructive interference occurs. In this state, the MR is referred as being at resonance condition. At this condition, periodic notches appear at the output ports of the MR, with the transmission spectrum at the output port (through port) showing a maximum in transmission, which corresponds to the resonant wavelengths (Figure 5). When an external electric field is applied, the effective refractive index ( $n_{eff}$ ) of the EO polymer ring waveguide will change and the resonant wavelength will shift.

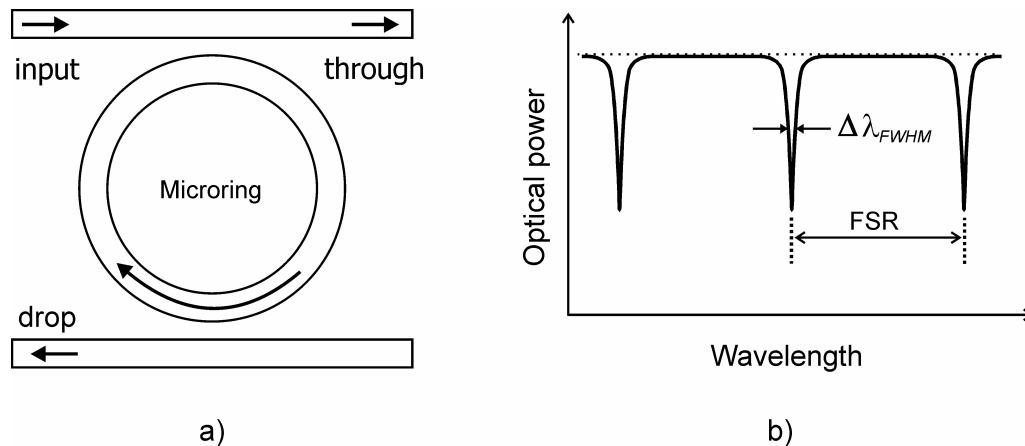


**Figure 5.** a) Schematic representation of a doubly coupled MR; b) Through port transmission spectrum.

The fabrication steps for the MR are shown in Figure 6. A racetrack kind of structure was used for the ring to increase the coupling between the ring and the bus waveguide. The radius of the ring was 200  $\mu\text{m}$  to keep the bending losses below 1 dB/cm. The waveguides were 2  $\mu\text{m}$  wide and 1  $\mu\text{m}$  thick to maintain the monomodal condition. The

fabrication starts with sputter deposition of the bottom electrode, a 250 nm thick gold layer, on a silicon wafer. A 6  $\mu\text{m}$  thick bottom cladding layer of VSC (a UV curable epoxy resin) was spun on top of the electrode, exposed to UV light and cured at 95  $^{\circ}\text{C}$ . Subsequently, the core layer, SU8-TCVDPA 15 wt%, was spun on the VSC to form a 1  $\mu\text{m}$  thick film. The doped SU8 layer was exposed to UV light through a contact chromium mask with the MR design. The film was then slightly cross-linked at 60  $^{\circ}\text{C}$  for 15 min and developed. Figure 7 shows the critical coupling section of the MR with the excellent result of the photodefinition process. A 6  $\mu\text{m}$  layer of VSC was spin coated as top cladding, UV exposed for 15 sec and cross-linked at 60  $^{\circ}\text{C}$  for 5 min. At this condition, the core layer and the top cladding are only slightly cross-linked. A top gold electrode was then sputtered and patterned. The processing temperature of the wafer after exposure of the core SU8-TCVDPA layer was limited to 60  $^{\circ}\text{C}$  to avoid further cross-linking of the core layer. Simultaneous poling and cross-linking of the MR was carried out in the same carefully controlled manner as for the unstructured film described in the previous section.

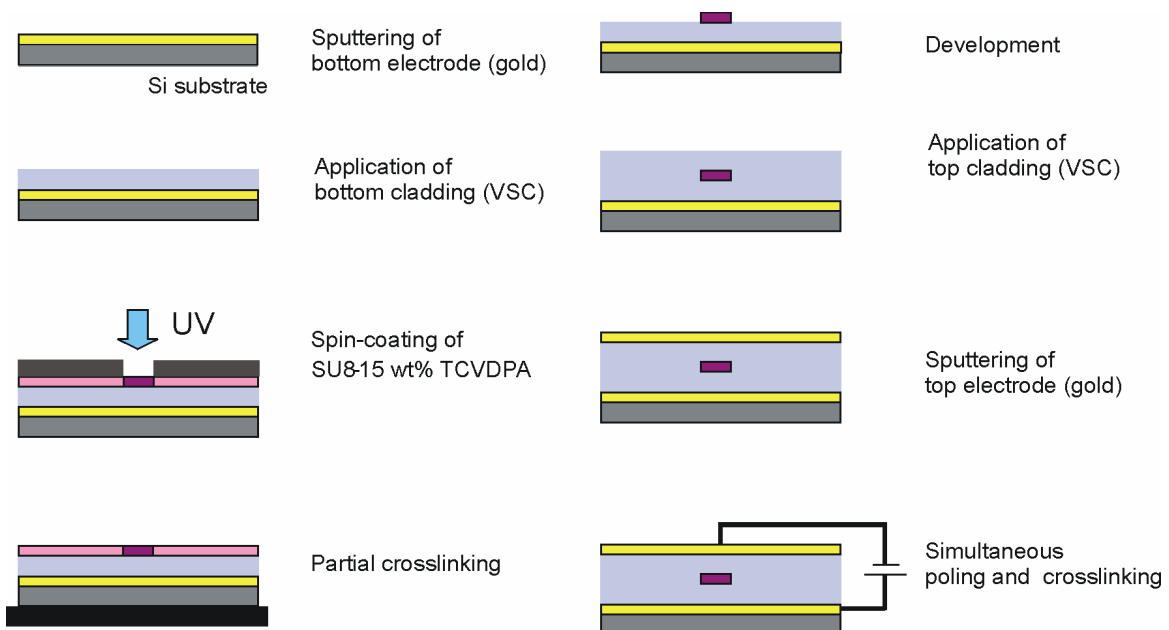


**Figure 6.** Fabrication steps for SU8-TCVDPA MRs.

The MR response was studied by coupling-in light from a broadband source emitting between 1530 and 1560 nm. The light coming out of the through and drop port was analyzed with a spectrum analyzer. Figure 8 shows the through port response of the MR with a dip of 11 dB, a free spectral range (FRS)<sup>17</sup> of 1 nm, a finesse (F)<sup>18</sup> of 6, and a ring waveguide loss of 25 dB/cm.

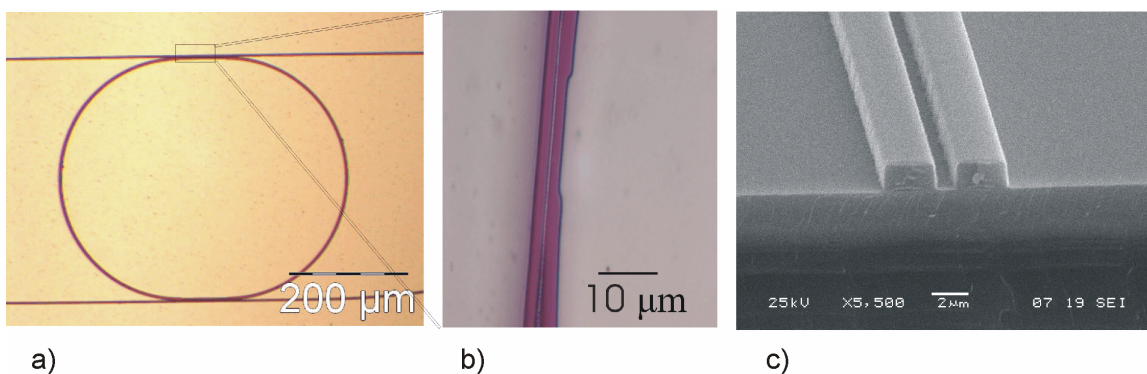


**Figure 7.** a) Microscope picture of a SU8-15 wt% TCVDPA MR; b) Detail of the coupling section with a 500 nm gap; c) SEM picture of the coupling section of a MR with 800 nm gap.

EO modulation up to 10 MHz was at 1550 nm, corresponding with an EO coefficient of about 11 pm/V. Because of the limitations of the experimental set-up, the modulation speed could not be further increased. The speed used, however, is sufficient to prove the pure EO origin of the modulation. In spite of the absence of any packaging or shielding from oxygen, the device has an extremely high photostability, showing no reduction of the  $r_{33}$  after illumination with a laser at 1550 nm for 100 h. This result confirms the exceptional photostability of the TCVDPA chromophore (1), even under high photon flux.

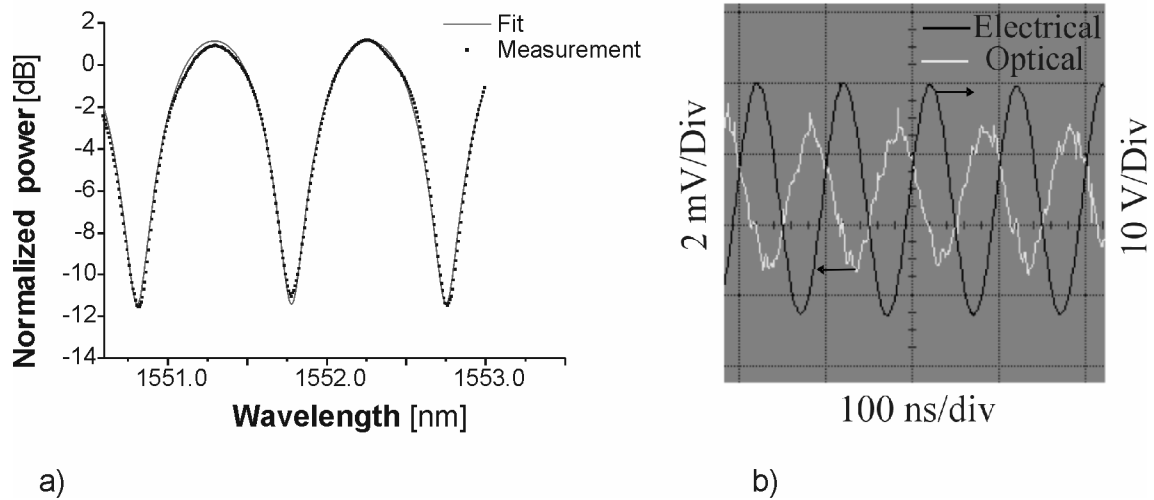


**Figure 8.** a) Through port response of the MR; b) EO modulation at 10 MHz.

### 6.2.5 Microring Resonator Fabrication by NIL.

By taking advantage of the low  $T_g$  of the SU8-TCVDPA-epoxy (**2**) system in the uncross-linked state, nanoimprint lithography (NIL) can be applied at lower temperature and pressure<sup>19</sup> than in conventional thermal imprints used for EO polymeric materials,<sup>20,21</sup> shortening imprint time and pattern distortion. The  $T_g$  of this patterned MR structures can then be increased after UV exposure and curing.<sup>22</sup>

To investigate the ability of patterning nanostructures on this system, preliminary UV-NIL experiments were carried out. A solution of 15 wt% TCVDPA epoxy (**2**) in SU8 was spin-coated on an approximately 4 cm<sup>2</sup> diced Si wafer and pre-baked at 90 °C for 10 min to remove the solvents. The size of the stamp and substrate were always comparable. Easy separation of stamp and substrate was facilitated by applying a fluorinated self-assembled monolayer to the stamp surface.<sup>23</sup> NIL was applied using a master with 2  $\mu\text{m}$  wide and 1  $\mu\text{m}$  thick inverted MR features. The gap between the ring and the straight waveguide was 1  $\mu\text{m}$ . The resulting spin-coated film (approximately 1.5  $\mu\text{m}$  thick) film was brought in contact with the master at room temperature, was then heated at 80 °C and 100 °C and pressure (1-2 MPa) was applied. After 10 min the system was cooled down to room temperature, the pressure was released and the substrate detached from the mold with little difficulty, exposed to UV light and cured at 120 °C for 10 min.



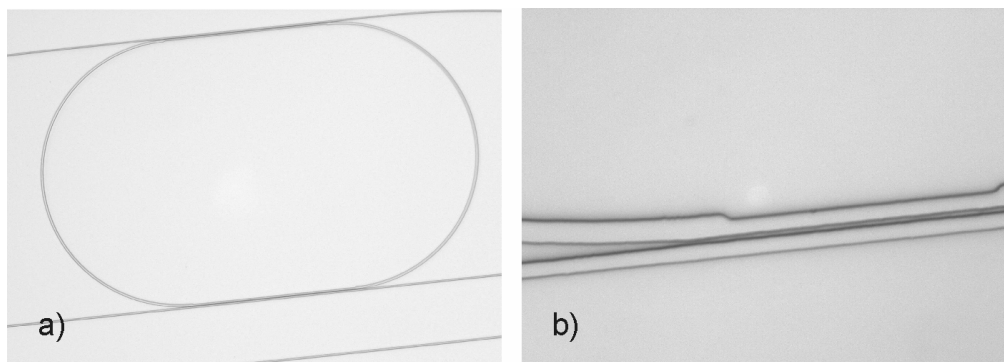


**Figure 9.** a) Microscope picture of the MR imprinted in SU8-TCVDPA epoxy (2) 15 wt%; b) detail of the 1  $\mu\text{m}$  open gap.

The imprinted films were analyzed by optical microscopy. Figure 9 shows that well defined microring resonator structures can be imprinted on the SU8-TCVDPA-epoxy (2) system. Moreover, the critical 1  $\mu\text{m}$  waveguide-ring gaps were successfully patterned. However, some defects can be noticed, probably due to the removal of the mold before cross-linking, since the material is still soft. This defect may be reduced by using a transparent mould, such as glass or quartz, which allow to apply UV light while mould and substrate are still in contact.

These results indicate that UV-NIL can be successfully applied to the SU8-TCVDPA epoxy (2) system for making low-cost, high fabrication throughput polymeric optical devices.

The performances of the device were not tested due to the presence of a thick background residue of EO polymeric material. Beyond a few hundred nm of residue insertion losses and waveguide bending losses become unacceptably high, and waveguides become multimode.<sup>24</sup> The thickness of the residue surrounding the waveguides has to be controlled and maintained at a tolerable level in order to achieve devices with the desired optical performances.

### 6.3 Conclusions

A laterally coupled EO microring resonator was fabricated by direct photodefinition on host SU8 with the TCVDPA chromophore (1) as guest, by exploiting the low UV

absorption window of the chromophore. The system showed an excellent photostability under high photon flux and an EO modulation with an  $r_{33}$  of 11 pm/V was demonstrated at 10 MHz. Functionalization of the **TCVDPA** chromophore with epoxy groups induced the formation of cross-links between the chromophore and the host polymer, resulting in a material with a 40 °C higher  $T_g$ . Exploratory UV-NIL experiments carried out on the SU8-**TCVDPA**-epoxy (**2**) system showed promising results for the high-volume and low-cost production of devices based on EO polymeric materials.

## 6.4 Experimental Section

**General Procedures.** All chemicals were of reagent grade and used without further purification. THF was freshly distilled from Na/benzophenone, and  $\text{CH}_2\text{Cl}_2$  from  $\text{CaCl}_2$ . All chromatography associated with product purification was performed by flash column techniques using Merck Kieselgel 600 (230-400 mesh). All reactions were carried out under an inert argon atmosphere. Melting points of all compounds were obtained with a Reichert melting point apparatus and a Kofler stage.  $^1\text{H}$  and  $^{13}\text{C}$  NMR spectra were recorded on a Varian Unity 300 using tetramethylsilane (TMS) or the corresponding residual solvent signal as internal standard. FAB-MS spectra were recorded on a Finningan MAT 90 spectrometer with *m*-nitrobenzyl alcohol (NBA) as a matrix. UV-Vis measurements were carried out on a Varian Cary 3E UV-spectrophotometer. HRS measurements were performed using the 800 nm fundamental wavelength of a regenerative mode-locked  $\text{Ti}^{3+}$  sapphire laser.<sup>25</sup> Measurements were carried out in  $\text{CH}_2\text{Cl}_2$ , with crystal violet chloride (CV) as an external reference ( $\beta_{\text{xxx}}$ ),  $338 \times 10^{-30}$  esu in methanol at 800 nm, taking into account the difference in symmetry (octopolar for CV and dipolar for the chromophores). The sample was dissolved in  $\text{CH}_2\text{Cl}_2$  and passed through 0.2  $\mu\text{m}$  filters. Dilute solutions ( $10^{-5}$ - $10^{-6}$  M) were used to ensure a linear dependence of  $I_{2\omega}/I_{\omega}^2$  on solute concentration, precluding the need for a Lambert-Beer correction for self-absorption of the second harmonic generation (SHG) signal. High-frequency femtosecond HRS was used to assess any multiphoton fluorescence

contribution at 400 nm. No fluorescence effects were observed at 400 nm for all chromophores.

For poled films, the  $T_g$  is defined as the temperature at which a change in the reflection of the top gold electrode is first noticed, by heating the sample is on a heating chuck, raising the temperature in steps of 10 °C and holding for 5 min at each step. The change of mobility in the material at the  $T_g$  causes the gold to buckle, hence losing perfect light reflectivity.

Compound **1** was prepared according to a literature procedure.<sup>26</sup> The synthesis of compound **3** is reported in Chapter 3.

**4, 4'-Bis(but-3-enyloxy)triphenylamine (5).** To a solution of **3** (2.0 g, 7.2 mmol) in dry CH<sub>3</sub>CN (300 mL) was added K<sub>2</sub>CO<sub>3</sub> (20 g, 145 mmol) and the mixture was stirred at rt for 30 min. After the addition of 4-bromo-1-butene (**4**) (10.4 mL, 102.0 mmol) and KI (14.4 g, 86.7 mmol), the reaction mixture was refluxed for 24 h. After evaporating the solvent, the residue was dissolved in CH<sub>2</sub>Cl<sub>2</sub> (250 mL) and then washed with a 10% HCl solution until neutral pH and water (3 × 150 mL). The organic phase was dried over MgSO<sub>4</sub>, concentrated under reduced pressure and the residue further purified by chromatography (hexane/CH<sub>2</sub>Cl<sub>2</sub> 4/1) to afford **5** as a yellowish oil (65%): <sup>1</sup>H NMR (CDCl<sub>3</sub>) δ 2.53 (q,  $J = 6.9$  Hz, 4H, CH<sub>2</sub>), 3.99 (t,  $J = 6.9$  Hz, 4H, OCH<sub>2</sub>), 5.11 (d,  $J = 10.2$  Hz, 2H, =CHH), 5.17 (d,  $J = 17.1$  Hz, 2H, =CHH), 5.91 (m, 2H, CH=CH<sub>2</sub>), 6.81 (d,  $J = 9.0$  Hz, 4H, ar-H), 6.84-6.90 (m, 1H, ar-H), 7.02 (d,  $J = 9.0$  Hz, 4H, ar-H), 7.16 (t,  $J = 7.8$  Hz, 2H, ar-H); <sup>13</sup>C NMR (CDCl<sub>3</sub>) δ 34.8, 69.1, 115.6, 116.4, 126.2, 130.3, 132.5, 134.7, 137.3, 146.5, 154.2; MS FAB<sup>+</sup>  $m/z$  385.2 ([M<sup>+</sup>], calcd for C<sub>26</sub>H<sub>27</sub>NO<sub>2</sub> 385.2).

**Chromophore 6.** To a solution of **5** (1.5 g, 4.2 mmol) in dry DMF (100 mL) was added TCNE (1.1 g, 8.5 mmol) and the resulting mixture was stirred at rt for 12 h. The solvent was removed under reduced pressure and the residue dissolved in CH<sub>2</sub>Cl<sub>2</sub> (200 mL) and then washed with water (3 × 100 mL). The organic layer was dried over MgSO<sub>4</sub> and the resulting solid was purified by chromatography (hexane/CH<sub>2</sub>Cl<sub>2</sub> 1/1) to give **6** as a purple solid (94%): mp 80-82 °C; <sup>1</sup>H NMR (CDCl<sub>3</sub>) δ 2.48 (q,  $J = 6.9$  Hz, 4H, CH<sub>2</sub>), 3.96 (t,  $J = 6.9$  Hz, 4H, OCH<sub>2</sub>), 5.00-5.09 (m, 2H, C=CH<sub>2</sub>), 5.12-5.15 (m, 2H, =CHH),

5.76-5.90 (m, 2H, =CHH), 6.75 (d,  $J = 9.3$  Hz, 2H, ar-H), 6.85 (d,  $J = 9.0$  Hz, 4H, ar-H), 7.06 (d,  $J = 9.0$  Hz, 4H, ar-H), 7.86 (d,  $J = 9.3$  Hz, 2H, ar-H),  $^{13}\text{C}$  NMR ( $\text{CDCl}_3$ )  $\delta$  33.5, 67.5, 79.7, 113.3, 113.5, 114.3, 115.9, 116.7, 117.2, 119.5, 128.1, 132.4, 134.1, 136.8, 137.5, 155.3, 157.8; MS FAB<sup>+</sup>  $m/z$  486.2 [ $\text{M}^+$ ], calcd for  $\text{C}_{31}\text{H}_{26}\text{N}_4\text{O}_2$  486.2.

**Epoxy chromophore 2.** To a solution of **6** (1.0 g, 2.1 mmol) in dry  $\text{CH}_2\text{Cl}_2$  (15 mL) was added *m*-chloroperbenzoic acid (3.9 g, 22.7 mmol). The resulting mixture was stirred at 0 °C for 1 h and then stirred at rt for 48 h. After filtration of the precipitate *m*-chlorobenzoic acid, the resulting solution was extracted with a  $\text{NaHSO}_3$  ( $3 \times 50$  mL) and a saturated  $\text{NaHCO}_3$  solution ( $3 \times 50$  mL). The organic layer was dried over  $\text{MgSO}_4$ , and the solvent was evaporated under reduced pressure to afford **2** as a purple solid (90%): mp 61-63 °C;  $^1\text{H}$  NMR ( $\text{CDCl}_3$ )  $\delta$  1.82-1.90 (m, 2H,  $\text{CH}_2$ ), 2.03-2.14 (m, 2H,  $\text{CH}_2$ ), 2.52 (dd,  $J = 2.7, 4.8$  Hz, 2H,  $\text{CH}_2\text{O}$ ), 2.77 (t,  $J = 4.8$  Hz, 2H,  $\text{CH}_2\text{O}$ ) 3.05-3.11 (m, 2H, CHO), 4.06 (m,  $J = 4.8$  Hz, 4H,  $\text{CH}_2$ ), 6.76 (d,  $J = 9.6$  Hz, 2H, ar-H), 6.87 (d,  $J = 9.0$  Hz, 4H, ar-H), 7.07 (d,  $J = 9.0$  Hz, 4H, ar-H), 7.86 (d,  $J = 9.6$  Hz, 2H, ar-H);  $^{13}\text{C}$  NMR ( $\text{CDCl}_3$ )  $\delta$  34.2, 48.5, 65.3, 91.8, 114.3, 116.0, 116.2, 119.5, 128.1, 132.3, 134.5, 136.7, 137.6, 145.3, 156.4; FAB<sup>+</sup>  $m/z$  518.2 [ $\text{M}^+$ ], calcd for  $\text{C}_{31}\text{H}_{26}\text{N}_4\text{O}_4$  518.2.

## 6.5 References

- 1 L. Eldada, L. W. Shacklette, *IEEE J. Sel. Top. Quantum Electron.*, **2000**, *6*, 54-68.
- 2 H. Ma, A. K. Y. Jen, L. R. Dalton, *Adv. Mater.*, **2002**, *14*, 1339-1365.
- 3 B. E. Little, S. T. Chu, *Opt. Photonics News*, **2000**, *11*, 24-28.
- 4 P. Rabiei, W. H. Steier, C. Zhang, L. R. Dalton, *J. Lightwave Technol.*, **2002**, *20*, 1968-1975.
- 5 A. Yariv, *Electron. Lett.*, **2000**, *36*, 321-322.
- 6 C. Y. Chao, W. Fung, L. J. Guo, *IEEE J. Sel. Top. Quantum Electron.*, **2006**, *12*, 134-142.
- 7 P. V. Lambeck, *Meas. Sci. Technol.*, **2006**, *17*, R93-R116.
- 8 M. Diemeer, L. Hilderink, R. Dekker, A. Driessen, *IEEE Photonic. Tech. L.*, **2006**, *18*, 1624-1626.

- 9 K. Enbutsu, M. Hikita, R. Yoshimura, S. Tomaru, S. Imamura, *Mol. Cryst. Liq. Cryst. B*, **1999**, 22, 441-444.
- 10 T. H. Dai, K. D. Singer, R. J. Twieg, T. C. Kowalczyk, *J. Opt. Soc. Am. B*, **2000**, 17, 412-421.
- 11 M. Balakrishnan, M. Faccini, M. B. J. Diemeer, W. Verboom, A. Driessen, D. N. Reinhoudt, A. Leinse, *Electron. Lett.*, **2006**, 42, 51-52.
- 12 L. J. Guo, *J. Phys. D Appl. Phys.*, **2004**, 37, R123-R141.
- 13 L. J. Guo, *Adv. Mater.*, **2007**, 19, 495-513.
- 14 C. C. Teng, H. T. Man, *Appl. Phys. Lett.*, **1990**, 56, 1734-1736.
- 15 L. R. Dalton, A. W. Harper, R. Ghosn, W. H. Steier, M. Ziari, H. Fetterman, Y. Shi, R. V. Mustacich, A. K. Y. Jen, K. J. Shea, *Chem. Mater.*, **1995**, 7, 1060-1081.
- 16 S. S. H. Mao, Y. Ra, L. Guo, C. Zhang, L. R. Dalton, A. Chen, S. Garner, W. H. Steier, *Chem. Mater.*, **1998**, 10, 146-155.
- 17 The distance between two adjacent transmission peaks, the free spectral range (FSR) can be described as

$$FSR = \frac{\lambda^2}{n_{eff}L}$$

where  $L$  is the length of the ring.

- 18 The finesse ( $F$ ) is a key specification of the MR and is defined as

$$F = \frac{FSR}{\Delta\lambda_{FWHM}}$$

where  $\Delta\lambda_{FWHM}$  is the peak width.  $F$  is dependent on both the internal loss and the coupling (that is, the external loss) of the resonator. The higher the total losses are, the lower the finesse of the resonator.

- 19 W. Hu, B. Yang, C. Peng, S. W. Pang, *J. Vac. Sci. Technol. B*, **2006**, 24, 2225-2229.
- 20 Y. Huang, G. T. Paloczi, A. Yariv, C. Zhang, L. R. Dalton, *J. Phys. Chem. B*, **2004**, 108, 8606-8613.
- 21 G. T. Paloczi, Y. Huang, A. Yariv, J. Luo, A. K. Y. Jen, *Appl. Phys. Lett.*, **2004**, 85, 1662-1664.
- 22 B. H. Ong, X. Yuan, S. Tao, S. C. Tjin, *Opt. Lett.*, **2006**, 31, 1367-1369.
- 23 U. Srinivasan, M. R. Houston, R. T. Howe, R. Maboudian, *J. Microelectromech. S.*, **1998**, 7, 252-259.
- 24 G. T. Paloczi, Y. Huang, J. Scheuer, A. Yariv, *J. Vac. Sci. Technol., B*, **2004**, 22, 1764-1769.

- 25 G. Olbrechts, R. Strobbe, K. Clays, A. Persoons, *Rev. Sci. Instrum.*, **1998**, *69*, 2233-2241.
- 26 C. Lambert, W. Gaschler, E. Schmalzlin, K. Meerholz, C. Brauchle, *J. Chem. Soc., Perkin Trans. 2*, **1999**, 577-587.

# Chapter 7

## **Electro-optic Active Cyclodextrin-based Rotaxanes**

*A Preliminary Study*

*NLO chromophores of which the  $\pi$ -electron bridge is encapsulated by a cyclodextrin macrocycle, to form an EO active rotaxane, were synthesized in water. Preliminary photobleaching tests demonstrated the enhanced protection against photochemical attack.*

## 7.1 Introduction

As outlined in Chapter 2, over the past two decades a wide variety of chromophores with an ever improved molecular optical nonlinearity has been synthesized and studied.<sup>1</sup> Very large hyperpolarizabilities have often been obtained in NLO chromophores with extended conjugated  $\pi$ -bridges between the electron donor and acceptor groups. However, the delocalized electronic structures of NLO chromophores inevitably makes them vulnerable to attack, because of a reaction with nucleophiles, electrophiles, or radicals, leading to the loss of their properties.<sup>2,3</sup> Therefore, the environmental reactivity and operational instability of organic dyes is often regarded as their main limitation. Blocking this unwanted reactivity is the key motivation for some of the ongoing research and several strategies have been employed to achieve this goal.

Among them, encapsulation of a conjugated molecule has resulted in substantial enhancements of the chemical and photostabilities.<sup>4,5</sup> A variety of macrocyclic receptors form inclusion complexes with rodlike guests; when the guest is long enough to protrude from both ends of the macrocycle these inclusion complexes are called pseudorotaxanes. The presence of bulky substituents at both ends of the guest results in a rotaxane structure, in which the dumbbell-shaped guest is trapped inside the cavity of the macrocycle (Figure 1).<sup>6,7</sup>

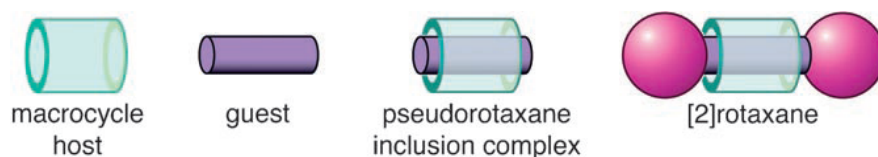


**Figure 1.** Introduction to the rotaxane terminology.

Mechanically interlocked molecules such as rotaxanes, catenanes, and knots have attracted a lot of attention as promising candidates for the development of functional molecular devices of high sophistication.<sup>8-10</sup> Many complexes of organic cyclic host compounds, such as donor-acceptor,<sup>11,12</sup> transition metal,<sup>13,14</sup> crown ether,<sup>15</sup> and hydrogen bond complexes of cyclic amides,<sup>8,16</sup> have been used for rotaxane synthesis, but



cyclodextrin (CD) inclusion compounds have been applied most. CDs are cyclic compounds consisting of six to eight glucose units, called  $\alpha$ -,  $\beta$ -, and  $\gamma$ -CD, respectively (Figure 2). They are known to form inclusion complexes with various low-molecular-weight compounds, ranging from nonpolar aliphatic molecules to polar amines and carboxylic acids.<sup>17</sup> CDs have a toroidal shape with the primary hydroxyl groups at the narrow side and the secondary hydroxyl groups at the wide side (Figure 2). CDs offer several advantages compared to other ring molecules: they are readily available in both high purities and large quantities. Furthermore, they are water-soluble, biocompatible and can be functionalized by a wide variety of synthetic methods.<sup>18,19</sup> CDs spontaneously incorporate guest molecules, a necessary prerequisite for rotaxane formation.

Threading a  $\pi$ -system inside the CD macrocycle to form a rotaxane can protect it from even the smallest and most reactive species, such as singlet oxygen. For example, a cyanine dye rotaxane, in which the chromophore is locked inside the cavity of a cyclodextrin is 40-times more stable towards photooxidation than the free cyanine dye.<sup>5</sup> Cyanine rotaxanes also display an enhanced redox reversibility as a result of the kinetic stability of their oxidized and reduced forms. Azo-dye cyclodextrin rotaxanes also exhibit enhanced chemical and photostabilities. These rotaxanes are more than 100-times less sensitive towards reductive bleaching, oxidative bleaching, and photobleaching than the free dye.<sup>4</sup>

The encapsulation is expected not only to provide a protection from photochemical attack of the vulnerable NLO chromophore, elongating its lifetime, but also to efficiently reduce the unfavorable intermolecular interactions among dipoles, which causes anti-parallel clustering of the chromophores and consequent reduction of the maximum achievable EO response. Theoretical and experimental findings have demonstrated that such interactions can be minimized by modification of the shape of the chromophore with bulky substituents, to obtain oblate-shaped and disk-shaped molecules.<sup>20,21</sup> Thus, a CD-based rotaxane, due to the bulkiness of the CD-macrocycle and to its intrinsically oblate-shaped structure, might be the perfect candidate. Moreover, supramolecular inclusion has been recently demonstrated as a promising strategy to increase the second-order nonlinear optical response of ionic organic chromophores. Incorporation of stilbazolium-

type dye in an amylose helix has been shown to enhance the hyperpolarizability by an order of magnitude.<sup>22</sup>

Kajzar *et al.* have investigated for the first time the EO properties of several rotaxanes based on dinitrone and furanamide threads and a benzylic amide macrocycle. These molecules could be processed into good optical quality films and poled with a static external field resulting in relatively low  $d_{33}$  values.<sup>23</sup>

In this Chapter the synthesis of NLO chromophores of which the  $\pi$ -electron bridge is encapsulated by a CD ring, to form an EO active rotaxane, is described. The electron donor and acceptor moieties must be bulky enough to act as stoppers in order to prevent the macrocycle to slip off from the molecule, leading to an unprotected chromophore (Figure 2).

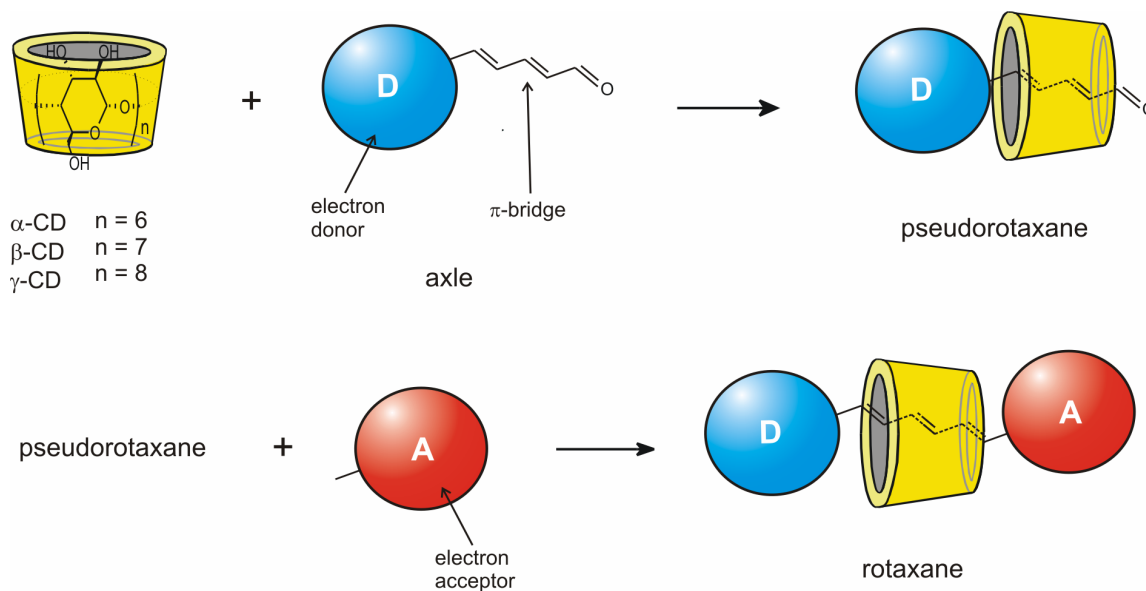


**Figure 2.** Schematic representation of the CD macrocycles and the rotaxane assembly applied on a NLO chromophore.

## 7.2 Results and Discussion

### 7.2.1 Synthesis

Our strategy for preparing EO-active rotaxanes is first to synthesize an axle, containing an electron-donor group. The axle must have the proper length for the

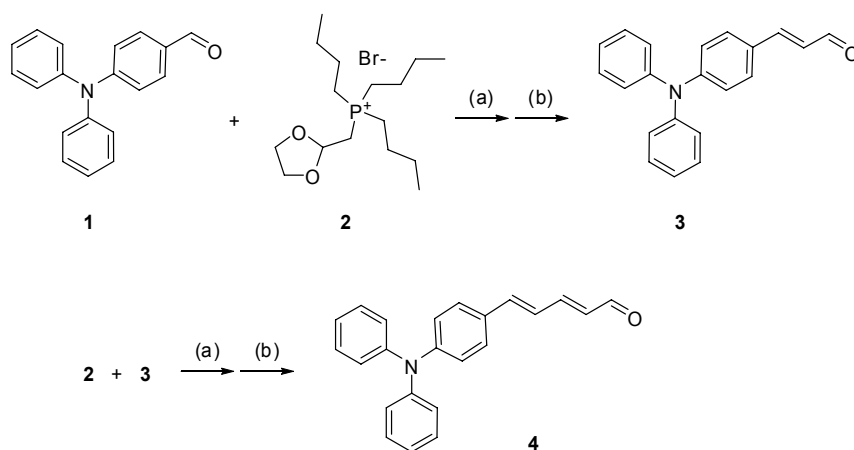
subsequent threading with  $\alpha$ -CD in water, to form a pseudorotaxane (Scheme 2).  $\alpha$ -CD was chosen for its smaller inner cavity that allow to form stronger inclusion complexes with elongated guests like linear alkanes and conjugated polymethine chains.<sup>24</sup> Moreover, it should possess a proper functionality to react with an electron acceptor group-containing stopper, ultimately resulting in rotaxane formation.<sup>25-27</sup>

Two different axles, possessing different electron-donor moieties, were synthesized.

### ***Triarylamine as electron donor.***

To synthesize an axle with an appropriate bridge length, the aldehyde functionality of 4-formyltriphenylamine **1**<sup>28</sup> was elongated via a Wittig reaction with the phosphonium salt of protected aldehyde **2**.<sup>29</sup> Subsequent cleavage of the protecting group by a strong acid gave aldehyde **3** (Scheme 1).

**Scheme 1.** Synthesis of triarylamine-containing axle **4**.<sup>a</sup>



<sup>a</sup> Reagents and conditions: (a) NaH, THF, rt, 24 h; (b) HCl, THF, rt, 15 min.

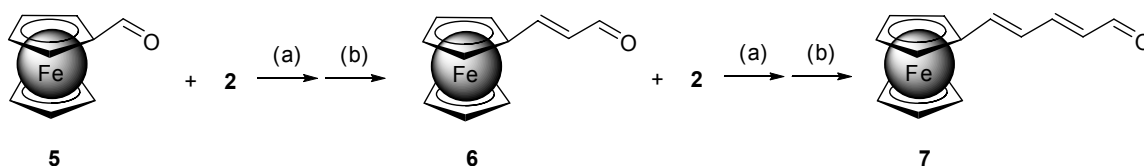
Subsequently, the same procedure was applied another time to give triarylamine-containing axle **4**. Its formation was demonstrated by the presence of four  $-\text{CH}=\text{C}$  hydrogens in the area between 6.21 and 7.19 ppm in the  $^1\text{H}$ -NMR spectrum, and confirmed by the molecular peak in the MS FAB<sup>+</sup> spectrum at  $m/z$  325.2.

**Ferrocenyl group as electron donor.**

Organometallic compounds are also used as NLO materials. Recently, ferrocenyl (Fc) containing chromophores reported the highest EO coefficient for an organometallic chromophore in a poled polymer matrix, being competitive with those of organic chromophores.<sup>30</sup> Moreover, the Fc moiety combines attractive NLO properties with a good thermal and photochemical stability, and redox-switching ability. The additional advantage of the Fc moiety in the EO rotaxane formation are the improved water solubility of the axle and its bulkiness to act as a stopper.

Using the same elongation procedure, ferrocenecarboxaldehyde **5** was reacted with phosphonium salt **2** to give, via aldehyde **6**, ferrocenyl-containing axle **7**. Its formation was demonstrated by the presence of four  $-\text{CH}=\text{C}$  hydrogens in the area between 6.23 and 7.26 ppm in the  $^1\text{H-NMR}$  spectrum, and confirmed by the molecular peak in the MS  $\text{FAB}^+$  spectrum at  $m/z$  267.0.

**Scheme 2.** Synthesis of ferrocenyl-containing axle **7**.<sup>a</sup>



<sup>a</sup> Reagents and conditions: (a) NaH, THF, rt, 24 h; (b) HCl, THF, rt, 15 min.

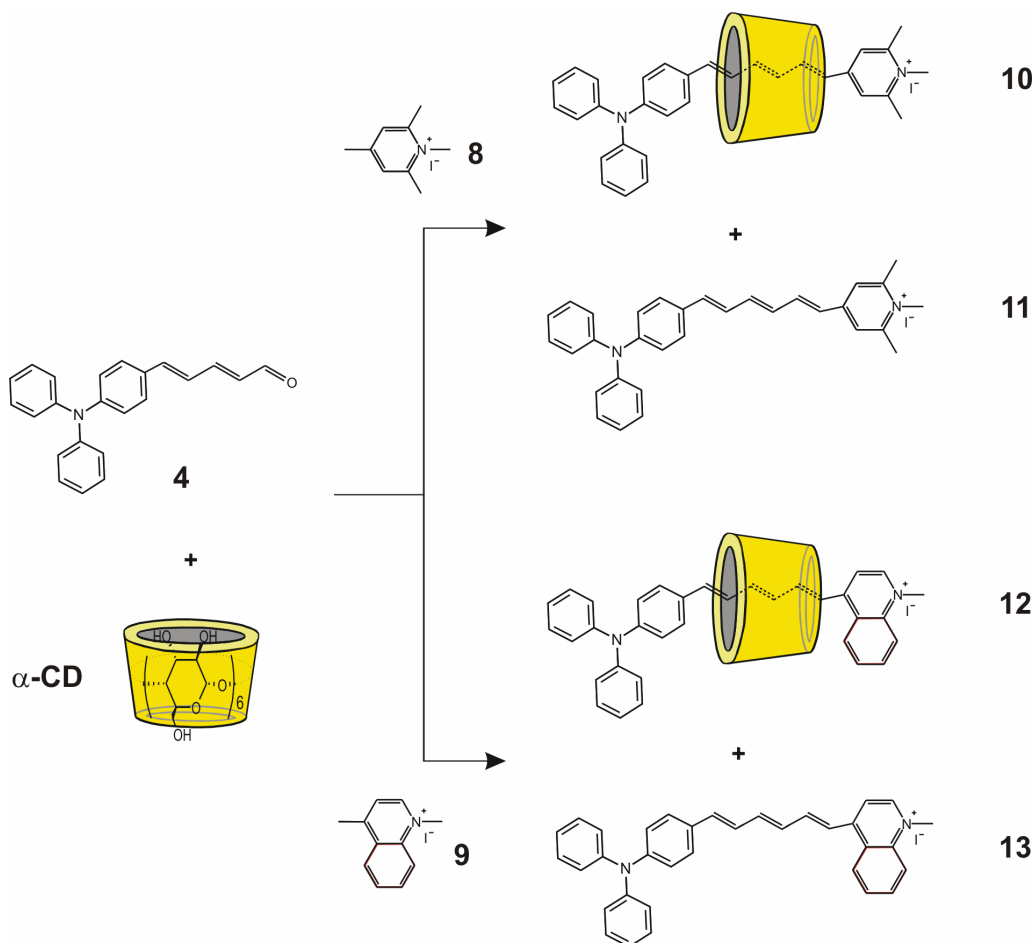
**Electron acceptor groups.**

In order to form an EO active rotaxane 1,2,4,6-tetramethylpyridinium iodide (**8**) and 1-methyl-4-lepidinum iodide (**9**) were chosen as electron acceptors. These charged compounds are able to react in water with an aldehyde to form a conjugated system. In addition, they are bulky enough to act as a stopper.

Rotaxane formation.

In general, the rotaxanes were synthesized by adding the iodine salts **8** or **9** to a 0.1 M NaOH solution of the corresponding axle **4** or **7** and a 4-5 fold excess of  $\alpha$ -CD. The reaction mixture was then stirred at 75 °C for 2 days, after which the rotaxane formation was verified by mass spectrometry (Scheme 3).

**Scheme 3.** Synthesis of rotaxanes **10** and **12** and their corresponding bare chromophores **11** and **13**.



Reaction between aldehyde **4** and pyridinium salt **8** (Scheme 3) led to the formation of both rotaxane **10** and the bare chromophore **11**. First, the basic aqueous reaction mixture was extracted several times with  $\text{CH}_2\text{Cl}_2$  to remove the unreacted aldehyde **4** and the bare chromophore **11** (partially). During the extraction a precipitate formed, which, after characterization, turned out to be free  $\alpha$ -CD. Characterization of both aqueous and

organic layers by MALDI MS revealed the presence of rotaxane **10** (and excess of  $\alpha$ -CD) in the aqueous layer.

Several techniques were tried to separate the mixture. Successively, normal phase silica (Kieselgel 60) with different eluents,<sup>31</sup> reversed phase silica (RP-18 F<sub>254</sub> S) with different eluents,<sup>5</sup> precipitation with a water-insoluble anion (PF<sub>6</sub><sup>-</sup>/ BF<sub>4</sub><sup>-</sup>), and size exclusion chromatography (SEC)<sup>4</sup> with Sephadex G-15 (molecular weight range  $\leq 1500$  D) with as eluent 0.1 and 0.01 M NH<sub>4</sub>HCO<sub>3</sub> were utilized. However, all techniques were not successful. SEC did not give complete separation between the rotaxane and the excess of free CD, probably due to the too small difference in molecular weights.

A MALDI MS characterization of the aqueous layer showed that the rotaxane **10** was the most intense peak at  $m/z$  1417, while showing, on the other hand, that free  $\alpha$ -CD was still present (Figure 3). The <sup>1</sup>H NMR spectrum showed broadened peaks, which could be due to both the movement of the ring along the axle and the presence of water and excess of  $\alpha$ -CD. Due to this excess of  $\alpha$ -CD it was impossible to fully characterize the rotaxane by <sup>1</sup>H NMR spectroscopy and to determine the position of the macrocycle around the chromophore.

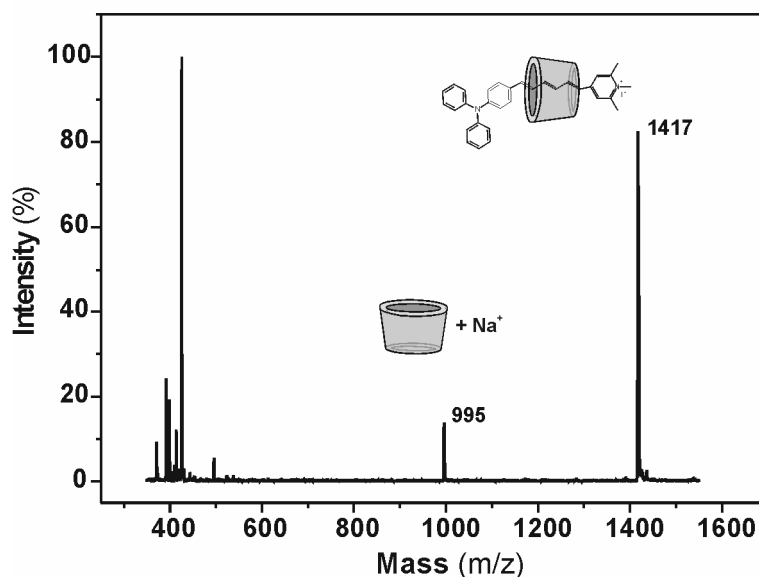
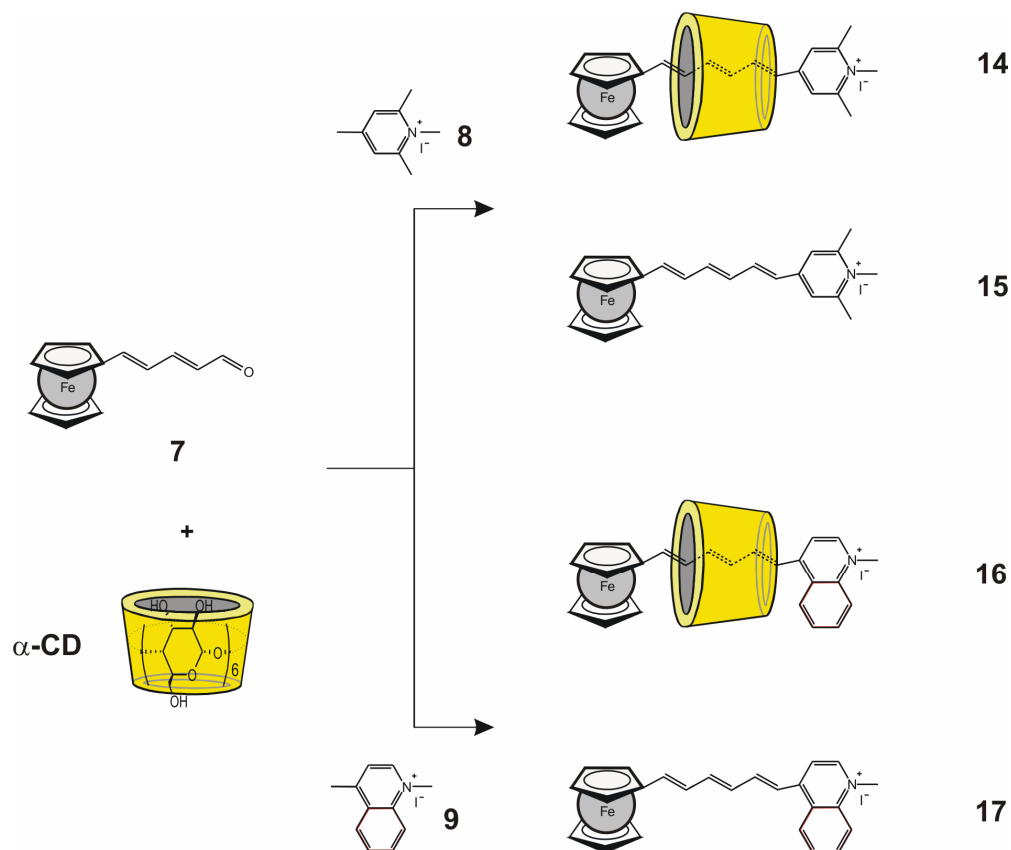


**Figure 3.** Mass spectrum of the rotaxane **10** ( $m/z$  1417) and CD mixture.

Chromophore **11** was independently synthesized in ethanol from aldehyde **4** and pyridinium salt **8** using a catalytic amount of piperidine as base. The formation of the chromophore **11** is confirmed by the complete disappearance of the aldehyde peak of the reagent at 9.61 ppm and by the shift from 6.23 to 6.50 ppm for the terminal  $-\text{CH}=\text{C}$  proton in the  $^1\text{H}$  NMR spectrum.

Reaction between aldehyde **4** and lepidinium salt **9** (Scheme 3) led, according to the MALDI MS spectrum, to the formation of the bare chromophore **13** while a signal of the corresponding rotaxane **12** was lacking. Apparently, the interaction between **4** and  $\alpha$ -CD was too low to give rotaxane formation.

**Scheme 4.** Synthesis of rotaxanes **14** and **16** and their corresponding bare chromophores **15** and **17**.



Rotaxane **14**: Reaction between aldehyde **7** and pyridinium salt **8** (Scheme 4) resulted in the formation of both rotaxane **14** ( $m/z$  1356) and the bare chromophore **15**, according to the MALDI MS spectrum (Figure 4).

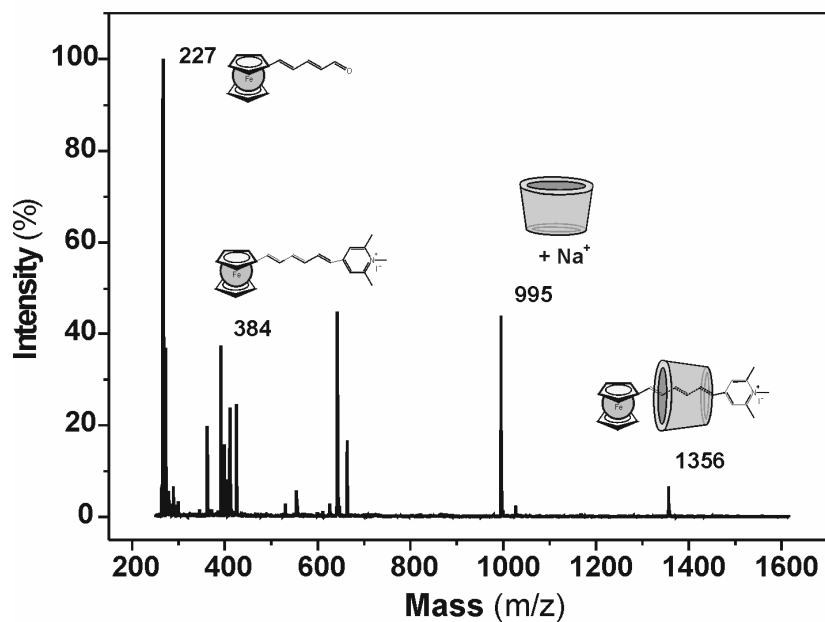


**Figure 4.** Mass spectrum of the crude reaction mixture containing rotaxane **14** ( $m/z$  1356).

Reaction between aldehyde **7** and lepidinium salt **9** (Scheme 4) led to the formation of both rotaxane **16** and the bare chromophore **17**, according to the MALDI MS spectrum (Figure 5). However, for both rotaxanes **14** ( $m/z$  1378) and **16** adequate separation could not be realized with SEC with as eluent 0.01 M  $\text{NH}_4\text{HCO}_3$ .

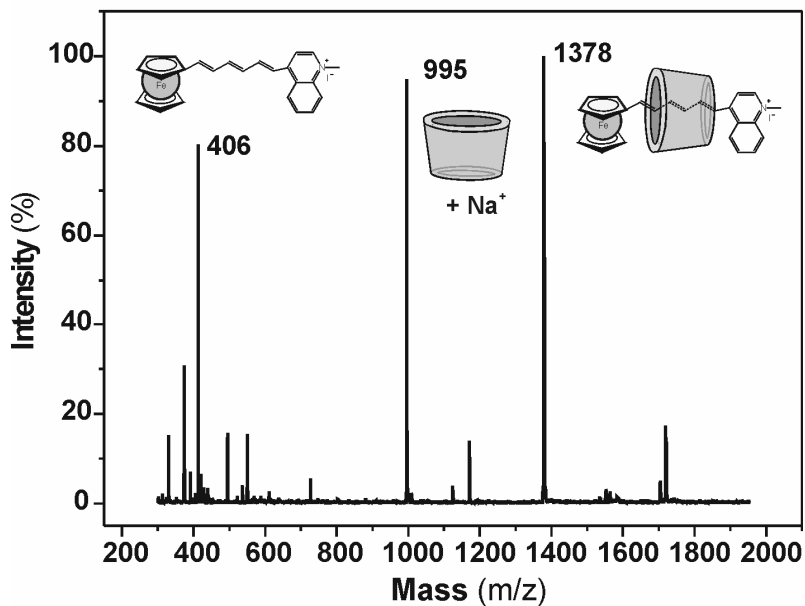


**Figure 5.** Mass spectrum of the crude reaction mixture containing rotaxane **16** ( $m/z$  1378).



### 7.2.4 Photobleaching Test

To have a preliminary indication of the expected enhanced photochemical stability induced by chromophore encapsulation, the straightforward and low-cost qualitative method described in Chapter 3 was used. It concerns the monitoring of the decrease in absorbance during irradiation of oxygen-saturated solutions of chromophores with visible white light. Photodegradation measurements were carried out in a dioxane/water 9/1 v/v mixture with rotaxane **10** and bare chromophore **11**, although rotaxane **10** was not completely pure.

The trend in Figure 6 clearly shows that the decay in the absorbance of bare chromophore **11** is faster than that of rotaxane **10**, demonstrating the effect of the protection of the  $\pi$ -electron bridge in rotaxane **10** by  $\alpha$ -CD. The conjugated alkene bonds are harder to be reached by the singlet oxygen, and thus lead to a reduced photodegradation reaction rate.

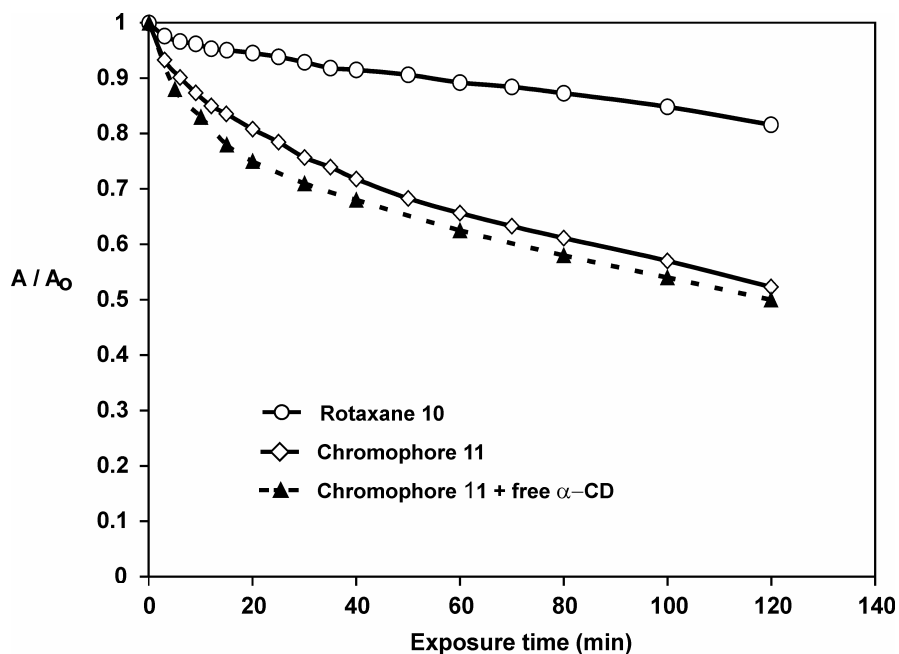


**Figure 6.** Photo-bleaching curves of the rotaxane **10**, chromophore **11**, chromophore **11** + free  $\alpha$ -CD in dioxane/water 9/1 v/v.  $A$  is the absorbance at time  $t$  and  $A_0$  is the initial absorbance. Photolyses were carried out in 10 mm quartz cuvettes with light from a 75 Watt halogen lamp. The samples were irradiated at a distance of 10 cm from the light source and were shielded from daylight.

However, since rotaxane **10** is not pure, but contains, as observed by  $^1\text{H}$  NMR experiments, an excess of  $\alpha$ -CD, a control experiment was performed to clarify whether this may influence the decay. Therefore a solution of bare chromophore **11** with a 10-fold excess of  $\alpha$ -CD was irradiated under the same conditions. The resulting decay curve (Figure 6) shows that the decay of bare chromophore **11** is barely influenced by the presence of the excess of  $\alpha$ -CD, validating the results obtained with the first experiment.

### 7.3 Conclusions

Three EO active rotaxanes having pyridinium salts as electron-acceptor and either triarylamine or ferrocenyl moieties as electron-donor were synthesized in water. The distinctive feature of these compounds is the encapsulation of the  $\pi$ -electron bridge of the NLO chromophores by  $\alpha$ -CD. Although their formation could be detected by mass spectrometry, attempts of purification with different separation techniques were not successful. Preliminary photobleaching tests were carried out with rotaxane **10** (with excess of free  $\alpha$ -CD) and bare chromophore **11**. Although rotaxane **10** was not completely pure, these experiments demonstrate the enhanced photostability provided by shielding of the chromophore by encapsulation.

### 7.4 Experimental Section

**General Procedures.** All chemicals were of reagent grade and used without further purification. THF was freshly distilled from Na/benzophenone, and  $\text{CH}_2\text{Cl}_2$  from  $\text{CaCl}_2$ . All chromatography associated with product purification was performed by flash column techniques using Merck Kieselgel 600 (230-400 mesh). Melting points of all compounds were obtained with a Reichert melting point apparatus and a Kofler stage.  $^1\text{H}$  NMR spectra were recorded on a Varian Unity 300 using tetramethylsilane (TMS) or the corresponding residual solvent signal as internal standard. FAB-MS spectra were recorded on a Finningan MAT 90 spectrometer with *m*-nitrobenzyl alcohol (NBA) as a

matrix. UV-Vis measurements were carried out on a Varian Cary 3E UV-spectrophotometer.

Compounds **1**,<sup>28</sup> **2**,<sup>29</sup> **8**,<sup>32</sup> and **9**,<sup>33</sup> were prepared according to procedures reported in literature.

**3-(4-Diphenylaminophenyl)-prop-2-enal (3)**.<sup>34</sup> To a solution of 4-formyltriphenylamine **1** (1.0 g, 3.7 mmol) in THF (40 mL) was added phosphonium salt **2** (4.2 g, 14.8 mmol). Then, NaH (60% dispersion in mineral oil; 740 mg, 18.5 mmol) was slowly added and the resulting mixture was stirred at rt for 24 h. Subsequently, HCl (10% in water) was added until pH  $\approx$  1, whereupon the reaction mixture was stirred for 15 min and extracted with CH<sub>2</sub>Cl<sub>2</sub> (2  $\times$  100 mL). The organic layer was dried with MgSO<sub>4</sub> and concentrated. The crude product was purified by silica gel chromatography (ethyl acetate/hexane 2/8) to afford **3** as a yellow solid (75%): <sup>1</sup>H NMR (CDCl<sub>3</sub>)  $\delta$  6.55-6.63 (dd,  $J$  = 8.4, 7.8 Hz, 1H, =CH-CHO), 6.97 (d,  $J$  = 8.7 Hz, 2H, ar-H), 7.03-7.22 (m, 6H, ar-H), 7.28-7.35 [m, 5H, (4H, ar-H and 1H, -CH=)], 7.41 (d,  $J$  = 8.4 Hz, 2H, ar-H), 9.65 (d,  $J$  = 7.5 Hz, 1H, CHO); MS FAB<sup>+</sup>  $m/z$  299.7 [ $M^+$ ], 300.7 ( $M^+$  + H), calcd for C<sub>21</sub>H<sub>17</sub>NO 299.4.

**5-(4-Diphenylaminophenyl)-penta-1,3-dienal (4)** was prepared following the same procedure used for compound **3** using aldehyde **3** (800 mg, 2.7 mmol), phosphonium salt **2** (3.1 g, 10.7 mmol), NaH (60% dispersion in mineral oil; 536 mg, 13.4 mmol), and THF (35 mL). Purification with silica gel chromatography (ethyl acetate/hexane 2/8) afforded **4** as a yellow solid (72%): <sup>1</sup>H NMR (CDCl<sub>3</sub>)  $\delta$  6.23 (dd,  $J$  = 8.1, 7.8 Hz 1H, =CH-CHO), 6.93 (d,  $J$  = 8.7 Hz, 2H, ar-H), 7.02-7.14 [m, 6H, (2H, ar-H and 2H, -CH=)], 7.23-7.26 [m, 5H, (4H, ar-H and 1H, -CH=)], 7.28-7.34 (m, 4H, ar-H), 7.36 (d,  $J$  = 8.7 Hz, 2H, ar-H), 9.61 (d,  $J$  = 7.8 Hz, 1H, CHO); MS FAB<sup>+</sup>  $m/z$  325.2 ([ $M^+$ ], calcd for C<sub>23</sub>H<sub>19</sub>NO 325.4).

**3-Ferrocenyl-prop-2-enal (6)** was prepared following the same procedure as for compound **3**. Reagents included ferrocenecarboxaldehyde **5** (3.0 g, 14 mmol), phosphonium salt **2** (8.1 g, 28.0 mmol), NaH (60% dispersion in mineral oil; 1.7 g, 42

mmol) and THF (75 mL). Purification with silica gel chromatography (CH<sub>2</sub>Cl<sub>2</sub>/hexane 1/1) afforded **6** as a red solid (80%): <sup>1</sup>H NMR (CDCl<sub>3</sub>) δ 4.15 (s, 5H, C<sub>5</sub>H<sub>5</sub>), 4.46-4.59 (m, 4H, C<sub>5</sub>H<sub>4</sub>), 6.34 (dd, *J* = 7.5, 7.8 Hz, 1H, =CH-CHO), 7.40 (d, *J* = 7.5 Hz, 1H, -CH=C), 9.69 (s, *J* = 7.8 Hz, 1H, CHO); MS FAB<sup>+</sup> *m/z* 240.0 ([M<sup>+</sup>-2H]), 241.0 (M<sup>+</sup>-H), calcd for C<sub>13</sub>H<sub>14</sub>FeO 242.1).

**5-Ferrocenyl-penta-1,3-dienal (7)** was prepared following the same procedure used for compound **3**. Reagents included 3-ferrocenyl-prop-2-enal **6** (550 mg, 2.3 mmol), phosphonium salt **2** (2.0 g, 6.9 mmol), NaH (60% dispersion in mineral oil; 458 mg, 11.5 mmol) and THF (25 mL). Purification with silica gel chromatography (CH<sub>2</sub>Cl<sub>2</sub>/hexane 4/6) afforded **7** as a red solid (75%): <sup>1</sup>H NMR (CDCl<sub>3</sub>) δ 4.09 (s, 5H, C<sub>5</sub>H<sub>5</sub>), 4.44-4.58 (m, 4H, C<sub>5</sub>H<sub>4</sub>), 6.21 (dd, *J* = 7.4, 7.8 Hz, 1H, =CH-CHO), 6.76-7.02 (m, 2H, -CH=C), 7.07-7.21 (m, 1H, -CH=C), 9.61 (d, *J* = 7.4 Hz, 1H, CHO); MS FAB<sup>+</sup> *m/z* 266.0 ([M<sup>+</sup>-2H]), 267.0 (M<sup>+</sup>-H) calcd. for C<sub>15</sub>H<sub>16</sub>FeO 268.1)

**Chromophore 11.** A solution of aldehyde **4** (146 mg, 0.45 mmol), 1,2,4,6-tetramethylpyridinium iodide (118 mg, 0.45 mmol), and a catalytic amount of piperidine in absolute ethanol (15 mL) was refluxed for 24 h. After cooling to rt, addition of diethyl ether (50 mL) led to the formation of a precipitate. The resulting solid was filtered and washed with ice cold methanol (5 mL). Trituration with water gave chromophore **11** as a dark solid (45%): <sup>1</sup>H NMR (CDCl<sub>3</sub>) δ 2.94 (s, 6H, CH<sub>3</sub>), 4.09 (s, 3H, N<sup>+</sup>-CH<sub>3</sub>), 6.54-6.56 (m, 2H, -CH=), 7.02-7.16 [m, 12H, (10H, ar-H and 2H, -CH=)], 7.21-7.35 [m, 6H, (4H, ar-H and 2H, -CH=)], 7.51 (s, 2H, ar-H); MS MALDI *m/z* 443.3, 444.3 (M<sup>+</sup>-I+H), ([M<sup>+</sup>-I] calcd for C<sub>32</sub>H<sub>31</sub>N<sub>2</sub>I 570.5).

## 7.5 References

- 1 L. R. Dalton, W. H. Steier, B. H. Robinson, C. Zhang, A. Ren, S. Garner, A. Chen, T. Londergan, L. Irwin, B. Carlson, L. Fifield, G. Phelan, C. Kincaid, J. Amend, A. Jen, *J. Mater. Chem.*, **1999**, *9*, 1905-1920.

- 2 A. Galvan-Gonzalez, M. Canva, G. I. Stegeman, R. Twieg, K. P. Chan, T. C. Kowalczyk, X. Q. Zhang, H. S. Lackritz, S. R. Marder, S. Thayumanavan, *Opt. Lett.*, **2000**, *25*, 332-334.
- 3 M. He, T. Leslie, S. Garner, M. DeRosa, J. Cites, *J. Phys. Chem. B*, **2004**, *108*, 8731-8736.
- 4 M. R. Craig, M. G. Hutchings, T. D. W. Claridge, H. L. Anderson, *Angew. Chem., Int. Ed.*, **2001**, *40*, 1071-+.
- 5 J. E. H. Buston, J. R. Young, H. L. Anderson, *Chem. Commun.*, **2000**, 905-906.
- 6 F. H. Huang, H. W. Gibson, *Prog. Polym. Sci.*, **2005**, *30*, 982-1018.
- 7 H. Tian, Q. C. Wang, *Chem. Soc. Rev.*, **2006**, *35*, 361-374.
- 8 O. Lukin, F. Vögtle, *Angew. Chem., Int. Ed.*, **2005**, *44*, 1456-1477.
- 9 V. Balzani, A. Credi, F. M. Raymo, J. F. Stoddart, *Angew. Chem., Int. Ed. Engl.*, **2000**, *39*, 3349-3391.
- 10 A. R. Pease, J. O. Jeppesen, J. F. Stoddart, Y. Luo, C. P. Collier, J. R. Heath, *Acc. Chem. Res.*, **2001**, *34*, 433-444.
- 11 A. H. Flood, R. J. A. Ramirez, W. Q. Deng, R. P. Muller, W. A. Goddard Iii, J. F. Stoddart, *Aust. J. Chem.*, **2004**, *57*, 301-322.
- 12 P. L. Anelli, P. R. Ashton, N. Spencer, A. M. Z. Slawin, J. F. Stoddart, D. J. Williams, *Angew. Chem., Int. Ed. Engl.*, **1991**, *30*, 1036-1039.
- 13 J. C. Chambron, V. Heitz, J. P. Sauvage, *J. Am. Chem. Soc.*, **1993**, *115*, 12378-12384.
- 14 J. M. Kern, J. P. Sauvage, G. Bidan, B. Divisia-Blohorn, *J. Polym. Sci., Part A: Polym. Chem.*, **2003**, *41*, 3470-3477.
- 15 H. W. Gibson, M. C. Bheda, P. T. Engen, *Prog. Polym. Sci.*, **1994**, *19*, 843-945.
- 16 F. Vögtle, T. Dunnwald, T. Schmidt, *Acc. Chem. Res.*, **1996**, *29*, 451-460.
- 17 A. Harada, *Acc. Chem. Res.*, **2001**, *34*, 456-464.
- 18 A. P. Croft, R. A. Bartsch, *Tetrahedron*, **1983**, *39*, 1417-1474.
- 19 A. R. Khan, P. Forgo, K. J. Stine, V. T. D'Souza, *Chem. Rev.*, **1998**, *98*, 1977-1996.
- 20 A. W. Harper, S. Sun, L. R. Dalton, S. M. Garner, A. Chen, S. Kalluri, W. H. Steier, B. H. Robinson, *J. Opt. Soc. Am. B*, **1998**, *15*, 329-337.
- 21 I. Liakatas, C. Cai, M. Bösch, M. Jäger, C. Bosshard, P. Günter, C. Zhang, L. R. Dalton, *Appl. Phys. Lett.*, **2000**, *76*, 1368-1370.
- 22 P.-M. Javier, A. Inge, S. Kai, C. Koen, Z. Yuxia, N. Hachiro, O. Shuji, N. Kyoko, K. Oh-Kil, J. Jongtae, M. Janka, M. Marc De, G. K. Mark, *J. Chem. Phys.*, **2007**, *126*, 074705.
- 23 V. Bermudez, T. Gase, F. Kajzar, N. Capron, F. Zerbetto, F. G. Gatti, D. A. Leigh, S. Zhang, *Opt. Mater.*, **2003**, *21*, 39-44.
- 24 M. V. Rekharsky, Y. Inoue, *Chem. Rev.*, **1998**, *98*, 1875-1917.

- 25 S. Anderson, T. D. W. Claridge, H. L. Anderson, *Angew. Chem., Int. Ed. Engl.*, **1997**, *36*, 1310-1313.
- 26 M. R. Craig, T. D. W. Claridge, M. G. Hutchings, H. L. Anderson, *Chem. Commun.*, **1999**, 1537-1538.
- 27 S. Anderson, W. Clegg, H. L. Anderson, *Chem. Commun.*, **1998**, 2379-2380.
- 28 G. F. Lai, X. R. Bu, J. Santos, E. A. Mintz, *Synlett*, **1997**, 1275-&.
- 29 C. W. Spangler, R. K. McCoy, *Synth. Commun.*, **1988**, *18*, 51-59.
- 30 Y. Liao, B. E. Eichinger, K. A. Firestone, M. Haller, J. D. Luo, W. Kaminsky, J. B. Benedict, P. J. Reid, A. K. Y. Jen, L. R. Dalton, B. H. Robinson, *J. Am. Chem. Soc.*, **2005**, *127*, 2758-2766.
- 31 R. Isnin, A. E. Kaifer, *J. Am. Chem. Soc.*, **1991**, *113*, 8188-8190.
- 32 S. R. Marder, J. W. Perry, W. P. Schaefer, *Science*, **1989**, *245*, 626-628.
- 33 V. Alain, A. Fort, M. Barzoukas, C. T. Chen, M. Blanchard-Desce, S. R. Marder, J. W. Perry, *Inorg. Chim. Acta*, **1996**, *242*, 43-49.
- 34 M. Liang, W. Xu, F. Cai, P. Chen, B. Peng, J. Chen, Z. Li, *J. Phys. Chem. C*, **2007**, *111*, 4465-4472.

# Summary

The research described in this thesis is concerned with the design and synthesis of new thermally and photostable electro-optic (EO) polymeric materials. In addition, emphasis is given to the thermal and photostability of these materials, being of critical importance for the long-term reliability of EO devices.

The importance of EO polymer-based devices to the development of a next-generation broadband communication network based on optical fibers is outlined in Chapter 1.

Chapter 2 first gives an introduction to the theory and concepts of nonlinear optics (NLO). Then it describes the recent developments in the field of second-order NLO polymers, including chromophore design and the different approaches for their incorporation in noncentrosymmetric materials. The different architectures are compared, together with the requirements for their incorporation into practical EO devices.

In Chapter 3 tricyanovinylidenediphenylaminobenzene (**TCVDPA**) was identified as the most promising NLO chromophore for its exceptional photostability and used as a base for structural improvements. A series of derivatives was synthesized applying shape modification, leading to a reduction of both the unfavorable dipole-dipole electrostatic interactions and the chromophore induced plasticization effect. Improvements of the macroscopic EO response were obtained for most of the derivatives when incorporated as a guest at high loading in polysulfone as host polymer. Specifically, functionalization with fluorinated aromatic substituents leads to a doubling of the EO activity at 30 wt % (25 pm/V at 830 nm) compared with the pristine **TCVDPA**. Furthermore, all chromophores in this study possess a good processability, and exhibit among the highest thermal and photochemical stabilities reported in literature.

In Chapter 4 the **TCVDPA** chromophore was covalently linked to a polycarbonate backbone, combining the good properties of polycarbonates with the improved stability of the poling order given by chromophore attachment. NLO polycarbonates with different

chromophore attachment modes and flexibilities were synthesized resulting in a significant improvement of over 100 °C of the material  $T_g$  compared with the guest-host system reported in Chapter 3, incorporating the same chromophore at similar high loadings. Poling efficiency and poling alignment stability are strongly dependent on structural parameters such as of polymer chain flexibility and the number of chromophore-to-polymer attachment points. Moreover, high thermal stabilities and excellent photostabilities were obtained.

Chapter 5 deals with the development of a generally applicable method for the synthesis of NLO polycarbonates. The modular approach involves first the versatile formation of a polycarbonate backbone possessing the desired physico-chemical properties (i.e. rigidity,  $T_g$ , thermal stability), followed by the introduction of the chromophore in the final reaction step. Chromophores with different structures and NLO activities were incorporated at high loadings, to give polymers with fairly high  $T_g$ s and thermal stabilities, good solubilities, and EO activities as high as 38 pm/V (at 1300 nm).

Chapter 6 describes the fabrication of a prototype integrated optical device, namely an EO microring resonator, by direct photodefinition on negative photoresist SU8, incorporating the **TCVDPA** chromophore as guest. **TCVDPA**, in contrast to most of the chromophores, possesses the unique feature of having a low absorption window in the UV region that allows to use UV-crosslinking for photodefinition without any chromophore bleaching. The resulting device showed an excellent photostability under high photon flux and an EO modulation was demonstrated at 10 MHz. Functionalization of the **TCVDPA** chromophore with epoxy groups induced the formation of cross-links between the chromophore and the host polymer, resulting in a material with a 40 °C higher  $T_g$ . UV-nanoimprint lithography (NIL) was explored on the SU8-**TCVDPA**-epoxy system as alternative technique for the high-volume and low-cost production of EO devices.

Chapter 7 describes the preliminary results of the synthesis of NLO chromophores of which the  $\pi$ -electron bridge is encapsulated by a cyclodextrin macrocycle, to form an EO active rotaxane. Three EO active rotaxanes having pyridinium salts as electron-acceptor and either triarylamine or ferrocenyl moieties as electron-donor were synthesized in water. Although their formation could be detected by mass spectrometry, attempts of



purification with different separation techniques were not successful. Preliminary photobleaching tests demonstrated the enhanced photostability provided by shielding of the chromophore by encapsulation.

In conclusion, new, highly stable polymeric materials were developed for EO applications. Some of the polymers presented in this thesis are among the most photostable structures ever reported, representing a step forward toward long-lifetime device-quality materials. In addition, the presented methodology for the synthesis of NLO polycarbonates opens new possibilities for the further development of high performing organic EO materials. The use of highly photostable chromophores in combination with UV-photolithography, demonstrated by the successful fabrication of a EO modulator device, represents a powerful tool for the high-volume and low cost production of devices based on EO polymeric materials.



# Samenvatting

Het onderzoek beschreven in dit proefschrift betreft het ontwerp en de synthese van nieuwe electro-optische (EO) polymere materialen die thermisch en fotochemisch stabiel zijn. De nadruk ligt op de thermische en fotochemische stabiliteit van deze materialen aangezien deze eigenschappen bepalend zijn voor hun duurzaamheid.

In het eerste Hoofdstuk wordt ingegaan op het belang welke apparaten gebaseerd op EO-polymeren hebben voor de ontwikkeling van de volgende generatie breedband communicatie netwerken die optische vezels als basis hebben.

Hoofdstuk 2 begint met een introductie over de theorie en de concepten van de nonlineaire optica (NLO). Vervolgens worden de recente ontwikkelingen binnen het gebied van de ‘second-order’ NLO-polymeren beschreven. Ook wordt ingegaan op het ontwerp van de chromoforen die hiervoor gebruikt worden en de manieren waarop deze in ‘uit-centrosymmetrische’ materialen verwerkt kunnen worden. De verschillende architecturen worden vergeleken, en de vereisten voor inbouw in EO instrumenten worden besproken.

In Hoofdstuk 3 wordt tricyanovinylideendfenylaminobenzeen (TCVDPA) als het meest geschikt NLO-chromofoor bevonden wat mede te danken is aan de exceptioneel hoge lichtstabiliteit. Deze structuur is dan ook als basis gebruikt voor de synthese van een serie derivaten, wat heeft geleid tot chromoforen met een verminderde ongunstige dipool-dipool electrostatische interactie en een verminderde plastificerende werking. Voor het overgrote deel van de derivaten wordt een verbetering in de macroscopische EO-respons gevonden wanneer ze in een hoge concentratie in het polymeer polysulfon worden verwerkt. Functionalisering met gefluorineerde aromatische substituenten leidt tot een verdubbeling van de EO-activiteit bij 30 wt % (25 pm/V at 830 nm) in vergelijking met de pristine TCVDPA. Daarnaast zijn alle hier beschreven chromoforen eenvoudig te verwerken in de beoogde materialen, en behoren ze tot de categorie chromoforen met de hoogste thermische en fotochemische stabiliteit bekend in de literatuur.

Hoofdstuk 4 beschrijft de covalente verankering van het TCVDPA chromofoor aan een polycarbonaat polymereer. Zo worden de gunstige eigenschappen van het polycarbonaat gecombineerd met een verbeterde stabiliteit van het chromofoor na uitrichten Experimenten waarbij het chromofoor op verschillende manieren verankerd wordt aan de NLO-polycarbonaten resulteren in een verbetering van de Tg waarde van meer dan 100 °C. Deze waarden zijn aanzienlijk beter dan wanneer hetzelfde chromofoor in eenzelfde concentratie verwerkt wordt in het polymeer, zoals beschreven in Hoofdstuk 3. De mate van uitrichten en de stabiliteit van de uitlijning zijn sterk afhankelijk van de structureigenschappen, keten flexibiliteit en het aantal chromofoor-polymeerbindingen binnen het polymeer-chromofoor materiaal. Bovendien zijn ook bij deze materialen hoge thermische en fotochemische stabiliteiten gevonden.

Hoofdstuk 5 behandelt de ontwikkeling van een algemeen toepasbare methode voor de synthese van NLO-polycarbonaten. In deze methode wordt als eerste een chemisch zeer toegankelijke polycarbonaatmatrix gesynthetiseerd met de vereiste eigenschappen (d.w.z. de juiste mate van stijfheid, Tg waarde en thermische stabiliteit) gevolgd door de verankering van een chromofoor als laatste stap. Op deze manier zijn een serie chromofooren met verschillende structuren en NLO activiteiten met een hoge dichtheid verankerd in het polymeer. Dit resulteerde in materialen met vrij hoge Tg waarden, thermische stabiliteiten, hoge oplosbaarheden en met EO activiteiten tot 38 pm/V (bij 1300 nm).

Hoofdstuk 6 beschrijft de constructie van een prototype geïntegreerd optisch instrument, een EO ‘microring resonator’, via directe fotodefinitie op een negatief fotoresist SU8 waarbij het chromofoor TCVDPA werd gebruikt. In tegenstelling tot de meeste chromofooren heeft TCVDPA een lage absorptie in het UV gebied. Dit maakt het gebruik van UV-crosslinking bij de fotodefinitie mogelijk zonder dat het chromofoor afbreekt. Het gefabriceerde prototype heeft een hoge fotochemische stabiliteit bij een hoge fotonflux en een EO-modulatie werd gevonden bij 10 MHz. Wanneer het TCVDPA chromofoor met epoxygroepen werd gefunctionaliseerd vindt er ‘cross-linking’ plaats tussen het chromofoor en het polymeer, resulterend in een materiaal met een 40 °C hogere Tg waarde. Als alternatieve techniek voor de eenvoudige constructie van EO

instrumenten werd onderzocht of UV-nanoimprint lithografie (NIL) met het SU8-TCVDPA-epoxysysteem gebruikt kan worden.

In Hoofdstuk 7 worden de voorlopige resultaten beschreven van de synthese van NLO chromoforen waarbij het  $\pi$ -elektronensysteem in een cyclodextrinering gecomplexeerd zit; op deze manier ontstaat een rotaxaan die EO-activiteit bezit. Drie EO-actieve rotaxanen met een pyridiniumzout als elektronen-acceptor en een triarylamine- of een ferrocenylgroep als elektronen-donor werden gesynthetiseerd in water. Met massaspectrometrie is aangetoond dat de rotaxanen gevormd zijn. Ondanks verscheidene scheidingprocedures was het onmogelijk om een zuiver product te verkrijgen. Uit de eerste resultaten blijkt dat de afschermdende werking van de cyclodextrinering de fotochemische stabiliteit van het chromofoor vergroot.

Concluderend kan gesteld worden dat er nieuwe polymere EO-materialen ontwikkeld zijn met een hoge stabiliteit, waarvan sommige behorend tot diegene met de hoogste fotochemische stabiliteit tot op heden bekend. Dit betekent een stap voorwaarts naar de ontwikkeling van materialen en instrumenten met een hoge duurzaamheid. Bovendien opent de beschreven synthesesmethode voor NLO polycarbonaten nieuwe mogelijkheden voor de verdere ontwikkeling van kwalitatief hoge organische EO-materialen. Uit de succesvolle constructie van een EO-modulatieinstrument via UV-fotolithografie in combinatie met fotochemisch stabiele chromoforen blijkt dat dit een veelbelovende manier is voor de goedkope massa productie van apparaten welke gebaseerd zijn op polymere EO-materialen.



# Thanks

Here I am, at the end of this four years long journey called a PhD, although I haven't fully realized yet that I've finally made it. Probably because I don't want to admit to myself that it's now difficult to leave, in spite for many years claiming the opposite. I'll probably have to wait for the 'Pedell' to drop his stick or for somebody to kick me out. Along the way I've met a lot of fantastic people who made my time both inside and outside the lab an unique experience. I would like to thank everyone who has supported me, believed in me, or just shared a moment of happiness with me.

First, I would like to express my appreciation to my promotor, Prof. David N. Reinhoudt for giving me the privilege of working as a member of SMCT. I've truly enjoyed the multicultural and the pleasant working atmosphere you have created in your group. Thank you for all the freedom that you have given me, for your honesty, and for your personal understanding and support during difficult moments.

I would like to thank my co-promotor, Dr. Wim Verboom, especially for the invaluable help in the final part of my PhD. Thank you for sharing with me your experience in writing scientific papers and for your meticulous yet fast corrections of my thesis.

Working in such a multidisciplinary project I had the chance to collaborate with many people with different backgrounds. A special thank goes to Muralidharan Balakrishnan who has been working with me throughout my PhD. Thank you Murali for all the measurements and all the hours spent in the cleanroom trying to make thin films or devices from the polymers I was synthesizing.

Dr. Mart Diemeer has been the mastermind behind the project, from the original idea to the practical work. Thank you for the useful scientific discussions, for your endless expertise, and for your kindness. It was a real pity that you couldn't be with us until the end. Prof. Alfred Driessen, head of the IOMS group, thank you for being the leader of the STW project that I've been involved in. I owe my appreciation to Prof. Koen Clays, Dr. Inge Asselberghs, and Ayele Gorfo from the Katholieke Universiteit Leuven for the HRS measurements and for the fruitful scientific

discussions. Clemens Padberg for the GPC measurements and for the assistance with the DSC and TGA machines.

I am grateful to the students who have worked on this project for a longer or shorter period of time: Zhipeng Hu, Maarten van Gils, Julia Garowska, Pim Voorthuijzen, and Riccardo Torosantucci.

I want to thank Aldrik Velders, Alessio Piermattei, and Albert Ruggi for reading and correcting my concept thesis, for giving me useful suggestions and nice feedback. Also thanks very much to Henk who translated the summary into Dutch.

Thanks goes to the SMCT-MNF staff members: Prof. Jurriaan Huskens, always expressing his appreciation for my T-shirts; Bart-Jan Ravoo (now Prof), Mercedes Crego Calama (Peace in the labs), and Aldrick Velders (certo che per essere solo un tecnico ti stai facendo un bel culo)

I must not forget to thank Marcel de Bruine for the technical support and patience (did my compounds arrive yet?), Richard Egberink for solving my computer-related issues and for closing an eye (or two) when passing by my bench, Tieme Stevens for the mass measurements, Bianca Snellink-Ruël for the help with the NMR. Thanks go also to all the secretaries of SMCT-MNF: Izabel Katalank, Marieke Slotman, and Danielle Heskamp.

I really believe that SMCT is more than a research group. I've really enjoyed the friendly working environment, all the discussions and jokes, the fights and the laughs. The 'social room' is where all the magic happens; it might be due to the mixed smell of food, coffee, solvents, and chemicals, but I've always seen it as a melting pot: if you want to be part of the group, just go there and blend in!

I would like to thank all my labmates: Alessio (grazie per il sostegno soprattutto nella parte finale della tesi e per ascoltare le mie chiamate quasi giornaliera), Henk (it has always been a pleasure to share my glassware with you), Xing Yi (always happy and supportive: "Mirko, come on, you can do it!") Thank you for sharing with me the secrets of NIL), Dominick (the unabomber), Manon (strong Dutch woman), Hans (pizza zonder kaas maar met mozzarella...thank you for trying to teach me Dutch), Albert (insieme abbiamo fatto le fiamme...rosse e di mezzo metro), Marta (la Reinoso!!), Martine (thank you for cheering me up, even when your own research wasn't going so good), Jealemy (for your help and patience with the UWV stuff), Laura, Moira (a bottle of what?), Elisabetta (fondatrice del ministero dell'amore,



grazie per aver cercato farmi vedere le cose sotto il tuo, sempre unico, punto di vista), Francesca (actually you were not in my lab, but I could hear you anyway...).

Shu Han (so cute!! I hope you've had as much fun with me, as I've had with you), Alberto (the TV series expert), Denis (the master of quenching), Arancha (sorry for the noise from the pump), Ben (your fumehood has always been so lonely), Srinidhi (I hope I've given you good tips about digital cameras), Xue-Mei (my personal Chinese cooking advisor), Fijs (what a party!...after you've left), Amela, Chien-Ching, Tian, Mustafa, Carmela & Carmela, Riccardone, Maarten, Pim, Rene, Arno, Bambang, Nuriman, Nadia, Silvia, and all the female polish Erasmus students who have spiced up our life.

I also want to say "thank you!" to all other SMCT-MNF members: Fernando (gracias a tu experiencia y tus consejos tan "sabios" he podido seguir adelante), Soco, Lourdes, Olga, Michel, Riccardino (collega nella ricerca del lavoro, torneremo mai in Italia?), Deborah, Janet, Monica (la carbonara col tofu??), Emiel (the plants are still alive! well..at least some of them), Barbara, Kim, Aldrick, Ignacio (your karaoke performances are stunning), Andrea (grazie per l'onore di avermi scelto come paraninfo e per i tuoi consigli sui film da scaricare), Dorota (are you still on the market?), Victoria (fiesta!!!!), Mariana (que tal? Cevere!), Oya, Veera, Sachin, Xuexin, Andras, Dae-June, Vijay, Gena, Nuria, Alart, Francesca (la Corbe), Huub, MengLing, Frederieke, David, Becky, Carmen, Pascale & Christiaan (who needs to watch reality shows on TV when you two are around?).

Although I like to complain a lot, I've really enjoyed living in the Netherlands. Enschede might not be Las Vegas, but it's the city where I've meet a lot of extraordinary people, who will always have a special place into my heart. I've always felt part of a big family, where I could always find people interested in going to parties, bbq's, dinners, traveling around the World or just a quiet beer in the center. Thanks to all of you who made the past four years unforgettable. Soco, mi mejor compañera de piso, siempre recordaré nuestras conversaciones mientras cocinábamos; Rob, it has been a pleasure to have you as forth housemate; Fernando & Alessio thank you for let me join you for the Tuesday's after-cleaning dinners. Thank you for the laughs, the jokes, I consider those moments as representative of our great friendship and I'll never forget them. Lourdes, gracias a tu optimismo y tu forma de ver la vida, me me hiciste creer que llegaría este momento: por fin he acabado la tesis! Olga, gracias por tus consejos en los momentos más difíciles. Il tuo romano sarà sempre migliore del mio. Mitchel, he descubierto tu amistad con el tiempo, pero ha ha merecido la pena esperar. Marina, al final hemos compartido muchas cosas,

fotografía y yoga entre las menos importantes. Xing Yi & In Yee, thank you for all the funny moments and for teaching me the secret recipe of Curry Chicken. Deborah, I'll never forget your pre-Birthday party! Kim, together we've made the best gay couple at the gym, not to mention about Amsterdam...what an experience! Francesca da quando stai Riccardo sei un'altra persona, molto piu rilassata, intanto però Riccardino è dimagrato 15 kili...come lo spiegate? Albert, sei pronto per la prossima sfida culinaria? Henk & Marloes, thanks for bringing a bit of Dutch flavour to our lives. Roald, has been fun to see you supporting Italy in Berlin; Ana, mi lavadora siempre estará disponible para ti; Denis, crazy people can also be nice; Eddy, quando parte il tour eno-gastronomico della Padania? W la Serenissima! Janet, how many durum do I have to eat to get the Turkish citizenship? Martine, my favorite French! The NMR (No More Resaca) group: Victoria, Aldrick, Jealemy, and Ignacio; Arancha, Alberto, la Corbe, la Reinoso, Irene, Sandra, Siggie & Bart-Jan, Janina & Bas, Wojtek (sailor, poet, and scientist), and the ones that I forgot...

I want to thank the photography team: Lourdes, Marina, Daisy, Leoni, Muriel, Rithyda, and our teacher Cees. I've really enjoyed the evenings in the darkroom as well as all the parties. When I first subscribed to a yoga course I thought it was going to be all meditation and spirituality. In the end it turned out to be great fun and a good way to release all of my stress. Thanks to all the people who shared this experience with me, walking like monkeys, frogs or whatever else: Marina, Xing Yi, Janina, Martine, Francesca, Melba, Pablo, Claudia, and thanks to Tamara for teaching us how to 'show the flowers'.

Un grazie ai miei paraninfi Alessio e Albert, tenetevi pronti a rispondere le domande di chimica, in caso ce ne sia bisogno. Non vorrete starvene 45 min senza far niente, vero?

Grazie anche ai miei amici in Italia: Francesco, Alex, Cassi, Caco, Teo, Roberto Francy, Laura, Luisa, Cristian, Igor, Rota, Beppe, Carlo e Valerio per essermi stati vicini in questi anni, nonostante la distanza.

Familia Arratibel (Anton, Ramoni, Irune y Aitor) muchas gracias por abrirme las puertas de vuestra casa en mis muchos viajes a España, por acogerme y cuidarme como un hijo más. Gracias por vuestro apoyo y vuestra amistad.

Alla mia famiglia, perché so che è stato difficile per voi quanto lo è stato per me. Grazie per avermi appoggiato in ogni mia scelta, per avermi capito e spronato nei momenti difficili. Papà,

Mamma, so che siete orgogliosi di me, e questo mi rende felice. Grazie per tutti i vostri sacrifici che mi hanno permesso di arrivare fin qui. Matteo, ti ho visto crescere e doverci rinunciare non è stato facile. Quando sono partito eri un bambino, e guarda adesso...spero di essere stato un buon fratello, nonostante la distanza.

Itxaro, come farei senza di te! La lontananza da te è stata la prova più dura, ma è stato proprio nelle difficoltà che ti ho sentita più vicina, con la tua allegria, il tuo sorriso, sempre pronta a mostrarmi il lato positivo quando faticavo a trovarlo. Hai sempre creduto in me, dandomi la forza per arrivare fino in fondo: “Peque, falta poco! Tu puedes!!” Ed avevi ragione: ce l’abbiamo fatta, insieme. Questa tesi è dedicata a te! Te quiero!

Mirko

